AN INVESTIGATION OF THE RELATIONSHIP BETWEEN TEMPERATURE, FORCES AND TOOL WEAR IN TURNING AND DRILLING

FATHI MOHAMED BOUD

Doctor of Philosophy

ASTON UNIVERSITY

September 1998

ASTON UNIVERSITY

AN INVESTIGATION OF THE RELATIONSHIP BETWEEN TEMPERATURE, FORCES AND TOOL WEAR IN TURNING AND DRILLING

FATHI MOHAMED BOUD

Doctor of Philosophy

September 1998

SYNOPSIS

Developing a means of predicting tool life has been and continues to be a focus of much research effort. A common experience in attempting to replicate such efforts is an inability to achieve the levels of agreement between theory and practice of the original researcher or to extrapolate the work to different materials or cutting conditions to those originally used. This thesis sets out to examine why most equations or models when replicated do not give good agreements. One reason which was found is that researchers in wear prediction, their predictions are limited because they generally fail to properly identify the nature of wear mechanisms operative in their study. Also they fail to identify or recognise factors having a significant influence on wear such as bar diameter.

Also in this research the similarities and differences between the two processes of single point turning and drilling are examined through a series of tests. A literature survey was undertaken in wear and wear prediction. As a result it was found that there was a paucity in information and research in the work of drilling as compared to the turning operation. This was extended to the lack of standards that exist for the drilling operation. One reason for this scarcity in information on drilling is due to the complexity of the drilling and the tool geometry of the drill. In the comparative drilling and turning tests performed in this work, the same tool material; HSS, and similar work material was used in order to eliminate the differences which may occur due to this factor. Results of the tests were evaluated and compared for the two operations and SEM photographs were taken for the chips produced. Specific test results were obtained for the cutting temperatures and forces of the tool. It was found that cutting temperature is influenced by various factors like tool geometry and cutting speed, and the temperature itself influenced the tool wear and wear mechanisms that act on the tool. It was found and proven that bar diameter influences the temperature, a factor not considered previously.

An existing predictive model for the forces in turning (Taibi's Model) was used to compare experimental results obtained from this work in turning, this model was adapted to the drilling operation by the use of Webb's model on the drill geometry. It found that the experimental and predictive results for the both turning and drilling forces in a sharp tool obtained good correlation, but not for worn tools. It was concluded that it may possibly be that Taibi did not take account of the wear mechanisms in his model. Also as a result of this work it was shown that extrapolation is possible between turning and drilling when using predictive models.

Keywords: metal cutting, prediction, wear mechanism, tool life equation, machining.

DEDICATION

To my parents Mohamed and Muna

ACKNOWLEDGEMENTS

I will always be greatly indebted to my supervisor Dr John D Maiden for his excellent supervision, invaluable advice and continued guidance, support and encouragement throughout this project.

Sincere thanks are due to Mr W L Flint, Dr S Murphy, Dr J E T Penny, Dr D P Upton, Dr M G Wood for their advice and interest shown in the research conducted, and Mr E R Fielding from the University of the Witwatersrand (South Africa).

My gratitude also extends to all the technicians in the Department of Mechanical and Electrical Engineering, especially Paul Pizer, Jim Jeff, James Duggins, John Thurgood, Alan Evitts, John Foden, David Farmer, Dr. Kameel Sawalha and Dr. Sayah Saied. I would also like to thank the secretaries of the department especially Miss Colette Kelly.

I wish also to thank Richard Goodwin, Erica Williams, and Bert Howarth from Dormer Tools Ltd. for supplying the drills for this work.

I would also like to thank Y. Adeeb for the typing of the manuscript.

Thanks are also due to ESRC for its financial support.

Finally, I wish to express my gratitude to all the members of my family especially my father Mohamed Boud and my mother Muna Khalil for their encouragement and support throughout this course.

TABLE OF CONTENTS

LIST OF FIGURES

LIST OF TABLES

Chapter 1

INTRODUCTION

The definition of wear has a number of variations on a theme (Neale 1995, Tucker 1986, Ruff et.al. 1986) but can be characterised by the following; it is:

- for the most part a surface related phenomena,
- damage occasioned to a solid surface by the removal of material through:
    - the mechanical action of a contacting solid in relative motion to the surface,
    - the action of a liquid or gas,
- generally progressive but can occur at catastrophic rates,
- a consequence, generally, of combinations of different mechanisms.

Fischer (1996) argues that the wear mechanisms and their combination are determined by the structure of the entire tribological system (broadly speaking, tribology encompasses friction, lubrication and wear). He reports that this system consists of four elements: body, counter body, interfacial medium, and surrounding medium as shown in figure 1.1.

Figure 1.1 Basic structure of a tribological system (Fischer 1996)

According to Fischer (1996) the system undergoes certain tribological stresses (arising from load, speed of relative movement, temperature and time), while the type of interaction between body and counter body may be sliding, rolling, impact or flow. Thus, the structure of a tribosystem and the characteristics of interaction define the combinations and order of influence of the wear mechanisms operating.

Similarly, Alden Kendall (1989) states that wear mechanisms in cutting are dependent upon the contact stress, relative velocities at the wear interface, temperature and physical properties of the materials in contact. This foreshadows and is entirely consistent with the comments of Fischer (1996) in the context of wear generally.

There are a number of ways of classifying the types of wear (Ruff et.al. 1986). The majority of these are based on observations of surfaces in advanced states of degeneration. Examples of wear mechanisms include:

- abrasion wear
- adhesion wear
- diffusion wear
- fatigue wear
- fretting wear
- chemical wear
- plastic deformation
- chipping and breakage
- oxidation

Ham (1968) argues that in some cases one type may dominate, and in others, all or some of them may occur simultaneously. This will be discussed in more detail in chapter 2.

One can argue that abrasion and surface fatigue are dominated by mechanical interactions, while adhesion and tribochemical reactions are governed by additional chemical effects.

Wear in cutting tools represents one of the more complex of wear situations involving as it does a number of different wear mechanisms and is the major cause of tool failure. Failure is usually brought about by one of or a combination of the following processes:

- gradual wear
- brittle fracture (chipping and breakage)
- plastic deformation

Under properly controlled cutting conditions and proper selection of tool material, a cutting tool usually fails by gradual wear, that is, by progressive loss of tool material due to mutual interactions between the tool and the chips (Ham 1968).

Cutting tools wear, according to Alden Kendall (1989), because normal loads on the wear surfaces are high and the cutting chips and workpiece that apply these loads are moving rapidly over the wear surfaces. The cutting action and friction at these contact surfaces increase the temperature of the tool material, which further accelerates the physical and chemical processes associated with tool wear. Thus, cutting tool wear is a production management problem for manufacturing industries.

A considerable amount of work has been and continues to be published about wear, and yet a fundamental understanding which enables a general application of the knowledge is still limited. Peterson (1974) argued that wear is given little consideration in design and he sees the main two reasons for the limited understanding about wear control as being: firstly, the work that has been done has not been put in a useful form so that it can be readily used by designers and engineers. Even research scientists who are familiar with the literature cannot easily predict wear in any given situation since much of it remains

buried in scattered technical articles. If even crude design techniques were available, there would be a better awareness of wear principles and a natural tendency to develop an understanding of them.

A second reason is that wear has come to be accepted as inevitable and unavoidable. Often materials are used with the idea that the part can be replaced after a given amount of wear. This practice of allowing parts to wear and replacing them frequently is much more expensive than one realises. The cost of the diagnosis, and replacement labour, and downtime on equipment must be considered. However, even these costs may be insignificant compared to the effect of wear on the operation of the machine.

Therefore, as Tucker (1986) states that the performance of equipment may slowly degrade so selecting the time to replace worn components (or selecting the best materials initially to combat wear) involves consideration of cost in light of the cost of improvement in process productivity or product quality and the cost of downtime.

Basically the implications of wear for industry are cost and performance, and therefore, generally can be summarised in any area where wear occurs, as being of an economic nature.

As has already been stated wear is a production management problem for manufacturing industries particularly those involving cutting processes. Alden Kendall (1989) points that to successfully manage machining processes, production engineers and managers need to establish a system that :-

- Selects the proper machine tools and cutting tools to produce the geometric features in a part being machined from a particular material.

- Ensures that the tool distribution system provides quality tools having the required geometry.

- Specifies the correct cutting velocity, tool feed rate, and tool engagements with the workpiece.

- Establishes on-line or off-line procedures to monitor the condition of the cutting tool and the quality of the surfaces machined by the tool.

- Has maintenance procedures that ensure consistent machine tool operation.

- Takes into account the cost of machine tool operation and tool use, permitting a clear idea of the economic objective for the machining system.

Such a system can provide the necessary information to determine when a tool should be changed. Unfortunately, there are many variables to consider; thus, it is not surprising that tool wear assessment and tool change decisions are difficult problems.

Tool wear, is also influenced by the constitution of the tool; the rigidity of the tool, workpiece, and machine tool system, and the proper positioning of the tool.

Information on tool materials, different machinery processes, and the mechanics of the cutting process - must be taken into account to avoid some undesirable tool wear side effects. This will be further discussed in chapter 2.

Sometimes tool wear is excessive even when the recommended cutting conditions are used. The cause of the problem may be the rigidity of the machine tool and work holding fixture. An older machine tool or one that has not been properly maintained can cause vibrations at the tool that accelerate the breakdown and wear of the cutting edge.

Even with a well-maintained rigid machine and workpiece system, improper positioning of the tool can cause tool wear problems. Excessive overhang of the tool can cause dynamic instabilities similar to those mentioned above. In the cutting zone, the cutting edge must be positioned so that clearance surfaces do not rub against the machined surface. For a single-point cutting tool, this requires correct alignment of the point of the tool with the rotating workpiece centreline and careful positioning of the rake and flank surfaces so that correct angles exist between the tool surfaces and the workpiece surfaces. A further discussion of tool geometry will be in chapter 2.

Each type of machining operation has such specifications, and the tool engineer needs to ensure that they are followed when tooling set-ups are made. Understanding the tool service environment and the conditions that cause wear is the first step in planning and controlling of tool use in machining. Tool replacement decisions are dependent on predicting or sensing the magnitude of the wear damage caused by the active wear mechanisms on critical wear surfaces.

Wear as a phenomenum is linked in the broad engineering definition with friction and lubrication and in the industrial context these are collectively classified under the heading of tribology. Bahadur (1978) reports that the most emphatic realisation of the economic benefits achievable through the rigorous practice of tribology was probably first provided through the publication of the Jost Report in the UK in 1966. Whereas great studies have been made in understanding lubrication and in exploiting that understanding to satisfy most commercial needs, the understanding of the phenomena of friction and wear is comparatively rudimentary. It is well recognised today that wear is the predominant cause of maintenance breakdowns in industry which results in severe economic losses. Consequently, wear research efforts can be observed throughout the industrial world.

There are a number of mechanisms such as adhesion, abrasion, surface fatigue, etc. involved in a wear process. Bahadur (1978) argued that whereas a limited understanding of these mechanisms has been developed, the general picture of wear is still missing because of the interplay of these mechanisms in an on line situation. The latter makes the understanding of wear very complex. With the advent of sophisticated experimental techniques and equipment, it is hoped that an all-encompassing picture of wear will gradually emerge.

Complex tool geometries and higher strength materials are required to meet higher specifications as products become more sophisticated. Fortin et al. (1990) argue that products must be manufactured to a higher quality standard, at a reduced cost and within a tighter schedule. In the context of cutting, therefore, tougher materials must be machined and superior cutting tools must be used in order to save production costs while maintaining tighter tolerances and decreasing manufacturing lead times.

Ludema (1974) refers to two separate and distinct needs for wear models. The first is to estimate the life of parts. This is usually done to make decisions on marketability, the replacement market, service, warranty, etc. The second need is to establish a method to evaluate materials either for redesign or for screening the material from suppliers. This need usually fosters the practice of the standard test and the accelerated wear test.

As Garbar (1995) states the selection of wear-resistant materials is usually based on long-term testing. The cutting activity is predominantly in the region of turning operations due to the consistency of the cutting geometry and the difficulty of coping with variability of geometry in a tool, like for instance in drilling, a further discussion about drilling takes place in chapter 2. Although most of the work is done in turning a lot of what has been done in turning can be applied to other processes, for example, one can monitor and use tool wear by using cutting force in turning which can also be applied to drilling. This will be further discussed and illustrated in chapters 9 and 10 of the force prediction models.

Monitoring the tool during cutting can give a pre-warning just prior to tool failure. With the trend towards automatic machining, it becomes increasingly important to monitor tool failure arising from tool wear, chipping and breakage. Lee et.al. (1994) argue that it is helpful to achieve more accurate monitoring of the cutting tool. Further, it is also possible to optimise tool geometry to improve the performance and increase the life of the cutting tool. Although much research has been done on tool failure, the mechanisms of chipping of the cutting edge and tool breakage are still not very well understood.

Numerous attempts have been made to design a suitable tool-wear sensor using parameters such as cutting force, temperature, acoustic emission, and so on. Monitoring machining forces, especially feed force, is among the most common techniques of wear detection, and much research has been done to establish a correlation between them; however, Stern et.al. (1993) argue that the results are extremely inconsistent and the detection device is frequently ignored in the shop environment. The relationship between flank wear and feed force is of particular interest because flank wear is the principal wear pattern generally used to evaluate the condition of the tool. More is discussed on this topic in chapters 6 and 7 of the forces in turning and drilling, and in chapters 9 and 10 of the force predictive models in turning and drilling.

Such a study would clarify previous works by showing how each of the wear patterns alters machining forces. The end result would lead to the design and/or development of a sensing technique which would accurately translate wear into an unambiguous pattern for tool wear detection.

Economic analysis can be used Alden Kendall (1989) states to establish a tool replacement strategy that optimises the performance objective associated with the making of each feature. Common objectives are minimum cost, maximum production

rate, and maximum profit; however, minimum acceptable reliability or minimum downtime could also be used.

Tools are replaced to minimise the probable consequences of a failure event. The tool wear environment is so complex that even with the utmost care it is possible that the tool may fail in service. A very conservative strategy may replace the tool frequently to reduce the probability of an in-process failure, but, as a consequence, interrupt the process so frequently that productivity decreases and tool costs increase. To establish the strategy objectively, a clear understanding of the failure event must be agreed upon, and suitable data concerning top performance and operating costs must be available.

Consider tool replacement methods oriented to the most effective operation of machines. Daschenko et.al. (1988) state that a probabilistic approach must be taken where tool durability is regarded as a random variable whose distribution can be found experimentally. Mean tool lifetimes are variable therefore, in order to reduce downtime for replacement, one should attempt to arrange matters so that all tools have a similar tool life, that is use a certain 'strategy' for cutting tool servicing and replacement. Thus such strategies as the replacement-by-failure, mixed replacement by failures and deliberate (forced) replacement before failure as a combined strategy can be employed in practice.

The published work on wear is still largely descriptive and not very analytical. According to Bahadur (1978) the whole subject is in a confusing state and things are getting more so, for many papers are difficult to assess because they provide data on materials tested under arbitrary conditions on machines of dubious value. Many authors fail to analyse their results, or deal with basic principles, or study the phenomena and mechanisms, involved. It is not surprising, therefore, that there is no generally accepted classification of wear regimes that would assist analytical studies towards a theory of wear for each defined category.

Meng (1994) makes the point that models of wear developed in various contexts are characterised by the fact that the developer of the model gets good agreement experimentally but that independent attempts to do so are not generally as successful. This is certainly the common experience in the field of cutting where most modelling effort has focused on the turning process. Here attempts to replicate results from the original experimental range or extend models to cover broader ranges of condition are generally unsuccessful. This is not surprising given the complexity of the cutting circumstances and the range of influencing factors. This, as implied by Alden Kendall (1989) and Fischer (1996), for example, suggest that it becomes self-evident that unless the wear mechanisms are properly identified that this will be the case.

It follows that unless a thorough understanding of the relative incidence and influence in cutting is gained then modelling will remain difficult to replicate range sensitive activity.

Much work has been done on the analysis and prediction of machining performance, including surface roughness, cutting forces and chip breakability; however, Fang (1994) argues, all of it is based on a basic assumption, that is machining with unworn cutting tools, and therefore may not represent "real" machining operations. It is also known that present machining theories and machinability databases are all established based on unworn or fresh cutting tools. In actual machining processes, however, the machining performance may vary significantly with the progression of overall tool wear, including major flank wear, crater wear, minor flank wear, nose wear and groove wear at minor cutting edge. This is because the tool wear formed at different tool faces alters the original tool geometry/configuration, thus resulting in unexpected machining performance. More details of this will be discussed in chapter 2.

In this sense, a truly effective estimation of machining performance (including surface roughness, cutting forces and chip breakability) should be set not only off-line, based on

the conditions under unworn cutting tools, but also on-line, based on the overall tool wear developed during the machining processes.

Fang (1994) continues that since present machining theories are inadequate to describe analytically the extremely complex interrelationship between the overall machining performance and the progression of various types of tool wear, a systematic experimentally-based approach becomes appealing - even inevitable - for tackling the problem. The tool replacement strategy is dependent on the mechanism by which wear and catastrophic-failure events influence the objective. A study based on the understanding of how tool wear affects tool geometry and the influence the two main wear patterns (flank and crater) have on the machining forces (cutting, feed and thrust) is essential.

1.1 SCOPE OF THE THESIS

The purpose of this thesis is to observe the cutting operations of single point turning and drilling. Specifically, the main objectives of this thesis are to:

- Gain an understanding of the wear mechanisms and their interaction over a range of cutting conditions.
- Investigate the influence of temperature on the tool wear and wear mechanisms and demonstrate its importance in the cutting operations of turning and drilling.
- Investigate the influence of forces on the tool wear and obtain results to use in a predictive model for forces in turning and drilling.
- Examine representative cutting theory against that understanding,
  - the degree to which they recognise the mechanisms of wear they purport to predict
  - the extent to which they account for all the influencing factors.

- To demonstrate the difficulty in using these is due to a partial failure in one or the other of these respects.
- To consider the parallel between single point turning and drilling.

To achieve the above there is a need

- To establish appropriate measurement techniques and standards.
- To look at the range of tool geometries as an influencing factor.
- To look at the range of cutting conditions as an influencing factor.

A detailed appraisal of the literature is included to give a clear and fundamental understanding of wear, wear in cutting and the cutting processes where wear has been and is being studied, also to give a detailed knowledge of current research and the directions in which current thinking is taking that work. The literature is investigated from 1907 (from the Taylor equation) to the present, covering all the areas which have been used in this research.

Chapter 2

LITERATURE SURVEY - Factors Influencing Wear

2.1 INTRODUCTION

The importance of the metal cutting process may be realised by a single observation; that nearly every device in use today has either a machined surface or a hole drilled in it. Tool and tool material have always played an important role in the development of society. Metal cutting is a very large segment of modern industry which attracts a large amount of investment in order to achieve higher production rates. Therefore there is a need for proper use of tools and the training of those involved in the metal cutting industry. So, producing new tool materials will not on its own give higher production rates; but this can increase productivity with the use of efficient tooling and proper training of those involved.

The literature survey has been divided into two chapters (chapters 2 and 3) for ease of presentation. The first chapter deals with factors influencing wear whilst the second chapter examines the literature covering representative models of tool wear in cutting. This chapter is further divided into three sections as follows:

- Section 1 covers literature on tooling (geometry, wear sites and mechanisms, tool life criteria etc.).
- Section 2 covers literature examining the relationship between temperature and wear and the interaction between tool geometry, tool/workpiece materials and cutting conditions in the context of that relationship.
- Section 3 covers literature which focuses upon the factors influencing the physical conditions at the contact interfaces of tool and workpiece.

2.2 TOOLING: Wear Sites, Mechanisms and Tool Life Criteria

2.2.1 Relationship between Tool and Cutting Geometry in Turning

Turning is a machining process for generating internal/external surfaces of revolution by the action of a cutting tool on a rotating workpiece, usually in a lathe. Turning, as Trent (1991) states, is one of the commonly employed operations in experimental work on metal cutting. The workpiece is held in the headstock of the lathe and rotated about an axis parallel to the lathe bed as shown in figure 2.1. The tool is rigidly held in a tool post and moved at a constant rate along the axis of the work material.

Figure 2.1 The Turning operation (Stephenson et al. 1997)

Three parameters associated with the cutting conditions must always be defined:

- The Cutting Speed is the relative rate of movement of the tool and workpiece, it is expressed in metres/min.

- The Feed Rate is the relative incremental movement of the tool into the workpiece and it is measured in mm/rev.

- The Depth of Cut is the thickness of metal removed from the bar, measured perpendicular to the axis of rotation of the workpiece in millimetres.

The product of these 3 variables gives the metal removal rate, a quantity which is used to measure the efficiency of cutting. The rate of removed material from the workpiece increases with growing cutting speed and feed. The ideal situation from an economic point of view as demonstrated by Carlsson et.al. (1992) is therefore to use as high speed and feed as possible. It seems that Carlsson et.al. are looking for the ideal situation, but this depends on whether the view is to maximise the production rate or to minimise production cost, however in either case, wear is the factor which determines the limit. As machining proceeds the face of the tool, as can be seen in figure 2.2 over which the chip passes in order to be discarded is the rake face. This face is inclined at an angle to the axis of the workpiece.

Figure 2.2 Cutting tool terminology (Trent 1991)

The angle formed between the rake face and a line parallel to the axis of the workpiece is know as the side rake angle. A 'negative rake' angle turns the chip through an angle greater than 90° causing the chip to flow back against the rotation of the bar. The tool terminates in an end clearance face, which also is inclined at such an angle as to avoid rubbing the freshly cut surface.

The nose of the tool is at the intersection of the 3 faces and may be sharp, but more frequently there is a 'nose radius' between the 2 clearance faces. The secondary cutting edge is formed by the intersection of the end clearance face and the rake face, the flank face and the rake face together form the primary cutting edge.

Figure 2.3 shows the two methods in which cutting usually takes place in single point turning: orthogonal (which is the method used in this study), and oblique (or non-orthogonal as it is sometimes referred to). In orthogonal cutting, only the primary cutting edge is used and this is typified by turning on the end of a tube, and the actual distinction is that the chip flow is perpendicular to the cutting edge. The speed, feed and primary cutting edge are all at right angles. Depending upon the material properties and cutting conditions, the chip can either be continuous or discontinuous.

Figure 2.3 (a) Orthogonal (b) Oblique cutting (Boothroyd et al. 1989)

According to Boothroyd et al. (1989), the wedge-shaped cutting tool consists of two surfaces intersecting to form the cutting edge, as seen in the figure above. The surface along which the chip flows is known as the rake face, and that surface ground back to clear the new or machined workpiece surface is known as the flank. Thus, during cutting a wedge-shaped 'clearance crevice' exists between the tool flank and the new workpiece

surface. The depth of the individual layer of material removed by the action of the tool is known as the undeformed chip thickness.

One of the most important variables in metal cutting is the slope of the tool face, and this slope, or angle, is specified in orthogonal cutting by the angle between the tool face and a line perpendicular to the new work surface, as seen in figure 2.3, and this angle is known as the rake angle. The tool flank plays no part in the process of chip removal; however, the angle between the flank and the new workpiece surface can significantly affect the rate at which the cutting tool wears and is defined as the clearance angle. Boothroyd et al (1989) state that from figure 2.3, the sum of the rake, clearance, and wedge angles equal to 90°, where the wedge angle is the inclined angle between the face and the flank.

Figure 2.4 Tool geometry (BS 1972)

According to Shaw (1991), the most important aspect of a lathe tool is its geometric form. The relief angles seem to decrease slightly as the hardness of the metal cut increases according to Shaw as shown in figure 2.4. In cutting very hard materials the relief angle should be as low as possible; and when the feed is also reduced, relief angles as low as 5° may be successfully used.

Kibbe et al. (1995) and Groover (1996) argue that the nose radius will vary according to the finish required. Nose radius determines to a large degree the texture of the surface generated in the operation. The smallest nose radius that will give the desired finish should be used. Tools are given a slight nose radius to strengthen the tip.

According to Kibbe et al. (1995), one of the most important aspects of cutting tool geometry is rake. Tool rake ranging from negative to positive has an effect on the formation of the chip and on the surface finish as seen in figure 2.5. Zero and negative rake tools are stronger and have a longer working life than positive rake tools. Negative rake tools produce poor finishes at low cutting speeds, but give a good finish at high speeds. Positive rake tools are freer cutting at low speeds, and can produce good finishes when they are properly sharpened. Machining with a high negative rake angle Kopalinsky et al. (1984) argue, can lead to instability (vibrations) in the chip formation process and rapid deterioration of the cutting edge.

Figure 2.5 (a) Positive rake (b) Negative rake (Boothroyd et al. 1989)

According to Shaw (1991), the recommended values of rake angle are seen to be such that the normal rake angle generally decreases as the strength of the metal cut increases. This decrease in the normal rake angle provides a greater wedge angle at the tool point to support a greater load. Under severe shock conditions it is frequently desirable to use negative values of rake angle with carbide-tipped tools. Due to the greater ability of HSS tools to absorb shock it is preferable to provide them with larger rake angles than is desirable with carbide tools in order to take advantage of the decreased cutting energy that accompanies a shift to a higher effective rake angle.

Figure 2.6 Effect of tool rake on tool life (Boothroyd et al. 1989)

According to Boothroyd et al (1989), figure 2.6 shows a typical relationship between rake angle and tool life, where the optimum rake is approximately 14 degrees when cutting high strength steel with a HSS tool. In curve *A* the feed is 0.127 mm and the cutting speed is 0.66 m/s; in curve *B* the feed is 0.508 mm and the cutting speed is 0.41 m/s. Boothroyd et al. (1989) claim that experience has shown that the optimum rake is roughly constant for a given work and tool materials, and these values are shown in the figure above.

Ahmad et al. (1989) have indicated that the presence of a small negative primary land at the cutting edge can have a significant effect on tool performance by prolonging tool life and by allowing the tool to be used over a much wider range of cutting conditions. The

negative primary rake places the edge in compression, a condition favourable to materials lacking toughness, whilst the positive secondary rake allows lower cutting forces and temperatures and easier chip flow. The optimum land width, as demonstrated through the maximum improvements in tool life and ease of chip removal, was found at the concomitant conditions of maximum chip thickness ratio, minimum chip-tool contact length and minimum interfacial temperature and was dependent on the cutting speed, feed and tool and work materials employed. However it was found that whilst the presence of a negative land improves tool performance, no universally ideal edge geometry exists but must be established for each set of cutting conditions chosen.

Boothroyd et al. (1989) have found that the width of the flank wear land is usually the limiting factor determining the life of the cutting tool. However, it has been shown that the physical conditions of stress, temperature, and speed that determine the wear rate on the tool flank are constant along the wear land, and for reasonably small wear lands these physical conditions are not greatly affected by changes in the wear-land width. For these two reasons it would be expected that the wear rate of the tool material normal to the resultant cutting direction would be constant and independent of the normal clearance. The rate of increase of flank wear-land width, on the other hand, is dependent on the flank clearance. Boothroyd et al (1989) state that in practice the normal clearance can not be made too large without running the risk of weakening the tool edge.

It is generally recognised that the wear process changes the geometry of the cutting tools, for example flank wear decreases the depth of cut for a lathe tool. According to Alden Kendall (1989) the changes in the geometry of the cutting tool could produce out-of-tolerance dimensions on machined parts. Wear on the cutting edge and on the rake surface alter the state of stress and strain in the cutting region, thereby changing cutting forces and the mechanics associated with the chip-making process. Severe geometric changes that decrease the angle between the rake and clearance surfaces can weaken the tool so that the edge may suddenly fracture. Wick (1988) argues that increasing the relief angle weakens the insert but permits more wear of the cutting edge before the maximum wear land develops, thus increasing tool life.

2.2.2 Relationship between Tool and Cutting Geometry in Drilling

Drilling is a metal removal process for producing holes in components. The process involves feeding a revolving cutting tool along its axis of rotation into a stationary workpiece. A circular hole is therefore generated in the workpiece. The feed velocity (or feed rate) is usually small compared to the peripheral tool velocity. (Armanego et al. 1969)

Drilling is a complex machining operation (Agapiou et al. 1990a). The twist drill is the most popular and often the only practical tool for boring holes (Ema et al. 1991). More details can be seen in chapter 7 section 7.3. Twist drills have been the subject of numerous investigations. The most notable are the works of Bird and Fairfield, Smith and Poliakoff, Benedict, Lukens, and Hershey, Boston, Oxford, and Gilbert, Opitz and Jansen, and Galloway and Morton. But Oxford (1955) points out that these investigations have been concerned principally with important external effects of drilling which can be measured by drilling tests on machines equipped with various types of dynamometric equipment, i.e., torque, thrust, and drill life as influenced by drill geometry, speeds, feeds, workpiece material, and coolants. Such data have been of great assistance to industry for setting up production drilling operation.

As will be seen throughout this work there seems to be a paucity of information in drilling as compared to single point turning. But nevertheless the two geometries will be presented here and the differences will be looked at, and at a stage when examining the consequences of these differences there is much more obvious contact.

As Armanego et al. (1969) stated relatively little work has been done to study the mechanics of drilling. The general approach has been to investigate the drill geometry with respect to the important variables for single point tools and hence qualitatively describe the drilling results in terms of the theories of orthogonal and oblique cutting.

A drill is an end-cutting tool which has one or more straight or helical flutes as can be seen in figure 2.7, and which may have a hollow body for the passage of cutting fluid and/or chips during the generation of a hole in a solid or cored material.

Figure 2.7 The Drilling operation (Stephenson et al. 1997)

Stephenson et al. (1997) state that twist drills are the most widely used drills in practice. Twist drills differs widely in the number of the flutes they contain, and in geometric characteristics such as the helix angle, relief (clearance) angle, point style, flute shape, web taper, web thickness and margin width (see appendix 2 for more terms and definitions). A standardised system of identifying or classifying twist drills made by different manufacturers has not yet been developed. More discussion and reasons as to why this is the case are shown in chapter 5.

One very important feature of a twist drill is its point geometry. The geometry of the point determines the characteristics of the drills three cutting edges: the main cutting edges or cutting lips, the chisel edge, and the marginal cutting edges. The geometry of the main cutting edges affects the drilling torque, thrust force, radial forces, power consumption, drilling temperature, and entry and exit burr formation. The chisel edge

positions the drill before the main cutting edges begin to cut, and stabilises the drill throughout the cutting process; it also affects the drill's centring characteristics (skidding and wandering at entry) and the thrust force. The margins guide and locate the drill and affect the hole straightness and roundness errors and the drilled surface finish.

The best point geometry for a given application depends most strongly on the drill and workpiece materials, hole depth and size, required hole quality, and expected chip form. Other factors to be considered include the entrance and exit surface orientation with respect to hole axis, hole interruption, burr formation and tool life concerns, and the presence or absence of a bushing. The principal geometric features of the point are the point angle, the chisel edge angle, and the relief angle.

The cutting edge length is inversely related to the point angle. An optimum point angle which yields maximum drill life and hole quality exists for every working material. Generally, a lower point angle reduces the thrust force while increases the torque; the thrust force varies with the point angle and reaches a minimum value at roughly 118°, the point angle used on standard drills. The cutting edge is formed by the intersection of the flute face and the flank face; the shape of lip is determined by the point angle, helix angle, and flute contour. A straight lip is desirable because it generally provides maximum tool life.

The helix angle is the angle between the leading edge of the land and the drill axis. As with this research, there are 3 angles (more on the angles can be seen in the appendix 2):

- Standard helix drills have a helix angle of approximately 30° and are used for drilling malleable and cast irons, carbon steels, stainless steels, hard aluminium alloys, brass, bronze, plexiglass, and hard rubber.

- Slow (low) helix drills have helix angles of approximately 12°. They have increased cutting edge strength and are used for drilling high temperature alloys and other hard-to-machine materials. They are also used for brass, magnesium, aluminium alloys and

similar materials, since they provide for quick ejection of chips at high penetration rates, especially for shallow holes.

- Fast (high) helix drills have helix angles of approximately 40°, as well as wide, polished flutes and narrow lands. They are used for drilling low strength non ferrous materials such as aluminium, magnesium, copper, zinc, plastics, and for low carbon steels.

The rake angle distribution across the main cutting edges depends on the flute helix angle. The flute helix reaches maximum at the margin and decreases to zero at the centre. Similarly, the rake angle decreases near the web; it is typically negative at the centre of a drill and roughly equal to the helix angle at the outer corner (more details on a recently developed geometrical model for drilling will be discussed when Webb (1990) is discussed throughout chapter 10). Lip correction can be used to reduce the rake angle and increase edge strength along the main cutting edge; it generates a constant rake (helix) angle along the entire length of the cutting edge. A high positive rake angle may leave the cutting lip vulnerable to wear when drilling hard materials. However, a small or neutral rake angle will not help chip evacuation and may cause build-up at the point in softer materials.

The chisel edge is the blunt cutting edge at the centre of a centre-cutting drill. It is formed by the flank surface ground on the drill web. The optimal web thickness depends primarily on the work material. Because it cuts slowly and has a large negative rake angle, Stephenson et al. (1997) point out that the chisel edge produces a chip by an extrusion or smearing action, rather than by cutting as shown in figure 2.8. Because chisel edge chips have a less direct path to the flutes, they are more likely to pack and build up in the hole. The chisel edge contributes substantially to the thrust force; the size of the contribution depends on the relative lengths of the chisel and main cutting edges.

Figure 2.8 Chip formation at different locations along the cutting edge of a conventional drill (Stephenson et al. 1997)

Two aspects of drill performance may be monitored during the drilling operation as stated by Webb (1990) (As mentioned earlier more will be discussed on the Webb model in chapter 10):

- The Drilling Torque - which is a summation of 3 components; the first is the torque required by the drill cutting edges in performing their metal removal operation. The second is the friction force between the drill shaft and the hole sides. The third is the friction force between the swarf material contained within the drill flute and the hole sides.

- The Drilling Thrust - which is a summation of 2 components; the first is the thrust required by the cutting edges in performing their metal removal operation, and the second is the thrust generated by the drill point or flank faces due to their lack of a positive cutting clearance towards the centre of the drill point.

Webb (1990) argued that there was a complete lack of any compatibility of describing the 'fundamental' geometry of the twist drill. The practical effect of this is to prevent accurate interpolation and extrapolation between sets of test data (further reference on extrapolation based on Webb's model can be seen in chapter 10). Webb (1990) stated that each and every new drill situation, therefore, requires the performance of a new testing program with subjective results provided by trial and error.

Prior to the research of Webb (1990), there was no method available which allows the cutting geometry of drilling to be defined numerically. Due to Webb's research at Aston University, (he devised a computer based system able to create a geometric model of the drill form and calculate 'fundamental' cutting geometry of that form), it has been possible to extrapolate a force predictive model that was originally devised for turning (by Taibi) to the drilling operation. More discussion is available on Taibi's force model in chapter 9, and Webb's model in chapter 10.

2.2.3 Wear Sites in Turning

Wear patterns, processes and rates vary with and are influenced by different tool materials, work materials and cutting conditions. A cutting tool wears in many different ways, depending upon the various factors involved in machining. Figures 5.1 and 5.2 in chapter 5 show the sites of wear in turning.

A cutting tool has two contact areas:
- The tool-work interface area on the flank and,
- the tool-chip interface area on the rake face.

During cutting and after the tool has been used for sometime, wear develops along the tool flank of the tool-work interface and on the rake face of the tool-chip interface (Ham 1968).

2.2.3.1 Flank Wear

Flank wear occurs on the relief face which results in the formation of the wear land. Damage to the surface is caused by the rubbing of the wear land against the machined surface.

According to the ISO (1993) the maximum flank wear for HSS is: VB_B max. = 0.6 mm if the flank wear is not regularly worn, scratched, chipped or badly grooved in Zone B as can be seen in figure 5.1 and photograph 5.2 in chapter 5.

The average flank wear for HSS is: VB_B Av. = 0.3 mm if the flank wear land is considered to be regularly worn in Zone B as can be seen in figure 5.1 and photograph 5.2 in chapter 5.

Flank wear grows progressively larger as cutting continues. It is usually not uniform around the cutting edge or the tool flank (Ham 1968). Figure 2.9 shows a typical graph of the progress of flank wear land width VB with time or distance cut. The curve can be divided into 3 regions which are also the three stages of flank wear as it progresses:

1 - The region AB where the sharp cutting edge is quickly broken down and a finite wear land is established (The initial break-in zone).
2 - The region BC where wear progresses at a uniform rate (The uniform (steady state) wear zone).
3 - The region CD where wear occurs at a gradually increasing rate (The rapid wear zone).

Region CD is thought, according to Boothroyd et al. (1989) to indicate the region where wear of the cutting tool has become sensitive to the increased tool temperatures caused by the presence of a wear land of such large proportions.

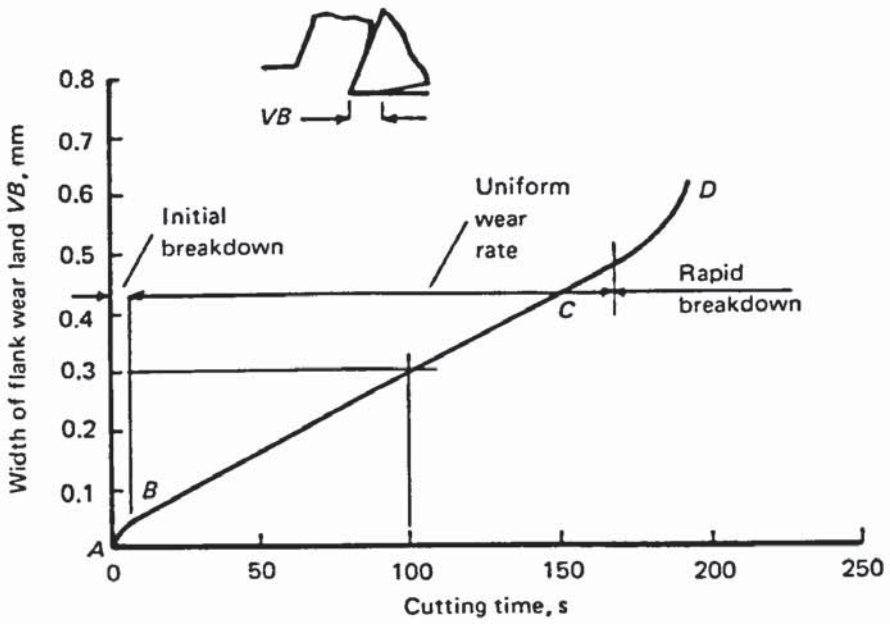

Figure 2.9 Development of flank wear with time
(for a carbide tool at a cutting speed of 1 m/s) (Boothroyd et al. 1989)

According to Ham (1968) in the initial break-in zone the tool develops rapid wear for a short duration as soon as it starts the cut. The uniform wear zone is also called 'the temperature insensitive zone'. In this zone the flank wear grows more or less linearly as the cutting time progresses. The rapid wear zone is called 'the temperature sensitive zone', and this is the zone where the rate of wear is rapid and dominated by increasing cutting temperature, and eventually results in catastrophic failure.

2.2.3.2 Crater Wear

It is stated in the ISO (1993) that crater wear, KT, occurs on the rake face and does not usually limit tool life. Although excessive crater wear weakens the cutting edge and can lead to deformation or fracture of the tool.

Crater wear grows in depth and length and grows progressively deeper as cutting continues. Ham (1968) argues that as the crater wear progresses the land between the cutting edge and the crater, and the location of the maximum depth changes. As the edge land decreases and becomes negligible, the crater boundary merges into the flank wear zones and the tool usually fails catastrophically.

2.2.3.3 Nose Wear

Nose wear, VB_C, according to the ISO (1993), occurs on the nose radius of the tool, on the trailing edge near the end of the relief face. It resembles a combined form of flank and notch wear.

2.2.3.4 Notch Wear

As stated in the ISO (1993), Notch wear, VB_N, occurs along the cutting edge, especially at the point of contact with the work surface. Notch wear is often caused by work hardening effects in the workpiece by the previous pass of the tool.

2.2.4 Wear Sites in Drilling

Twist drilling is a metal cutting operation where cutting speed and cutting angles vary along the cutting edge.

Characteristic wear patterns for conventional twist drills are shown in figure 5.6 and photograph 5.7 in chapter 5, Stephenson (1997) sights four types of wear are commonly observed (more details is in chapter 5):

- chisel edge wear
- lip wear
- margin wear
- crater wear

2.2.4.1 Chisel Edge Wear

This occurs at the central chisel edge of the drill and results from abrasion or plastic deformation, this is seen in chapter 5 figure 5.6 and photograph 5.7. This form of wear may double or triple the thrust force on the drill and affect the drill's centring accuracy.

2.2.4.2 Lip or Flank Wear

This occurs along the relief face of the drill's cutting lips and results from abrasion, plastic deformation insufficient flank relief caused by improper point grinding, or excessive dwelling at the bottom of blind holes. Lip wear increases the thrust force, power consumption, and maximum lip temperature, which in turn leads to an increase in thermal softening and further wear. Lip wear also increases the size of the burr produced when drilling through holes. When lip wear becomes excessive, the drill may cease to cut and fail by chatter or breakage.

2.2.4.3 Margin or Land Wear

This occurs at the outer corner of the cutting lip or on the land which contacts the drilled surface. Margin wear results from abrasion, thermal softening, or diffusion wear. Excessive margin wear results in poor hole size control and surface finish. Generally margin wear produces an undersized hole unless it is accomplished by built-up edge formation or centring errors, in which cases it produces an oversized hole.

2.2.4.4 Crater Wear

This occurs on the flute surface (see figure 5.6 in chapter 5) and results from thermal softening or diffusion wear. Moderate crater wear is usually not of concern, but excessive cratering weakens the drill's cutting edge and can lead to edge deformation, chipping, or breakage.

Stephenson et al. (1997) argue that at low to medium cutting speeds, abrasive wear is usually dominant and most wear occurs at the outer corner near the margins. At higher cutting speeds, in addition to abrasive wear, workpiece deposits may form on the drill lips and the margins, especially when drilling aluminium. Generally, the tool life decreases as the speed is increased when drilling abrasive materials. The feed rate should be maintained above a minimum level to avoid rubbing along the drill lips.

The tool wear can be classified into flank wear and crater wear. Liu et al. (1994) state that flank wear, which is a good indication of the drill condition, is caused by friction between the contact area on the clearance surface and the workpiece being machined. Crater wear is due to high temperature conditions along the rake surface. Flank wear is a good indication of the drill condition and has been widely used to indicate the severity of drill wear.

2.2.5 Wear Mechanisms in Cutting Operations

Economy in metal cutting is associated with an increase in production rates, with acceptable dimensional accuracy and finish. The useful life of a cutting tool is limited by wear. Hence, Battacharyya (1969) argues that productivity is directly affected by the wear of cutting tools. The principal concern of machinability research has been to investigate the basic mechanism of 'wear' by which tool life is governed.

Ham (1968) states that the basic mechanism of tool wear has been investigated for many years but is still not fully understood despite the large amount of data and knowledge accumulated. Much remains to be studied to explain fully the causes, processes, and the nature of wear for the improvement of tool material for better tool life.

According to Hastings et al (1976) there are 3 main types of wear mechanisms: abrasion, adhesion and diffusion, but there are several wear mechanisms, which contribute to the process of wear, these include oxidation and plastic deformation.

Current knowledge of tool wear provides for several basic causes of tool wear: abrasion, chipping and fracture, adhesion, diffusion, oxidation, some of which are illustrated in figure 2.10 (Ham 1968).

2.2.5.1 Abrasion Wear

The mechanism of abrasion wear Hoglund (1976) argues, occurs when the softer metal may contain appreciable concentrations of hard particles, and Smith (1991) suggests, for example, sand pockets, 'scabs' from the casting process of hard oxide coatings on hot-rolled bar stock. In these conditions the hard particles act as small cutting edges like those of a grinding wheel on the surface of a hard metal which in due course, is worn out through abrasion. Hoglund (1976) found that individual hard particles in the chip's underside plough into the tool surface's bonding material and expose the harder phase, or even break the brittle carbides. In each 'collision', the particle which is the hardest at that particular moment survives.

Smith (1991) states the nature, shape and size of the hard inclusions will affect how they abrade the tool's surface, for example, the ones with angular sharp inclusions are much more effective at increasing the wear-rate than those that are smooth and spherical. While the hard angular inclusions produce a micro-cutting effect on the tool, the more spherical types tend to deform the surface plastically, with a grooving action.

The effect of the cutting speed on wear rate Loladze (1976) and Brun et al. (1985) argue, indicates that the wear mechanism is also sensitive to temperature, and Brun et al. (1985), Kramer (1986), Rubenstein (1976) state that the cutting temperatures in abrasive wear are relatively low, also the wear rate is dependent on the hardness of the tool material.

Abrasive wear Ham (1968) states, is the result of the abrasive action of hard inclusions - such as carbides, oxides, other hard micro constituents in the work material, or hardened fragments of built-up edge - as they plough over the tool surfaces. In general the abrasive action is relatively more severe on the tool flank because of the nature of contact. And according to Bhattacharyya et al. (1969), abrasion occurs due to ploughing the softer matrix by hard constituents such as segregated carbides and inclusions.

2.2.5.2 Adhesion Wear

When a softer metal slides over a harder metal so that it always gives a newly-formed surface to the same portion of the hard metal, and because of friction, high temperature and pressure, particles of the softer material welds to a few high spots of the harder metal. Therefore, as a result of this flow of the softer metal over the surface of the hard metal past the cutting edge becomes irregular; a BUE may be formed and contact with the tool may be less continuous.

This mechanism is associated with relatively low cutting speed, when temperatures are low. According to Hastings et al. (1976) in the low temperature range adhesion is the principal factor controlling tool wear, passing through a maximum value of wear rate around 600°C and thereafter falling off rapidly with further increase in the temperature. The main characteristic determining the life of a tool material, in adhesion wear conditions, is resistance to micro-contact damage due to the periodic effect of local adhesion forces. A further characteristic is the adhesion activity between the tool and the workpiece material.

Lo Casto et al. (1993) argue that when machining AISI 1040 steel with ceramic tools hot metallic particles were found to be projected onto the rake face and were 'welded' to the ceramic surface, at this stage of the process there is also the occurrence of chemical reaction between alumina and iron which would increase the adhesive strength and decreases the mechanical strength of Al_2O_3. The subsequent flow of the chips collide with the particles that were pasted on the alumina earlier and drag them along, and therefore increasing the wear rate. The alumina based tools exhibit high chemical inertness but are very sensitive to thermally induced stresses and show chemical reactivity with oxidation products of steel chips. This behaviour explains 'chipping' and adhesive wear.

Adhesion wear is also sometimes referred to as attrition wear. Shaw (1991) explains that if the particles that are removed are very small, that is, submicroscopic, then this process

is referred to as attritious wear. But if the particles are visible under the microscope then the process is referred to as 'galling'. In all the cases the mechanism is the same except for the size of the particle generated.

Trent (1991), Hoglund (1976) and Juneja (1987) argue that sooner or later some of these fragments which may have grown up to microscopic size are torn from the surface of the hard metal. When this process continues for sometime, it appears as if the surface of the hard metal has been nibbled away and made uneven.

The high cutting temperature and extreme pressure acting at the interfaces may result in a strong bonding between a tool-work pair along the real area of contact. And therefore, Ham (1968) states that subsequent shearing may chip-off adhered tool material, thus causing the adhesion and transfer type wear.

Adhesion and formation of metallic bonds, as Bhattacharyya et al. (1969) states, are formed over the rubbing surfaces subjected to pressure with subsequent rupture of these bonds followed by transfer of elementary particles.

Many investigators, as demonstrated by Ham (1968) have studied adhesion wear from various points of view, as partially indicated in the following discussion. Dawihl in 1940 and 1941 conducted an extensive study on the adhesion temperatures of various tool-work parts and emphasised the influences of the interface temperature and the alloying elements of the tool materials on adhesion wear. Trent in 1952 and 1963 through his extensive analysis of tool wear from the metallurgical point of view, proposed a theory of crater wear based on adhesion, diffusion and alloy formation at the tool-chip interface. Trigger and Chao in 1956 made a significant contribution to a better understanding of crater wear from both experimental and theoretical points of view, particularly in relation to the interface temperature. And finally Ham (1968) indicates that Loladze in 1958 has carried out very extensive tool wear studies, especially on adhesion and diffusion wear, and has clarified many problems involved in the wear mechanism.

2.2.5.3 Diffusion Wear

According to Hoglund (1976) when a metal is in sliding contact with another metal and the temperature at their interface is high, conditions are favourable for atoms from the harder metal to diffuse into the softer matrix, so increasing the latter's hardness and abrasiveness. Also, on the contrary atoms from the softer metal may also diffuse into the harder medium and, therefore, weakening the surface layer of the latter to such an extent that particles on it are dislodged, torn, or sheared off, and are carried away by the flowing medium.

The diffusion wear mechanism becomes significant with the increase in cutting temperature. According to Hastings et al. (1976) at temperatures above 800°C diffusion becomes the dominant factor in tool life. Loladaze (1981) suggests that high temperature, large rate of deformation and continuous contact at the interface zone facilitate the initiation of intermetallic diffusion between the tool and work material.

Under conditions of diffusion wear the material of the tool should be inactive towards the work material. Depending on the properties of the work material, different grades of tool material manifest specific properties. For example, Loladze (1981) states that when cutting steel at high speeds, a tool material containing titanium carbide or titanium-tungsten carbide gives better results than one containing tungsten carbide only.

Lo Casto et al. (1993) and Pashby et al. (1993) found that ceramic tools cover a wide range of chemical composition and therefore their solubility in iron varies. For example, alumina-based inserts are interesting because the free energy of formation of Al_2O_3 is high and inhibits solutions in iron even at high temperatures. However, there is a high chemical affinity between iron and silicon nitride, and at high temperature, zirconia exhibits lower chemical wear. The inclusion of TiC to Al_2O_3 gives an increased resistance to edge fracture but is only beneficial, in terms of tool life, when machining annealed materials at 150m/min. In all other cases the chemical interaction of TiC with the workpiece gives wear levels similar or more than those in the Al_2O_3 tools.

Chemical wear processes are reported by Pashby et al. (1993) as being responsible for the wear of Sialon tools when machining iron based materials; only when cutting annealed material at a speed of 150m/min are temperatures low enough to prevent rapid interaction between workpiece and tool. With respect to diffusion wear, the ceramic material (corundum) is an ideal tool material for machining steel; since corundum does not dissolve appreciably in steel up to its melting point. If the ceramic material has sufficient strength, Loladze (1981) argues, it will be a more effective tool material for machining steel than the carbide materials.

It has been demonstrated by many investigators, as Ham (1968) shows, that at high temperature, that is, well above 900°C, diffusion mass transfer may take place at the interfaces, particularly on the rake face where chips slide over the contact surface. The tool material is usually an alloy of several elements, e.g., a mono-carbide tool material of C-6 grade consists of tungsten (W), carbon (C), and cobolt (Co). When temperature and time are favourable for the reaction, diffusion takes place, i.e., atoms of different elements in the tool material are simultaneously introduced into the work material. The carbon atoms diffuse at a faster rate and decarbonisation of the tungsten-carbide (WC) tool material might take place first. This might transform WC into tungsten-rich WC. The loss of carbon as a result of decarbonisation softens the tools, but according to Ham (1968), Loladze stated in 1958 that the diffusion wear is usually not observed on the tool surface. Thus Ham (1968) argues it can be assumed that only diffusion of tungsten into the chip or work material determines the extent of diffusion wear at the cutting conditions subject to the diffusion process, i.e. at high cutting speeds.

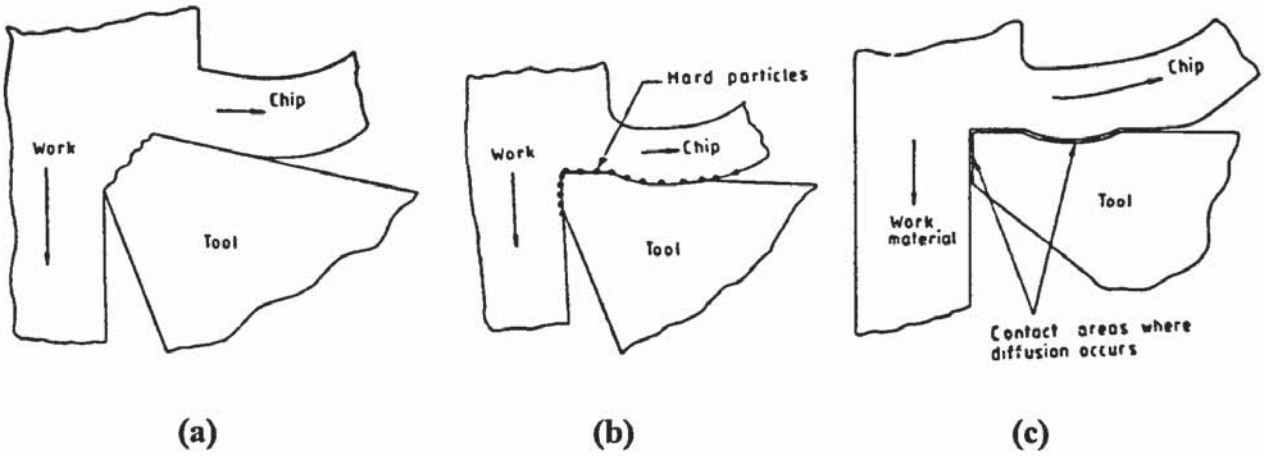

(a) (b) (c)

Figure 2.10 Wear mechanisms (a) Abrasive wear (b) Adhesive wear (c) Diffusive wear (Juneja 1987)

2.2.5.4 Chipping and Fracture Wear

In some cases, a tool fails from mechanical wear caused by chipping and brittle fracture. Usually this type of wear occurs as a result of the brittle nature of the tool material itself, or because of undesirable chatter vibrations, poor tool design and selection, improper cutting conditions, etc. Ceramic tool tends to wear in this process because of its brittle nature, while HSS tool is much more resistant to impact and to this type of wear (Ham 1968) as can be seen in tables 2.2 and 2.4.

2.2.5.5 Oxidation Wear

At high cutting speeds, i.e., in high cutting temperature range, oxidation also causes tool wear. According to Ham (1968) Opitz in 1966 reported that a high wear rate partly caused by oxidation is often found on the trailing ends of the tool-work contact zone, around the cutting edge. When oxidation wear occurs it is usually easily identified by visual inspection. Actually the oxidation of the carbide in the tool material leads to a weakening of the tool matrix and the strength of the cutting edge.

Practical wear situations rarely involve only one type of wear, and there are also important interactions, for example, adhesive wear is often accompanied by oxidation of the wear debris which may also act as a solid lubricant to reduce further adhesive wear or as a hard particle which causes abrasive wear.

According to Hoglund (1976), in general at low cutting speeds it is considered that adhesion and abrasion wear are the main mechanisms of flank wear in the steady-state region, and the diffusion wear increases in the accelerated wear region when temperatures increase. The major of the wear mechanisms are dependent on temperature as shown in figure 2.11 (Barth 1985).

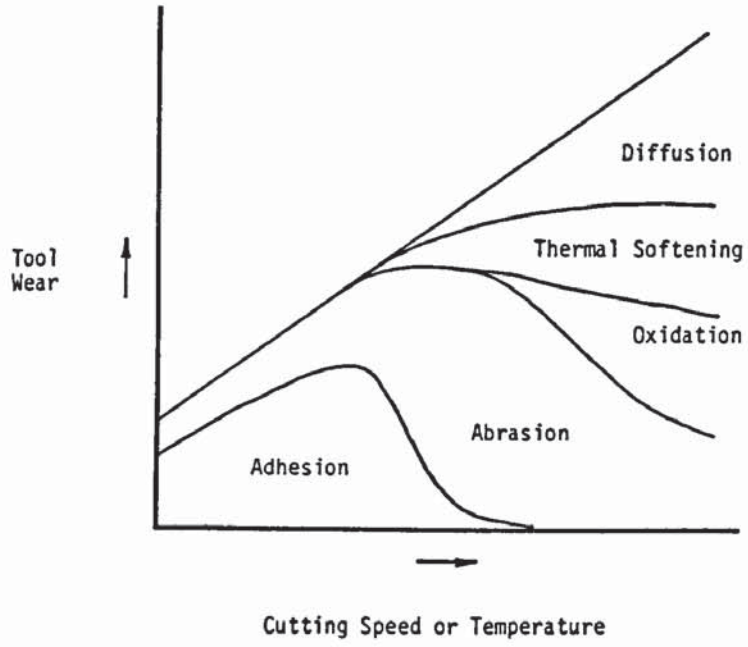

Figure 2.11 Shows relationship of tool wear mechanisms to speed and temperature (Barth 1985)

In figure 2.12 (a) the relative magnitudes of the various tool wear processes as function of the cutting speed (or temperature) can be seen as suggested by Viergge and figure 2.12 (b) is a similar diagram as proposed by Konig (Hastings et al. 1976).

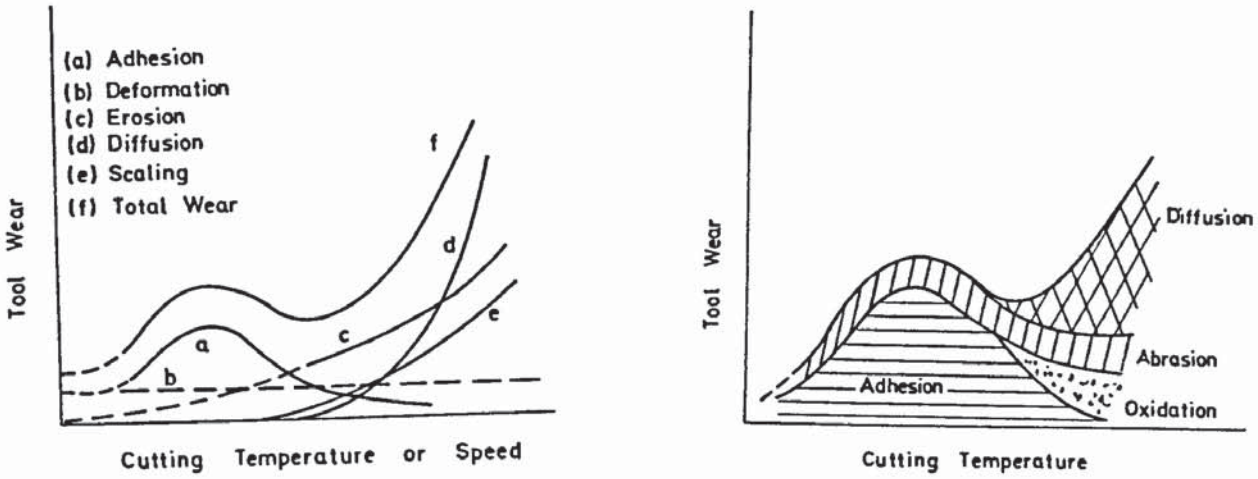

Figure 2.12 (a) and (b) shows various wear processes as function of the cutting speed (or temperature) (Hastings et al. 1976)

Not all wear processes that are listed above will occur simultaneously, nor in some cases will they appear at all in the useful life of a tool, especially if that life expires before total tool failure occurs. The type of wear causing tool failure, that is, by abrasion, adhesion or diffusion, etc., however, is related to the cutting conditions and the tool material, work material combination. The above wear mechanisms and their dependence on temperature will be further discussed in chapter 8, also the figures above of 2.11 and 2.12 can be see as to how they relate to the findings in this work.

A particular wear mechanism, Alden Kendall (1989) and Bhattacharyya et al. (1969) argue is dependent upon the contact stress, relative velocities at the wear interface, temperature, and physical properties of the materials in contact.

Initial Wear Mechanisms - The two materials in contact have surface roughness (SR) irregularities in the form of protrusions or asperities. At the interface, asperities from the two materials touch, creating tiny contact areas. The total area from these contact points is a fraction of the projected area of the contact surface. The stresses and heat are intensified in the asperities, and partial removal may occur due to seizure accompanied by fracture of the asperity or melting in the asperity. As these asperities are removed, the

initial SR is altered and the contact area increases. If the force conditions remain unchanged, pressure decreases and the active wear mechanisms change to plasticity and/or mild oxidation/diffusion dominated wear. This initial wear period creates small, visible wear surfaces (Alden Kendall 1989).

Steady-State Wear Mechanisms - The wear surfaces get progressively larger, if the wear surfaces are plastically dominated, small particles of material are mechanically deformed and fractured away from the wear surface. Abrasion is the most common wear process along the clearance surfaces of most tools (Alden Kendall 1989).

Normal stress and temperature vary over the wear surfaces so that a plasticity mechanism that dominates in one wear zone may not dominate in another. The maximum tool surface temperature occurs on the rake surface a small distance from the cutting edge. This is where the crater wear occurs, with diffusion wear often being the dominant mechanism. The high temperature and pressure cause atoms to move between the contacting materials, and this diffusion process locally aids in the removal of tool material to form the crater.

Venkatesh (1978) argues that a BUE condition affects the process in two ways. Near the cutting edge, the higher pressures could cause particles of work material to adhere to the cutting tool in the sticky zone. If the shear forces due to chip movement are high enough, the bond will be temporary and the adhered material will fracture away from the tool surface. When it fractures, small particles of tool material may be removed with the previously adhered material. This then is a wear process and would be associated with conditions in the safe zone just outside the BUE line. The second effect on the process occurs when the BUE is not fractured away by the chip motion and remains to alter the geometry of the cutting edge. The presence of the BUE changes the shear angle, causing instabilities in the chip-forming process and damage to the machined surface.

Wear can also occur as chipping along the cutting edge. Such chipping more commonly occurs when the cutting edge intermittently removes chips. This results, according to Alden Kendall (1989) and Ramaswani (1971) in cyclic impact and thermal loading of

the cutting edge. These two cyclic loading states can initiate small cracks or other residual cracks to form the chips.

Lim et al. (1993a) argue that abrasion, oxidation, diffusion, and chipping wear mechanisms that occur at operating conditions within the safe zone cause the initial wear surfaces to enlarge over time.

According to Alden Kendall (1989) the Tertiary Wear Mechanisms - The steady-state period of wear eventually enlarges the wear surfaces to a critical size that triggers accelerated wear. The pressures and velocities on these enlarged surfaces begin increasing the temperature so that the rapid oxidation/diffusion and local seizure or melting conditions exist, causing rapid destruction of the tool.

2.2.6 - Wear Standards in Cutting

Shaw (1991) notes that British, German and American standards differ in terms of the nomenclature and the definitions of positions of the tool, for example, of the tool face relative to the tool base. This illustrates how extremely complex things can be without standardisation. But in the case of the discussion here the two standards used are the British and the ISO which will be indicated throughout the discussion, more on standards can be seen in chapter 5.

What does exist in terms of standards are:
- BS 1296:1972 Part 2 - Specifications for Single-point cutting tools (BS 1972).
- ISO 3685: 1993 - Tool-life testing with single-point turning tools (ISO 1993).
- BS 328:1993 Part 1 - Specification for twist drills (BS 1993).

Some of the relevant information to this work of the nomenclature, terms and definitions are shown in the appendix 2 (Terms and Definitions).

Due to the complexity of the drill geometry leading to variation of speed and cutting angles across the lip of the drill, and also the difficulty in measuring wear in drilling as

it is compared to single point turning, makes the process complicated to investigate by researchers. In addition there is no International Organisation for Standardisation for drill tool life testing as there is for single point turning. The scarcity in the information about the drilling operation may be due to several reasons. It could be that due to the area being a complicated and difficult one the researchers are reluctant in taking up research into this area rather than another. This might explain why there are so fewer publications for drilling as compared to single point turning. Therefore, many researchers/investigators develop their own understanding of the process, as will be shown in chapter 5 where standards for measurements in drilling has been developed for this work.

2.3 - THE INFLUENCE OF TEMPERATURE UPON WEAR

2.3.1 - General Considerations

The cutting temperature plays an essential role in the performance of the cutting tool because as Zakaria et al. (1975) stated the wear rate and the type of wear mechanism are strongly influenced by the prevailing temperature in the contact zones. The temperature generated at the cutting edge Trent (1991) argues, is a deciding factor for the control of the maximum possible rate of metal removal when machining materials like iron, steel and nickel alloys with high melting points. In chapter 8 temperature and their influences were discussed in depth.

According to Boothroyd et al. (1989) heat is generated in 3 major zones (section 8.2 in chapter 8 gives more details of the zones):

- The primary shear zone - heat is generated because of the deformation of the work material.

- The secondary shear zone - In the area of the chip-tool interface heat is generated because of the shearing of the chip.

- Heat can also be generated at the flank face where heat is generated by the interaction of the workpiece with the tool. This can be kept to a minimum with a sharp cutting tool (Boothroyd et al. 1989).

During machining the generation of heat in the chip as seen in figure 2.13 occurs due to deformation on the primary shear plane Smith (1991) argues. The temperature of the chip is not usually very high unless machining is performed at very high speeds. There is a high temperature in the contact zone between the tool and the workpiece, and this leads to thermal softening when the cutting-tool material's specific temperature threshold is reached, in the case of metallic-based tools. Stephenson et al. (1997) argue that it has been shown that under most normal cutting conditions, nearly all the work done is in chip forming at the shear plane, and that most of this generated heat is passed into the chip, with a proportion being conducted into the workpiece and tool. The heat conducted into the chip is greatest some way up the rake face, and this results in eventual crater wear occurring in the tool at this position. According to Boothroyd et al. (1989), the chip material has a much greater capacity for the removal of heat than the tool because it is flowing rapidly near the tool face.

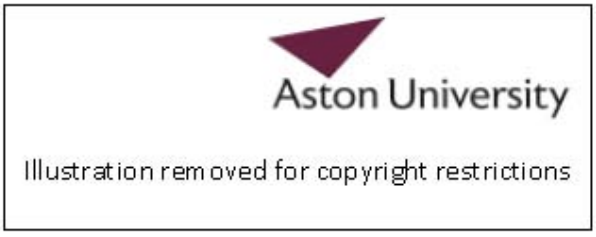

Figure 2.13 Temperature distribution in workpiece, chip and tool during orthogonal cutting (Stephenson et al. 1997)

Therefore, according to Boothroyd et al. (1989), this can be shown in the equation:

$$P_m = \Phi_c + \Phi_w + \Phi_t$$

P_m total rate of heat generation

Φ_c rate of heat transportation by the chip

Φ_w rate of heat conduction into the workpiece

Φ_t rate of heat conduction into the tool

The chip material has a much greater capacity for the removal of heat than the tool because it is flowing rapidly near the tool face. Therefore Φ_t , which usually forms a very small proportion of P_m , may be neglected except at very low cutting speeds.

A successful technique has been developed for temperature determination according to Trent (1991), when using HSS tools. This is useful for temperatures above 600°C, above this HSS are over tempered quickly. These structural changes can help to determine the temperatures within 25°C. The limitation of the technique is that it only applies to HSS tools and that the temperature has to be between 600°C - 900°C to cause recognisable structural changes.

Therefore the temperatures at the tool/work interface increase with cutting speed, and it is this rise in temperature which sets the ultimate limit to the practical cutting speed for higher melting point metals and their alloy.

The most important heat source responsible for raising the temperature of the tool Trent (1991) argues, has been identified as the flow-zone where the chip is seized to the rake face of the tool. The amount of heat that is needed to raise the temperature of the very thin flow-zone may represent only a small fraction of the total energy expended in cutting, and the volume of metal heated in the flow-zone may vary considerably. Therefore, there is no direct relationship between cutting forces or power consumption and the temperature near the cutting edge.

The cutting temperatures, as stated by Agapiou et al. (1994), strongly influence both tool life and the metallurgical state of the machined surface. Temperatures are particularly important in drilling, since the chips, which absorb much of the cutting energy in the form of heat, are produced in a confined space and remain in contact with the tool for a relatively long time. Tool temperatures therefore tend to be higher in drilling than in other processes under similar conditions. Drilling also differs from some other processes in that both transient and steady state temperatures are of interest. In many cases, a steady state is never established; tool temperatures simply increase with hole depth (Agapiou et al. 1988). The transient response becomes important in these cases if the temperature must be kept below a critical limit, since it then determines the maximum acceptable hole depth (Agapiou et al. 1994). Agapiou et al. (1994) argue that the point and helix angles both influence drill temperatures. Increasing the point angle shortens the cutting edge and increases the temperatures. Increasing the helix angle increases the effective rake and reduces the temperatures.

According to Zakaria et al. (1975) temperature, as one of the main parameters of the cutting process, may be viewed from two different angles. On one hand, the cutting temperature is recognised as a dependent variable whose magnitude reflects the severity of the cutting conditions. In this regard, the cutting speed is known to have the largest influence on the temperature. On the other hand, the cutting temperature may be thought of as an independent variable whose influence on tool wear has been clearly demonstrated. In the context just described, Zakaria et al. (1975) argue that the cutting temperature may be sensed and used effectively as an indicator of the cutting performance. For example, as an independent variable, the cutting temperature when sensed may be expected to indicate in some way the severity of the cutting conditions. For example, at a given moment, if a larger depth of cut or a harder work matrix is encountered, the measured temperature would be expected and is observed to increase. In turn, when temperature is viewed as a dependent variable, a higher temperature level is most likely to lead to increased tool wear; hence it may be expected that sensing the cutting temperature may reflect the on-going rate of tool wear.

One of the most important factors in the investigation of tool wear processes, is the measurement of tool temperatures in metal cutting. The importance of temperature in the study of metal cutting was realised early this century as mentioned by Barrow (1973). In 1907 Taylor noted the influence of temperature on the wear of cutting tools.

According to Taylor (1962), although more energy is consumed as wear proceeds and hence more heat is generated, more than 75% of the heat liberated is carried away by the chip. The real contact area increases, and therefore Taylor (1962) argues, it is not necessary for the temperature to increase in order for more heat to be conducted away from the contact area. Under constant cutting conditions, the temperature at the tool-workpiece interface has been observed to rise generally with machining time. This increase Sadat (1994) argues, is usually attributed to the increase in the cutting forces due to increase in total wear.

The wear mechanisms of a cutting edge are closely related to cutting temperature as is shown by Kannateys-Asibu's (1985) argument. Low cutting temperatures produce pressure welding, which results in a built-up edge, while high cutting temperatures enhance diffusion and oxidation processes. Diffusion processes between the chip and the top rake surface of the cutting edge result in crater wear, and oxidation reactions with the environment produce scaling of the cutting edge (Gruss 1989). For conditions where adhesive wear is important, it predominates in the intermediate steady-state stages, but the degenerative effects of wear and temperature makes diffusion a considerable factor in the later stages and definitely predominant in the accelerated wear region. There is a critical temperature at which accelerated wear begins. Below that temperature, flank wear increases uniformly with time. Above that temperature, the wear increases exponentially with temperature. The exponential rise in wear above the critical temperature is due to the dominating influence of diffusion.

Adhesion and diffusion wear mechanisms, both show a high degree of sensitivity to cutting temperatures. Various experimental studies have shown including Hastings et al. (1976), that the tool temperature may be related to the cutting speed and feed. In the low temperature range adhesion is the principle factor controlling tool wear, as can be seen

in figure 2.12 a and b. The adhesion wear mechanism tends to become insignificant as a cause of tool wear with the rising cutting temperature, therefore, the diffusion wear mechanism becomes significant and increases rapidly with increases in temperature.

Leshock et al. (1995) presented the analysis of the relationship between tool wear and temperature by applying the tool-work thermocouple technique. Flank wear appears to have no effect on the average temperature. On the other hand, the temperature measured by the tool-work thermocouple method shows that temperature has a strong effect on the crater volume wear rate, as is expected since crater wear is dominated by diffusion. Tool temperature is a very important parameter in the analysis of metal cutting. For many cases where the exact temperature distribution of the tool is not required, the tool-work thermocouple is a viable option for temperature measurement. The benefits of using the tool-work thermocouple are its ease of implementation after it has been calibrated, and its low cost.

Young (1996) states that the fact that the machining temperature has a critical influence on tool wear and tool life has been well recognised since the work of Taylor. Such a concept was applied by Trigger and Chao (Young 1996), who found that the growth of crater wear at the tool-chip interface was directly governed by the temperature distribution along the interface. Furthermore, Sata (Young 1996) showed, experimentally, a close correspondence between crater wear and the cutting temperature. In practice, according to Young (1996) the amount of flank wear is used more often in determining the tool life.

2.3.2 - Cutting Forces

The forces present during the cutting process Trent (1991) argues, can be resolved into 3 components which are shown in figure 2.14. The first component is the cutting force (F_c), which is the largest force acting on the rake face in the direction of the cutting velocity (YO). Second is the feed force (F_f) which acts parallel to the direction of the tool feed (OX) and finally the radial force which tends to push the tool away in a radial

direction (OZ). Most analyses ignore this third component which is small compared to the other two.

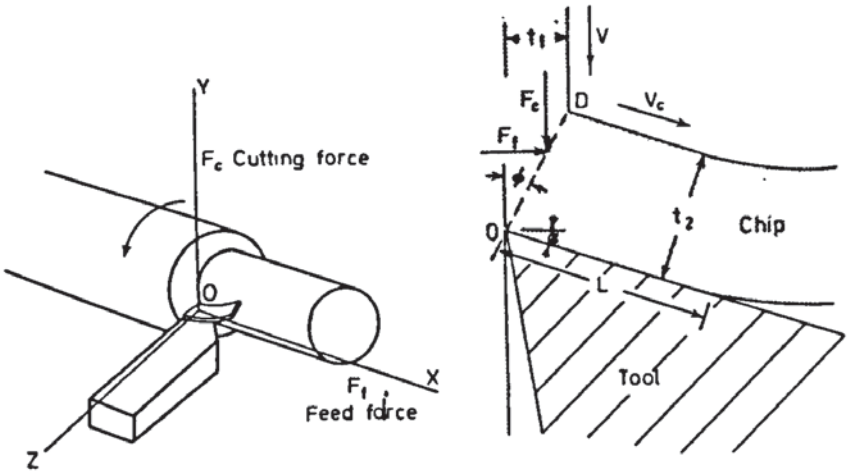

Figure 2.14 Forces acting on cutting tool (Trent 1991)

According to Trent (1991) the maximum compressive stress acts on the cutting edge and reduces to zero when approaching the end of the contact zone. Turning materials which produce discontinuous chips tend to produce lower forces due to the shorter contact length. Increase in the feed rate will increase the contact length between the chip and the tool, resulting in higher force generation. Chapters 6 and 7 deal with forces in turning and drilling respectively. Also details about force prediction models can be seen on chapters 9 and 10 for turning and drilling respectively.

Lee et al. (1989) point out that in 1946 Arnold suggested four causes for fluctuations in the cutting force. The first arises from variable speed of the tool relative to the work. With this condition it is found that dynamic instability would induce vibration. Energy is fed into the system by the variable force created and controlled by the vibration. Vibration or chatter was one of the aspects that Taibi looked at when developing a predictive model of the forces in turning (more details are discussed in chapter 9 and 10 of the model as it was replicated for turning and extrapolated to drilling with the force results obtained from this work).

The second factor relates to the influence of the cutting action of the flat at the tool point. During the half-cycle when the tool is moving downwards the flat is in contact with the workpiece. The force on the tool is expected to increase during this period. The magnitude of influence is dependent on the extent of wear on the flank face. The other two influences are the variable depth of cut produced by the movement of the tool point and the variable top rake resulting from the change of slope, but these are likely to be relatively less significant.

Another factor which influences the cutting forces is the rake angle according to Rowe et al. (1967). Selection of a tool with a larger rake angle will require lower forces but the increase in the rake angle will have the tendency to weaken the cutting edge thereby creating conditions of tool failure.

Flank wear Lim et al. (1993a) argue, generally causes an increase in the cutting force and the interfacial temperature, leading normally to dimensional inaccuracy in the workpieces machined and to vibration which makes the cutting operation less efficient. It has been observed that under conditions of flank wear during cutting, forces tend to increase with increase in tool wear.

2.3.3 - Tool/Workpiece Materials

The cutting tool material is one of the most important elements of the machining system. According to Shaw (1991), the tool materials which have survived today are not necessarily the ones that give the longest life. It is those which have satisfied the demands put on them in terms of the life of the tool, the rate of metal removal, the surface finish produced, the ability to give satisfactory performance in a variety of applications, and the cost of tools made from them that are still commercially available.

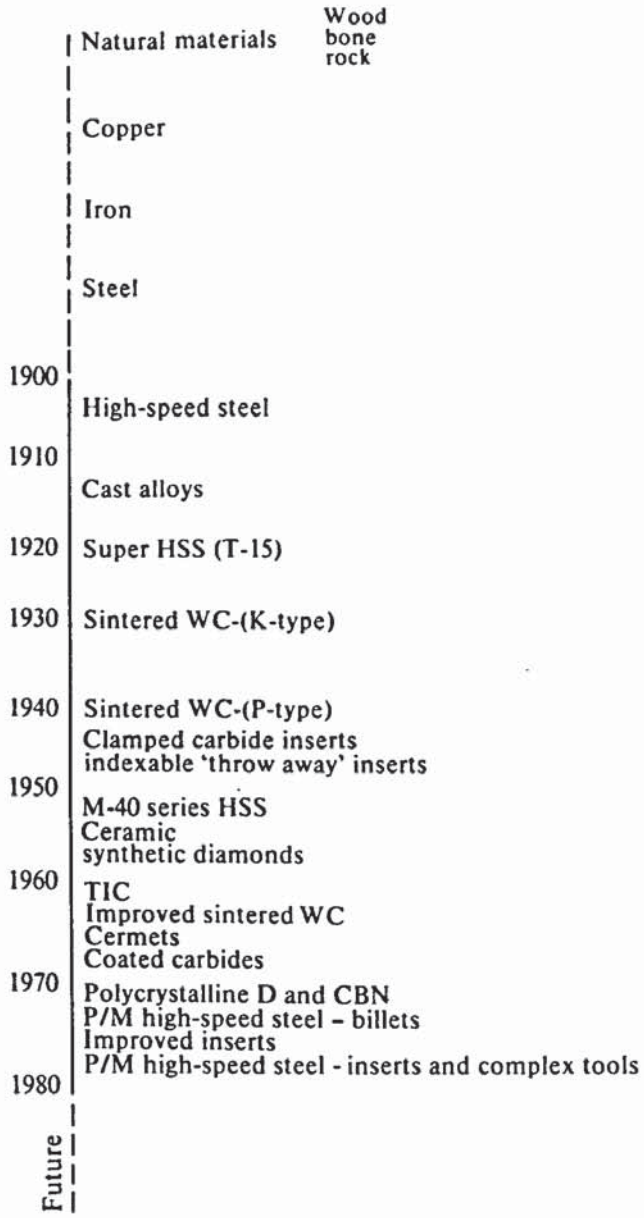

Table 2.1 Tool material development (Shaw 1991)

Table 2.1 shows a chronological list of the major developments relative to tool materials from 1900 to the present (Shaw 1991). The rate of increase in the introduction of new materials was partly due to a fast growing improvement in materials technology and in part to the need for special machining characteristics. A number of materials for cutting tools are composed on the basis of iron, carbides, ceramics or carbon. But some of the later discoveries have introduced combinations of the individual groups as well.

The tool/workpiece materials covered in this section are for the purpose of a general literature survey, but as far as tests in this work only HSS tools and some carbides were used. More details of the tool materials that were used can be seen in chapter 4. These tool materials were used as they were made available for the interest of research. Also as it happens, they are the same materials that were used by Taibi (1994) when he carried out his research at Aston University, this therefore facilitates the replication and extrapolations of the model so as to eliminate discrepancies concerning these factors. More can be seen discussed in chapters 9 and 10.

2.3.3.1 Tool Material Requirements

Cutting tools can be put through rough conditions, such as high temperatures and stresses. Severe frictional conditions can also occur between the tool and chip and between the tool and the newly machined workpiece surface.

The main properties, that Boothroyd et al. (1989) list which determine the usefulness of cutting tool materials are:

1 - High temperature physical and chemical stability, particularly high-hot hardness.

2 - High wear resistance.

3 - High resistance to brittle fracture.

High performance in all these three attributes is generally not possible. In general, materials with increased high temperature resistance and high wear resistance will also have reduced resistance to brittle fracture. In figure 2.15 an iron - iron carbide equilibrium diagram where the phases of the iron can be seen and in this kind of diagram, for example, the presence of other elements can be seen to change the phases and alter the diagram.

Figure 2.15 Iron - Iron Carbide Equilibrium Diagram (Pollack 1988)

The lifetime of a cutting tool is effectively controlled by the environment in which it is operated in as can be seen in tables 2.2 and 2.3. Edwards et al. (1990) argue that as increasing the cutting speed decreases the cycle time for a given cutting operation, then the highest cutting speed possible is required; the limitations to such a strategy has been tool material performance.

Table 2.2 Comparison of hardness and toughness for the cutting tool materials (Stephenson et al. 1997)

Table 2.3 The effect of tool material on cutting speed (Stephenson et al. 1997)

Other factors which influence the performance of cutting tools are (Boothroyd et al. 1989):

1 - Relative hardness of the tool and work material.

2 - Abrasive particles, such as scale, on the surface of the workpiece.

3 - Chemical compatibility of the tool and work material.

4 - Cutting temperatures.

5 - Condition of the machine tool; rigidity.

6 - Type of machining operation, in particular whether continuous or interrupted cuts occur, which is important for materials with a low resistance to brittle fracture.

Table 2.4 Major types of cutting tool material (Boothroyd et al. 1989)

The major types of cutting tool materials are shown in table 2.4, as this list is descended, the strain at fracture decreases.

The coated tool materials Alden Kendall (1989) states have good wear resistance until the hard coating is removed, exposing the softer core material. In the tests carried out by S. C. Lim et al. (1993b) of HSS tools which were used to machine (without fluid) medium-carbon steel, it was demonstrated that changes in wear rate can be obtained by altering both feed rate and cutting speed. HSS tools are used as an example here for mapping of wear.

Several mechanisms have been reported (Lim et al. 1993b) to describe the flank wear observed in HSS using single-point turning. These include diffusion wear, adhesion

wear mechanism depends on the machining conditions: the diffusion-controlled area is essentially the regime where diffusion wear operates; the plasticity-controlled regime covers the area where the machining conditions are insufficiently severe to generate a high temperature to cause diffusion wear.

Though there are many factors affecting wear of tools, the development of high precision machine tools can eliminate almost all the factors attributable to the wear caused by machine tools such as vibration as argued by Wada et al. (1980). The properties of workpiece material, therefore, directly determine the wear of the cutting tool in large extent.

2.3.3.2 Carbon Steel Tools

Before 1870 all lathe tools were made from plain steel. Carbon steel tools were used successfully for cutting copper at speeds as high as 110 m/min., but for cutting iron and steel speeds were normally kept to about 5-7 m/min. (Trent 1991) to ensure a reasonable tool life. Different carbon steels bring on different cutting force, temperature, tool face stress, and thus crater wear states Usui et al. (1978).

At the end of the last century, Trent (1991) reports, there was a need to develop improved tool materials due to the high costs resulting from the very low productivity of machine tools operating at very low speeds. Steel had become the most important of materials in engineering and the criterion of an improved tool material was its ability to cut steel at high rate of metal removal. They are still the most popular tool materials.

2.3.3.3 High Speed Steel (HSS)

A range of alloy steel was introduced at the beginning of this century to try to overcome the low cutting speed restriction of carbon steel; this was introduced by Robert Mushet in 1870 (Boothroyd et al. 1989, Shaw 1991, Smith 1991, Bayer et al. 1989). The steel retained its hardness at higher temperatures than previously, so that it could be used at speeds of up to 8 m/min. (Smith, 1991). By using a different heat treatment the tools were now capable of machining steel at 30 m/min. (Trent 1991).

In 1901 F. W. Taylor and M. White greatly improved the stability of these tools by increasing the amount of tungsten and the replacement of manganese by chromium, as well as using different heat treatment which became known as High Speed Steels. The cutting speeds used were reaching 19 m/min. (Shaw 1991, Bayer et al. 1989).

During the next ten years a rapid development of HSS took place. In 1904 Dr. J. A. Matthews found that additions of vanadium improved the material's resistance to abrasion (Boothroyd et al. 1989, Smith 1991). By 1910 the content of tungsten had increased to 18%, the chromium content to 4% and the vanadium to 1%. This became known as the 18:4:1 HSS which was the standard HSS for the next 40 years.

In 1923 a modification of HSS occurred as the 'super' HSS. According to Edwards et al (1990), Gill reduced the tungsten content to allow the material to be hot-worked. In the present M2 HSS, introduced in the USA in 1950, some of the tungsten content has been replaced by molybdenum (Edwards et al. 1990). It withstands temperatures approaching 650^{o}C and still maintains a cutting edge.

Date	Development
1903	0.70% C, 14% W, 4% Cr prototype of modern high-speed tool steels
1904.....	0.30% V addition
1906.....	Introduction of electric furnace melting
1910.....	Introduction of first 18-4-1 composition (AISI T1)
1912.....	3 to 5% Co addition for improved hot hardness
1923.....	12% Co addition for increased cutting speeds
1939.....	Introduction of high-carbon high-vanadium super high-speed tool steels (M4 and T15)
1940–1952.....	Increasing substitution of molybdenum for tungsten
1953.....	Introduction of sulfurized free-machining high-speed tool steel
1961.....	Introduction of high-carbon high-cobalt super hard high-speed tool steels (M40 series)
1970.....	Introduction of powdered metal high-speed tool steels
1973.....	Addition of higher silicon/nitrogen content to M-7 to increase hardness
1980.....	Development of cobalt-free super high-speed tool steels
1982.....	Introduction of aluminum-modified high-speed tool steels for cutting tools

Table 2.5 Development of HSS (Alden Kendall 1989)

Table 2.5 shows the significant dates in the development of high-speed steels. The most essential characteristics of HSS are wear resistance, hot hardness and toughness as well as improved speed at which steel was cut compared to carbon steel tools. But the loss of strength and permanent changes in structure of high speed steel when heated above 600°C, limit the rate of metal removal when cutting higher melting metallic and alloys.

According to Cook (1973), tool softening (tempering) leading to gross, very rapid loss of the entire cutting zone, appears to be a prevalent failure mode with high speed steel tools under high speed cutting conditions.

2.3.3.4 Cemented Carbides

These are a range of very hard, refractory, wear resistant alloys introduced in 1928 in Germany by powder metallurgy. In the simplest composition, cemented carbides Edwards et al. (1990) and Kempster (1984) inform are made up of tungsten carbide as a hard material and cobalt as a binder.

The early 'carbides', Smith (1991) reports suffered from a chipping tendency (brittleness), there were difficulties in brazing and grinding them, and most lathes were not sufficiently powerful or rigid to use them adequately. There was also a tendency to cratering, especially when machining steels.

Improved grades of carbides Santhanam et al. (1989) state, were produced with greater shock resistance, but they were used mainly to turn cast iron and non-ferrous metals due to the greater tendency for steel to cause tool face cratering. To improve resistance to cratering, Shaw (1991) suggests tantalum carbide and titanium carbide are added to the basic composition, resulting in tungsten-tantalum carbide or tungsten-titanium carbide.

Cemented carbides are available in many different grades, which differ in hardness and wear resistance. Increasing the cobalt content of the material Ber (1972) reports generally increases the toughness but reduces the hardness. All cemented carbides can be used at elevated temperatures compared to high speed steel, but these materials are relatively brittle and can fracture easily when interrupted cuts are used (Kramer 1987). It was found by Ber (1972) that the hardness of a cemented carbide grade decreases with the rise of temperature. Test results Bhattacharyya et al. (1970) believe indicate favourable agreement for machining steel with carbide tools.

2.3.3.5 Coated Carbides

One of the challenges in the design of cemented carbide tools is the optimisation of toughness associated with straight WC-Co alloys with the superior crater wear resistance of alloyed carbides containing high levels of titanium carbide. This challenge has led to the development of coated carbide tools.

The success of coated carbides is based on their proven ability to extend tool life on steels and cast irons by at least a factor of two to three. This is accomplished by a reduction in wear processes, especially at higher cutting speeds.

In the 1960s developments in the production of coated carbide tools enabled higher cutting speeds in steel machining but also reduced crater wear on the tool. Santhanam et al. (1989) argue the metal cutting productivity increased with the use of these laminated tools, which consisted of a base of WC-Co alloy with a sintered layer of high TiC composition, but the thermal expansion mismatch between the substrate and the surface layer caused thermal stresses during metal cutting, and the laminate tended to spall during use. In coated tools, the fracture toughness of the coating is almost always lower than that of the substrate. In addition, Kramer (1993) states the presence of the crack in the coating increases the stress intensity penetration of the crack into the substrate.

In 1969 further developments of laminated tools were superseded by the application of a thin layer (5 and 8 μm) of hard TiC coating to the cemented carbide by chemical vapour deposition (CVD). Eventually when the coating has been worn away by abrasion, the wear rate becomes the same as that for the uncoated tool.

A coated carbide insert is more expensive than an uncoated one, but Chen et al. (1989) state it has higher wear resistance and therefore a longer life. For example, Dearnley (1985) demonstrates that coated cemented carbides are more effective in resisting wear than uncoated ones when cutting GA iron (pearlitic grey cast irons containing flake) in the absence of BUE at 200 m/min.

2.3.3.6 Ceramics

The use of ceramic tools was first proposed in Germany as early as 1905 (Kopalinsky et al. 1984). Desirable properties of these tools include high hot hardness, and resistance to wear (both abrasion and cratering), good chemical inertness, high resistance to plastic deformation, high compressive strength (Campbell et al. 1994), and a low coefficient of friction (Tonshoff et al. 1988). Most of the heat generated during cutting is carried away in the chips, resulting in less heat build-up in the workpiece and tooling.

Relatively low tensile and transverse rupture strengths of most ceramics limit their resistance to shock loads. Boothroyd et al. (1989) state that premature failure of ceramic inserts is generally the result of chipping, cracking, or breakage, typically caused by improper edge preparation, overloading, shock, or a combination of these.

Pashby et al. (1993) state that a range of ceramic cutting tools have been developed to address one of the critical restrictions of all ceramic tool materials, a relative lack of toughness. There are three major categories of ceramic tool materials today; the pure oxide, mixed oxide and the nitride ceramic (Komandur et al. 1989). Alumina (Al_2O_3) is predominant in the pure oxide and mixed oxide ceramics while silicon is predominant in the nitride ceramics. It is therefore useful to classify ceramic tools into two categories; the alumina and silicon based materials. Alumina-based inserts include plain (pure), composite, and whisker-reinforced ceramics. Silicon nitride-based inserts include sialons.

Plain oxide ceramics are highly pure alumina. Some contain zirconium oxide (ZrO_2) as a sintering aid and to improve the fracture toughness and its resistance to thermal stresses (Lo Castro et al. 1993). Small amounts of magnesium oxide are sometimes added to inhibit grain growth, and molybdenum to help refine grain structure.

The aluminium oxide provides high chemical stability and hot hardness with good oxidation resistance. Edge build up is minimal, and cratering is generally only

encountered with heavy roughing cuts. Wear resistance is also excellent for machining many materials. Advantages of whisker-reinforced ceramics Narutaki et al. (1993) state include improved strength and wear resistance.

According to Buljan et al. (1989) the silicon nitride-based inserts have higher degrees of fracture toughness, thermal shock resistance, and edge strength than those made of plain oxide or composite ceramics, with comparable hardness, temperature resistance, and chemical stability. The sialons Billman et al. (1988) argue generally have higher diffusion wear resistance than the densified silicon nitride ceramics, but their rupture strength is usually lower, especially at higher temperatures. Composite silicon nitride ceramics generally have higher hardness and fracture toughness than sialons.

Inserts made from silicon nitride-based ceramics are being primarily used for machining cast irons. Their use for machining steels has been limited because of chemical interactions at the tool-workpiece interface. Modifications to the compositions of the ceramics and/or coating the inserts, however Gruss (1988) informs, minimise this problem.

2.3.3.7 Diamond and Cubic Boron Nitride (CBN)

Diamond and CBN are very similar in many ways: they are the two hardest materials known, they share the same crystallographic structure, and they exhibit exceptionally high values of thermal conductivity. In other ways they are very different; diamond oxidises in air, reacts with ferrous workpiece material at moderate temperature, and is subject to graphitisation. CBN is thermally quite stable both in air and in contact with ferrous workpiece materials. As a result of these property differences, Heath (1989) states that diamond is used in the machining of non ferrous materials, while CBN is used in the machining of ferrous materials.

CBN is less expensive than diamond, but over 20 times more costly than carbide. The high cost is counterbalanced by a considerably increased tool life (up to 50 times longer than carbide) (Boothroyd et al. 1989). It is also possible Schaible (1991) suggests, to

produce polycrystalline diamond (PCD) or polycrystalline cubic boron nitride (PCBN) by sintering (or binding) many individual crystals of diamond or CBN together to produce a larger polycrystalline mass.

Kozak et al. (1994) inform that PCD is an extremely tough and strong material. In simple abrasive wear situations, PCD is significantly more wear resistant than any other cutting tool material. PCD is approximately 10 times more wear resistant than PCBN and 100 times more wear resistant than cemented carbide. PCD are used for cutting low melting temperature materials such as alloys based on aluminium or copper. They are used at very low cutting speeds for hard materials such as ceramics. CBN is specially used for materials that are difficult to machine such as case-hardened steels, cast irons and some nickel alloys.

2.4 THE RELATIONSHIP OF THE PHYSICAL CONDITION OF THE CONTACT INTERFACES AND WEAR

2.4.1 - Relationship between Chip Formation and Wear

Chip formation in general has been considered by previous researchers but their concentration has been principally on chip formation in isolation and the factors it influences as will be seen below. However, one can argue that an understanding of the chip formation process also helps in the understanding of the development of the wear process because these factors also relate to forces, pressures, etc. (More can be seen in chapters 6 and 7).

It has long been known according to Jawahir et al. (1995) that chip control in metal machining, particularly in continuous mode operations such as turning, is vital owing to its significant role in producing small handleable sized chips for disposal, and in protecting the machined work surface, cutting tool and machine tool. As Boothroyd et al. (1989) demonstrated in turning operations, when the tool is continuously removing metal for a long period, a continuous chip can become entangled with the tool, the workpiece, or the machine-tool elements. Unless controlled properly, it can result in mechanical chipping of the cutting edge.

Chip formation takes place by a process of shear in a region known as primary deformation zone which Bailey (1975) argues extends from the tool cutting edge to the junction between the surfaces of the chip and workpiece. The chip is generated from the deformed work material and according to Li et al. (1995) flows along the tool rake face under the action of large normal and shear stresses. Figure 2.16 illustrates the major areas of deformation and friction that occur during the generation of chips.

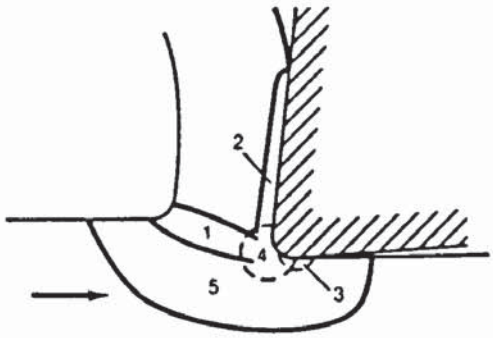

Figure 2.16 Zones of deformation and friction in chip formation (Nachtman 1989)

In figure 2.16, zone 1 indicates the area of strain hardening that forms in the material being cut ahead of the tool. Microcracking can take place in the zones and relatively high temperatures result from the deformation and resultant strain hardening. In zone 2, the deformed chip moves out of the shear zone and flows up the surface of the tool. As the chip slides up the face of the rake of the tool, it generates more heat as a result of friction between the chip and the tool. In zone 3, as the tool traverses the freshly cut surface, further rubbing of the tool against the workpiece material takes place, thus generating friction and additional deformation. As chip formation proceeds, the tool edge forms a BUE (zone 4), which creates more local plastic deformation and friction. In zone 5, below the area of primary metal removal, additional plastic deformation takes place, along with some strain hardening. The geometry of the chips varies with the workpiece material and the cutting conditions.

Types of chip formed by cutting generally fall into one of 3 main groups (Chapman 1981):

a- Discontinuous without built-up edge - a discontinuous chip which is formed by unsteady plastic deformation and periodic fracture on the shear chip, and use of an efficient cutting lubricant, low speed and brittle material (figure 2.17a).

b- Continuous without built-up edge - a continuous chip is formed by steady plastic deformation in the primary shear zone. Use of ductile work materials, high speeds and unlubricated conditions give rise to this type of chip (figure 2.17b).

c- Continuous with built-up edge - a continuous chip which forms over a built up edge adhering to the rake face. Higher values of feed, low speed and also poor properties of the lubricants give rise to this type of chip (figure 2.17c).

In practice, there is a gradual change from one distinctive type to another. The distinction between different chip types is not always obvious.

Figure 2.17 Types of chips obtained in metal cutting, (a) Discontinuous chip, (b) Continuous chip without BUE, (c) Continuous chip with BUE (Chapman 1981)

The form of a chip, at the instant it leaves the cutting zone, depends on three basic chip form parameters: up-curl, side-curl, and chip flow angle. For instance, a combination of the first two usually leads to cylindrical-helical chips whereas the addition of the third to this combination leads to conical-helical chips. However, Venuvinod et al. (1996) argue there are no analytical models available which possess the ability to predict, with sufficient robustness, the magnitudes of these basic chip form parameters for given input conditions. The problem is further exacerbated by the fact that chips often substantially change their form or, even break (which is generally desirable) when they encounter an obstacle after they have exited from the cutting zone.

Elbestawi et al. (1996) looked at chip formation mechanism in hard-turning. It was observed that the chip formation starts with initiation of a crack at the free surface of the workpiece which further propagates towards the cutting edge of the tool. The crack soon ceases to grow at a point where severe plastic deformation of the material exists under

high level of compressive stresses. The chip segment caught up between the tool rake face and the crack is pushed out while the material in the plastic region just below the base of the crack is displaced along the tool rake face thus forming saw-toothed chips.

The cutting edge of the tool is positioned a certain distance below the original work surface during machining and this corresponds to the thickness of the chip prior to chip formation t_o . The chip increases in thickness to t_c as it forms along the shear plane. The chip thickness ratio *r*: is the ratio of t_o to t_c

$$r = \frac{t_o}{t_c}$$

The chip ratio will always be less than 1.0 as the chip thickness after cutting is always greater than the corresponding thickness before cutting. An important relationship is established among the chip thickness ratio, the rake angle, and the shear plane angle due to the geometry of the orthogonal cutting model (Groover 1996). Let l_s be the length of the shear plane. A substitution $t_o = l_s \sin\phi$, and $t_o = l_s \cos(\phi - \alpha)$. Therefore,

$$r = \frac{l_s \sin\phi}{l_s \cos(\phi - \alpha)}$$

This can be rearranged to determine ϕ as follows: $\tan\phi = \dfrac{r\cos\alpha}{1 - r\sin\alpha}$

The chip shape and its behaviour can cause a variety of problems. In the single-point turning process, where the tool is continuously removing metal for a long period, a continuous chip can become entangled in the tool, the workpiece, or the machine tool elements, therefore Yee et al. (1986) argue causing damage to the surface finish of the part or interfering with workpiece or tooling changes. If a coolant is being applied, the chip may interfere with the flow of coolant, causing alternate heating and cooling of the cutting edge. The resulting thermal stresses can reduce the tool life.

At low cutting speeds, the chips usually have a natural curl and tend to be brittle. According to Sukvittayawong et al. (1991) with a new tool and under a low feed rate a long chip is produced. Under the same cutting conditions, the chip length, when a worn tool is used, is shorter than when a new tool is used. In chapter 8 more detailed discussion of the chip and its relation to temperature is shown.

Koelsch (1993) argues that the classic, tightly curled 6 or 9 chip is not always best for optimum performance, but a process that tolerates a more open chip requires less cutting force and, therefore, enjoys longer tool life. Deeper cuts speed tool wear, and faster feeds can diminish surface finish and taper quality, by doing this chip control is improved.

2.4.2 Relationship between BUE and Wear

The presence of BUE on the tool face during cutting can affect the tool-wear in various ways, sometimes decreasing the life of a cutting tool and sometimes increasing it. With an unstable BUE the highly strain-hardened fragments, which adhere to the chip underface and the new workpiece surface, can increase the tool-wear rate by abrading the tool faces. However, Boothroyd et al. (1989) state that a BUE can also contribute to sudden tool failures when tools with carbide inserts are used. For example, when a tool is suddenly disengaged, a portion of BUE (welded during cutting to the tool face) may be torn off, taking with it a fragment of tool material. More is discussed about BUE and also SEM photographs are shown in chapters 6 and 7.

When very hard materials are cut, the presence of a stable BUE can be beneficial. A stable BUE protects the tool surface from wear and performs the cutting action itself. According to Ramaswami (1971) the presence or absence of BUE is important in relation to tool wear and surface finish. Abrasion and adhesion are the two types of wear influenced mostly by BUE. Abrasive wear occurs by ploughing of hard particles on the underside of the chip to remove material from the tool face by mechanical action. The hard particles are strain-hardened fragments of an unstable BUE and cause both crater and flank wear. As a result of the irregular and less laminar flow of the work material

past the tool, Lim et al. (1993a), and Ohgo (1978) argue that a BUE always forms at the tool edge at low cutting speed; the shearing and breaking down of the BUE during unstable cutting tend to pull away fragments of the tool materials underneath this BUE, giving rise to adhesive wear.

Materials transferred from a workpiece to a cutting tool is deposited on the rake face or the flank face of the cutting tool and reduces the service life of the tool for machining. Ohgo (1978) had reported a BUE forms on the rake face of the tool with low speed cutting, and peeling of the BUE from the rake face causes adhesive wear of the tool which results in a reduced tool life.

According to Yaguchi (1988) the BUE, which is a stagnant piece of work-piece material adhered at the tool edge, is very important in relation to various aspects of machinability and may be either harmful or beneficial depending on the cutting conditions and the machinability criteria. Yaguchi has found that the presence of a small and stable BUE is generally beneficial to the machinability of free-machining steels with uncoated HSS tools except when very tight size tolerance or surface finish should be obtained. But for most non-free-machining steels, the BUE is generally undesirable. Since too large a BUE is also undesirable, cutting conditions should be selected so as to produce a small and stable BUE.

Therefore, as Shaw (1991) states, BUE has opposing actions relative to tool wear. The rough particles of hard highly worked BUE passing off with the chip tend to increase abrasive wear while BUE actually protects the cutting edge from wear. On the other hand, cutting with a large undesirable BUE always give rise to a substantial increase in surface roughness.

When cutting mild steel, aluminium and other ductile materials under certain conditions; at relatively low speeds and feeds, Bandyopadhyay (1984) states that BUE often appears on the tool as seen in figure 2.18. Under these conditions the friction between the chip and the tool is so great that the chip material welds itself to the tool face.

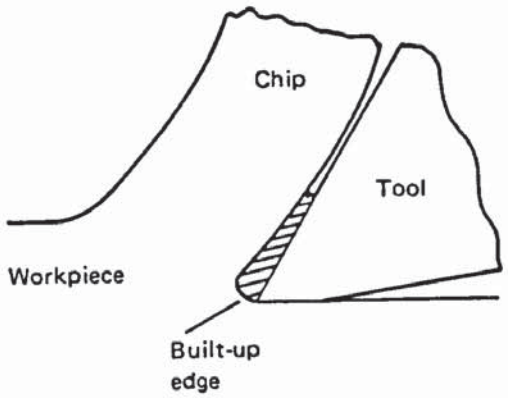

Figure 2.18 Built-up edge on Tool (Boothroyd et al. 1989)

It is well known that BUE has a large effect on surface roughness. The top of the BUE is only semi-stable and this Boothroyd et al. (1989) argue, leads to the formation of scales on the workpiece surface. Increasing of speed or feed result in an increase in the temperature on the tool face. At low speeds increases in tool-face temperatures tend to reduce friction at the chip-tool interface and hence tend to prevent the formation of a BUE; at high speeds increases in tool-face temperatures tend to increase the rate of crater wear.

At very low cutting speeds the interface is contaminated with oxide, oil, air, etc. and the metal machined behaves in a brittle manner as the primary shear plane exhibits low compressive stress, the chips produced are often discontinuous and slide easily along the rake face with low forces which encourages segmentation. Discontinuous chip formation results in irregular variation in tool forces. Workpieces machined under these conditions show relatively smooth areas where cutting has occurred and fractured areas. In the fractured areas segments of the work material have been removed from the surface leaving cavities. At higher speeds the contaminated layer is removed and bonding of the chip to the tool can take place and a BUE may form.

As previously stated at low cutting speeds the tool intermittently cuts and fractures the chip from the bar and hence a surface containing a fracture and cut component exits. As the speed increases the temperature generated by shearing is such that the cracking becomes shortened, ductility increases chip to tool contact and compression minimises cracking. Smaller areas of fracture are left with the material.

At higher speeds the surface layer of the tool is cleaned and the bonding forces are high. These conditions give rise to a continuous chip. Continuous chip is formed by steady plastic deformation in the primary shear zone. Increasing speed gives rise to eventually no BUE formation.

It appears that the initial form of BUE is very important in controlling machinability throughout the whole machining operation. For example, Yaguchi (1988) states that groove wear proceeds at the same location; it is rare that groove wear is covered by a new BUE in the middle of machining.

2.4.3 Relationship between Surface Roughness and Wear

Surface roughness (SR) is an important measure of quality in metal cutting. Yang et al. (1994) argue that the surface roughness is caused by the fact that the tool generates its shape into the surface. Boothroyd et al. (1989) explain that the final SR obtained during a practical machining operation may be considered as the sum of two independent effects:

i) The 'ideal' SR, which is a result of the geometry of the tool and the feed or feed speed. This represents the best possible finish that may be obtained for a given tool shape and feed and can be approached only if BUE, chatter, inaccuracies in machine-tool movement, and so on, are eliminated. Practical cutting tools are usually provided with a rounded corner, and figure 2.19 shows the surface produced by such a tool under ideal conditions (Boothroyd et al. 1989).

ii) The 'natural' SR, which is a result of the irregularities in the cutting operation. Usually it is not possible to achieve conditions such as those in (i) in practice, and normally the natural SR forms a large proportion of the actual roughness. One of the main factors contributing to natural SR is the occurrence of a BUE. The BUE may be continually building up and breaking down, the fractured particles being carried away on the undersurface of the chip and on the new working surface. Thus, it would be expected

that the larger the BUE, the rougher would be the surface produced, and factors tending to reduce chip-tool friction and to eliminate or reduce the BUE would give improved surface finish.

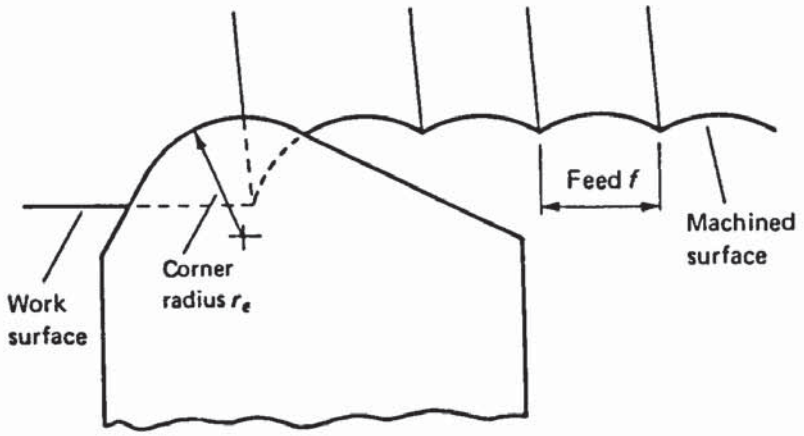

Figure 2.19 Idealised model of surface roughness for a tool with a rounded corner, where r_ε is the corner radius (Boothroyd et al. 1989)

Factors tending to reduce or eliminate BUE giving improved surface finish include increase in cutting speed and feed rate, the introduction of free machining materials such as leaded or resulphurised steels, the application of the correct cutting lubricant at low cutting speeds, etc. In 1957, Nakayama, according to Trent (1988) suggested that sulphur greatly improves the surface finish at low cutting speeds but causes a slightly poorer finish at high speeds, therefore, due to this sulphur tends to cause an unusually stable BUE. The change in SR, Yang et al. (1994) argue is primarily caused by cutting tool flank wear.

The SR obtained in lathe turning, aside from being dependent on workpiece material and hardness, is influenced by tool material and its relation to speed and feed rate, by tool design (particularly tool nose radius), by the rigidity of the machine tool and the tool, and Field et al. (1989) argue, by the type and effectiveness of cutting fluid used. It is found that the harder the tool material, the lower the SR.

The most commonly used measuring technique for SR, according to Boothroyd et al. (1989), employs a mechanical-electronic device where the read out shows the roughness of the surface profile taken during the passage of a small radius stylus over a short straight line path on the surface.

Goller et al. (1995) state that the SR produced by a turning tool is influenced by a number of factors and is therefore difficult to predict in practice. The roughness of the machined surfaces depends on the progressive changes which take place on the tool peripheral surface. This, in turn, depends on the wear resistance of the tool materials. Komaraiah et al. (1993) found that the harder the tool material, the lower the SR. According to Wada et al. (1980) it is expected that the finished SR of the workpiece may be greatly affected, if some wear occurs on the cutting edge. Yang et al. (1994) state that the change in SR is primarily caused by cutting tool flank wear. According to Selvam et al. (1974) that one of the parameters affecting SR is that crater wear on the rake face mainly affects the life of the tool but grooving wear modifies the profile of the nose radius.

Matsumura et al. (1993) have suggested that when considering tool wear and surface roughness simultaneously, machining operations are optimised to minimise cost by predicting flank wear analytically based on metal cutting theory and by predicting surface roughness with a neural network. Therefore, flank wear considering initial wear, and surface roughness considering tool wear can be predicted through adaptive prediction.

Wilkinson et al. (1997) argue that the precision and surface profile of the machined profile of the machined surface are key indicators of tool wear, so that any cutting tool wear monitoring system should have a surface parameter as part of the input.

2.4.4 The Influence of Lubrication upon Wear

Metal cutting involve a complex set of operating parameters, and the choice and effectiveness of cutting fluid is determined by several factors relating to the machine tool, operating conditions, cutting tool, surface coating, and workpiece.

When properly applied, cutting fluids can increase productivity and reduce costs by making possible the use of higher cutting speeds, higher feed rates, and greater depths of cut. The effective application of cutting fluids can also lengthen tool life, decrease surface roughness, increase dimensional accuracy, and decrease the amount of power consumed as compared to cutting dry. Trent (1991) states that improved surface finish is a major objective of cutting lubricants. In this respect they are particularly effective at rather low cutting speed and feed rates in the presence of a BUE. Reduction in the size of BUE causes great improvements in surface finish.

Cutting fluids are applied to the chip formation zone to improve the cutting conditions (compared to dry conditions). These improvements can take several forms, depending on the tool and work materials, the cutting fluid, and to a large extent the cutting fluid can act as a coolant and as a lubricant.

According to Boothroyd et al. (1989), quantitative information on the effect of a coolant on cutting-tool life has been obtained mainly from drill life tests; these tests clearly demonstrated improvements in drill life owing to the application of a coolant. It seems most likely that these improvements are caused by some reduction in temperature in the region of the drill point, but work on cutting temperatures suggests that the heat losses from the exposed surface of the tool and workpiece have quite a small effect on the temperatures in the region of the tool cutting edge. It can only be assumed, therefore, that the tool-wear rate is extremely sensitive to the small changes in temperature in the region of the wearing surfaces that result from the application of a coolant.

The function of cutting fluid in lathe turning according to Field et al. (1989), is to cool workpieces and tools, to cool and flush away chips, to promote cutting action by

minimising adherence of tool and workpiece, and to protect the workpiece from corrosion.

In high speed cutting operations, the cooling provided by the cutting fluid is its most important function. At moderate cutting speeds Li et al. (1995) argue, both cooling and lubrication are important, but at low speeds, lubrication becomes the dominant function of a cutting fluid.

In cutting metals, Hong et al. (1993) state, a shearing action between workpiece and tool generates a heat due to a plastic flow in the chip and a friction between the surfaces which may cause a continuous build-up of welded debris and reduce the efficiency of the operation. Therefore, cutting fluids are used to remove the frictional heat. Also, cutting fluids must function under boundary lubrication by a chemical reaction between fluid and workpiece surface to prevent welding of metal debris to the tool edge.

Boothroyd et al. (1989) argue that under certain conditions the application of a lubricant to the cutting process can result in a reduction in friction on the tool face; this friction reduction on the tool face can cause a reduction in power consumption, an increase in tool life, and, most important, an improvement in the surface finish of the machined component by reducing the occurrence of a BUE.

Boothroyd et al. (1989) argue that the extremely high pressures existing in the region of the chip-tool interface during machining do not allow complete hydrodynamic lubrication, where the chip and tool would be separated by a thin film of fluid. Indeed, it has been known for some time that the lubricating action of cutting fluids is mainly of a chemical nature. For example, the lubricating effect of carbon tetrachloride (CCl_4) when copper is machined; at low cutting speeds friction at the chip-tool interface is reduced considerably by the application of the fluid.

It has been shown, by Boothroyd et al (1989), that this effect results from the formation of a low-shear-strength film of copper chloride at the chip-tool interface, which acts as a boundary lubricant, preventing, to a large extent intimate metallic contact between chip

and tool. Under dry cutting conditions the intimate contact between chip and tool results in an extensive secondary deformation zone that has the appearance of a stable BUE. The effect of the lubricant is to reduce the intimacy of chip-tool contact, thereby eliminating the BUE and secondary deformation causes a reduction in friction at the chip-tool interface, reducing the forces required to form the chip.

According to Koelsch (1993) the coolant is part of chip control, and chip breakage improves as the tool wears. It is also argued by DeVries et al. (1994) that controlling wear at the cutting edge, and the temperatures that the part experiences, are the main purposes of a fluid.

The wear mechanisms of a 3Y-TZP ceramics/GCr15 steel reciprocating sliding couple have been investigated as a function of sliding speed and normal load under water lubrication. Liu et al. (1996) found that the dominant wear mechanism of 3Y-TZP ceramics under mild wear conditions is plastic deformation, whereas under severe wear conditions it is surface fracture. In the transition region, 3Y-ZTP ceramics undergo microploughing and microcracking. The mild and severe wear mechanisms of GCr15 steel are plastic deformation and abrasive wear, respectively. Water lubrication can reduce the friction coefficient of the 3Y-TZP/GCr15 sliding couple. Under certain sliding conditions, water lubrication can improve the wear resistance of 3Y-TZP ceramics, but over a certain criterion, water lubrication would cause deterioration of the wear resistance of 3Y-TZP ceramics.

2.5 CONCLUSION

The above survey has looked at all the influencing factors influencing wear in cutting. From this, it can therefore be seen that in metal cutting there are many factors that need to be taken into consideration when machining. This research investigated various aspects of the two operations.

The survey took a detailed and historical look at the tool material, but tests in this work focused on HSS. This was partly chosen due to the intention of this work to look at the comparability between the single point turning and drilling operations, and to investigate the possibility of using simple turning tests to examine the state of the drilling operation, and since drills in the main are made in HSS, it was convenient to conduct the tests in HSS.

This work also looked at such parameters as the cutting speed and their influence on cutting temperature, and in turn, how the temperature itself has effects on many factors such as wear mechanisms, tool geometry, forces and so on. These will be discussed in more detail throughout the work and in chapter 8 which specifically discusses temperature. Also it will be shown that forces are of great importance and how they are affected by temperature and other factors. These can be seen in chapters 6 and 7.

In terms of prediction theories, tool wear prediction theories are discussed in chapter 3 and these can be related to the force prediction models in turning and drilling in chapters 9 and 10 where it is attempted to replicate and extrapolate an existing force prediction theory to the results of this work. This will highlight issues discussed in the above chapter relating to tool geometry, temperature, wear mechanisms and others.

Chapter 3

WEAR PREDICTION MODELS

3.1 INTRODUCTION

This chapter is divided into two sections which examine tool life equations. The first section looks at tool life equations in relation to single point turning, and the second section examines the tool life equations in relation to the drilling operation. Before examining the tool life equations in single point turning and drilling, it is important to note some of the important differences and similarities between the two.

The differences between the single point turning and the drilling include:
- variable cutting geometry in the drill,
- variable cutting speed across the drill,
- difference in the heat sink capacity ratio between tool and workpiece in drilling as opposed to turning.

The similarities between the single point turning and drilling include:
- similarity of drill outer corner and turning nose wear as a criteria for failure,
- same kinds of wear mechanisms.

Tool life equations, like other areas in this study where drilling is concerned, has not been investigated by many researchers and therefore much fewer equations are considered in drilling, as will be explained in more detail in chapter 5. A selection of investigations has been looked at that included equations about tool life and wear that relate to different conditions.

Since tool life has a strong economic impact in production operations, the development of quantitative methods for predicting tool life has long been a goal of metal cutting research. The need for accurate assessment of tool life has increased considerably with the development of numerically controlled machine tools and optimisation procedures.

The general trend has been the development of equations relating tool life to the machining variables involved.

Barrow (1972) states that when considering the validity of tool life equations it should be remembered that they are all empirical in nature. It is therefore impossible to make any ordered decision that a particular equation is valid for all cutting conditions.

3.2 SINGLE POINT TURNING

3.2.1 Tool Life Criteria

Before considering the form of tool life equations it is important that the end of the life of a cutting tool is specified. It is proposed in ISO 3685 (1993) that the time at which a tool ceases to produce workpieces of the desired size and surface quality usually determines the end of useful tool life. However, the reasons for which tools may be considered to have reached the end of useful life will be different in each case depending upon, for example, cutting conditions, the material combinations used, etc.

Barrow (1972) suggests that a tool may reach the end of its useful life by any of the following modes:

1- clearance or flank face wear,

2- rake face or crater wear,

3- plastic deformation of the cutting edge,

4- thermal cracking and mechanical chipping of the cutting edge.

Tool failure in the case of 3 and 4 is generally catastrophic in nature and should be avoided. Therefore, it is normal to consider tool life in terms of flank or crater wear. In many cases thermal deformation of a mild form does not lead to immediate tool failure, but accelerates the rate of flank wear.

Because catastrophic tool failures should be avoided, it is essential that certain limits on wear should be stipulated. ISO (1993) recommends the following common criteria (see figure 5.1 in chapter 5):

Carbide Tools

- Maximum width of the flank wear land (if flank wear is not regularly worn in zone B) - VB_B max = 0.6 mm.
- Average width of the flank wear land (if flank wear is considered to be worn in zone B) - VB_B = 0.3 mm.
- The depth of the crater KT given by the formula: $KT = 0.06 + 0.3f$ where f is the feed/mm per revolution.
- The crater front distance reduces to a value of KF = 0.02 mm.
- The crater breaks through at the minor cutting edge, causing a poor finish of the machined surface.

Ceramic Tools

- Maximum width of the flank wear land (if flank wear is not regularly worn in zone B) - VB_B max = 0.6 mm.
- Average width of the flank wear land (if flank wear is considered to be worn in zone B) - VB_B = 0.3 mm.

High Speed Steel

- Maximum width of the flank wear land (if flank wear is not regularly worn in zone B) - VB_B max = 0.6 mm.
- Average width of the flank wear land (if flank wear is considered to be worn in zone B) - VB_B = 0.3 mm.
- Catastrophic failure.

Complete failure of HSS is particularly recommended for cases in which material build-up on the tool makes measurement very difficult. Although the failure of tools by crater wear does occur, provided the correct tool material is used, failure by flank wear is usual. In view of this, Barrow (1972) states that the tool-life equations are usually developed using a flank-wear criterion.

3.2.2 Tool Life Estimation

Tool life estimation is an important factor in all machining operations. Tool life equations were determined experimentally as early as 1907 by Taylor (1907). Since then numerous investigations have been carried out to determine the tool life as a function of cutting conditions, and the type of workpiece materials. Aside from the problem of experimentally determining the parameters in these equations, El-Wardany et al. (1997) point that there are inherent variations in tool life for a given set of machining conditions.

Koren et al. (1984) presented a series of state models for flank wear in metal cutting which are potentially useful for on-line estimation or control. These models will be discussed later in the chapter. They argued that tool wear measurement, and prediction, is potentially useful for scheduling tool changes and for adaptive control. Numerous techniques have been proposed and investigated for tool wear measurement. No practical direct measurement methods are currently available, and indirect methods rely on relationships between tool wear and other process variables such as temperature, force, tool vibration, or acoustic emissions.

It is postulated by Koren et al. (1984), that the state of wear of a cutting tool is one of several state variables which characterise the state of a metal cutting process. Koren et al. (1984) contend that tool wear, however, is not directly measurable in a practical on-line manner and thus outline an approach to estimate or observe the state of wear of a cutting tool from a measurement of an output variable such as cutting force. This approach relies on the availability of a model of the metal cutting process which can provide quantitative relationships between input, state, and output variables.

3.2.2.1 Taylor

The oldest and simplest tool life equation, and best known, is the Taylor Equation.

$VT^n = C$

where V is the cutting speed (ft/min); T is the tool life (min); C is a constant, dependent on cutting conditions; n is the exponential constant, dependent on cutting conditions.

It expresses the relationship between the cutting speed and tool life in terms of two constants (n and C) that are functions of the cutting conditions involving a particular tool material machining a specific work material. The exponent n determines the slope of the tool life curve and depends primarily on the tool material.

Typical values according to Stephenson et al. (1997) are as follows:
0.1 - 0.17 for HSS tools
0.2 - 0.25 for uncoated WC tools
0.3 for TiC or TiN WC tools
0.4 for Al_2O_3 coated WC tools
0.4 - 0.6 for solid ceramic tools

The constant C varies widely with the tool material, work material, and tool geometry.

Rubenstein (1976) argues that attention has often been directed to the fact that there are many occasions when a log V-log T does not produce a straight line (as required if the Taylor law is obeyed) but a curve. Barrow (1972) has listed four conditions most likely to lead to deviations from Taylor's law. These include the machining of high-strength, thermally resistant workpieces, machining under conditions leading to long tool lives, at high rates of metal removal and in finish turning conditions.

There are many cases in which these general rules are contradicted. But, until the mechanism of tool wear is more fully understood, it is impossible to define clearly the conditions in which a Taylor equations with constant n applies. These general rules do,

however, indicate the conditions in which extreme care in determining tool life is advisable and indicate the dangers of extrapolating tool-life curves.

Linearity of the logV-log-T lines can be directly related to the predominant wear mechanism i.e., abrasion wear mechanism usually is linear and diffusion wear mechanism is usually non-linear.

The Taylor equation seems to be reasonably valid as Barrow (1972) notices when machining carbon and low alloy steels with all types of tool material in semi-roughing conditions (depth of cut 0.050 - 0.150 in (1.27 - 3.81 mm) and feeds of less than 0.020 in (0.508 mm)) when cutting with speeds to give a tool life of between 10 and 50 min. Barrow (1972) stated that when using carbide throw-away tools, one is chiefly interested in tool lives of 10-50 min, because it is in this region that optimum economic conditions are approached. An exception to this is in the case of transfer lines, where it is usual to change tools at half or full shift intervals (that is, tool lives of 240 min and more). This is usually the region of maximum curvature and extrapolation of a Taylor curve into this region can give considerable errors.

Kronenberg (1970) has proposed a straightening factor, K_S, which was a constant and could be added to the tool life or the cutting speed which straightened the curved log T-log V plot. The factor was normally added to the cutting speed and re-plotting the results in the form

$$(V \pm K_s)T^{n_1} = (C \pm K_s)$$

The curvature of the original data determines whether the straightening factor is added or subtracted. Kronenberg used trial and error methods to determine K_S and checked his guess by the equation

$$n_1 = \frac{\log\left[V_2 + (k_s / V_1) + K_s\right]}{\log(T_1 / T_2)}$$

Taylor's equation only relates cutting speed to tool life for a particular tool-workpiece combination, and does not consider other cutting variables and tool geometry.

To connect tool life with several variables, Taylor derived the equation

$$VT = \frac{C_1\left[1-8/7(32r_\varepsilon)^2\right]}{\left\{S^{2/5}+5+(2.12/32r_\varepsilon)(48a/32r_\varepsilon)^{2/15}+0.16(32r_\varepsilon)^{1/2}+0.8(32r_\varepsilon)/\left[6(32r_\varepsilon)+48a\right]\right\}}$$

where V_T is the cutting speed (mm/min) for tool life T, S is the feed, a is the depth of cut, r_ε is the tool nose radius, and C_1 is a constant.

This equation includes the important variables, feed and depth of cut, although Taylor considered that feed and depth of cut could not be combined into a single variable. But Kronenberg used the data obtained by Taylor and found that in most cases the area of cut ($S.\ a$) could be used as a single variable. By plotting data in the form of log V_T-log A, he developed the relationship

$$V_T = \frac{C_2}{(1000A)^z}$$

where C_2 is a constant, that is the cutting speed for an area of cut of 0.001 in^2, A is the area of cut and z the slope of the *log* V_T-log A plot.

Combined with Taylor's relationship $VT^n = C$ the above equation becomes

$$VT^n = \frac{60^n C_2}{(1000A)^z}$$

A shape effect was introduced by considering the slenderness ratio $G=a/S$, so that

$$VT^n = \frac{C_2(G/5)^u 60^n}{(1000A)^z}$$

where u is a constant and the term G/5 relates G to an average value of G which Kronenberg considered to be 5.

Although the above equation considers both feed and depth of cut, the nose radius is not taken into account. Thus, the equation omits a relatively important variable and is felt to be inferior to equations using the concept of 'chip equivalent' which is discussed later in the chapter.

3.2.2.2 Extended Taylor Equation

According to Stephenson et al. (1997), Taylor's equation reflects the dominant influence of the cutting speed on tool life, but does not account for the smaller but significant effects of the feed rate and the depth of cut. For this reason, a modified version of Taylor's equation, called the 'extended Taylor equation' is often used:

$$VT^n f^a d^b = K_t$$

Stephenson et al. (1997) state that for HSS tools, typical values of n, a, and b are 0.17, 0.77 and 0.37 respectively when T is given in minutes, V in ft/min, and d and f in inches. K_t varies considerably with the rake angle of the tool, but is typically 500 for mild steels and 200 for cast iron. The extended Taylor equation treats the influences of the feed rate and depth of cut independently.

Barrow (1972) argues that although Taylor connected tool life with cutting speed, feed and depth of cut in separate equations but never attempted to combine them together. He states that this is now done regularly.

$$T = \frac{C_3}{V^{1/\alpha} S^{1/\beta} a^{1/\gamma}}$$

C_3, α, β, and γ being constant.

This equation is used extensively but it omits tool geometry and assumes that the exponents α, β, and γ are constant. As in the simple Taylor equation this is not generally so and large errors can occur. Barrow (1972) argues that provided α, β and γ are reasonably constant, the above equation is quite useful, but the evaluation of α, β, γ, and C_3 is, however, quite laborious as at least 3 sets of tests involving fifteen tool-life values are required.

Taylor's equation has been applied in the determination of optimum conditions in machining economics. However, Nagasaka et al. (1982) state that when surface roughness is one of the constraints in the machining process, it must be represented as a function of the amount of tool wear, and when the conditions vary in cutting something such as a stepped part, tool life equations are needed in which the amount of tool wear is considered. To obtain such equations, a multiplication model (a modified form of Taylor's equation) and a polynomial model are presented by Nagasaka et al. (1982). These models agree with the wear process which involves gradual or little wear after rapid initial wear, but there is disagreement between observations and the model equations at the third stage of the wear process which consists of very rapid or catastrophic wear.

A tool life equation is proposed which describes the 3 stages of the wear process (as shown in figure 2.9 in chapter 2) with a single mathematical model. The model is compared with multiplication and polynomial models. The sensitivity of the analysis of the model is considered by Nagasaka et al. (1982) by investigating the effect of variation in the parameters on its accuracy.

There is a general relation between the cutting time t and the flank wear V_B when cutting conditions are constant. That is, the wear process follows three stages: rapid initial wear which is followed by gradual or little wear and finally very rapid or catastrophic wear as the cutting time increases. If it is assumed that the wear process curve approximates to a curve having asymptote $t = T_o$ then the relationship between V_B and t is given by

$$t = T_0 \exp\left\{-\exp(b) V_B^{\,n}\right\} \qquad n < 0 \qquad \text{Eq 1}$$

where b and n are constants and T_0 is designated as the critical cutting time. In equation 1 , if T_0 is a function of the cutting conditions,

$$T_0 = a V^{n_1} f^{n_2} \qquad \text{Eq 2}$$

where a, n_1 and n_2 are constants, V is the cutting velocity and f is the feed rate. The depth of cut is not taken into account because its effect on tool life is almost negligible. By substituting equation 2 in equation 1, equation 3 is obtained:

$$t = a V^{n_1} f^{n_2} \exp\left\{-\exp(b) V_B^{\,n}\right\} \qquad \text{Eq 3}$$

Substitution of the appropriate value of V_B as the tool life criterion in eq 3 yields the ordinary Taylor equation.

The multiplication model is a modified form of Taylor's equation:

$$t = a_0 V^{a_1} f^{a_2} V_B^{a_3} \qquad \text{Eq 4}$$

where a_0, a_1, a_2 and a_3 are constant. The polynomial model can be obtained by a stepwise regression procedure. The contribution of each term in the second order polynomial is calculated in terms of cutting velocity, feed and amount of flank wear after logarithmic transformation and removal from the model of any term which provides a non-significant contribution. The parameters of the two models are estimated with the same data as in the proposed model.

According to Nagasaka et al. (1982), that for practical applications of the tool life equation to analytical methods such as the determination of economically optimum cutting conditions, the polynomial model is of no practical use because of its complexity. The multiplication model is intended for practical use, e.g. to optimise cutting processes. The proposed model is similar in form to the multiplication model, which indicates the utility of the proposed model.

Improvements in cutting tool performance are usually achieved either through modifications to the tool material properties or by the use of suitable tool geometries. Tool material and geometry are normally considered as dependent variables since using the correct geometry allows harder, more brittle tool materials with improvements in the cutting conditions, whilst the selection of a particular tool material places restrictions on the geometry that can be used.

An analysis, by Rubenstein in 1976 (Lau et al. 1978), of tool life based on flank face wear was performed in which Taylor's tool life equation was obtained theoretically and an expression for the Taylor constant, C, was derived. For a given workpiece material, a given tool material, a given flank wear criterion, a given feed and a given depth of cut, this expression reduces to a relation of the form,

$$C \propto \left\{ (\cot\beta - \tan\alpha)^n K^{1/\varepsilon} \right\}^{-1} \qquad \text{Eq 1}$$

where, β is the clearance angle of the tool, α is the rake angle of the tool, n is the Taylor exponent for the particular tool/workpiece combination at the selected cutting conditions, and K is the constant appearing in the equation.

$$\theta_f = K(H_m)^{\rho} V^{\varepsilon} f^{n} l_f^{\delta} W^{\gamma} \qquad \text{Eq 2}$$

relating the flank face temperature, θ_f, to the workpiece hardness, H_m, the cutting speed, V, the feed, f, the depth of cut, W and the wearland l_f.

For a chosen tool/workpiece combination, a fixed cutting edge radius and a given cutting medium, K is a function of the rake angle, α, and of the clearance angle, β, i.e. K may be expressed as $F(\alpha, \beta)$ so that equation 1 may be rewritten

$$C \propto \left\{ (\cot\beta - \tan\alpha)^n F(\alpha,\beta)^{1/\varepsilon} \right\}^{-1} \qquad \text{Eq 3}$$

Subsequently, the theoretical deductions obtained by Rubenstein in 1976 (Lau et al. 1978) were compared, where possible, with published experimental data when it was found that although a certain amount of evidence concerning the influence of tool geometry on tool life exists (Lau et al. 1978), a search of the literature failed to reveal any measurements of the variation of the Taylor constant, C, with different tool geometries. Accordingly, Lau et al. (1978) decided to attempt to determine to what extent experimentally obtained data conform to equation 3 - a task seriously complicated by the fact that they are ignorant of the form of the function $F(\alpha, \beta)$.

Clearly, Lau et al. (1978) suggest that the way to minimise the consequences of this ignorance is to seek experimental conditions within which α and/or β produces minimal change in $F(\alpha,\beta)^{1/\varepsilon}$. (It was found that in the low speed range, $1/\varepsilon$ is smaller than in the high speed range. Accordingly, the effect of a change in $F(\alpha,\beta)^{1/\varepsilon}$ will be less if experiments are performed in a low rather than in a high speed range).

It was then noted by Lau et al. (1978) that equation 2 has been obtained from a knowledge of the factors influencing the mean workpiece/tool thermocouple temperature, θ, and by making the assumption that $\theta_f = k\theta_m$, i.e. the coefficient k is incorporated in the coefficient K. k will be a function of the tool geometry and it maybe argued that k will be more sensitive to changes in the rake angle than to changes in the clearance angle as follows. For a fixed rake angle, θ_f and θ_m will both decrease as the clearance angle increases. On the other hand, they argue that with a fixed clearance angle, a change in rake angle will affect θ_f much less than it will affect θ_m. Accordingly, it may be expected that in order to minimise the change in $F(\alpha,\beta)^{1/\varepsilon}$, the range of variation of the rake angle should be limited in relation to the range within which the clearance angle is varied.

Finally, Lau et al. (1978) argued that suppose that cutting were to be performed in the presence of an infinitely efficient cutting fluid. Then, in such an ideal case, the tool temperature would remain constant (at the room temperature value) i.e. the indices p, ε, n, δ and γ would be zero and, more to the point, K and hence $F(\alpha,\beta)$ would be

constant. Hence, it may be concluded that cutting in the presence of an efficient cutting fluid would help to minimise the change in $F(\alpha,\beta)$ as α and/or β are varied.

The experiments were planned and carried out by Lau et al. (1978) on the basis of these considerations: Work material is annealed mild steel tubes (50.8 mm o.d., 2 mm wall thickness), feed is constant at 0.10 mm/rev, Tool material is MTM 41 HSS (throw away tips), and average flank wear land is 0.18 mm.

In orthogonal cutting of mild steel by HSS, it was concluded that:

1- the Taylor constant, *C*, increases as the included angle of the tool decreases.

2- The values of the Taylor exponent usually quoted for HSS i.e. 0.1-0.2 appear to be appropriate only to cutting conditions leading to relatively low cutting tool temperatures. At speeds above *ca.* 55 m/min, the value of *n* is *ca* 0.44 in air and is somewhat lower in the presence of a coolant fluid.

3- With respect to changes in the clearance angle when the rake angle is constant, $C \propto (\cot\beta - \tan\alpha)^{-m}$ where $m \cong n$ only at low cutting speeds when cutting in air but even at high cutting speeds when cutting in the presence of a cutting fluid when cutting at high speeds in air $m \neq n$.

4- With respect to changes in the rake angle when the clearance angle is constant, $C \propto (\cot\beta - \tan\alpha)^{-m}$ where $m \cong n$ only when cutting in the presence of a cutting fluid. When cutting in air, the values of *C* deviate significantly from this relation.

5- When cutting at conditions such that $\{F(\alpha,\beta)\}^{1/\varepsilon}$ is constant i.e. when $C \propto (\cot\beta - \tan\alpha)^{-n}$, it can be seen that in the practical range of geometries, i.e. $\alpha \approx 12^{\circ}, \beta \approx 8^{\circ}$, the tool life for a given included tool angle, say 65°, will be greater if the clearance angle is increased by 5° than if the rake angle is increased by 5°. There it can be seen that reducing the included angle by 20° by reducing the rake angle from -10° to +10° causes C to increase from 67 to 78 i.e. a 17% increase. A reduction in the included angle of 18° (obtained by increasing the clearance angle from 2 to 20°) on the other hand causes *C* to increase from 70 to 105 i.e. a 50% increase in *C*.

In a later paper, Lau et al. (1982) tested MTM 41 HSS cutting tool using DF 2 cold worked steel, low carbon steel and mild steel. They argue that although the influence of rake angle and of clearance angle on the mechanics of metal cutting has been established, the effect of the plan approach (side cutting) angle *Cs* has been ignored. They argue that changing the side cutting angle results in an increase in tool life.

For a given tool life criterion, the tool life can be related to the uncut chip dimensions by an expression of the form of the extended Taylor tool life equation:

$$VT^n t_1^a W^b = C$$

where C is constant for a given tool/workpiece combination and for given tool geometry. At a given cutting speed,

$$Tt_1^{a/n} W^{b/n} = (K_1)^{1/n} = K \qquad \text{(a constant)}$$

Let *Ts* be the tool life when the plan approach angle is *Cs*, then $T_s(f\cos C_s)^{a/n}(B\sec C_s)^{b/n} = K = T_0 f^{a/n} B^{b/n}$, where T_0 is the tool life when $C_s = 0$

Hence,

$$T_s = T_0(\sec\ C_s)^{(a-b)/n}$$

Now empirically it is found that $a > b$ hence $(a-b)/n$ is positive whence it follows that as C_s increases, so does the tool life.

3.2.2.3 Chip-Equivalent Concept

In the 1930s Woxen (Barrow 1972) proposed a method utilising the chip equivalent method. This related tool life to cutting temperature. The chip equivalent is defined as:

$$q = L / A \ in^{-1}$$

He showed that cutting temperature was a direct function of the chip equivalent, q, for a given cutting speed and tool-workpiece combination, where L is the length of the tool edge and A is the area of cut:

In some cases the inverse of the chip equivalent is used and is called the equivalent-chip thickness, h_e

Barrow (1972) stated that the proposal by Woxen that temperature is a function of chip equivalent has been substantiated by several workers using tool-work thermocouple techniques. Woxen assumed that the conditions resulting in constant temperature also resulted in a constant tool life. He proposed the tool-life equation:

$$V_T = G_T(q_o + q)$$

These plots tended not to be linear and a factor $(1/1 + gq)$ was introduced to account for this fact and he amended his equation to,

$$V_T = G_T\left(\frac{q_o + q}{1 + gq}\right)$$

where g is a constant.

Tool life T was introduced as a separate factor and it gave the following equation:

$$V = \left(\frac{T_x}{T}\right)^{\alpha} G_s\left(\frac{q_o + q}{1 + gq}\right)$$

where T_x is a certain tool life, say 30 min, and G_s is a constant, dependent on the work and tool materials and is related to T_x.

This assumed that the Taylor equation was generally valid. Woxen recognised that the Taylor exponent, α, could vary and added a further term to overcome this difficulty, thus

$$V = \left[\left(\frac{T_x}{T}\right)^{\alpha} + g_1 T\right] G_s \left(\frac{q_o + q}{1 + gq}\right)$$

where g_1 is a constant.

Although the equations are valid over a wide range of cutting conditions, they are rather complex and difficult to use. The complexity of the equations is mainly because of non-linearities and if log V_T is plotted against log q then the plot is often linear and the equation can be simplified to:

$$VT = Jq^{j}$$

where J and j are constants

The above equation can be expanded to include tool life as a separate term, resulting in

$$VT^{\alpha} = C_4 q^{j} \qquad \text{or} \qquad VT^{\alpha} q^{\delta} = C_4$$

Colding, and Brewer and Rueda (Barrow 1972) used relationships of the form of the above equation and showed that the exponents α and δ are not necessarily constant. Using dimensional analysis, Colding (Barrow 1972) proposed an equation of the form

$$K + aX + bY^2 + cY + dY^2 + eZ^2 - Z + fXY + gYZ + hXZ = 0$$

where $X = \log q$, $Y = \log V$, and $Z = \log T$, and a, b, c, d, e, f, g, and h are constants.

Barrow (1972) states that the above equation is valid over a wide range of cutting conditions, and can cope with tool-life curves with considerable curvature, but the evaluation of the constants to a reasonable accuracy requires at least twelve tool-life points.

Konig and Depiereux (Barrow 1972) developed an equation to accommodate non-linearities in the log T-log V and log T-log S plots. The equation formed is:

$$T = \exp\left(\frac{-K_V}{m} V^m - \frac{i_S}{n} S^n + C\right)$$

If the slope of the log T-log V curve is constant the equation is modified to

$$T \exp\left(\frac{-i_S}{n} S^n + C\right) V^{-K}$$

This technique is useful as it only requires five points in order to predict the tool-life curves.

Carlsson (1992) produced a statistical model which uses ideas from the theory of reliability and statistical quality control. He uses it to implement a statistical optimisation of the cutting process by identification and prediction of the tool condition and lifetime. It is consistent with Taylor equation, therefore uses existing information about relations between cutting data and tool life.

The rate of removed material from the work piece increases with growing cutting speed and feed. The ideal situation from an economical point of view, he suggests, is therefore to use as high speed and feed as possible. However, as the life of the cutting tool is limited and becomes less, the more intensively the tool is stressed. For each occurrence of tool replacement, costs emerge for a new tool and for idle time. The relationship of tool wear and tool life to the cutting conditions, such as feed and speed, are therefore essential for the economical utilisation of the cutting process.

The classical formula interrelating those variables is the Taylor equation. Carlsson argues that Taylor's equation gives a rough estimate of the relationship between mean values, but does not take into account the extensive spread of the tool life. It must be remembered that there can be considerable variations of the Taylor equation constants from one tool and workpiece to another.

A criterion for optimisation of the cutting conditions Carlsson suggests, is the Colding productivity formula below. It is here represented by two variants, whereby the second takes into consideration variations of cutting data during the tool life.

$$P = \frac{h_e v T}{T + T_v}$$

$$P = \frac{\sum_{i=1}^{n} h_{ei} v_i t_i}{T_v + \sum_{i=1}^{n} t_i}$$

$$T = \sum_{i=1}^{n} t_i$$

$$h_e = \frac{af \sin K}{a - r(1 - \cos K)rK + f \sin K / 2}$$

where P is the productivity and T_v is the equivalent tool replacement time into which tool costs as well as idle time are included. The Woxen chip thickness h_e, according to Carlsson includes in one parameter feed (f), depth of cut (a), nose radius (r) and cutting angle (k).

To find the optimum productivity point, a variant of the Taylor equation is used, where α and m vary with speed v, and chip equivalent h_e (and thereby feed),

$$T = \frac{C_T}{V^{\alpha} h_e^m}$$

$$\alpha = \alpha(h_e, v)$$

$$m = m(h_e, v)$$

The above presented formulas give a general idea of the relationships between cutting data and tool wear. The experimental test that Carlsson carried out were for a number of purposes:

a- to confirm the validity and accuracy of the model.

b- to distinguish measurement errors from variation of wear.

c- to investigate the influence of variations of cutting data during the process.
d- to evaluate the feasibility of the control algorithm, using the results achieved in a-c.

To achieve reliable results, Carlsson argues, it is necessary to conduct large, and thereby time-consuming, test series. At first, constant cutting data were used during the tool life for different feeds. To achieve statistical variation, 5 tests were carried out for each feed. Secondly, the tests were repeated for the same feeds, but now varied during the tool life in all permutations of feeds, at intermissions as well as in process. Finally, the control algorithm was tested.

3.2.2.4 Further Equations

It was mentioned above that a series of state models for flank wear in metal cutting is presented by Koren et al. (1984). The simplest model considers only a speed input, a second model considers both speed and feed input, and a third model incorporates temperature effects. They used experimental data to determine typical parameters for the first model. All three models are limited by the various assumptions used in the derivations. Thus, their applicability is expected to be limited to certain specific cutting conditions. Refinements to the model can ease these restrictions, but will also complicate the model.

To develop a simple model, Koren et al (1984) assumed that cutting conditions are such that crater wear can be neglected and flank wear is selected as a state variable. It is further assumed that the flank wear versus time has the characteristic behaviour (as shown in figure 2.9 in chapter 2). That is an initial high wear rate is followed by an almost constant wear rate. The constant wear rate dominates from about T_o to T_f at which time the wear rate may increase abruptly as the tool fails. The time T_f can be considered to be useful life of the tool. Thus, it is assumed that over the useful life of the tool we can express,

$$w(t) = w_o + \left(\left(w_f - w_o\right) / T_f\right)t \qquad \text{Eq 1}$$

For a constant depth of cut a, and a constant feed f Taylor's tool life equation can be written as,

$$T_f v^n = c_1 \qquad \text{Eq 2}$$

where v is the cutting speed. The exponent n and the constant c_1 depend on the tool and workpiece materials. Combining equations 1 and 2 leads to,

$$w(t) = w_o + K_1 v^n t \qquad \text{Eq 3}$$

where it is defined,

$$K_1 = \left(w_f - w_o\right) / c_1 \qquad \text{Eq 4}$$

and assumed that K_1 and consequently w_o, w_f, and c_1 remain constant. With these assumptions one can differentiate equation 3 to obtain the state equation,

$$w(t) = K_1 v^n \qquad \text{Eq 5}$$

Based on experimental data, they represent for constant a and f the cutting force as a function of flank wear,

$$F = Fo + K_f w \qquad \text{Eq 6}$$

where F_o is the initial cutting force. Equation 6 incorporates the assumption that F as well as the parameters F_o and K_f are independent of the speed v over a practically useful range of cutting speeds. Equation 6 can be rewritten as,

$$\Delta F = F - F_o = k_f w \qquad \text{Eq 7}$$

Several extensions of this basic model is considered to increase the complexity of the model. Koren et al. (1984) first consider the effect of relaxing the constant feed assumption. When the feed f is not constant equation 2 can be replaced by the extended Taylor's tool life equation.

$$T_f v^n f^m = c_2 \qquad \text{Eq 8}$$

When f is not constant F_o in equation 6 can be expressed as,

$$F_o = a\left(k_S f^P - K_v v\right) \qquad \text{Eq 9}$$

K_f in equation 9 can depend on f. As stated by Koren et al. (1984), the appropriate selection of the cutting force component to be used as the output variable F can help to minimise the effects of v and f on K_f.

Next the influence of temperature is considered, which can be expected to be significant. Koren et al. (1984) use equation 10,

$$w(t) = K_2 v^n f^m \qquad \text{Eq 10}$$

together with the following empirical relationship

$$\theta = K_3 v^k f^l F \qquad \text{Eq 11}$$

where θ is temperature, and the constant K_3 and exponents k and l depend on material properties and the constant depth of cut a. This leads to

$$w = \left(K_2 / K_3\right) v^{n-k} f^{m-l} \theta F^{-1} \qquad \text{Eq 12}$$

and taking the natural logarithm of both sides as before gives,

$$\ln w = \ln K_2 - \ln K_3 + (n-K)\ln v + (m-l)\ln f + \ln\theta - \ln F \qquad \text{Eq 13}$$

Finally regarding crater wear and the proposed model. Koren et al. (1984) state that crater wear which has been neglected here can have a significant effect on the force levels as cutting proceeds. The effects of cratering become most pronounced at high speeds and are strongly dependent on the cutting speed. An important extension of the models that are presented here is to develop some approach to handling crater wear. Otherwise the models are limited to situations where flank wear is dominant.

A physical model of the flank wear, based on a feedback mechanism has been presented by Koren (1978). Two principal mechanisms were assumed as wear causes: a thermally activated one and a mechanically activated one.

The total wear occurring on the flank surface of the cutting tools is equal to the sum of the wear due to the separate effects of these mechanisms. The model yields a mathematical expression describing the wear land growth with time. Good agreement with practical data has been demonstrated by Koren (1978).

The parameters of the model can be evaluated directly from experimental wear curves with an additional measurement of the cutting force. As a consequence, the relative weight of the thermally and mechanically activated wear components is known (Koren (1978). The model yields the tool life as a function of the cutting speed, and provides a formula for the tool life which is not based on Taylor's equation.

$$T = \frac{C_o / K_3}{K_1'\left(e^{-\theta_a/273+\theta_a} \right) + K_2 v}$$

In addition the experimental results were fitted to the model providing estimations for the activation and the coefficient of the mechanically activated wear.

θ - constant - depending on the activation energy, K_3 - constant - speed dependent, K_1 & K_2 - parameters dependent on cutting speed as well as on the other cutting conditions, T - tool life, V - cutting speed, C_0 - parameter - speed dependent, and θ_a - Average value of temperature for a certain speed.

Takeyama et al. (1963) investigated tool wear and tool life from the viewpoint of flank wear. The mechanism of tool wear in turning can be classified into 2 basic types:
- Mechanical Abrasion - which is directly proportional to the cutting distance and independent of the temperature.
- Physicochemical type which is considered to be a rate process closely associated with the temperature. (Here there is a large probability that some components of the tool

material react chemically with the machining atmosphere, the cutting fluid, or the material cut).

Although it depends upon the cutting condition which type of wear plays a more important role, the latter is predominant under usual conditions.

According to the analyses and the experimental results, it has been found out that the tool life from the standpoint of flank wear can be predicted to a first approximation by the initial cutting temperature.

The physicochemical mechanism can be considered to be a sort of rate process, which greatly depends upon the temperature. According to Takeyama et al (1963) Trigger and Chao in 1956 applied such a concept to the crater wear of cemented carbide tools, and Ling in 1956 treated with the tool life of HSS tools, which is defined by the complete failure, on a similar basis after Schallbroch in 1938. Sata in 1959 also pointed out the close relationship between crater wear and cutting temperature experimentally.

Takeyama et al. (1963) extended the theory of rate process to the problem of flank wear. They argued that if the total amount of tool wear is assumed to be the addition of the terms due to brittle fracture, mechanical abrasion, physicochemical mechanism or rate process, and other mechanisms, if any, the equation of wear will be as follows:

$$W = W_b(n,\sigma_s) + W_a(L,\sigma_a) + W_r(\theta,T) + W_i \qquad \text{Eq 1}$$

Where W - total amount of wear, W_b - amount of wear due to brittle fracture, W_a - amount of wear due to mechanical abrasion, W_r - amount of wear due to 'rate' process, W_i - amount of wear due to other mechanisms.

These wear types are functions of the following:

σ_s - resistance against brittle fracture of tool material, σ_a - abrasion resistance of tool material, n - number of shocks, L - cutting distance, θ - absolute temperature at cutting edge, and T - cutting time

The concept of rate process could be extended even to the mechanical type of wear assuming that the probability for the fracture of wear to occur is proportional to the function $\exp\left[-\frac{Q}{K\theta}\right]$, where Q is the activation energy presumably affected by the temperature, K the constant, and θ the absolute cutting temperature.

However, in the paper the mechanical type of wear is differentiated from the physicochemical type in the sense that the former is independent of the temperature. In a continuous cutting such as turning under normal conditions, the term W_b can be ignored. Also neglecting the term W_i for the time being - equation 1 becomes

$$W = W_a(L_1\sigma_a) + W_r(\theta, T) \qquad \text{Eq 2}$$

Considering that always new abrasives in the work material abrade the tool, and the distribution of the abrasives is uniform, W_a will be proportional to the cutting distance and independent of the temperature as assumed previously. Since W_r is the term of rate process, it can be assumed to be proportional to the cutting distance and independent of the temperature as assumed previously. Since W_r is the term of rate process, it can be assumed to be proportional to $\exp[-E / K\theta]$, where E is the activation energy. K the constant associated with diffusive wear, and θ the absolute temperature. Thus the total wear rate dW/dT becomes as follows,

$$dW / dT = V(\theta, f)A + B\exp(-E / K\theta) \qquad \text{Eq 3}$$

where V is the cutting speed, A and B the constants associated with the tool and work material, and f the feed.

On the other hand, the specific wear per unit cutting distance dW/dL is described as follows

$$dW / dL = A + (B / V)\exp(-E / K\theta) \qquad \text{Eq 4}$$

Takeyame et al. (1963) carried out experiments to study the effect of the cutting temperature upon the rate of tool wear or tool life from the viewpoint of flank wear, and to investigate how the cutting conditions affect the cutting temperature.

They concluded that:

1- The mechanism of flank wear has been analysed experimentally, and it has been verified that in a continuous cutting the wear mechanism can be classified into two, that is rate process and mechanical abrasion, the latter mechanism being actuated in the case where the cutting temperature is low or the cutting conditions are mild. However, the former mechanism is controlling in machining with carbide tools under usual conditions. In this case the rate of tool wear for a definite combination of tool and work materials is proportional to $\exp[-E / K\theta]$, regardless of the cutting conditions, where E is the activation energy, θ the absolute cutting temperature, and K the constant.

2- Fundamental formulas of tool wear and tool life (flank wear) have been proposed analytically.

3- It has been verified experimentally and analytically that flank wear tool life of carbide tools under usual condition is proportional to $\exp[-E / K\theta]$ regardless of the cutting conditions. As a matter of fact, the tool life for a definite combination of tool and work materials can be predicted only by the cutting temperature θ_0.

4- The activation energy E is of the same order of the diffusion energy for heavy metals.

The work presented in this thesis shows, as Takeyama et al., that temperature influences the wear mechanisms. Further discussions of how temperature is related to wear mechanisms can be seen in chapter 8.

Rubenstein (1976) proposes an equation where by the rate of wear, or loss of material from the tool, is considered as the rate of production of 'wear' particles multiplied by the volume of the wear particles. This leads to the following equation:

$$Q = v_t dn / dt$$

$$= k_1 p n_0 W l_f V r h$$

which takes account of diffusive wear through the term h, which is in effect the depth into the tool that diffusion takes place. h is considered to be affected by both temperature and by duration of tool contact. It is also considered to follow the equation

$$h = h_0\left(1 - e^{-\delta r}\right)$$

Through approximation due to short contact time, $h = h_1 r / V$, where r is the radius of the area of contact, and therefore the following equation is arrived at:

$$\frac{dl_f}{dt} = \frac{k_1}{\pi} c_1 g^2 h_1 p\left[\cot\beta - \tan\alpha\right]\frac{H_m}{H}$$

Bhattacharyya et al. (1969) suggest a statistical model, which starts from an energy position and by considering the effects of friction upon the energy distribution within the tool material.

This leads to the idea of 'wear particles', the production of which are considered to be a function of the cutting speed, the area of contact and time.

Through various stages of integration in ascertain various 'constants' the following equation emerges:

$$h_f(T) = K'' V_c T^{1-\alpha}$$

Kannatey-Asibu (1985) proposed an equation for conditions of diffusive wear. He observes that there is a 'critical temperature'. Below this critical temperature, the flank wear increases uniformly, and linearly, with time. However, above this temperature, suddenly the wear begins to increase exponentially. This temperature is dependant upon the workpiece and tool combination. By assuming a uniform temperature distribution in

the tool face an equation for diffusive wear is formed. By also including an equation for adhesive wear a highly complicated equation appears, with three constants formed from other variables.

No single model can adequately describe the wear behaviour in all situations and it would seem appropriate to model the individual mechanisms or in combinations that are likely to occur together so that the appropriate model can be used for any given situation.

$$\frac{dc}{dt} = D\frac{d^2c}{dx^2} + D\frac{d^2c}{dy^2} - V\frac{dc}{dx}$$

A complete analysis of the diffusion problems in orthogonal metal cutting should thus be based on the above equation. A solution of the equation will produce a complete representation of the state of the diffusing species in the workpiece and chip (with appropriate modification of the velocity term and axes rotation).

A relationship is derived for the rate of flank wear on the basis that tool wear occurs primarily by adhesion (during steady-state wear) and diffusion. The objective has not been to obtain another form or improved version of Taylor's Law, but to enable a prediction of the onset of the tertiary stage of wear, with the reasoning that this stage is entered when diffusion begins to dominate the wear process.

High temperature, large rate of deformation and continuous contact at the interface zone facilitate the initiation of intermetallic diffusion between the tool and work material. Assuming that the tool wear occurring in a certain case is only due to diffusion wear, in the case of orthogonal cutting, Loladze (1981) argues that it is possible to determine the magnitude of wear at the rake and flank surfaces of the tool.

Obtained theoretical tool life equation for machining of steel and other alloys with carbides shows the satisfactory confirmation with practical data. He produces the final expression - (the substance M in terms of mass units)

$$m_{rake} = \frac{2}{\sqrt{\pi}} \rho c_1 pT \left(\frac{v}{c_n}\right)^{1/2} D^{1/2} \left(KB_{[a]}\right)^{1/2}$$

M - the quantity of substance in terms of mol, T - tool life, $KB_{[a]}$ - length of contact, v - speed along the rake surface, c_n - chip thickness ratio, ρ - mass density of the diffusion layer, c_1 - fraction of total mass, pT - area of chip on the tool., and D - coefficient of diffusion

He concludes that it is possible to select and design the most effective tool material and assign reasonable working conditions for every work material, depending on its chemical mature and mechanical characteristics.

Under conditions of diffusion wear the material of the tool should be inactive towards the work material. Depending on the properties of the work material, different grades of tool material manifest specific properties. Loladze's diffusion wear model for a carbide tools are used by Venkatesk (1978) to project a diffusion wear model for HSS tools at low and medium and at high speeds.

Venkatesh (1978) concludes that the model shows how the white diffusion layer is formed at low to medium and at high speeds. Though the amount of diffusion wear may be small, it causes depletion of carbon and chromium from the tool surface, thus making it more prone to wear by abrasion and by plastic deformation. It can be said that when HSS tools are used for machining mild steel, the crater is formed as a result of diffusion wear, plastic deformation and wear be abrasion.

Kramer (1986) integrated Rabinowiczís abrasive model with his of the chemical dissolution wear model in order to provide an algorithm that predicts the wear rates of hard coating throughout the speed range of application of HSS and cemented tungsten carbide tooling.

Abrasive wear model

$$Vm = \frac{xL\tan\theta}{3P_t} \qquad P_t / P_a < 0.8$$

$$Vm = \frac{xL\tan\theta}{53P_t}\left(\frac{P_t}{P_a}\right)^{-2.5} \qquad 1.25 > P_t / P_a > 0.8$$

$$Vm = \frac{xL\tan\theta}{2.43P_t}\left(\frac{P_t}{P_a}\right)^{-6.0} \qquad P_t / P_a > 1.25$$

where: tan θ - the average tangent of the roughness angle of the abrasive grains (a measure of the particle shape or sharpness), L - The applied normal force between the surfaces, P_t - the tool hardness, and P_a - the hardness of the inclusions

The absolute abrasive wear rate calculated as:

$$A*V*K*\left[Pa\hat{}(n-1)\ \right]/\left[Pt\hat{}(n)\right]$$

Chemical Dissolution Wear model

$$C_{A_xB_y} = \exp\left[-\frac{1}{x}\left(\frac{\Delta G_{A_xB_y} - x\Delta G_A^{-xs} - y\Delta G_B^{-xs} - yRTIn\frac{Y}{x}}{(x+y)RT}\right)\right]$$

where:

$C_{A_xB_y}$ - the chemical solubility of the coating material in the workpiece (mole fraction)

$\Delta G_{A_xB_y}$ - the free energy of formation of the coating material, AxBy

ΔG_A^{-xs} - the relative partial molar excess free energy of solution of component A of the tool material in the workpiece material

ΔG_B^{-xs} - the excess free energy of solution of component B

R - the universal gas constant

T - the absolute temperature

Composite Wear rate

$$\left(A*V*K*\left[Pa\hat{}(n-1)\right]/\left[Pt\hat{}(n)\right]\right)+\left\{B*M*C\left(V\hat{}0.50\right)\right\}$$

Another approach to wear is to consider the forces acting upon the tool as proposed by Oraby et al. (1991). They developed mathematical models to describe the wear-time and the wear-force relationships for steady centre lathe turning conditions. Such models, Oraby et al. (1991) argue have been found to accurately represent the gradual wear development within the initial and constant wear rate domains. Cutting forces have been found to correlate well with wear progress and with tool failure.

The measurement of the variation of the ratio between the radial and vertical force components (F_z/F_y) has been found to provide a practical method for an in-process approach to the quantification of tool wear and failure and, at the same time, to eliminate variation in workpiece hardness so that the proposed approach could be more universally implemented.

One of the most promising techniques of tool wear detection and breakage involves the measurement and the use of cutting forces. In turning operations, it is convenient to consider the tool forces as a three-component system (as seen in chapter 2 figure 2.14). These are the vertical component F_y, the horizontal (feed) component F_x, and the radial component F_z. Even though it has been agreed among many investigators that the change of tool forces represent an accurate and reliable approach to assess tool wear and failure, disagreement still exists over which force component (or combination) is the most sensitive and reliable.

Oraby et al. (1991) investigated the cutting force characteristics within the different phases of the tool working life for a possible correlation with the various forms of tool failure. The effect of the different forms of tool wear and failure on the various force components is studied. Force-wear inter-relationships are formulated for possible use for in-process tool-state monitoring through measurement of the variation in cutting forces.

The experimental procedures of Oraby et al. (1991), resulted in 669 data points for each of the 3 wear measures and 3 force components measures, together with the cutting time. These data were used to develop mathematical models of the different outputs of the turning operations using regression analysis techniques (which make use of the least-squares method).

Friedman & Field in 1975 (Oraby et al. 1991) suggested that the relationship between tool life T and cutting variable: speed V, feed f, and depth of cut d, may take the form:

$$T = a_0 V^{a1} f^{a2} d^{a3}$$

This equation is extended Taylor's equation.

However, for p independent variable, the cutting response R may take the general non linear multiplicative form:

$$R = c\left[\prod_{j=1}^{p} \xi_j^{\beta j}\right]\bar{\varepsilon}$$

where ξj are the machining variables, c and βj - model parameters, $\bar{\varepsilon}$ - multiplicative random error.

Linearized -

$$\ln R = \ln c + \Sigma_{j-1}^{p} \beta j \ln \xi j + \ln \bar{\varepsilon}$$

Wear developed on tool edge can be expressed as:

$$W = W_0 + \Delta W$$

or

$$W = W_0 + mt$$

ΔW - wear increase, W_0 - initial wear, m - slope of the wear-time curve, t - cutting time.

Since the wear increase ΔW at a particular cutting time is dependent on the cutting conditions employed, the wear level may be expressed as:

$$W = W_o + a_0 V^{a1} f^{a2} d^{a3} t^{a4}$$

where V, f and d are the cutting speed, feed, depth of cut respectively.

However, the wear-time models are generally incapable of estimating the wear level in the 3rd stage at which a very high wear rate occurs, according to Oraby et al. (1991). Random disturbances such as tool chipping and fracture are usually not detectable using this technique. Therefore, a better and more reliable approach for in-process tool wear monitoring is still required, - wear-force interrelation.

In Oraby's et al. (1991) research, however, the wear developed on the clearance face does not conform to a uniform pattern; due to the frequent but irregular chipping and fracture of the cutting edge. Moreover, the cutting force proved to be very sensitive to any disturbances within the entire span of the tool life. A correlation exists between the force characteristics and the wear progress. This appears to give good correlation with wear progress up to tool failure. They propose the equation below.

$$W = b_0 V^{b1} f^{b2} d^{b3} + b4\left(F_z / F_y\right)^{b5}$$

b_0 - coefficient - dependent on tool geometry, workpiece hardness and type of lubricant.

This is highly useful from the point of view of actual machine control, as the forces are very simple to measure automatically.

Koren et al. (1991) use the forces as method of formulating their equations. They use cutting force measurements to estimate the flank wear. The force depends on the cutting variables: the cutting speed, v, the feed, f, and the depth of cut, d, as well as on the tool wear W, namely $F(v,f,d,W)$. The wear itself also depends on the cutting variables, that is, $W(v,f,d)$. Since the measured force is affected by both tool wear and the changing cutting conditions, and the wear itself depends on the cutting conditions, any change in a cutting condition affects the force measurement both directly and also indirectly through the

wear. The problem is to change the direct effect of the wear on the force measurement from the effect due to changing cutting variables.

The effect of the cutting variables $d, f,$ and v on each of the three force components, for a sharp tool, can be expressed in terms of the following empirical relationship:

$$F_0 = K_s d^{\alpha 3} f^{\alpha 2} v^{\alpha 1} \qquad \text{Eq 1}$$

where K_s, α_1, α_2, and α_3 depend on the tool geometry and workpiece material.

The growth of the wear on the flank face of the tool consists of three distinct stages, as shown in figure 2.9 in chapter 2: a short initial region of rapid wear, an approximately constant wear-rate region, and finally a very rapid wear-rate region which indicates tool failure. In practice, the tool is replaced during the second stage.

Therefore, during most of the cutting process the flank wear may be approximated by

$$W = W_0 + Wt \qquad \text{Eq 2}$$

where W represents the wear-rate in the second region, W_o is the intercept with the wear axis, and t is the time.

The flank wear can be represented by utilising the extended Taylor tool life equation

$$Tv^{\gamma 1} f^{\gamma 2} d^{\gamma 3} C_n = 1 \qquad \text{Eq 3}$$

where C_n, γ_1, γ_2, and $\gamma 3$ depend on the workpiece material and the tool's material and geometry. The tool life T may be defined by a final flank wear $W(T) = W_f$ at which the tool is replaced. Combining equations 2 and 3 yields

$$W = \left(W_f - W_0\right) C_n v^{\gamma 1} f^{\gamma 2} d^{\gamma 3} \qquad \text{Eq 4}$$

where typically, $\gamma_1, > \gamma_2, > \gamma 3$

The initial wear develops rapidly in the first few seconds of the cut, and experience shows that it is not possible to measure the initial force level F_o or the sharp tool. In practice, they measure an initial force $F_0 = F_0^* + KW_0$. Consequently, the additional measured force component due to wear is $\Delta F = KWt$, or

$$\Delta F = C_p v^{\beta 1} f^{\beta 2} d^{\beta 3} W\left(v^{\gamma 1} f^{\gamma 2} d^{\gamma 3}\right) t \qquad \text{Eq 5}$$

The wear rate is expressed in equation 5 as a function of the cutting variables. If the validity of the Taylor tool life equations had been assumed, then equation 4 could have been substituted into equation 5. Instead, they consider the use of estimation methods to obtain the wear rate from force measurements. The case is considered where the wear rate depends on the cutting conditions, but only one of the cutting variables varies. Then equation 5 can be rewritten as

$$\Delta F = Cb^{\beta} W\left(b^{\gamma}\right) t \qquad \text{Eq 6}$$

where b is the particular cutting variable which varies (that is b might be $v, f,$ or d). The coefficient C depends on the tool and workpiece material as well as on the other cutting variables that do not vary. A change in b has both a direct effect on the force measurement through equation 1 and b^{β} in equation 6, and an indirect effect through the change in the wear rate W.

Many equations similar to those discussed in this section have been proposed by researchers. Simple tool life equations are useful mainly for comparative purposes, for example, for ranking the general machining performance of insert grades. Taylor tool life tests performed according to defined standards are also useful in ensuring results from different sources are consistent. Tool life predictions based on these relations, as Stephenson et al. (1997) point out are generally not quantitatively reliable as the empirical constants are estimated from tool life tests in which tool life is assumed to have ended when a specified level of flank wear is reached. In practice, tools are not used when the part's dimension, form accuracy, or surface finish is out of tolerance. A variety of mechanisms other than flank wear may produce such conditions.

3.3 DRILLING

This section looks at the drilling operation and tool life equations related to wear. as mentioned earlier in the introduction, drilling, unlike single point turning, has not been an area where there has been much research. Even in terms of standards, there has not been international or even British standards concerning tool life criteria (as discussed in chapter 5). Therefore, this section is not proportional to the previous section due to the lack of information and research in the drilling operation.

3.3.1 Drill Life Criteria

Individual researchers have come up with their own versions of drill life criterias because of this lack in standards. Singpurwalla et al. (1966) stated that drill life means different things to different people, and they characterised it by three criteria:

- A change in colour of the drill.
- A change in sound of the drill or a 'cry' while drilling continuously.
- Complete destruction of the drill or its inability to drill any further.

Soderberg (1978) that tool life is always defined as the time to failure, and that other possible criteria as flank wear, crater wear or increase in torsional moment show bad correlation to the failure criterion. It is, therefore important he states, to correlate the sudden failure of the drill with the wear mechanisms operating during cutting. Examination of drills after failure is difficult since failure is followed by a rapid destruction of the drill. According to Soderberg, a typical feature when drilling carbon steel is the sudden breakdown of parts of the lip which seems to happen either at the periphery or near the centre. While when drilling direct hardening steel, failure is preceded by a rapid increase in wear rate at the periphery. Failure initiates when the drill material starts flowing by plastic deformation at the periphery and the flow then rapidly spreads inwards.

3.3.2 Tool Life Estimation

In process tool failure poses a serious threat to unmanned manufacturing systems, such as flexible machining centres. Developing effective means to monitor and manage cutting tools, in order to avoid off-quality product and/or system damage, Jalili et al. (1991) argue, presents a significant problem for manufacturing research. They focus on these issues relative to drilling processes involving steel.

Effective tool management requires machinability models that are as simple as possible, yet provide information regarding tool wear and breakage. Direct experimentation is typically the basis for tool life and cutting force models. Jalili et al. (1991) measured tool life in minutes of HSS drills, torque in kg-mm (in-lbs) on the drill, and thrust in kg (lbs) on the drill.

The scope of the experiment included 4 independent variables:
1- Surface speed of the drill ranging from 162-330 mm/s (32-65 sfpm)
2- Feed ranging from 0.0635 - 0.381 mm/r (0.0025 - 0.015 ipr)
3- Drill diameter ranging from 7.54 - 14.68 mm (0.2969 - 0.5781 in)
4- Work material, steel, hardness ranging from 146 - 330 Brinell hardness number, BHN

Difficulties are encountered in metal cutting due to the large number of variables involved. Jalili et al. (1991) examined four variables: cutting speed, feed, drill diameter, and work material hardness. Other work piece variables such as tensile strength and yield strength were not considered because they are mathematically related to hardness. The thermal conductivity of the steel was not considered, since it was nearly constant. The effects of machining variables other than speed and feed (i.e. vibration, deflection, and thermal expansion) were also ignored. The tool variables such as point angle, relief angle, and helix angle were nearly constant.

The experiments involved HSS twist drills, drilling low carbon steel of variable hardness. The data obtained were used to develop a statistical model to predict tool life (min) as a function of machining, tool, and work piece variables (i.e. cutting speed in

mm/s (sfpm), drill feed in mm/r (ipr), drill diameter in mm (in), and steel hardness in BHN. The thrust and torque models consider drilling time as well as speed, feed, diameter and hardness as independent variables.

The objective of developing the tool life model was that once the tool life of a drill is predicted for a drilling set-up, it may be used to determine the maximum thrust limit for that drilling set-up, by using the thrust prediction model. The thrust measure is useful to help detect a chipping or catastrophic failure mode. And also the tool life predicted may be used as the maximum cutting time a drill is allowed to cut, in the case where the drill fails due to the criterion of wear.

The predictive model for tool life was developed as a function of the independent variables:

$$T_1 = f(V_1 F_1 D_1 H) \qquad \text{Eq 1}$$

where T_1 is the tool life (min), V is the cutting speed, mm/s (sfpm), F is the feed, mm/rev (ipr), D is the drill diameter at periphery, mm (in.), and H is the steel hardness.

The predictive models for cutting forces, torque in kg-mm (in-lbs) and thrust in kg (lbs), were developed as a function of independent variables as seen in equations 2 and 3 for torque and thrust respectively:

$$T_q = f(V, F, D, H, t) \qquad \text{Eq 2}$$

$$T_h = f(V, F, D, H, t) \qquad \text{Eq 3}$$

where T_q is torque, T_h is thrust, and t is time of cut (min).

The tool life model is a complicated one. As Jalilia et al. (1991) point out, it is difficult to explain the effects of the independent variables on tool life merely by inspecting individual terms. One must consider the effect of all terms containing a given independent variable simultaneously. They concluded that the cutting speed, feed, and steel hardness have a very significant inverse effect on tool life (i.e. tool life decreases

very significantly by increasing the cutting speed, feed or steel hardness). Also that the drill diameter has a significant inverse effect on tool life (i.e. tool life decreases significantly by increasing the drill diameter).

Jalali et al. (1991) suggest that in terms of tool management, their tool life equation provides the basis for a simple cutting time tool management system, and that through the use of a real-time torque/thrust monitoring system, one may use the torque/thrust models as tool management guides for either wear or tool breakage.

Tool life is the period of economical use of a tool and differs from tool wear. However, Subramanian et al. (1977) argue that the two are closely related. It is the extent of wear on the tool that determines whether a tool has reached the limit of its economical life or not. Drill life varies greatly but there has been very limited testing under 'industrial' conditions. Drill life of repeated grinds is a function of thermal history of the drill during its previous tool life, the grinding practice used, the point geometry, and the accuracy of the geometry. Drill life is also affected by the nature of the operation - blind hole, through hole on cast surface, through hole on milled surface, intersecting holes, angle of entry, bushing location, coolant application, etc.

Subramanian et al. (1977) state that torque, thrust, and power are basic process variables that depend solely on the cutting condition and the tool condition. Their variation in any situation, such as single or multiple tool operations, if all operating parameters remain constant, depends only on the condition of the individual tool in question. It is assumed here that the individual drilling spindles are driven independently and that their speed of revolution remains constant. In general the wear observed on a drill is extensive on the flank of the tool but negligibly small on the rake face (generally known as crater wear). It is known that the flank wear of the tool increases rapidly at the end of tool life. If it is true that the torque, thrust, and power vary with the flank wear, then the changes in these variables should be significant and rapid at the end of the drill life. A careful constant monitoring of these variables during the life of a drill should indicate their changes and thus a parallel indication or predication of the flank wear (Subramanian et al. 1977).

The equation to calculate torque generated during a drilling operation with gradual tool wear is:

$$M = \frac{H_B d^2 f}{8} + \frac{H_B d^2 r}{4\cos\alpha_p} + \frac{H_B d^2 w}{24\cos\alpha_p}$$

where M is the torque applied, H_B is the Brinell hardness of the work material, d is the diameter of the drill, f is the feed per revolution, r is the radius at the edge of the tool (not the nose radius), w is the average flank wear and α_p is the inclination of the cutting force on the cutting edge with the axis of the drill.

The equation to calculate the thrust force generated during a drilling operation with gradual tool wear is shown in the equation below:

$$T = H_B(P + Qw)$$

where T is the thrust force, P and Q are constants and w is the flank wear.

Therefore, as stated above torque, thrust and power increase as the flank wear of the drill increases. By using the basic principles of the mechanics of metal cutting, Subramanian et al. (1977) derive a relationship between torque and flank wear and also between thrust and flank wear in the drilling operation. Therefore, one can conclude that from the above research tool wear prediction may be linked to the prediction of the torque and thrust.

3.4 CONCLUSION

The above section looked at the single point turning and drilling operations in relation to tool life equations and wear. It can be seen from the proportion of the two sections, drilling has not been researched like single point turning in terms of tool life equations in relation to tool wear, as will be seen throughout many areas of this work, one reason of this lack in drilling research could be due to the complexity of the drill geometry across the lip, variation in angles and speed.

As can be seen that published work focuses on particular factors and are therefore incomplete. The reality is that any factor in a machining process which impacts upon heat input or the paths by which heat is executed will influence wear. For example bar diameter (in turning) does not appear in any equation, but can be demonstrated to influence the heat flow efficiency into the workpiece as will be shown in chapter 8.

The above survey showed that research had not been found where tool life equations have been related to different wear mechanisms, or that an attempt has been made to extrapolate models from one process to another. It is therefore important that when considering a tool life equation and wear that all factors must be considered.

Therefore, the Taibi (1994) model that was used in order to apply the force results obtained in this work to it, was partly chosen as it claimed to accommodate a wide variety of cutting conditions. Its extrapolation for use with the force results obtained in the drilling operation was made easier due to the existence of the Webb (1990) geometric drill model, as will be seen in chapters 9 and 10.

Chapter 4

EXPERIMENTAL METHODS

4.1 INTRODUCTION

The literature review carried out in the previous chapters showed that further research is required to investigate various influences on the tool's condition in turning and drilling. As part of this work a comprehensive series of experimental tests was conducted to study the influence of cutting temperature and forces on the turning and drilling operations over a range of cutting conditions (such as cutting speed, depth of cut, etc.). The results of both processes were examined and compared in order to determine the similarities and differences between them.

The worn tools were examined in order to observe the wear mechanisms and how these were affected by the nature of the workpiece, tool materials and variables such as cutting speeds and flank and rake angles. Measurements were carried out to determine the value of the forces and temperature. Chapters 6 and 7 deal with the forces in turning and drilling respectively in more detail. Chapter 8 discusses temperature in more detail.

The experimental conditions used for the cutting tests, such as cutting conditions, tool and workpiece material, are described in the following sections, as well as the measuring techniques and the general experimental procedure.

4.2 WORK MATERIALS

4.2.1 Turning

The workpiece material used for the single point turning operation was solid carbon steel bar BS970 080A42, and the microstructure can be seen in figure 4.1, by using the optical microscope (Swedish optical microscope POLYVAR).

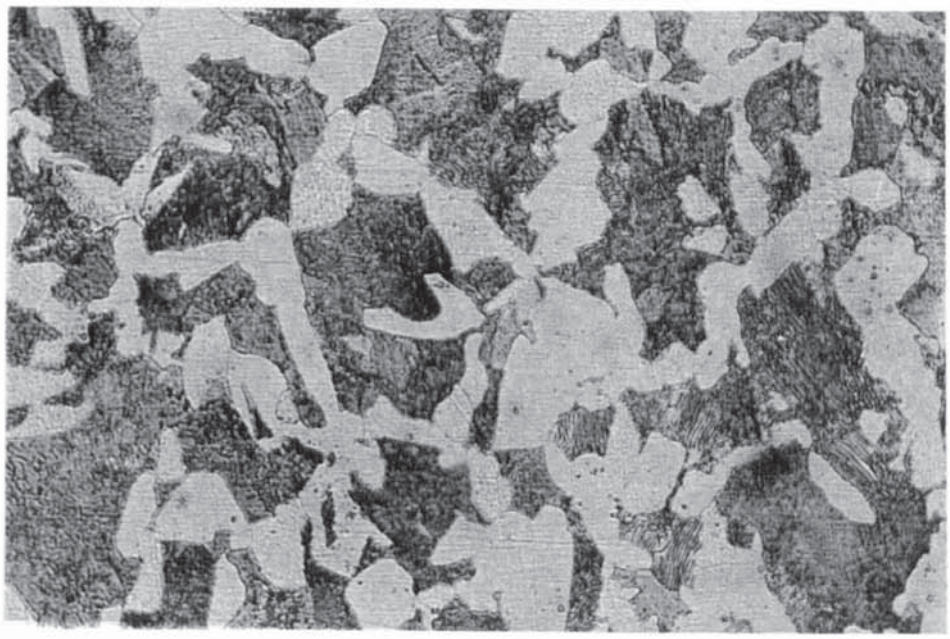

Figure 4.1 Microstructure of BS970 080A42 (X 500)

The typical applications of this type of carbon steel are for forgings and general engineering parts not subject to high stresses or severe wear. Owing to its low hardenability its use in the hardened and tempered condition is not recommended for large masses as the improvement in mechanical properties over the normalised condition is insufficient in such cases to justify the additional processes required. These steels can be surface hardened by flame or induction methods giving a case hardness of 365-510 HV suitable for general gearing and parts not subject to high stresses. This steel is widely used for applications where better properties than mild steel are required but the expense of an alloy steel is not justified. Hardness of BS970 080A42 is 190 HV.

The chemical composition of this material is given in table 4.1:

%C	%Si	%Mn	%S	%P
0.4 - 0.45	0.05 - 0.35	0.7 - 0.9	0.06 max.	<0.06

Table 4.1 Chemical composition of BS970 080A42

4.2.1.1 Preparation

The workpiece material was supplied in a 3m (approx.) long bar and of 76 mm (approx.) diameter, from the supplier. The bars were cut into six 0.5 m sections. The hard outer skin of the bar was removed beforehand with a 1 mm skim in order to eliminate hardness of the material, and to remove any defective material. Three discs between the bars were cut to measure the hardness across the bar. A series of hardness values were measured from each of three bars. All tests were undertaken between 75 mm and 27 mm diameter.

4.2.2 Drilling

The workpiece material used for the drilling operation was plain carbon steel BS970 080A40, and its microstructure can be seen, by using the optical microscope, in figure 4.1.

BS970 080A40 is widely used for applications where better properties than mild steel are required, but the expense of an alloy steel is not justified. A moderate wear resistance can be obtained by flame or induction hardening giving a case hardness of 365-510 HV depending on the carbon content of the steel. Typical applications include: connecting rods, studs, bolts, highly stressed gears, spindles, roller and many vehicle and general engineering components.

The chemical composition of this material is given in table 4.2:

%C	%Si	%Mn	%S	%P
0.35 - 0.45	0.05 - 0.35	0.6 - 1.0	0.06 max.	0.06 max.

Table 4.2 Chemical composition of BS970 080A40

4.2.2.1 Preparation

BS970 080A40 and is supplied from the supplier in a beam of 3 m long, 200 mm width and 25 mm thickness. It is then cut into suitable size (200 x 50 x 25 mm) which is appropriate for the machine. The material was cleaned from oil and grease with acetone before the testing.

4.3 TOOL MATERIAL

4.3.1 Turning

The tool material used for the single point turning operation were:

1 - Moly M2 HSS billet (BS4659 BM2), 12.7 mm square, and 101.6 mm long. Figure 4.2 shows the microstructure of Moly M2 HSS. Hardness of Moly M2 HSS is 850 HV.

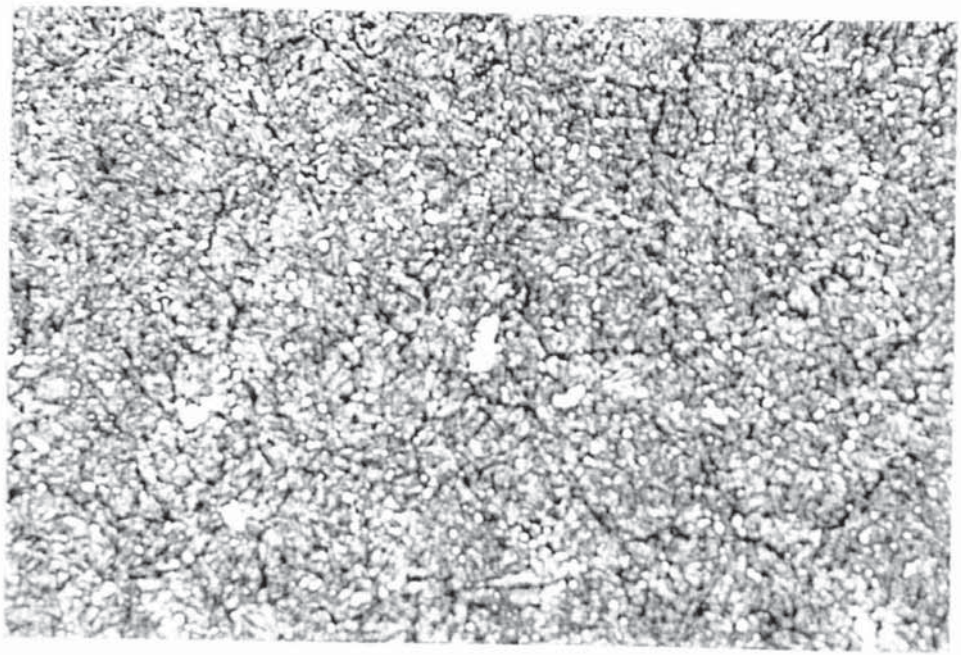

Figure 4.2 Microstructure of Moly M2 HSS (X 500)

The Nominal composition is seen in table 4.3:

%C	%Cr	%W	%Mo	%V
0.85	4	6	5	2

Table 4.3 Chemical composition on Moly M2 HSS

2 - Uncoated BT42 (BS4659 BT42) (0.4 mm nose radius) and TiN coated BT42 (0.8 mm nose radius) HSS inserts. The microstructure of BT42 HSS can be seen in figure 4.3. These were manufactured by a cold-press-and-sinter powder metallurgy technique from water atomised powder. Hardness of BT42 is 912 HV.

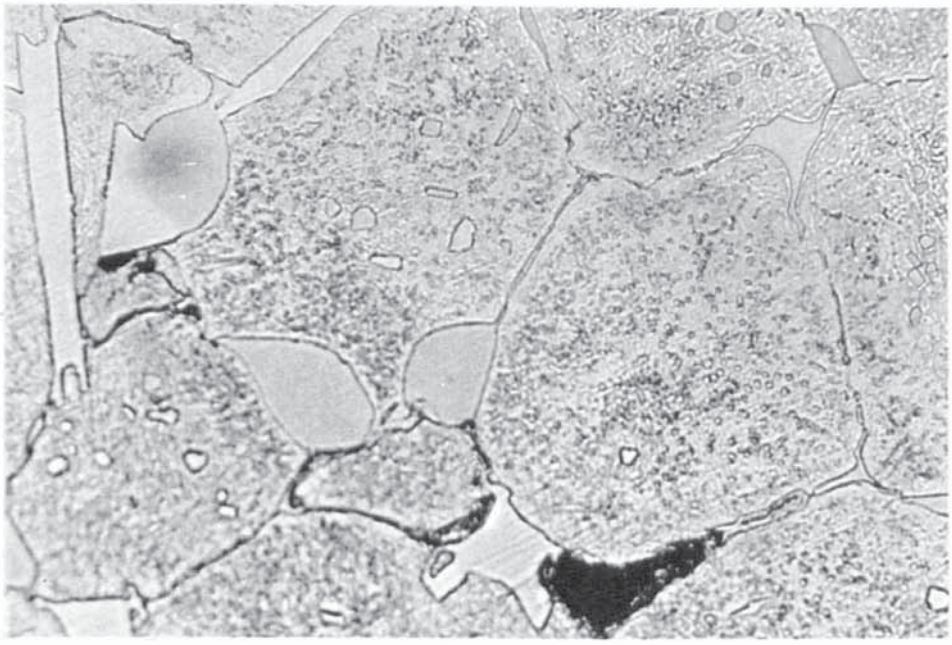

Figure 4.3 Microstructure of BT42 HSS (X 500)

The Nominal composition is seen in table 4.4:

%C	%Cr	%W	%Mo	%V	%Co
1.3	4	9	3	3	9.5

Table 4.4 Chemical composition of BT42 HSS

3 - Carbide Tools: uncoated K68 and K313, and coated KC850, in Kennametal classification (ISO classification: K05-K15/M10-M20 for K68 and K313, and M25-M45/P25-P45 for KC850, details on composition is in appendix 1). They all have 0.4 mm and 0.8 mm nose radius.

4.3.1.1 Preparation

The angles of the Moly M2 HSS tool were ground by using the Cutter grinding C5807-9 Cincinnati grinding machine. Flank and rake angles of the Moly M2 HSS billets were checked using the toolmakers microscope, (Swiss Toolmakers Microscope - MU-214B with a Sylvac 25 digital probe in chapter 5 figure 5.5), a device which uses stylus probe with accuracy of 1 min which is equal to 1/60 degrees. The inserts were mechanically clamped in a tool holder (CT GPL-2020K16).

4.3.2 Drilling

The tool material used for the drilling tests was M2 HSS and its microstructure can be seen in figure 4.2. The types of drills used varied as seen below:

1 - Three different helix angle (fast, slow and standard) M2 HSS drills, of 13 mm diameter were used:

2 - M2 HSS standard helix angle of 9 mm diameter (pilot drill).

The Nominal composition is seen as above in table 4.3.

4.3.2.1 Preparation

The drills were labelled and the datum marked using the Taylor-Hobson resistance etcher. The datum position was measured using the toolmaker's microscope. This gave an unworn initial position of the lips before degradation. The drill quality was checked in case of any chips etc. The toolmaker's microscope was also used to measure and check the chisel angles, helix angles, clearance angles, point angles, fluted land width, cutting land width, total point clearance, minimum diameter, body clearance, web thickness and relative lip height, see figure 5.5 in chapter 5 for the photograph of measuring equipment. More details of the terms and definitions are shown in the appendix 2.

Prior to taking the wear measurements, the drills were 'squared' by measuring the position of the datum lines. These lines were measured prior to any drilling, and were defined as the perpendicular distance between the two datum marks across the chisel edge. This was done so that accurate placement of the drill could be ensured before measurement was carried out.

Measurement of wear was taken at three points across the lip of the 9 mm drill: for both lips, corner wear and 1 and 2 mm from the corner and land wear. Measurements of wear on the 13 mm drill were for the corner wear, average and maximum wear on the lip and land wear. More about the wear measurements will be discussed in chapter 5 section 5.3.1.

4.4 MACHINING

4.4.1 Turning

The single point turning was confined to orthogonal machining. The experiments were carried out on a CNC Torshalla lathe, (Swedish made Torshalla S160 CNC Lathe with Japanese control GE Fanuc OT - fully computer controlled. (Speed: 0-4800 rev/min.)). When cutting fluids were used in the tests, the fluid used was 4% Shell Dromus Oil B @ 4 litres/min., which was checked, before the tests, by using the Futikoki refractometer. The test was stopped to measure the average and maximum flank wear, that is, wear in each tool life was measured using the toolmaker's microscope. Also the forces had been measured using the dynamometer and monitored against time via the Apple Macintosh Computer using Chart software. Figure 4.4 shows the Torshalla CNC lathe with the dynamometer attached to it. The chips were collected for the different speeds for each test to be analysed at a later stage under the Scanning Electron Microscope (SEM). The tool was also examined under the SEM for tool wear. (Test conditions can be seen in tables A1.1 to A1.9 in appendix 1).

Figure 4.4 Photograph of Torshalla CNC lathe with force equipment

4.4.2 Drilling

Two machines were used for these tests: the Bridgeport series 1 Interact milling/drilling machine for the lower speed tests and the Bridgeport machine centre milling/drilling for the higher speeds. (Bridgeport series 1 Interact milling/drilling machine, (Speed: 50-3750 rev/min.) and Bridgeport machine centre milling/drilling machine, (Speed: 100-10000 rev/min.)), as seen in figure 4.5 with the dynamometer attached to it for the force readings. Two different size M2 HSS drills with straight lip were used: the 9 mm drill with standard helix angle with oxide finish (pilot), and 13 mm at three different helix angles, that is, slow, standard and fast.

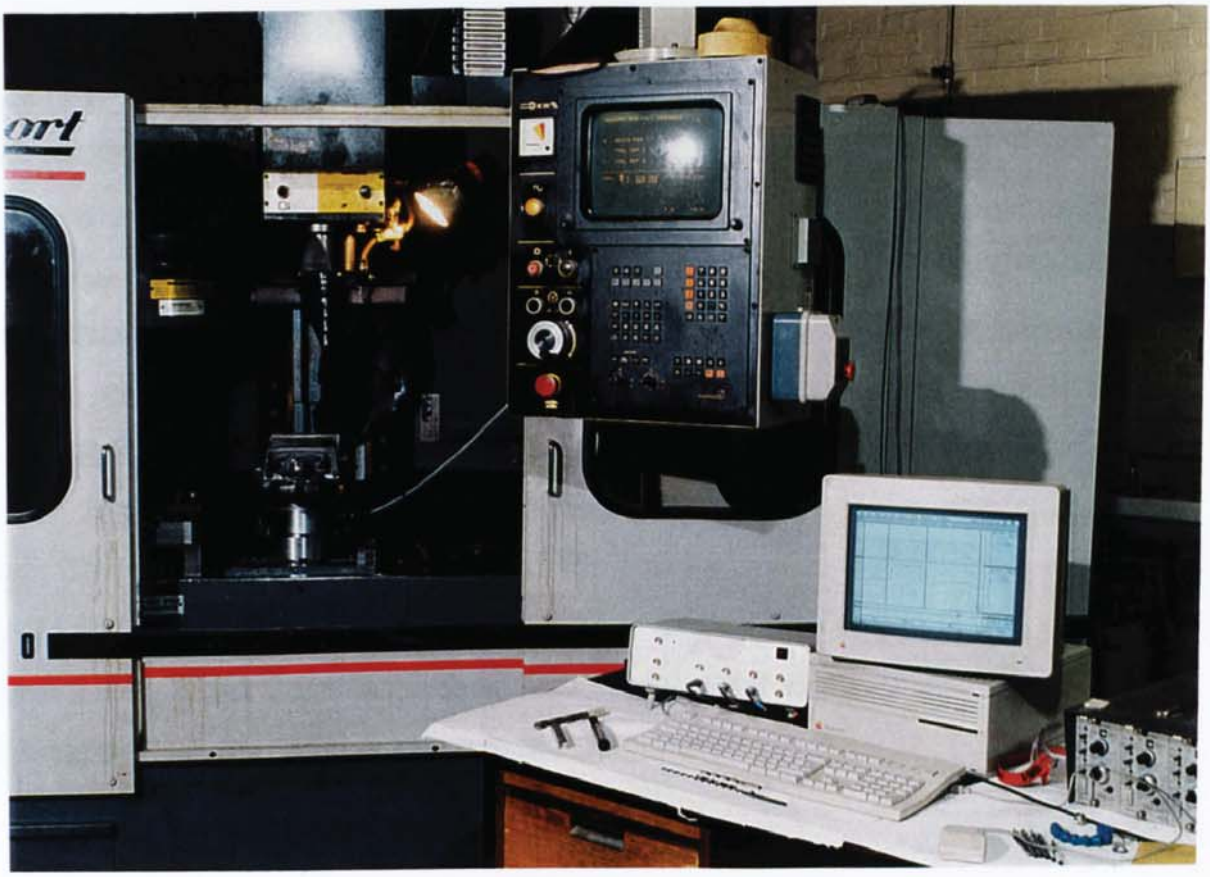

Figure 4.5 Photograph of Bridgeport machine centre with force equipment

The first hole was made by using the 9 mm standard helix drill. Then for each test a 13 mm drill was used in order to give each lip cutting 2 mm in order to enlarge the hole. After the first hole the drill was measured for wear by using the toolmakers microscope with a Sylvac 25 digital probe as seen in chapter 5 figure 5.5. The forces: torque and thrust, were measured by using the dynamometer which is connected to the Apple Macintosh computer. The chips were collected to be examined under the SEM at a later stage. (Test conditions can be seen in tables A1.10 to A1.12 in appendix 1).

4.5 MEASUREMENT OF WORN TOOLS

In turning, by conforming to the ISO guidelines regarding the criteria of tool life, a measurement of maximum and average flank wear and where possible nose wear was taken. By using 40X magnification on the Swiss tool makers' microscope, maximum and average flank wear was taken for the 13 mm drill. As for the 9 mm drill measurements were taken for corner wear and 1 and 2 mm from the corner and land wear, due to the lack of standards, International and British, standards have been established by the author for this work of which more details will be seen in the next chapter. Also in drilling, using the same microscope, measurement was taken not for the wear scar but a measurement was taken for the total distance from the datum to the cutting edge (lip), and subsequently a measurement was taken from the datum to the wear. Therefore, it was possible to assess the increase in wear and decrease in the area by subtracting the latter from the former. More details can be seen in chapter 5, and figure 5.5 in chapter 5 shows the equipment used for measuring the wear in turning and drilling, and also for the angle measurement in drilling.

4.6 MEASUREMENT OF CUTTING FORCES

For measuring the cutting forces to a considerable accuracy, several types of cutting force dynamometers have been developed and are now in use. In most metal cutting force dynamometers the tool force is determined by measuring the deflections or strain in the elements supporting the cutting tool. It is essential that the instrument should have high rigidity and high natural frequencies so that the dimensional accuracy of the cutting operation is maintained and the tendency to chatter, or vibrations, must, however, give strains or displacements large enough to be measured accurately.

In this work, in order to record the levels of cutting and feed force in turning and torque and thrust force in drilling experienced during machining, a three-component piezo-electric dynamometer Kistler type 9257B was used along to record the cutting forces. The outputs of the dynamometer are filtered in a low pass filter of 10Hz, amplified

through a Kistler charge amplifier which was connected to the Apple Macintosh computer. MacLab software was used on the Applemac to convert, read, store and generally manipulate the data obtained from the transducers on the lathe and the drilling machine. Figures 4.4 and 4.5 show the dynamometer attached to the Torshalla lathe and the Bridgeport machine respectively. The Chart software enabled a number of analysis and mathematical processes to be carried out. Data taken for all the tests was saved onto floppy disk for more investigation. The dynamometer has a great rigidity and consequently a high natural frequency. Its high resolution enables the smallest dynamic changes in large forces to be measured.

The dynamometer consists of four three-component force sensors fitted under high preload between a base plate and a top plate. Each sensor contains three pairs of quartz plates, one sensitive to pressure in the z direction and the other two responding to shear in the x and y direction respectively. The force components are measured practically without displacement.

The current methods of monitoring drilling is the use of a four axis dynamometer load cell. The workpiece is held in a vice mounted on the dynamometer. This allows the torque and thrust force of the process to be measured and recorded throughout the drilling operation.

In chapter 6 more details are discussed relating the effect of the forces on the turning operation and the materials. Chapter 7 discusses in more details the effect of the forces on the drilling operation and the materials.

4.7 MEASUREMENT OF TEMPERATURE

To measure the temperature, a glass-fibre insulated, K-type, thermocouple with conductors of 0.1 mm diameter had been used. The thermocouple junction is formed by capacitor-discharge welding the ends of the wire, which produces a roughly spherical

bead. Thermal contact is maximised by flattening the bead and welding the resulting junction to the cutting tool.

The thermocouples were connected to the auto-cold junction thermocouple amplifier using compensating lead and thermocouple connectors as seen in a block diagram in figure 4.6, in order to minimise cold junction errors.

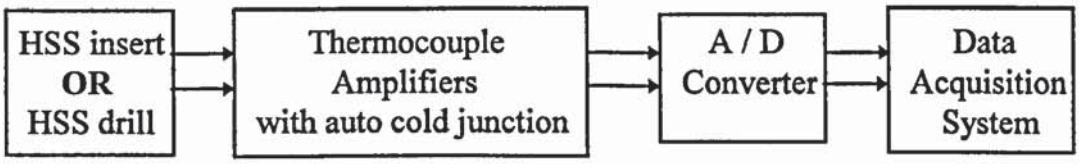

K - Type Thermocouple

Figure 4.6 Diagram showing thermocouple connection

A large soldering iron was placed in contact with the cutting edge of the tool and the thermocouple output monitored. For calibration an area of flank and face was dipped in hot oil (low temperatures) and molten lead (high temperatures), this area was approximately the same as the area of contact between workpiece chip and tool during cutting, the technique was also used by Redford et al. (1976).

In this work, in turning, the temperature was measured by placing thermocouples in the cutting tool; in the insert for the single point turning operation and through the oil hole in the drill for the drilling operation. In figure 4.7 the experimental set up for the temperature measurement with the display unit is shown. It can be seen from the photograph that the set up is for the drilling operation. The set up for the turning operation is the same as the drilling but the attachment is made to the Torshalla CNC lathe instead of the Bridgeport machine.

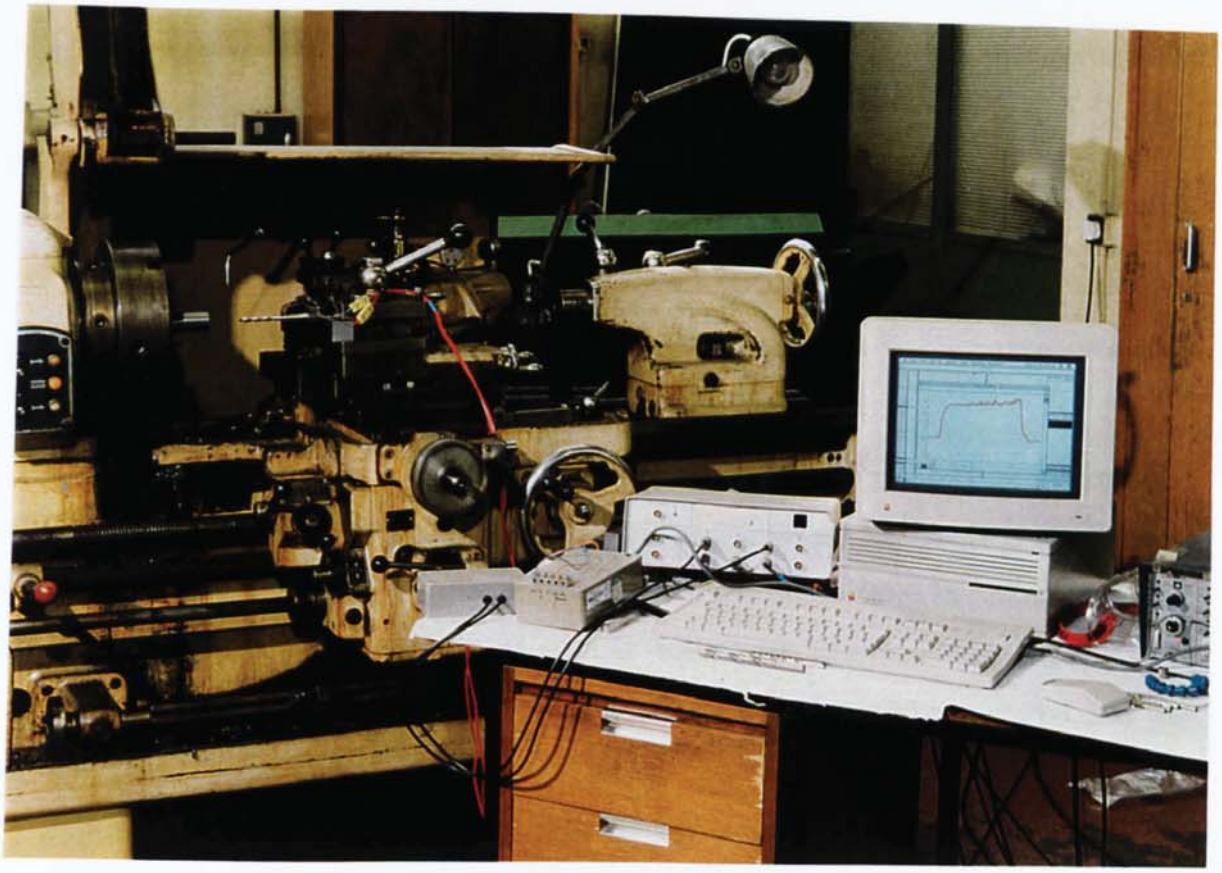

Figure 4.7 Photograph of experimental set up for temperature measurement

More details and results of the tests about temperature and the technique of thermocouples in the cutting tool will be discussed in chapter 8. (Test conditions for turning can be seen in tables A1.13 to A1.19, and tables A1.20 to A1.25 for drilling in appendix 1).

4.8 ANALYSIS OF THE CHIP SURFACE

An analysis of the chip surface using ESCALAB 22-D, (made by VG Scientific. (Technique used X-ray Photoelectron Spectroscopy (XPS)), was undertaken by the Applied Physics department as seen in more detail below and in chapter 8.

The surface of the chip was examined in order to analyse and detect the free iron and oxide iron content on the surface of the chip. The sample of the chip has been placed in liquid nitrogen as soon as it was produced until it was ready to be analysed, therefore in

order to stop the oxidation process going any further the analyses was carried out immediately after being produced. The analysis takes place in only 60 - 100 Å (1 nm = 10 Å) depth of the surface of the chip.

4.9 SCANNING ELECTRON MICROSCOPE

Both the tool and the chip were examined by using the Scanning Electron Microscope, (Cambridge Instrument Stereoscan S90). It was used to examine the wear mechanisms and wear scar by looking at the flank wear, crater wear, nose wear in both turning and drilling, notch wear in turning, and corner wear and land wear in drilling. The examination of the wear scar was obscured due to the built-up edge material that was welded over the flank face and rake face, which made it difficult to identify the wear mechanism. Therefore there was an attempt to remove the BUE which was successful sometimes.

Before examination took place under the SEM, the tools were cleaned in acetone in an ultrasonic bath, and attached to aluminium stubs.

4.10 CONCLUSION

The work depends substantially upon the accurate measurement of wear, and in the author's opinion it is important to talk about the International standards and the way in which the research material either conforms to them or offers a standard where wear is measured. In this section a brief mention is made of how wear is measured in turning and drilling but due to the importance of this subject, and also since a comparison is intended to be made between turning and drilling, the next chapter deals with the whole issue of measurements in terms of what standards exist or do not and what sites and protocols are used in general and what was used throughout this work.

Chapter 5

MEASUREMENT: STANDARDS, SITES AND PROTOCOLS

5.1 INTRODUCTION

In practical/workshop situations, the time at which a tool ceases to produce workpieces of the desired size and surface quality usually determines the end of a useful tool life. The period up to the instant when the tool is incapable of further cutting may also be considered as useful tool life. However, the reasons for which tools may be considered to have reached the end of useful tool life will be different in each case depending upon cutting conditions etc.

To increase reliability and comparison of test results, it is essential that tool life is defined as the total cutting time of the tool to reach a specified value of tool-life criterion. As mentioned throughout this chapter the author did not find any international or British standards which concerns tool life testing for drilling.

Standards, in metal cutting, are needed as they contain recommendations which are applicable in laboratories, manufacturing, industrial units etc. These recommendations are intended to unify procedures in order to increase reliability and comparability of test results when making comparisons of cutting tools, work materials, cutting parameters or cutting fluids. In order to come as close as possible to these aims, recommended reference materials and conditions are included and should be used as far as is practical.

In addition, the recommendations can be used to assist in finding recommended cutting conditions, in wear measurement, or to determine tool life and machining characteristics such as cutting forces, machined surface characteristics, chip form etc.

Many International Standards have equivalent Standards issued by the British Standards Institution or similar institutions from other countries. Shaw (1991) demonstrates how British, German and American standards differ in terms of the nomenclature and the definitions of the positions of the tool. To reach international agreement on all aspects of the nomenclature, bearing in mind the desirability of providing terms which could be translated, without double meaning, from one language into another, some compromises and some changes from accepted usage in individual countries are inevitable.

The existence of standards for tool life and measurements of wear in single point turning and drilling will be discussed in this chapter as it has been discovered that although International standards for tool testing and wear measurements exist for single point turning, for drilling they are non-existent, there is nothing to follow, but in order to establish a comparative set of results with those of turning, then criteria have been established by the author in order to accomplish some of the objectives of this work. A brief look will be taken at some of the standards that were used in this research, for instance those related to definitions, nomenclature and others.

An understanding of tool life requires an understanding of the ways in which tools fail. Broadly, tool failure may result from wear. Tool wear may be classified by the region of the tool affected or by the physical mechanisms which produce it. The sites of wear on the tool will be discussed in this chapter for both turning and drilling.

What is usually measured in terms of wear and the procedures of their measurements in this research as well as those of other investigators will also be investigated and discussed.

5.2 TURNING

5.2.1 Standards

The main standards that were used in this work relating to single point turning are:

BS 1296:1972 - Specifications for Single-point cutting tools. Part 2 - Nomenclature (1972)
This British Standard defines terms for certain concepts concerning single-point cutting tools; it deals with those features which are necessary to define the geometry of the cutting part. It defines the general terms applicable to single-point tools, the types and shapes of single-point tools and the hand of tools. It also defines tool elements, tool surfaces, cutting edges, surfaces on the workpiece, tool and workpiece motions and certain specific dimensions.

ISO 3685:1993 - Tool-life testing with single-point turning tools (1993)
This International standard specifies recommended procedures for tool-life testing with high-speed steel, cemented carbide and ceramic single-point turning tools used for turning steel and cast iron workpieces. It can be applied to laboratory testing as well as in production practice.

This International Standard is concerned with recommendations for testing which results predominantly in tool wear. This International Standard establishes specifications for the following factors of tool-life testing with single-point turning tools: workpiece, tools, cutting fluid, cutting conditions, equipment, assessment of tool deterioration and tool life, test procedures and the recording, evaluation and presentation of results.

Through the ISO guidelines the following criteria were selected in order to determine the end of a useful tool life:

- Average flank wear: > 0.4 mm
- Maximum flank wear: > 0.7 mm
- Notching at nose or depth of cut: > 1 mm
- Rake face crater wear: > 0.14 mm
- Fracture of insert or flaking of the cutting edge, or catastrophic failure.

These criteria are used for single point turning. As far as this work is concerned we are interested with the criterion of the tool of uniform (steady-state) flank wear as shown in figure 2.9.

5.2.2 Sites

As far as this work is concerned the wear measured was: average and maximum flank wear, and nose wear when possible. Wear on the flank face is called flank wear and results in the formation of a wear scar. Rubbing of the wear scar against the machined surface damages the surface and produces large flank wear which increases deflections and reduces dimensional accuracy. The extent of flank wear is characterised by the average or maximum land width. The flank wear scar is generally of uniform width, with thicker sections occurring near the ends (Stephenson et al. 1997).

Figure 5.1 shows the flank wear scar and rake face wear crater according to the ISO Standard, and a photograph of this can be seen in figure 5.2.

Figure 5.1 Characterisation of flank wear scar and rake face wear crater (ISO 1993)

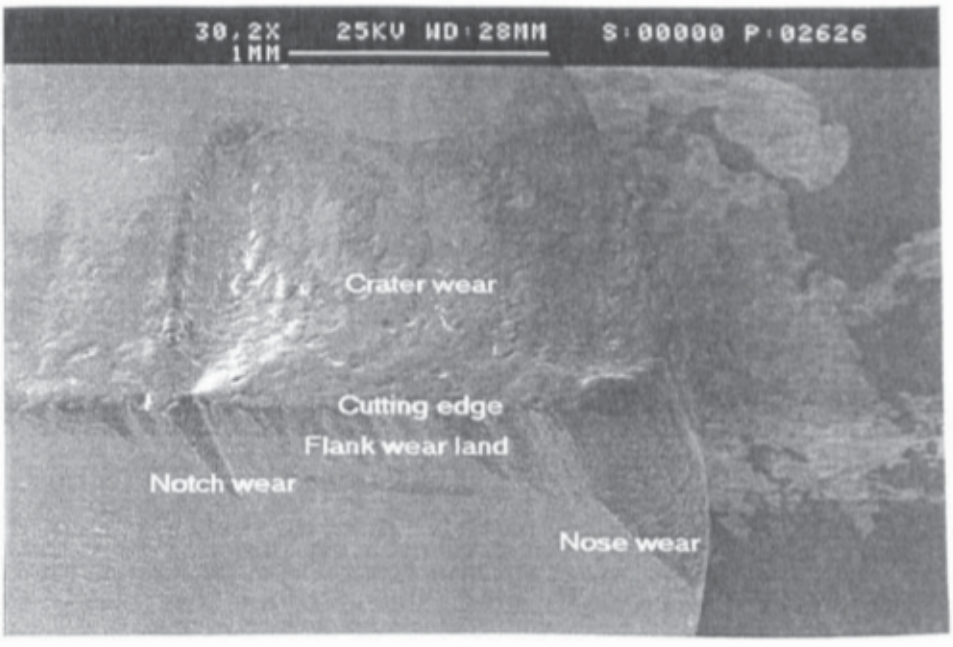

Figure 5.2 Photograph of wear sites in turning

Also measured in the turning operation when possible is nose wear. (Nose wear was not possible to measure because of the tool geometry). Nose radius wear occurs on the flank face near the nose, on the trailing edge near the end of the relief face. It resembles a combined form of flank and notch wear. Severe nose radius wear degrades the machined surface finish.

5.2.3 Protocols

The standard tests strictly define the tool geometry, workpiece, cutting conditions, machine tool characteristics, and tool life criteria needed to construct repeatable tool life curves. They typically use a maximum and average flank wear criterion to define tool life; in the ISO turning test. The flank wear criterion is used because flank wear is normally the most 'desirable' form of wear; the flank wear rate is relatively low and repeatable, so that tools which fail due to flank wear have comparatively long and consistent lives.

The use of a flank wear criterion, however, requires periodic measurement of the wear scar width during testing. Since these measurements must be made off-line with a microscope, such measurements contribute significantly to the time required to perform the tests.

In the above tests, Built-up Edge (BUE), that is, particles adhering to the flank directly under the wear scar can give the appearance of a larger width of the wear scar. This BUE caused a problem by covering the cutting edge.

In order to maintain consistency, the same datum and cutting edge was always used, also the same set up for equipment. The equipment was tested every time before testing the tool, it was reset and a test carried out to make sure that the measurements are correct.

5.3 DRILLING

5.3.1 Standards

Compared to other cutting processes, drilling is manifestly more complex in its tool geometry, such as variation of speed and angles across the lip of the drill, the tool obliquity changing along the cutting edge, and wear measurements are more difficult than in single point turning. As Kaldor et al. (1980) state the twist drill geometry is often referred to as one of the most complicated in cutting tools. In view of this complexity, it is not surprising that little progress has been made in the search of a unified theory of tool-life criteria for drilling (Rubenstein 1991).

The BS and ISO standards that exist as concerning this work for drilling are:

BS 328:1993 - Drills and Reamers. Part 1 - Specification for twist drills (1993)
This standard indicates preferred drill sizes and tolerances as a means of rationalising both the production and the use of drills.

ISO 5419:1982 - Twist drills - Terms, definitions and types (ISO 1982)
This International Standard gives for each of the geometrical terms relative to twist drills, a standard definition which will be valid internationally, the corresponding term being chosen as far as possible in each language in such a way as to be a direct reflection of the meaning of the definition. See appendix 2 for more details on terms and definitions.

An extensive search of literature and checks with the relevant authorities, revealed evidence of no standards, British or International, existing for tool life testing and wear measurement in drilling, and one main reason found for this scarcity is due to the complexity of the drilling operation and the tools (Stephenson 1997, BSI 1997, Howarth 1998).

Having no standards for tool life makes it more difficult for researchers who are testing to know what criteria to test against. Therefore researchers or companies tend to make their own standard, for instance, the concept of the end of tool life is reached when the wear scar covers the land has become like a 'rule of the thumb'. Other investigators that set their own criteria include Boulger (1978) who mentioned three criteria for tool failure: complete destruction of the cutting surface, wear of the tool to the extent that the quality of the machined surface becomes unacceptable, and wear of the tool surface to some predetermined level.

Singpurwalla et al. (1966) suggest other criteria, such as a change of colour of the drill, due to the loss of temper, a change in the sound of the drill, or a complete destruction of the drill, or its inability to drill any further. According to Soderberg (1978), tool life is always defined as the time to failure. Other possible criteria such as flank wear, crater wear or increase in torsional moment show poor correlation with the failure criterion. To Subramanian et al. (1977) failure of the tool was considered as the end of useful life of the drill. Failure of the drill was determined when the tool would not produce a hole. While others considered the number of holes drilled as a tool life criteria.

Other investigators who devised their own method of measuring and calculating flank wear in drilling include Subramanian et al. (1977), where the drill was held vertically and the different wear measurements were made on the flank, using an optical microscope at 5X magnification. The drill was always located in the same direction, using a reference in the shank, so that the successive wear measurements refer to the same cutting edge.

$$\text{Flank wear} = \frac{A+B+C+D}{4}$$

The measuring procedure that Liu et al. (1994) carried out was for both cutting edges of the drill. The measurement was done at three places on each lip as shown in figure 5.3, and average flank wear V_b is calculated as:

$$V_b = \frac{(A+B+C+D+E+F)}{6}$$

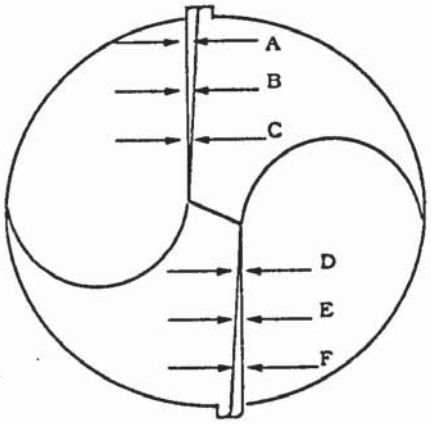

Figure 5.3 Measurement and Calculation of Average Flank Wear (Liu et al. 1994)

All these illustrate how extremely complex things can be without standardisation.

5.3.1.1 Standards Set in This Work

It is important that there should be a standard which others can understand, the following section presents the way the standards were set by the author for measuring wear in the drill in this work.

The method devised for taking the wear measurement in this research is as follows. Six measurements were taken; that is, of the corner, 1 mm and 2 mm from the corner for each lip in the 9 mm drill, in order to know the variation in drill geometry such as the angles and speed. The measurements were chosen as such in order to keep consistency by awareness of the cutting speed, rake angle and flank angle. This can be seen in figure 5.4. Measurements were also taken for the 13 mm drill of the average and maximum flank wear.

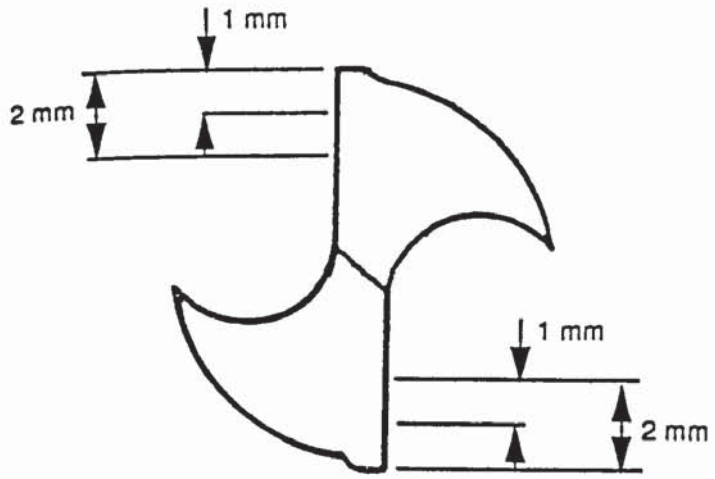

Figure 5.4 Diagram of the wear measurements

In measuring wear it is important that there are standards so that all tests carried out by any individual or organisation can validate it by having followed a certain criteria. Because the measurement of wear scar is very small in dimension; less than 1 mm, therefore there is a need to be highly accurate with the measurements and use highly accurate equipment, because the slightest error in measurement can give a high percentage error. Therefore any slight variations may make a difference in the actual measurement taken. Figure 5.5 shows the equipment used for the measurement of wear in turning and drilling (Swiss Toolmakers Microscope MU-214B with a Sylvac 25 digital probe), and for the angle measurement in drilling. In the photograph, the probe used for measuring can be seen, as well as the electronic display.

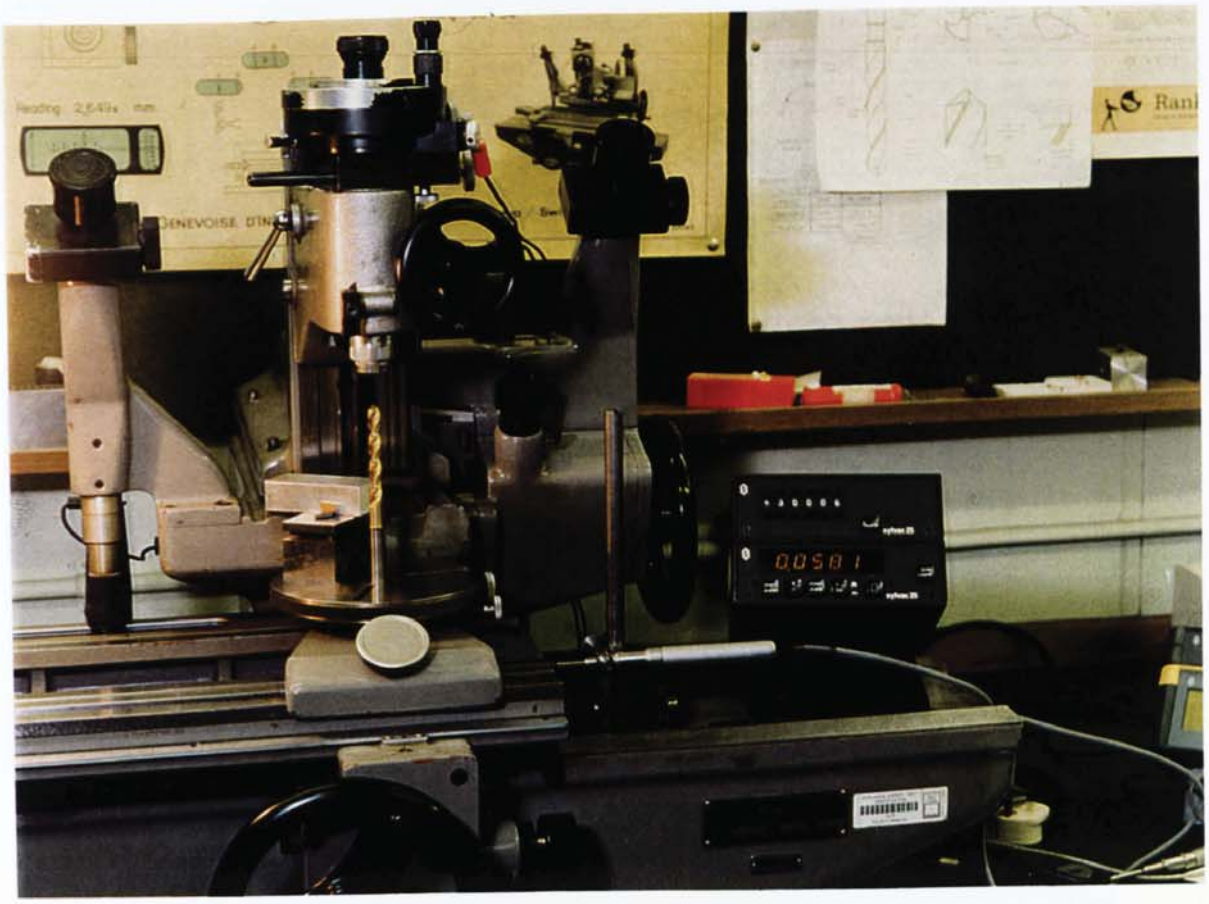

Figure 5.5 Swiss Toolmakers Microscope MU-214B with a Sylvac 25 digital probe.

5.3.2 Sites

As mentioned in the previous section, in the drilling operation, measurements of wear were taken. A measurement of the outer corner wear and land wear was taken for both drill sizes 9 mm and 13 mm. But an average and maximum flank wear measurement was taken only for the 13 mm drill, while for the 9 mm drill a measurement of 1 mm and 2 mm from the corner was taken.

Figure 5.6 shows the sites of drill where the above wear can occur, and figure 5.7 a photograph of the wear sites in drilling can be seen.

Aston University

Illustration removed for copyright restrictions

Figure 5.6 Sites of drill wear (Stephenson et al. 1997)

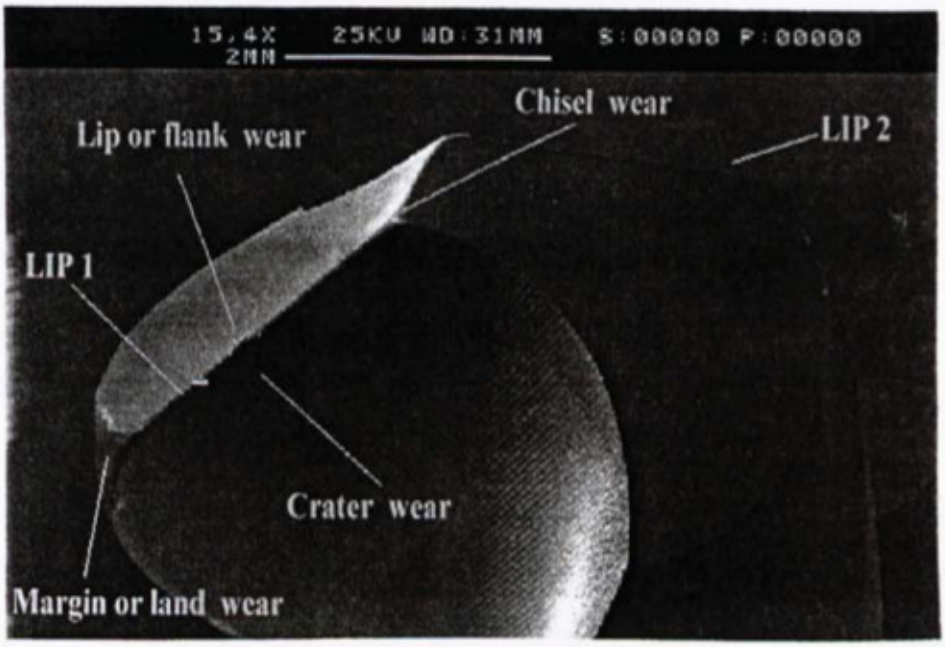

Figure 5.7 Photograph of wear sites in drilling

Lip or flank wear occurs along the relief face of the drill's cutting lips. Margin or land wear occurs at the outer corner of the cutting lip or on the land which contacts the drilled surface.

5.3.3 Protocols

As mentioned above, there are no International or British standardised tests for tool life in drilling. In some cases drills are tested to failure, and the number of holes required to produce failure is the primary test output; the drill thrust force, torque, hole surface finish, or hole diameter may be monitored, however, as an indication of the progress of drill wear throughout the tests.

In this work the techniques that were used were distinct from others, the wear measurements that took place are as mentioned in section 5.3.2. Since the drill geometry varies across the lip, measurements of the corner, 1 mm and 2 mm from the corner were taken in the 9 mm drill in order to keep consistency. Again BUE caused a problem as in turning, by covering the cutting lip.

In order to keep uniformity, the same datum and cutting edge was always used, also the same set up for equipment. In drilling the set up and accuracy of the equipment and how the tests are carried out are important and are checked in the same way as they were for the turning tests.

5.4 CONCLUSION

Therefore, from the above one can see the importance of having standards. The non existence of International or British standards for tool life testing for drilling is confirmed by several sources: the author of this work, Stephenson et al. (1997), Bert Howarth (1998) and BSI (1997). Without having standards to adhere to or to follow, for this research, it is more difficult carrying out tests, for reasons explained above.

It is very important to have standards for such things as tool life testing in order for researchers to follow and to compare results to. In this work the standards and recommended sites were used for turning, but as for drilling and as mentioned above,

although there are recommended sites and some kind of protocols, there are no international standards. Therefore the author has established new standards for measuring wear in this work for drilling as was discussed in more detail above, which may be followed by other researchers when measuring wear in drilling.

Chapter 6

FORCES IN TURNING

6.1 INTRODUCTION

Force is one of the most important variables that describes the characteristics of many mechanical systems and processes, such as machining processes. Cutting forces are of great practical interest. The knowledge of these cutting forces is therefore essential for those involved with the manufacture and design as well as the purchase of machine tools. Cutting forces are also needed for working out power requirements and help in determining the tool geometries. The cutting forces vary with the tool angles, and accurate measurements of these forces would be a helpful factor in optimising tool design.

This chapter examines the results obtained in the experimental activity of this work concerning the forces in single point turning. But in order to place the context clearly, this chapter contains an extension of the early literature to forces in chapter 2, but which is more specific to the material in this chapter. The methods of the measurements of forces can be seen in chapter 4 and figure 4.4 shows the dynamometer for measuring the forces attached to the Torshalla CNC lathe for force measurement.

The forces acting on a cutting tool can be seen in figure 2.14 in chapter 2 and figure 6.1 below. In both oblique and orthogonal cutting conditions, the cutting force generated by the bar's rotation is by far the largest force; it will vary in magnitude depending upon whether a positively or negatively-inclined insert is used. If a positive insert is in use, then a lower force will result, and vice-versa. The feed force is much smaller than the cutting force component, and is determined by the feedrate: if the feedrate is increased, there will be a higher feed force. Thus the feedrate will influence the feed force - but not in isolation, since it will also lead to increases in the cutting force. The radial force is usually assigned to the plan approach angle: as this increases, so will the radial force.

The radial force will occur with both positive and negative plan approach angles. The nose radius of the insert will also produce a small radial force.

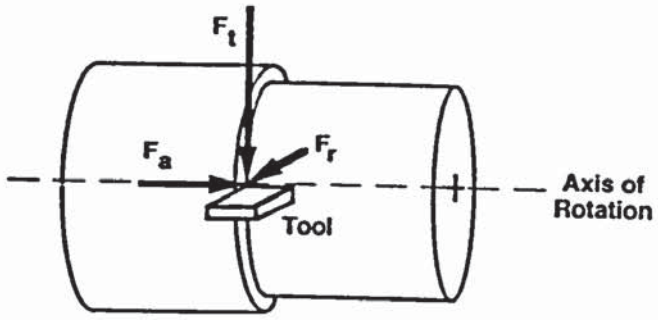

Figure 6.1 Forces on cutting tool (Stephenson et al. 1997)

The forces involved in machining are relatively low compared with those in other metal working operations because the layer of metal being removed, i.e. the chip, is thin. The force required to form the chips is dependent on the shear yield strength of the work material under cutting conditions, and on the area of the shear plane. Trent (1991) points out that in general the shear strength of metals and alloys in cutting has been found to vary only slightly over a wide range of cutting speeds and feeds. The area of the shear plane is very variable, and it is this area which exerts the dominant influence on the cutting force, often more than outweighing the effect of the shear strength of the metal being cut.

6.2 TOOL REGIONS AND FORCES

The forces increase in direct proportion to increments in the feed and depth of cut, which, Trent (1991) argues, are two of the major variables under the control of the machine tool operator. The shear plane angle, however, is not directly under the control of the machinist, and in practice it is found to vary greatly under different conditions of cutting, from a maximum of approximately 45 degrees to a minimum which may be 5 degrees or even less.

Apart from the shear plane angle, the other main region in which the forces arise is the rake face of the tool. Trent (1991) shows that for the simple case where the rake angle is 0 degrees, the feed force is a measure of the drag which the chip exerts as it flows away from the cutting edge across the rake face. The rake angle will be discussed in more detail in a later section 6.4.1 in this chapter.

6.2.1 Shear Plane

In orthogonal cutting the area of the shear plane is geometrically related to the undeformed chip thickness (the feed), to the chip width (depth of cut) and to the shear plane angle.

The force to cause the chip to move over the tool surface is mainly that required to shear the work material in the flow-zone across the area of seizure. Under most cutting conditions, the contribution to the feed force made by friction in the non-seized areas is probably relatively small. The feed force can, therefore, be considered as the product of the shear strength of the work material at this surface and the area of seized contact on the rake face.

In orthogonal cutting the width of the contact region is usually equal to the depth of cut, or only slightly greater, although with very soft metals there may be more considerable chip spread. The length of contact is always greater than the undeformed chip thickness, and may be as much as 10 times longer; it is usually uneven along the chip width, and a mean value must be estimated. The contact area is mainly controlled by the length of contact. It is a most important parameter, having a very large influence on cutting forces, on tool life and on many aspects of machinability.

According to Trent (1991), when the cutting tool is sharp, the forces related to strain on the shear plane and movement of the chip across the rake face of the tool are the only forces which need to be considered. A force must arise also from pressure of the work material against a small contact area on the clearance face just below the cutting edge. This force is small enough to neglect as long as the tool remains sharp and the area of

contact on the clearance face is very small. If use in cutting results in a wearland on the tool parallel to the cutting direction on the clearance face, the area of contact is increased. The forces arising from pressure of work material normal to this unworn surface and movement of the work parallel to this surface may greatly increase. The increment in force may be used to monitor wear on the tool.

6.2.2 Rake Face

The area of contact on the rake face, in some pure metals and alloys e.g. iron, nickel, copper, aluminium etc. is found to be very large, the shear plane angle is small and the very thick, strong chips move away at slow speed, and Trent (1991) argues that the high forces are related to the large contact area.

Reduction in forces by restriction of contact on the rake face may be a useful technique in some conditions, but in many cases it is not practical because it weakens the tool. It must be noted that not all pure metals form such large contact areas with high forces, e.g. when cutting commercially pure magnesium, titanium and zirconium the forces and contact areas are much smaller and the chips are thin.

Wallace et al. (1964) presents an analysis of the physical variables in metal cutting. This allows the force acting on the tool rake face to be separated from the force acting in the region of the tool nose.

In orthogonal cutting, the action of the tool on the workpiece causes a portion of the work to be displaced and to slide up the tool rake face. In figure 6.2, the side view of a tool with the contact area between tool and work material are shown.

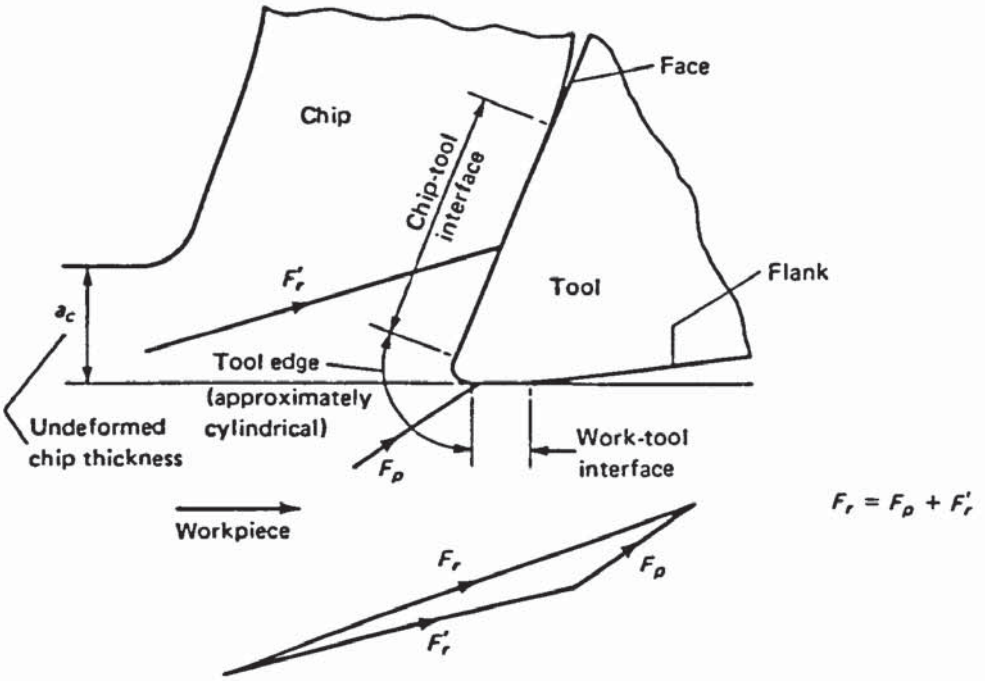

Figure 6.2 Contact regions on a cutting tool (Boothroyd et al. 1989)

Wallace et al. (1964) divided these into two main regions. One is: the rake face of the tool which contacts the chip and transmits most of the force necessary to perform the cutting action. The second region is the tool nose region, which comprises two subsidiary regions:

- The finite radius of the tool edge (the transition surface between the rake and flank faces) which contacts the work material at the point where the chip and workpiece separate,
- A small area on the tool flank face which may rub against the newly cut work surface.

The first complete analysis of the mechanics of orthogonal cutting was proposed by Merchant (1945b). This analysis was based on the model of chip formation as shown in figure 6.3.

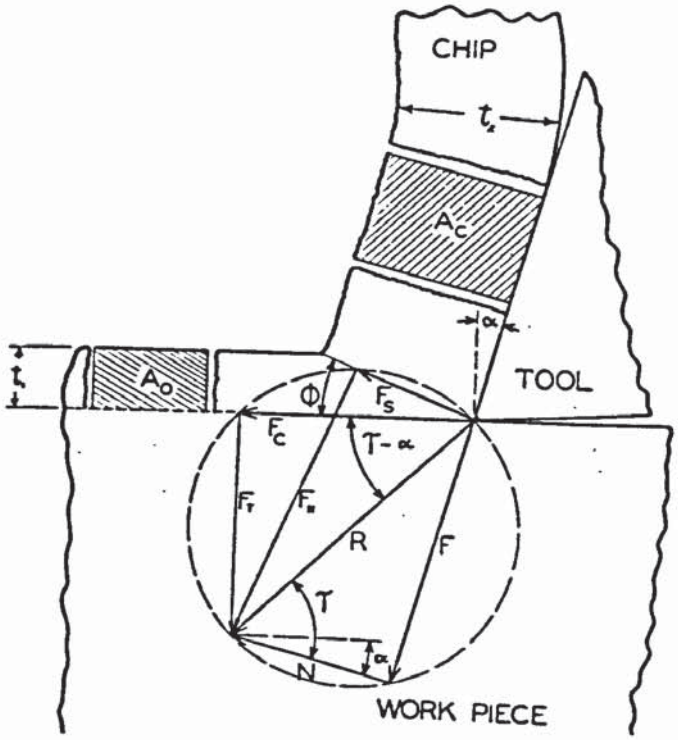

Figure 6.3 Shear plane theory of orthogonal cutting (Merchant 1945b)

Here the metal is assumed to shear across a plane, i.e. the shear plane, extending from the tool edge to the junction of the chip and work surface ahead of the tool. The work materials having passed through the shear plane is then assumed to slide, as a rigid body, up the tool rake face.

6.2.3 Tool Nose

Merchant (1945b) assumed that the force on the tool nose was negligible when the tool had been freshly ground, and hence that the entire resultant tool force could be regarded as acting on the tool rake face. But when calculating the coefficient of friction in this way, it was found to vary considerably with changes in the depth of cut, rake angle, and cutting speed.

The shear strength of the work material on the shear plane was also calculated and it was found that the values obtained increased as the depth of cut became smaller. This apparent dependence of the strength of the material on the depth of cut was not

explained by Merchant (1945b). However, according to Wallace et al. (1964), it was suggested by Backer, Marshall, and Shaw that this increase in apparent shear strength was a 'size-effect' and could be explained by the metal approaching its theoretical strength at very small depths of cut.

Wallace et al. (1964) also state that Kurrein showed that severe localised deformation occurs near the tool nose where the workpiece and chip separate. Since the tool cutting edge can never be perfectly sharp, it is certain that some force acts on the tool nose as it 'ploughs' through the material and rubs against the newly cut workpiece surface. Thus even with a freshly ground tool the total forces applied to the tool during cutting will be transmitted across both contact regions.

Two methods have been proposed in the past for the determination of the nose force (which is the force on the tool nose). First Albrecht (Wallace et al. 1964) suggested that the nose force depended on the radius of the tool nose only and that the rake-face force depended on the depth of cut only. In applying these postulates to experiment Albrecht varied the nose radius from 1 per cent to a maximum of approximately 50 per cent of the depth of cut to determine the nose force. The geometry of the tool rake face was thus altered over a length of up to half the depth of cut by changing part of the rake face into a larger tool nose. Since it has been shown from photoelastic studies that the highest stresses on the tool act near the tool edge, it is likely that alterations of the nose radius by the amounts quoted not only altered the nose force but also the force on the rake face; Albrecht's postulate would therefore appear to be invalid under these conditions.

Another method of evaluating the force on the tool nose was proposed by Takeyama and Usui (Wallace et al. 1964) who controlled the length of contact between chip and tool by grinding back the rake face. They produced variations of the tool force by changes in contact length; it was suggested that the force intercepts at zero contact length were the relevant components of the force acting at the tool nose.

The implication in Takeyama and Usui's (Wallace et al. 1964) analysis was that the force on the tool rake face was a function of the contact length only; as the contact

length approached zero by extrapolation so did the magnitude of the rake-face force. Since the rake-face force is also likely to be a function of the depth of cut, this analysis is incomplete. Considering the results of Takeyama and Usui (Wallace et al. 1964), it can be seen that the tangential component of the resultant tool force is proportional to the contact length and substantially independent of both the depth of cut and the normal force for a given value of contact area.

The assumption made by Wallace et al. (1964) in their previous work, that the entire resultant tool force acts on the rake face has not been supported by experiment. It is assumed in the present work that the resultant force acting on a cutting tool is distributed over both the tool rake face and the tool nose, i.e., over the contact regions.

Wallace et al. (1964) found that when cutting an aluminium alloy a tool force existed which did not act on the tool rake face but on the tool nose. The results indicate that this force was independent of the depth of cut, the chip-tool contact length and the chip thickness, under the cutting conditions investigated.

Wallace et al. (1964) also found that when the force acting on the rake face was used to calculate the specific cutting pressure and the mean shear strength of the work material, both remained constant with respect to depth of cut. The existence of a force on the tool nose, which does not contribute to the removal of the chip, gives an explanation of the apparent variation in the shear strength of the work material with depth of cut found by previous workers.

Dan et al. (1990) found that during external high-feed turning tests, rapid deformation of the tool nose resulted in higher values for the feed force and radial force components.

Taibi (1994) states that the effect of the tool nose was analysed by Wu (1989) when the resultant force in the feed direction and resulting from the material deformation under the cutting edge was assumed to be proportional to the deformed volume of the work material. The vertical nose force was determined from the feed force by assuming a constant friction angle along the contact area. Theoretical predictions were compared to

previously published data and showed good prediction of the dynamic force variation in both feed and cutting direction. However, in this model, the friction coefficient along the flank was assumed constant and its values were determined from published data. Moreover, the derivation of the vertical force from the feed force was then made by neglecting the roundness of the cutting edge and by considering the tool flank parallel to the mean cutting direction.

Cutting theory to date has been concerned with analyses of the chip flow on the tool rake face using a perfectly sharp tool. Some efforts have been put forward to introduce the effect of the radius of the cutting edge. None of the existing theories have provided an analytical formulation of the forces acting on the tool nose and the secondary edge of the cutting tool. Moreover, analytical formulations of these forces have to be developed to account for the flank wear effect.

Taibi (1994) in his investigation has shown the possibility of machining forces during turning by considering both contact between the tool and the chip along the rake and the deformation around the tool nose and along the flank of the tool. He attributed the former action to the shearing process and the latter to the ploughing mechanism.

Taibi's (1994) dynamic force model considers the effect of the indentation around the nose of the cutting edge. As the tool moves into the work material, a certain amount of material deforms elastically and plastically because of the roundness of the cutting edge leading to additional forces upon the flank face of the tool. These forces will act as a positive damper thus increasing the stability of the machining systems. The turning force is therefore the resultant of the turning force along the rake face of the tool responsible of the shearing process and of the ploughing force acting along the flank face of the tool.

The cutting forces are affected by several parameters such as feed rate, depth of cut, cutting speed and tool geometry.

6.3 TOOL GEOMETRY

In turning, the insert geometry can be extremely varied, with a wide range of shapes, nose radii, plan approach angles, angular inclination etc.

6.3.1 Rake Angle

Tool geometry also influence the tool forces, the most important parameter being the rake angle. As a more positive angle is used the chip is deformed less and both cutting force and feed force are lower (a bigger decrease in the cutting force). However, at high positive rake angles the strength of the tool edge is weakened and thereby creating conditions of tool failure. The strongest tool edge is achieved with negative rake angle tools, and these are frequently used for the harder grades of carbide and for ceramic tools which lack toughness. The high forces make negative rake angle tools unsuitable for machining slender shapes which may be deflected or distorted by the high stresses imposed on them.

Taibi (1994) found that in the presence of the BUE, the effective rake angle appreciably increases over its nominal value set by the tool geometry. He argued that the dynamic force is dependent on both the tool displacement and the velocity of the tool vibration. Moreover, the expressions of the turning force components show that an increase the tool rake angle results in a decrease of the effect of the velocity of the tool vibration.

Cherry (1961) argued that no appreciable reduction in cutting force is shown when rake is increased beyond 20 degrees, and since tool failure is mainly the result of the friction heat generated by the cutting force, no advantage is to be gained by increasing rake angle beyond this point; indeed, this will only reduce the heat dissipation capacity of the tool section and so reduce tool life.

Bailey (1975) argues that tool forces are important in machining because they determine the energetics of the process. For a given work-tool combination tool forces depend on

tool geometry, depth of cut, width of cut, feed, cutting speed and the type of chip produced.

In contrast to previous studies, Bailey (1975) suggested that the friction depends on the tool rake angle and upon the cutting conditions. It has been generally observed that an increase in the tool rake angle at constant cutting speed produces a decrease in the mean coefficient of friction and in the resulting cutting forces. According to Bailey (1975), Zorev (1966) observed that the mean friction angle depends also on the depth of cut because of the presence of the forces on the tool nose. Nonetheless, Taibi (1994) argues that when the tool forces are corrected for the presence of the tool nose forces, the mean friction angle becomes independent of the depth of cut. However, at small depths of cut, a BUE tends to develop on the rake of the tool which changes the effective rake and henceforth affects the calculated values of the friction angle. He shows that the force acting on the tool nose and along the clearance face of the tool decreases for higher clearance angle and, for a constant depth of cut, this force is decreasing as the tool vibration increases.

6.3.2 Other Angles

Depending on the plan approach angle, the cutting action of the insert will be orthogonal or oblique. Other changes in practical cutting geometries such as changes in plan approach angle, clearance angle, and tool corner radius have virtually no effect on the magnitude of the cutting forces with the exception of depth of cut for which increases in force are proportional to increases in depth. Taylor (1962) argues that the clearance angle variations have little effect on the cutting forces.

6.4 CUTTING CONDITIONS

6.4.1 Cutting Speed

It is a common experience, when cutting most metals and alloys, that the chip becomes thinner and forces decrease as the cutting speed is raised. Trent (1991) shows that the decrease in both cutting force and feed force with cutting speed is most marked in the low speed range. This drop in forces is partly caused by a decrease in contact area and partly by a drop in shear strength in the flow-zone as its temperature rises with increasing speed.

Alloying of a pure metal normally increases its yield strength, but often reduces the tool forces, because the contact length on the rake face becomes shorter. Trent (1991) demonstrated that in each case the tool forces are lower for the alloy than for the pure metal over the whole speed range, the difference being greatest at low speeds. With steels, a BUE forms at fairly low speeds and disappears when the speed is raised. Where it is present the forces are usually abnormally low because the BUE acts like a restricted contact tool, effectively reducing contact on the rake face.

Amongst many others, Pashby (1992) has investigated the effects of workpiece material, machining conditions and tool geometries on the forces produced in single point turning. He found that at low cutting speed the presence of BUE restricts the contact length between the chip and tool rake face, resulting in a decrease in the expected value of force.

Mills et al. (1983) argue that increases in cutting speed in general reduce both the tangential and normal cutting forces but the effect is usually small. It is argued that as the cutting speed is increased, the temperature in both the primary and secondary deformation zones rises and this results in a 'softening' of the workpiece.

Taibi's (1994) study of the steady state turning process showed two distinguishable cutting speed regions. At the low cutting speed region, the magnitudes of the cutting

force components fluctuate following a certain pattern as the cutting speed increases. This is due to the presence of the BUE during machining. At the low cutting speed region, the fluctuation pattern of the measured force is actually dominated by the fluctuation pattern of the height of the BUE versus the cutting speed. At the high cutting speed region, BUE disappears and the magnitude of the turning force components decreases as the cutting speed increases owing to the effect of the temperature which softens the workpiece material flowing through the cutting zone. The obtained dynamic turning force components however show different tendencies with the cutting conditions from what was shown by the steady state forces.

At low cutting speeds, it is well known that a BUE is increasing in size and after reaching a maximum of size this part of workpiece metal is torn away by the flowing chip and a new edge starts to build-up on the rake of the cutting tool. Moreover, it is also well known that the machining force components are decreasing with the size of the BUE. The instantaneous variation of the size of the BUE will lead therefore to important perturbations in the dynamic turning force through its effect upon the instantaneous rake angle.

6.4.2 Cutting Feed

The contact length between the chip and the tool is increased when the feed rate increases which causes the forces to rise. Trent (1991) argues that machining of materials with high stresses on the shear plane subsequently results in a large amount of heat generated in the cutting zone. With the increase in heat the yield strength of the tool material drops rapidly. Kopalinsky et al. (1984) suggest that the main factor which causes the force ratio of feed force to cutting force to increase as the undeformed chip thickness decreases is the temperature at the tool-chip interface.

Trent (1991) concludes in his stress analysis of metal cutting under seizure conditions that the contact area on the tool rake face is seen to be a most important region, controlling the mechanics of cutting. This is the reason for lower cutting forces for materials which have discontinuous chips.

6.4.3 Cutting Fluid

Finally, the contact length and tool forces may be greatly influenced by cutting lubricants (Trent 1991). In relation to forces, lubricants can act to reduce the seized contact area, and thus the forces acting on the tool. They are most effective in doing this at low cutting speeds and become largely ineffective in the high speed range (Dan 1990).

6.5 TOOL WEAR

The research work for determining the correlation between cutting forces and tool wear started some years ago. The relationships between tool wear and cutting forces have been extensively investigated. Cutting forces, Dan et al. (1990) argue, change as the tool wears and have often been used to detect tool wear in the laboratory.

There have been many attempts at using force patterns as an indication of tool wear for the turning processing. A force tranducer was developed to measure the dynamic forces from the chip formation process. This sensor used a piezo electric element which, when dynamically compressed, produced an electrical output, proportional to the dynamic forces transmitted through it. Extensive cutting tests have shown that it could be used to indicate flank wear.

Dan et al. (1990) report that some experimental results showed that the feed and thrust forces are influenced much more by tool wear than the main cutting force. Some results showed regimes where a linear relationship between these forces and tool wear existed. Yet another method using force measurements is based on an experimental result that the pattern of the curve which shows the relationship between the feed force and the feed per revolution is strongly influenced by tool wear (Dan et al. 1990).

Dan et al. (1990) also state that another study has contradicted the above findings and showed that the main cutting force gave the best indication of tool wear at any given

time, and that the radial and feed force components were not suitable for in-process monitoring of tool wear. The feed force showed a linear relationship with flank wear up to a limit of 0.508 mm of the average flank wear width, while heavily depending on the feed rate. At low feed rates, such as those used in finish turning, the increase in feed force due to flank wear was so small that difficulties were encountered in its detection, and that the radial force showed no notable change with the progression of tool wear. The high frequency component and amplitude of feed force were found to keep increasing during the normal wear stage, whilst subsequently decreasing during advanced wear or when breakage took place.

According to Dan et al. (1990), there has however been one early work that claimed that it was impossible to derive accurate information on tool wear based on measurements of cutting forces in turning, where it was shown that significant increases in force occurs only at the moment of tool failure. This technique is therefore limited to detect failure only and not wear in its many forms.

Extensive practical experience and a number of experimental studies, such as that of Kobayashi et al. (1960), indicate that flank wear is strongly related to the increase in force on the tool.

In the cutting operation, the tool initially makes a line contact with the new work surface, and removing a chip having a rectangular cross section. MacAdams et al. (1961) assume that, as the tool wears, a wearland develops on the tool flank, so that the worn tool makes an area of contact with the new work surface.

Merchant (1945a) analysed the forces acting on a cutting tool. The chip is held in equilibrium by the action of two equal and opposite resultant forces. The forces are assumed to be collinear and it is assumed that the chip is of continuous type without BUE. The tool is ideally sharp, in that it presents a line contact with the new work surface. The vertical force is the same as the feed force, and the horizontal force on the shear plane is the same as the cutting force, as seen in figure 6.3. But MacAdams et al. (1961) argue that since the tool dulls with time, a more realistic view is, of a worn tool

and in which the feed force acting on the tool is shared between the shear plane and the wearland. The vertical force on the shear plane is less than the applied force.

The conventional analysis of forces on an ideally sharp cutting tool has been extended to a tool exhibiting flank wear. If constant tool rake angle, friction angle, and shear angle are assumed, then it can be concluded that tool depth of cut is proportional to that part of the feed force acting on the shear plane. If one assumes that the friction process is adequately described by Shaw et al. (1955), then for a constant applied feed force the depth of cut is a linear function of the area of the wear land, provided the shear stress required to rupture the friction welds remains constant and that the welded fraction of the real contact area does not change.

Various tool wear monitoring techniques have been developed to enhance the operation efficiency of automated manufacturing systems. Among these techniques, cutting forces have been often used to monitor the evolution of tool wear due to the simplicity, fairly straightforward means of measurement, and close association with the tool condition. Tool wear monitoring based on the cutting force response relies mainly on the observation that the cutting forces increase with the real contact area on the flank face, whereas rake face wear reduces the cutting forces since it increases the effective rake angle (Cho et al. 1988). Another characteristic feature is that the feed force gradient at the beginning of each cutting pass increases with tool wear.

Approaches based on mechanistic models have been used to determine the cutting forces for various tool materials and cutting conditions. Koren (1987) developed an on-line method that predicts tool wear from the cutting force response and distinguishes the effect of tool wear on the cutting forces from that due to variations in cutting depth. This method has been extended by Koren (1991) to include the effects of feed rate and cutting speed. Ko et al. (1989) proposed a model that relates the change of the cutting forces to the amount of wear occurring on the nose and the flank face. Nair (1992) studied the effect of feed rate on the cutting forces of unworn tools and obtained a linear relationship between the cutting force and the cross-sectional area of the uncut chip. Danai (1992) adopted this model to simulate the variation of the cutting force with the

feed rate. However, the previous models are based on the assumption that rake face wear is negligibly small compared to flank face wear (Cho et al., 1988).

Findings vary significantly among the various investigators concerning how much tool wear influences the increase in the cutting forces. As a rule of thumb, Lee et al. state that for each 0.1 mm width of wear land, the tangential force increases typically by 10%, the feed force by 25% and the radial force by 30%. Tarman et al. in 1974 and Wolf et al. in 1981, according to Taibi (1994) used the increase of the cutting force with the increase of the contact between the tool and the workpiece to monitor the tool wear. This relationship is not as simple as first appears, as, while the cutting forces are sensitive to tool wear they are also sensitive to changes and variations in the cutting conditions, tool geometry, tool and workpiece material. To overcome the influence of some unneeded parameters, some workers (Mackinnon et al. in 1986 and Goforth et al. in 1983) tried to use the ratio between the components of the machining force instead of their amplitudes. This technique presents the same difficulties in tool wear prediction as the cutting conditions and the changes in the tool geometry lead to different tendencies in variations of the machining force ratio (Taibi, 1994).

Furthermore, Taibi (1994) found that the sensitivity of increase of turning force components depends upon the amount of wear and the cutting speed. At low cutting speed the feed force increases by 40% while at higher speeds as 7.27 m/s it increases by 94% as the wear increases up to 280 μm. Whereas, for the same increase of flank wear, the cutting force increases by 14.5% when cutting at 2.28 m/s and by 7.31% at cutting speed of 7.27 m/s. The sensitivity of the feed force to flank wear is increasing while that of the cutting force is decreasing with cutting speed. No consistent trend can be found between the sensitivity of flank wear increase and feed rate. In other words, the variation of the turning force components with flank wear does not appear to be a simple linear function of the feed. Similar results were obtained by Shi (1990) where feed force was found to increase more rapidly with flank wear than the cutting force.

It is shown, by Taibi (1994), that feed force is more suitable for flank wear monitoring at high speed and flank wear levels while at low speeds and low values of flank wear

cutting force is more convenient for wear monitoring. Both feed and cutting force are linearly increasing with flank wear for constant cutting conditions.

However, as experimental results (Ridley 1982) show the feed force is more sensitive to flank wear than the cutting force, it is therefore understandable that there is a deformation of the material in the feed direction. This deformation results in an additional feed force by resistance of the work material to deformations and in a tangential or vertical force introduced by friction (Lau & Rubenstein 1972) (Taibi 1994).

At high values of flank wear the dynamic turning force components are expected to decrease with subsequent flank wear. Lee (1989) analysed the dynamic feed and cutting forces when the flank wear is varied up to 700 μm. In their experimental results the dynamic components of turning force were found to decrease rapidly for flank wear above 500μm, a decease which was attributed to the chipping of the cutting edge.

Oraby et al. (1991) found that one technique for tool wear detection and breakage involves the measurement and the use of cutting forces (Oraby 1991, Ravindra et al. 1993), even though it has been agreed among many investigators that the change of tool forces represent an accurate and reliable approach to assess tool wear and failure, disagreement still exists over which force component (or combination) is the most sensitive and reliable (Ravindra et al. 1993). The force variation during cutting has been found not only to correlate well with the wear level on the clearance face but also to be very sensitive to any tiny disturbances such as tool chipping and machining instability. Each of the feed force and the radial force are found to be very sensitive to the gradual progress of tool wear and fracture. The nose wear has the strongest influence on the force components with its highest effect on the radial force. The flank wear equally affects both the feed and the radial forces. The notch wear has the least effect on all force components Oraby et al. (1991) argued.

Cutting forces change as the tool wears, and are often used to detect the tool wear during machining. Major flank wear and crater wear have been found to be the most significant factors influencing cutting forces. Many experimental results Fang (1994) argues have

shown that among three components of cutting forces, the force in the feed force is most affected by the change of tool wear situation as it is directed on the major flank. However, a contradictory finding, that feed and radial forces are not significantly sensitive with the progression of tool wear, especially for low feed conditions, has also been reported. The explanation given for this by Fang (1994) is that the complex relationship between cutting force components and tool wear is also dependent on the combined effects of work material properties, cutting tool materials and variations of other machining conditions.

The existence of increasing wear rates is not inconsistent with the observed data on cutting forces; it is a matter of common experience that the force increases as the tool becomes blunted through use (Taylor 1962). Cutting force components have been found by Lee et al. (1989), and Ravindra et al. (1993) to correlate well with progressive wear and tool failure. The cutting force generally increases with flank wear due to an increase in the contact area of the wear land with the workpiece. Zorev (1966) and De Filippi and Ippolito (1969) according to Nair et al. (1990), were among the first who demonstrated the direct effect of flank wear on the cutting force.

6.6 TOOL/WORK MATERIAL

Tool wear is influenced by the characteristics of the tool-work material pair and working conditions. Among the tool-work material characteristics, material hardness plays a significant role. Variations in work material hardness (hot hardness) have been shown to be a contributing factor for stochastic variations in tool life. Further, the mean and variance of tool life are functions of cutting conditions.

Forces are a function of cutting conditions, properties of tool and work material, structural rigidity of the machine, status of lubrication etc. Hence the direct use of forces will require a threshold based on the working conditions. The effects of feed and speed on forces have been indicated from such data, it is possible to model forces as functions

of cutting conditions. The effects of other variables, such as tool and work materials, status of lubrication etc., are more subtle and complex and difficult to quantify.

According to Trent (1991) the tool material can also influence the tool forces, when one major type of tool material is substituted for another, the forces may be altered considerably, even if the conditions of cutting and the tool geometry are kept constant. This is probably caused mainly by changes in the area of seized contact.

Gorczyca (1987) states that the mechanics of the cutting process deals primarily with the analysis of the forces acting between the tool and the work material. By analysing forces that act in particular directions relative to the tool and work material, we can gain insight into a basic understanding of the cutting process.

Cutting forces reflect the effectiveness of the cutting tool as well as the resistance that the work material offers to the cutting operation.

Beside the shear process occurring in the cutting zone, contacting deformation of the workpiece material and the tool also occurs in the contacting area between the tool and the workpiece as a result of the ploughing process. Because the hardness of the workpiece material is relatively low with respect to the hardness of the tool material, the occurrence of the contacting deformation is mostly on the workpiece side. The turning force components affected by the contacting deformation is the feed force, the magnitude of which can be increased because of the material work hardening during the ploughing process. The degree of the ploughing process affects more the turning force components at low frequencies as the deformation can be considered as a relatively slow process.

Different factors such as the existence of soft or hard particles in the work material and the machine structure are responsible for the tool oscillation during machining. When the tool wear is introduced the metal cutting configuration becomes more complicated and demanding for close analysis. As the flank wear is usually modelled by a flat

surface, corresponding to zero degrees of flank angle, the trace of the work surface will be geometrically the same as the geometry of the cutting edge.

By using a coated carbide tool at a lower depth of cut, the coating peels off and the tool itself does not wear (Ravindra 1993).

6.7 EXPERIMENTAL RESULTS AND DISCUSSION

More details about the experimental methods and equipment can be seen discussed in chapter 4, and the test conditions for the turning tests can be seen in appendix 1 tables A1.1 to A1.1.

6.7.1 Uncoated BT42 HSS

6.7.1.1 Effect of feed rate and cutting fluid

The graphs shown in figures 6.4 and 6.5 are forces vs. cutting speed. The uncoated BT42 HSS tool material was machined using four different speeds: 10, 20, 30 and 40 m/min. The rake angle was 6°, the flank angle 5°, depth of cut 2 mm, and the nose radius 0.4 mm. Two different feed rates were used 0.15 and 0.18 mm/rev., both of which were used with and without coolant. Therefore all conditions used in both the graphs were the same but figure 6.4 shows the cutting force vs. cutting speed while figure 6.5 shows the feed force vs. cutting speed. (See appendix 1 tables A1.5 to A1.8 for test conditions).

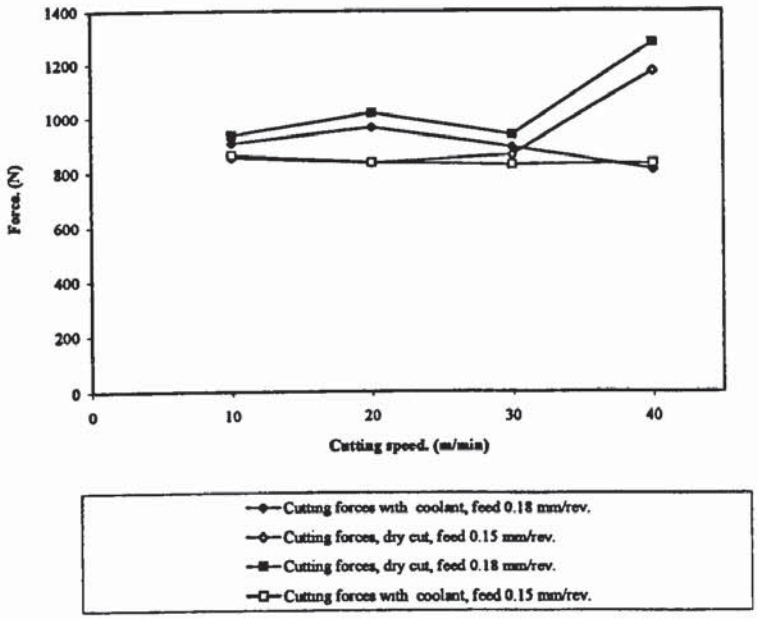

Figure 6.4. Force *vs*. cutting speed for uncoated BT42 HSS insert, with 2 mm DOC, 6 &5 deg. rake and flank angles, 0.4 mm nose radius.

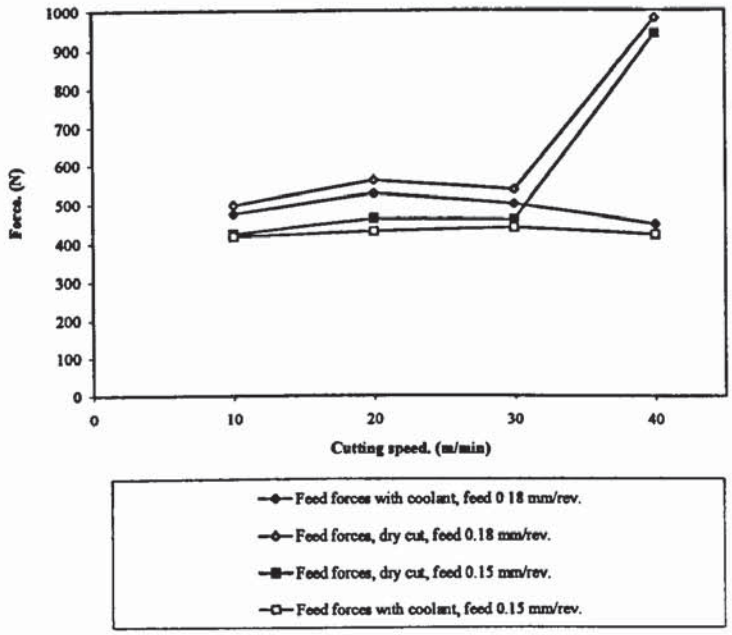

Figure 6.5. Force *vs*. cutting speed for uncoated BT42 HSS insert, with 2 mm DOC, 6 &5 deg. rake and flank angles, 0.4 mm nose radius.

The effect of feed rate on the cutting forces can be seen in both figures. When using the feed rate of 0.18 mm/rev., it is seen that both the cutting forces and feed forces are higher for the speeds of 10, 20 and 30 m/min. than when using 0.15 mm/rev. feed rate. The increase in the feed rate results in higher force generation as is also shown by Trent (1991), due to the increase in the contact length between the chip and the tool.

But at the speed of 40 m/min., it can be seen that both forces are higher when the cut was dry. Again, for this speed, both forces are also higher when using 0.18 mm/rev. feed rate than when using 0.15 mm/rev. feed rate.

The forces in the dry cut are higher than when using coolant due to tool wear acceleration which causes tool failure.

Trent (1991) shows that when cutting at very low speed the lubricant may act to prevent seizure between the tool and work and thus greatly reduce the forces.

Although the difference between the two feed rates is not great, the difference which they cause in the forces is still significant. Therefore if the feed rates used were very different than one can expect that they will produce forces which are of greater difference.

6.7.2 Coated BT42 HSS

6.7.2.1 Effect of cutting speed

Figure 6.6 shows the forces vs. cutting speed. the tool material used was coated BT42 HSS at speeds of 30, 40, 45, 50, 60, 65 and 70 m/min. The feed rate was 0.18 mm/rev., rake angle 6° , flank angle 5° , depth of cut 2 mm, and nose radius 0.8 mm with coolant. (See appendix 1 tables A1.5 to A1.8 for test conditions).

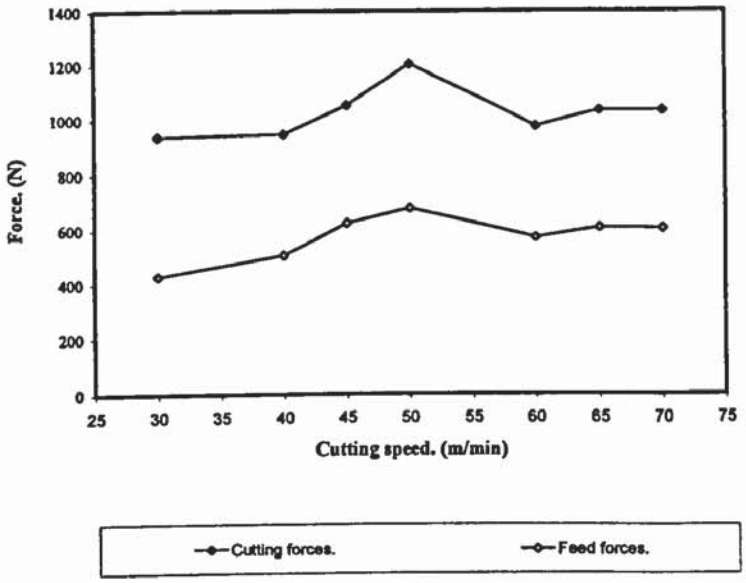

Figure 6.6 Force *vs*. cutting speed for coated BT42 HSS insert, 6 & 5 deg. rake & flank angles, DOC 2 mm, 0.8 mm nose radius, feed rate

It can be seen that both cutting and feed forces increase to a maximum at the cutting speed of 50 m/min., then at 60 m/min. they begin to decreases again. This is due to the change of the wear mechanism with the cutting speed and the effect of BUE, different types of wear mechanisms can be seen in figures 6.42, 6.43, 6.44 and 6.45.

The drop in forces, Trent (1991) argues is partly caused by a decrease in contact area and partly by a drop in shear strength in the flow zone as its temperature rises with increasing speed.

This is a common experience, Pashby (1992) also suggested the cutting forces is seen to fall because the chip becomes thinner as the speed rises and the higher temperatures present at high speed reduces the strength of the material.

It has been determined by many workers that the cutting forces are directly proportional to the length of contact between the chip and the tool. This means that the materials producing discontinuous chip generate very low cutting forces. As the cutting speed increases there is a corresponding increase in the shear angle, which helps generate thinner chips resulting in a considerable reduction in the contact length and hence cutting forces. The tool forces rise as the tool is worn out because the area of contact at the clearance face increases.

6.7.2.2 Effect of cutting fluid

In figure 6.7 the forces vs. cutting speed for coated BT42 HSS is shown. The speed used was 10, 30, 50 and 60 m/min. The feed rate was 0.15 mm/ rev., the rake angle 6°, the flank angle 5° , the depth of cut 2 mm and the nose radius was 0.8 mm. The speeds of 10, 30 and 50 m/min. were carried out in dry conditions and with using a coolant. But for the speed of 60 m/min, the tests were carried out only with a coolant. (See appendix 1 tables A1.5 to A1.8 for test conditions).

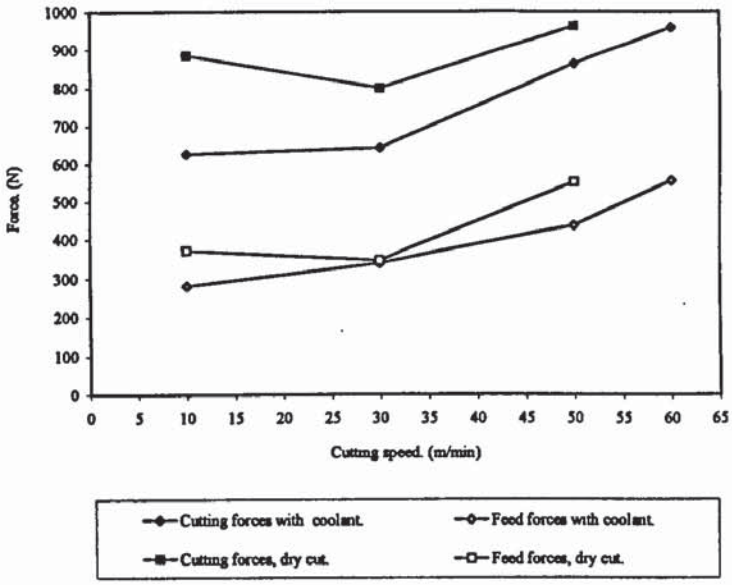

Figure 6.7 Force vs. cutting speed for coated BT42 HSS insert, 6 & 5 deg. rake & flank angles, DOC 2 mm, 0.8 mm nose radius, feed rate

The effect of using a coolant can be shown in this figure. The cutting forces and the feed forces are lower when a coolant is used. in both cases however, that is testing in a dry cut and using a coolant, the forces start high, they then decrease at the cutting speed of 30 m/min. and start to increase again at the cutting speeds of 50 and 60 m/min.

This can only be caused by the temperature which affects wear mechanism, as seen in figures 6.37 to 6.46 and therefore affects the forces. This influence of the temperature on the wear mechanisms is discussed in more details in chapter 8.

6.7.3 M2 HSS

6.7.3.1 Effect of depth of cut on forces

Forces vs. cutting speed is shown in figure 6.8. M2 HSS billet was used with the cutting speeds of 10, 20, 30 and 40 m/min, and a feed rate of 0.18 mm/rev. rake angle of 15°, and flank angle of 8°.Two depths of cuts were used: 2 mm and 1 mm with coolant. (See appendix 1 tables A1.1 to A1.4 for test conditions).

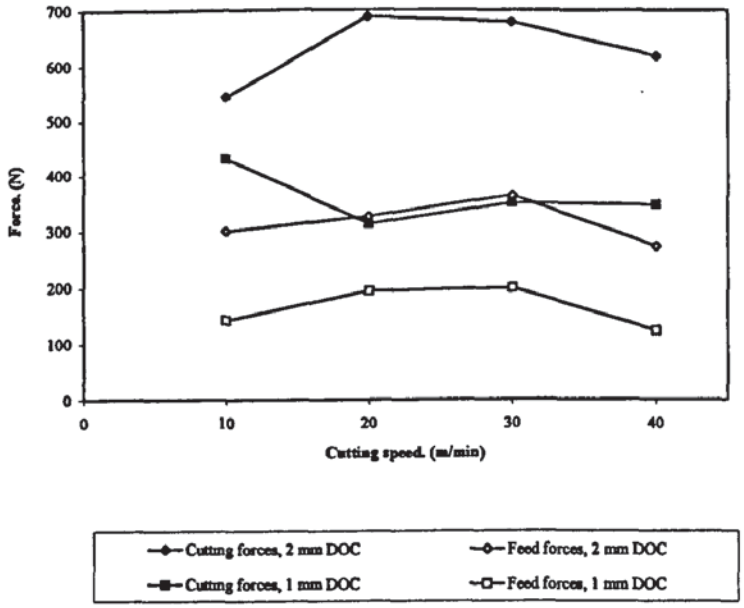

Figure 6.8. Force vs. cutting speed for M2 HSS billet, 15 & 8 deg. rake & flank angles, feed rate 0.18 mm/rev., with cooling.

This figure shows the effect of depth of cut on cutting forces. It can be seen clearly from this figure that a 2 mm depth of cut the forces are much higher than for a depth of cut of 1 mm for both cutting forces and feed forces for the four different cutting speeds.

Once again it is seen at 40 m/min cutting speed the forces decrease for both depth of cuts, this is caused by the temperature which effects the wear mechanism, as shown in figure 6.45. Rahman (1988) has also noticed that as the depth of cut increases, the forces increase.

6.7.3.2 Effect of flank angle on forces

The effects of flank angle on forces can be seen in figures 6.9 to 6.12.

The forces vs. cutting speed are shown in figures 6.9 to 6.12. M2 HSS billet was used for four different speeds: 10, 20, 30 and 40 m/min. A feed rate of 0.15 mm/rev. was used and a depth of cut of 2 mm in a dry cut. The flank angles were varied at 5° , 10° and 15° . In all four figures the tests used the same conditions except the rake angles were fixed at 6°, 10° , 30° and -6° for figures 6.9, 6.10, 6.11 and 6.12 respectively. (See appendix 1 tables A1.1 to A1.4 for test conditions).

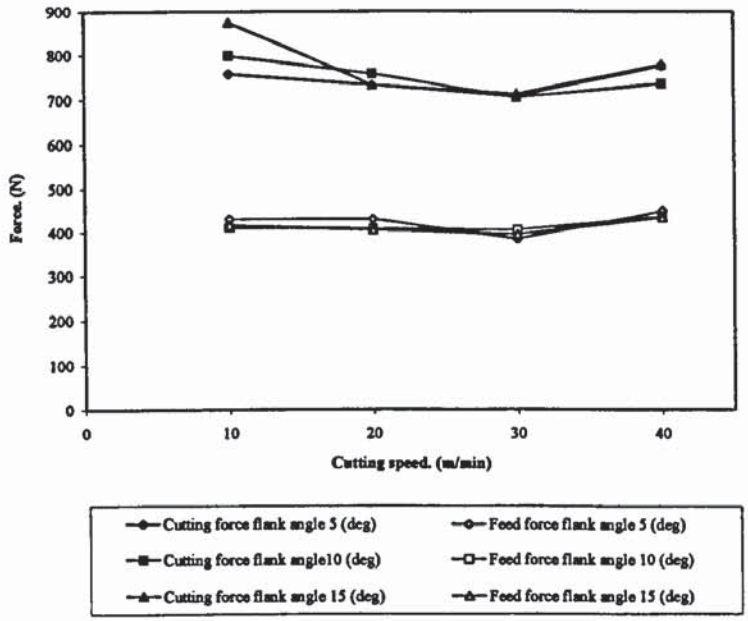

Figure 6.9. Force *vs*. cutting speed for M2 HSS billet, 6 deg. rake angle, DOC 2 mm, feed rate 0.15 mm/rev., dry cut.

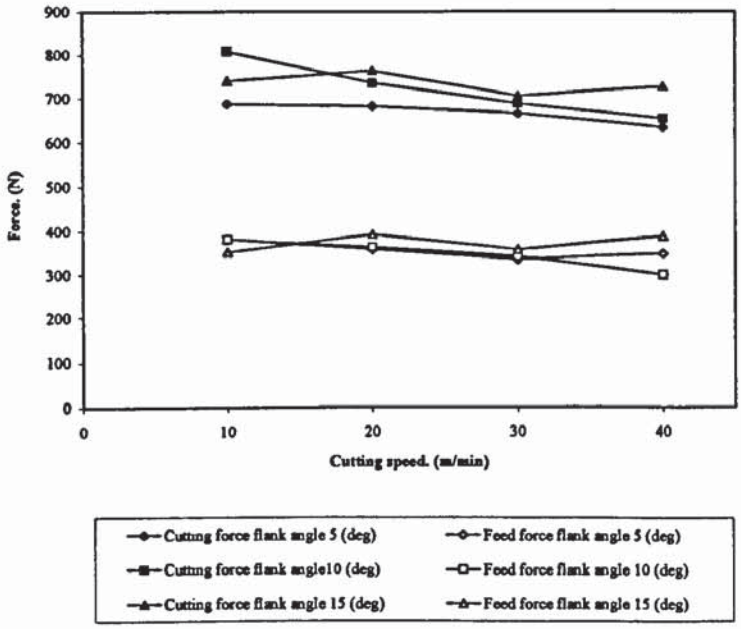

Figure 6.10. Force *vs*. cutting speed for M2 HSS billet, 10 deg. rake angle, DOC 2 mm, feed rate 0.15 mm/rev., dry cut.

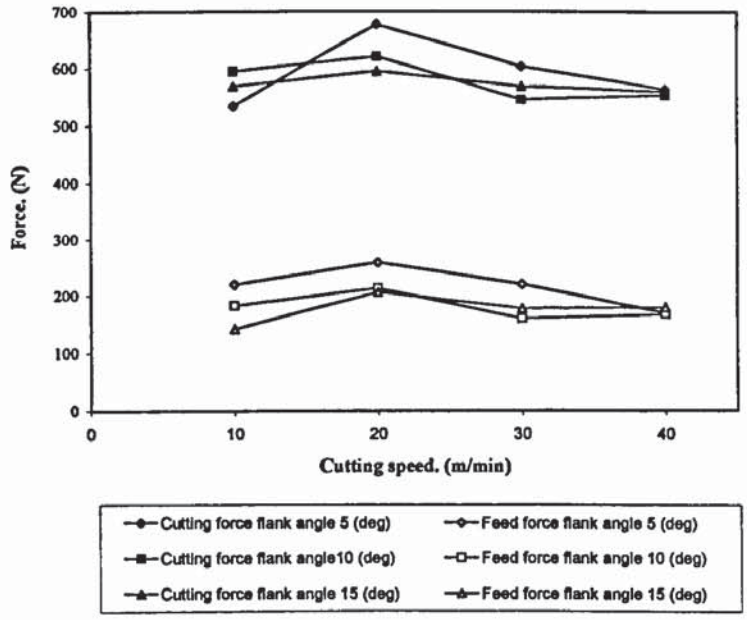

Figure 6.11. Force *vs*. cutting speed for M2 HSS billet, 30 deg. rake angle, DOC 2 mm, feed rate 0.15 mm/rev., dry cut.

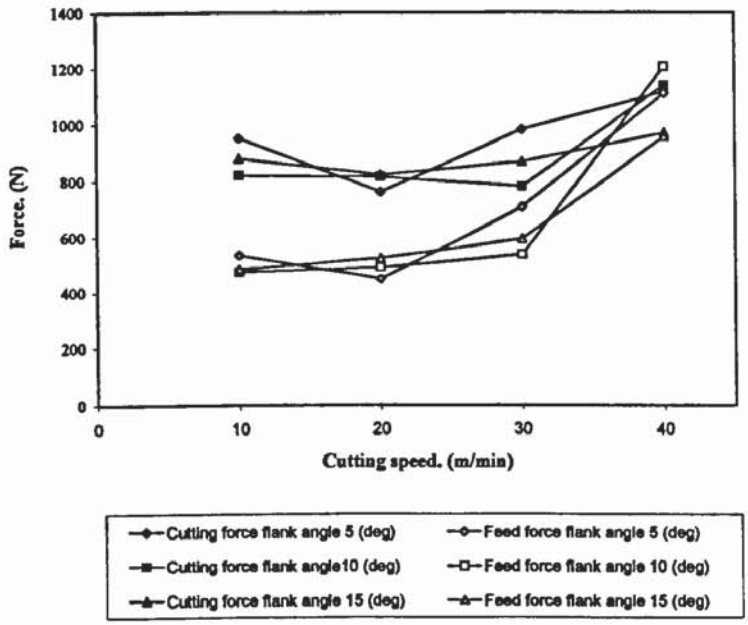

Figure 6.12. Force *vs*. cutting speed for M2 HSS billet, -6 deg. rake angle, DOC 2 mm, feed rate 0.15 mm/rev., dry cut.

By fixing the rake angle (as mentioned above for each test) and changing the flank angle from 5°, 10° and 15°, it is seen that for all four cutting speeds for the four figures the cutting and feed forces are very similar. It can, therefore, be concluded that, as expected, for the above conditions, flank angle variation has no effect on both the cutting and feed forces.

6.7.3.3 Effect of rake angle on forces

Figures 6.13 to 6.18 show the effect of the rake angle on forces. (See appendix 1 tables A1.1 to A1.4 for test conditions).

Figure 6.13, 6.14, 6.15, 6.16, 6.17, and 6.18 show the force vs. cutting speed for M2 HSS billet using four different speeds: 10, 20, 30 and 40 m/min., with a feed rate of 0.15 mm/rev., and a 2 mm depth of cut at dry cut. The rake angles were varied at 6°, 10°, 30° and -6°. All the above conditions were similar for all the graphs the only difference is that the cutting and feed forces are shown in separate figures, and the flank angles were fixed at 5° for 6.13 and 6.14 for cutting force and feed force respectively. A flank angle of 10° was fixed for figures 6.15 and 6.16 for cutting force and feed force respectively

and a flank angle of 15° was fixed for figures 6.17 and 6.18 for cutting force and feed force respectively.

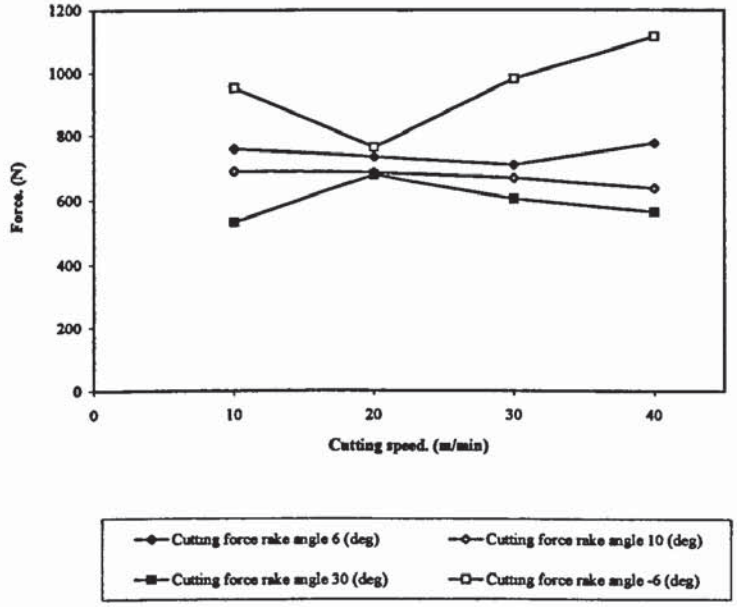

Figure 6.13. Force *vs*. cutting speed for M2 HSS billet, 5 deg. flank angle, DOC 2 mm, feed rate 0.15 mm/rev., dry cut.

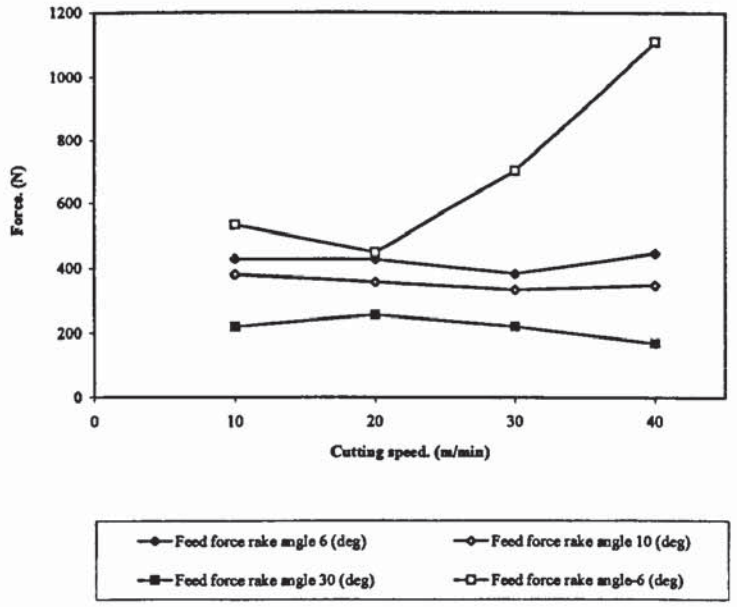

Figure 6.14. Force *vs*. cutting speed for M2 HSS billet, 5 deg. flank angle, DOC 2 mm, feed rate 0.15 mm/rev., dry cut.

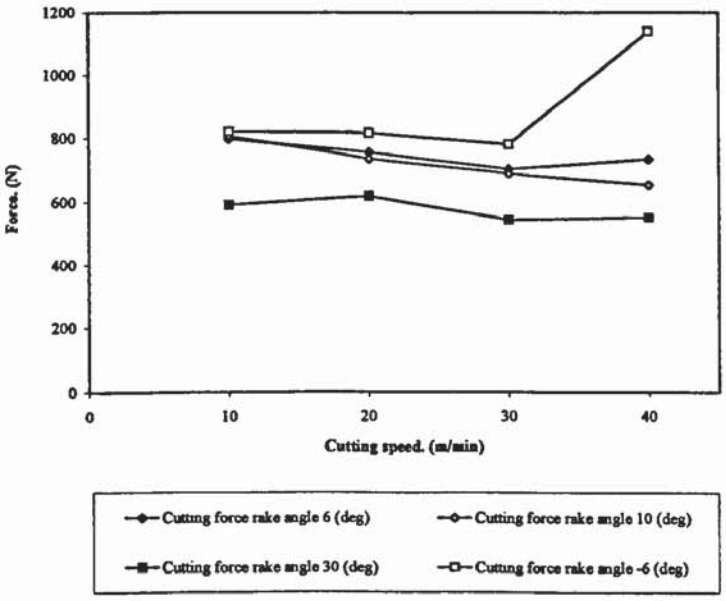

Figure 6.15. Force *vs*. cutting speed for M2 HSS billet, 10 deg. flank angle, DOC 2 mm, feed rate 0.15 mm/rev., dry cut.

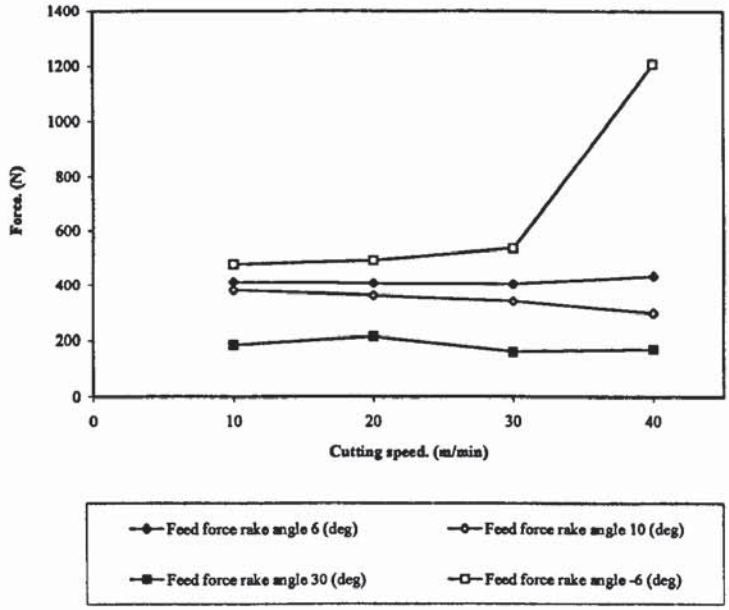

Figure 6.16. Force *vs*. cutting speed for M2 HSS billet, 10 deg. flank angle, DOC 2 mm, feed rate 0.15 mm/rev., dry cut.

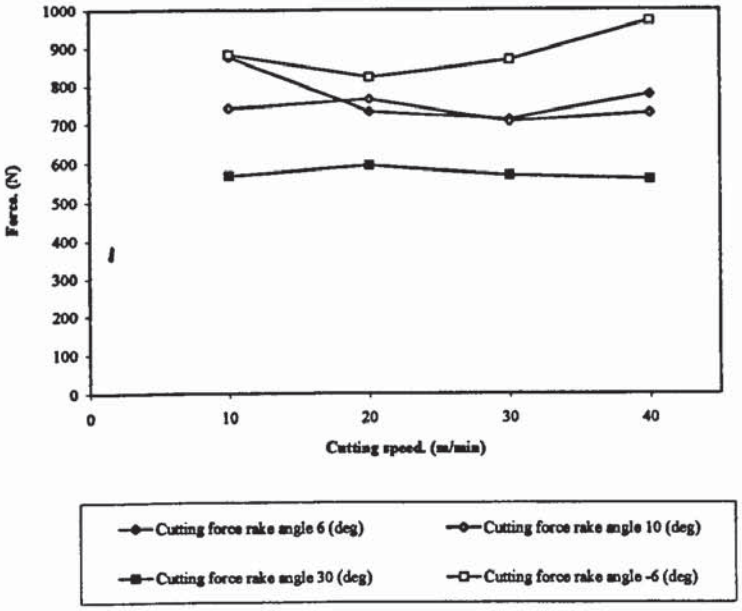

Figure 6.17. Force *vs*. cutting speed for M2 HSS billet, 15 deg. flank angle, DOC 2 mm, feed rate 0.15 mm/rev., dry cut.

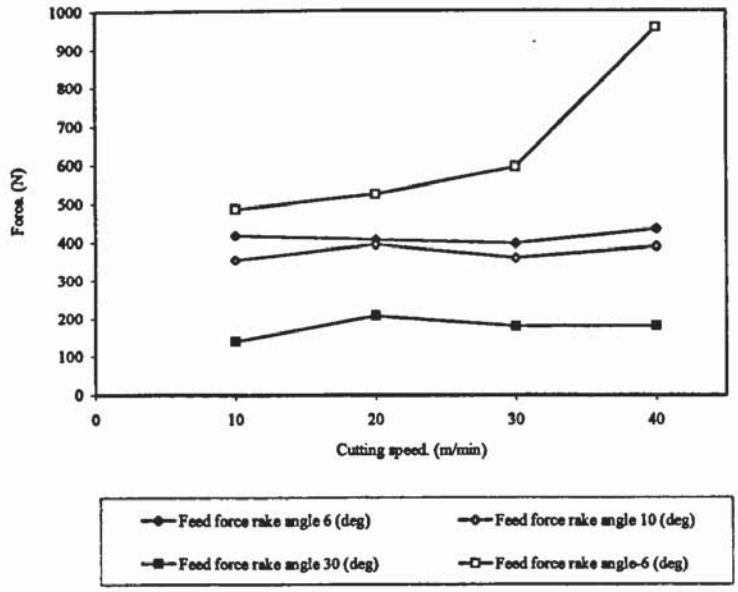

Figure 6.18. Force *vs*. cutting speed for M2 HSS billet, 15 deg. flank angle, DOC 2 mm, feed rate 0.15 mm/rev., dry cut.

The tests were to see if the rake angle has any effect on the forces. From all the figures it can be seen that by changing the rake angle the forces change.

For all the four cutting speed, in all the figures when the rake angle is at 30° then the forces are lowest than at the other three rake angles. At -6° rake angle the forces were the highest compared to the others. This effect was similar for both cutting and feed forces.

Smith (1989) shows that by using negative geometry inserts, a large wedge angle occurs, they must be inclined in order to give a clearance angle to avoid rubbing on the workpiece. This inclination produces a strong blunt edge and causes the cutting forces to be increased accordingly, so a rigid machine-tool structure and higher power are required than if a positive geometry insert is used.

Positive inserts allow a smaller wedge angle to be utilised, resulting in lower cutting forces and less tendency for vibration because the shear plane is reduced. The main drawback with positive inserts is that, owing to the smaller wedge angle, tool life is reduced if heavy roughing cuts are taken.

Taibi's (1994) results also agree with these results, he suggests that the increasing characteristic of the forces curves can be attributed to the decrease in the effective rake angle, resulting from the decrease of the BUE size by the increase of the cutting speed.

6.7.4 Carbide tools

Three different carbide tool materials were tested: KC850, K68 and K313, and the results shown in figure 6.19 for force vs. cutting speed. The cutting speeds used were: 30, 40, 50, 60 and 70 m/min. with 0.18 mm/rev feed rate, 6° rake angle, 5° flank angle and 2 mm depth of cut using coolant. (See appendix 1 tables A1.9 for test conditions).

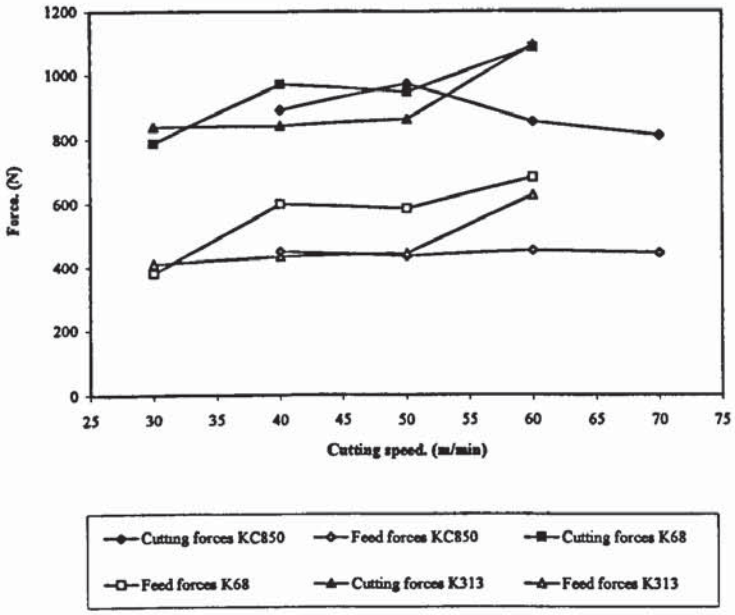

Figure 6.19 Force *vs*. cutting speed for carbide insert, 6 & 5 deg. rake & flank angles, DOC 2 mm, feed rate 0.18 mm/rev., coolant.

The speeds of 40, 50, 60 and 70 m/min. were used for KC850 while for K68 and K313 the speeds used were 30, 40, 50 and 60 m/min.

As can be seen from the figure 6.19 that there is not much change for the cutting force and feed force for the above test conditions for the three carbide material.

The force vs. cutting speed can be seen in figure 6.20 for the carbide tool materials. K68 and K313 for cutting speeds of cutting speeds of 40, 50 and 60 m/min. The test conditions used were: 0.15 mm/rev feed rate, 6° rake angle, 5° flank angle, 2 mm depth of cut at dry cut.

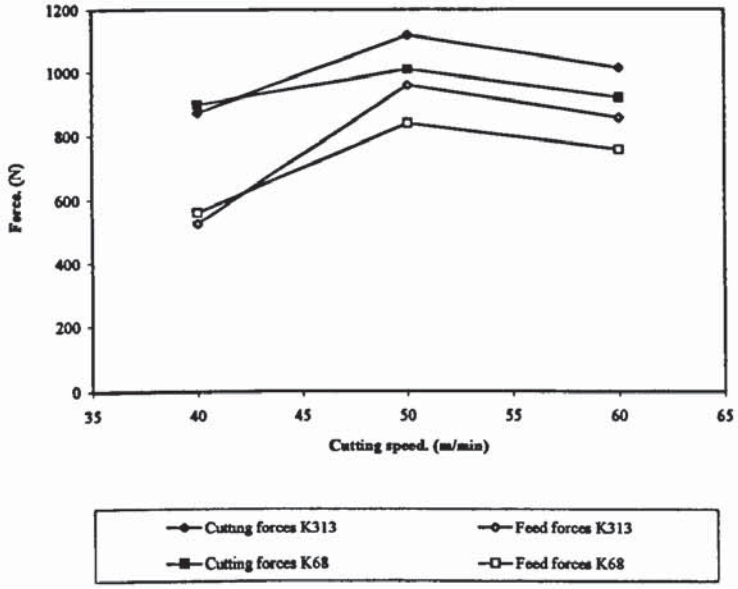

Figure 6.20 Force *vs*. cutting speed for carbide insert, 6 & 5 deg. rake & flank angles, DOC 2 mm, feed rate 0.18 mm/rev., dry cut.

Both cutting and feed forces begin to decrease at the cutting speed of 60 m/min, again this is due to the temperature which affects the wear mechanisms.

6.7.5 Effect of wear on the forces

6.7.5.1 Uncoated BT42 HSS

figures 6.21, 6.22, 6.23 and 6.24 show the force vs. average flank wear for cutting speeds 10, 20, 30 and 40 m/min respectively for uncoated BT42 HSS insert. The feed rate used was 0.15 mm/rev, the rake angle 6^{o} , the flank angle 5^{o} , the depth of cut 2 mm, and the nose radius 0.4 mm at dry cut. (See appendix 1 tables A1.5 to A1.8 for test conditions).

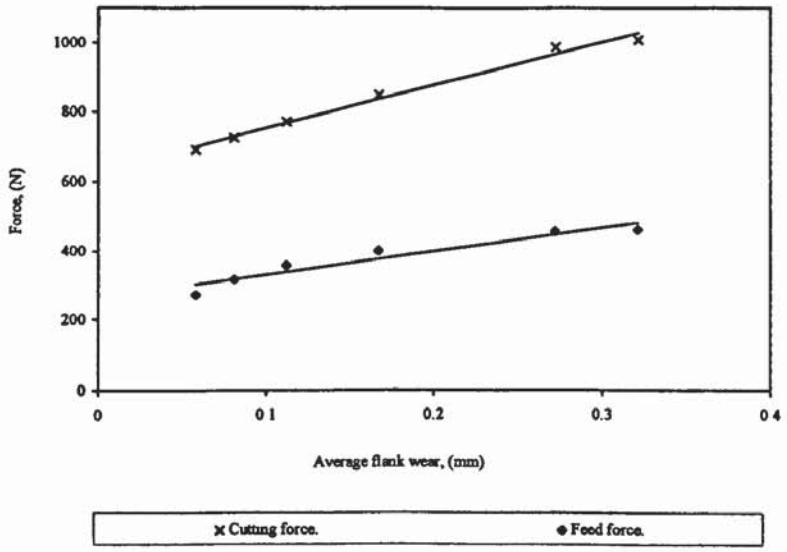

Figure 6.21. Force *vs* . average flank wear for uncoated BT42 HSS insert, at cutting speed of 10/min., with 2 mm DOC, 6 & 5 deg. rake & flank angles, 0.4 mm nose radius, feed rate 0.15 mm/rev., dry cut.

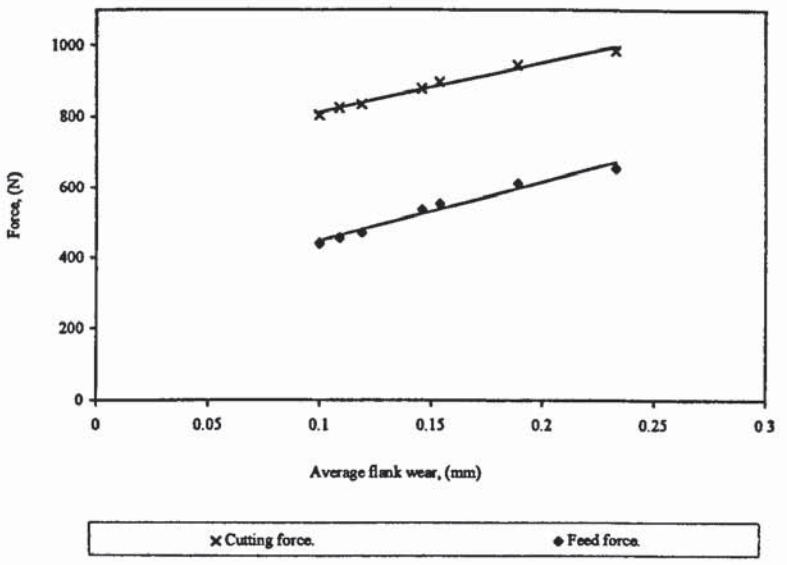

Figure 6.22. Force *vs* . average flank wear for uncoated BT42 HSS insert, at cutting speed of 20/min., with 2 mm DOC, 6 & 5 deg. rake & flank angles, 0.4 mm nose radius, feed rate 0.15 mm/rev., dry cut.

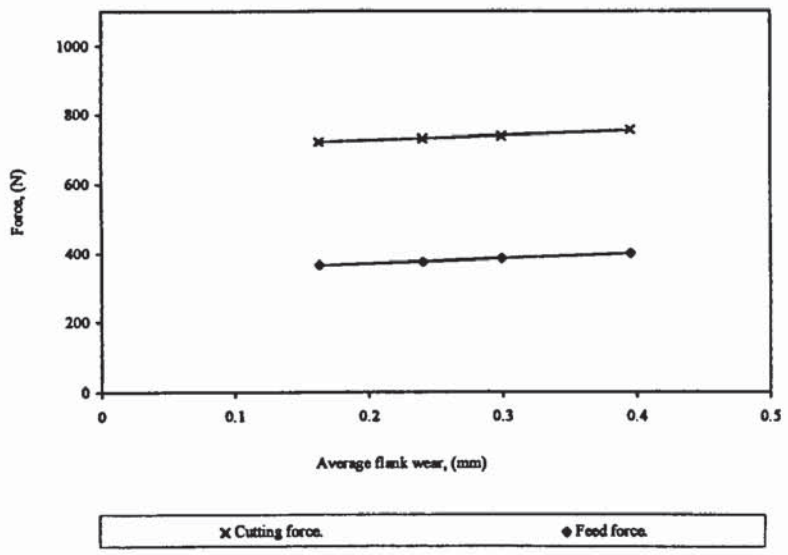

Figure 6.23. Force *vs*. average flank wear for uncoated BT42 HSS insert, at cutting speed of 30/min., with 2 mm DOC, 6 & 5 deg. rake & flank angles, 0.4 mm nose radius, feed rate 0.15 mm/rev., dry cut.

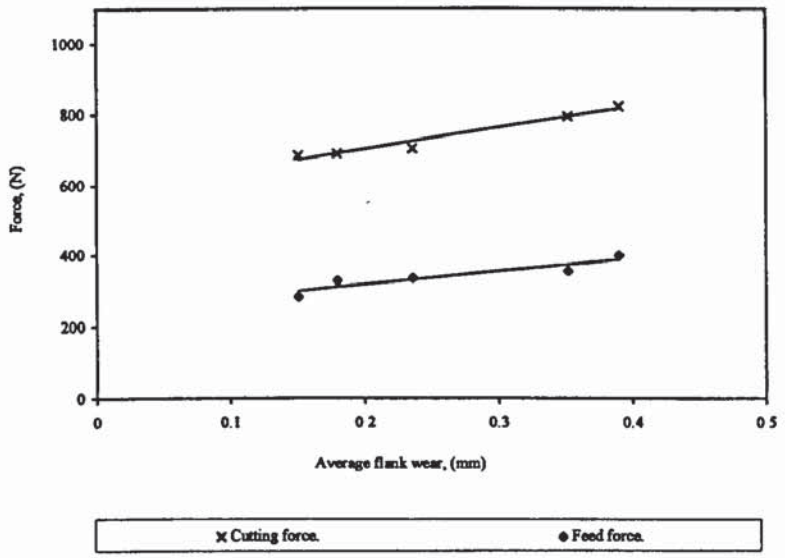

Figure 6.24. Force *vs*. average flank wear for uncoated BT42 HSS insert, at cutting speed of 40/min., with 2 mm DOC, 6 & 5 deg. rake & flank angles, 0.4 mm nose radius, feed rate 0.15 mm/rev., dry cut.

For the four figures it is seen that the cutting forces and feed forces increase with the increase in the average flank wear. But the rate of increase for the four speeds can be seen to differ when comparing the four graphs. For instance, at figures 6.21 and 6.22 where the cutting speeds are 10 and 20 m/min respectively, as the average flank wear is increased both cutting and feed forces show a steep increase, very rapidly. While in figure 6.23 for the cutting speed of 30 m/min by increasing the average flank wear there

is a steady increase in both cutting and feed forces. This is put down to the speed, temperature and wear mechanism. At the speed of 40 m/min in graph 6.24 again the difference from the other three figures is due to the speed, temperature and wear mechanism which can be seen in figures 6.45 and 6.46.

Many investigators argue that as flank wear increases so do the forces. Takeyama et al (1963) showed that cutting forces exhibit a good linear correlation with the rate of tool wear but results obtained by Filippi and Ippolito indicated a wider scatter (Lee 1986).

As the tool wear the contact area between the tool and the workpiece increases which tends to increase the cutting forces.

Taibi's (1994) results agree with these, it can be seen that both cutting and feed forces are increasing with flank wear as expected. As the flank wear increases, the volume of the deformed material increases. This leads to an increase in feed force as the resistance of the material to deformation is in the direction of the feed.

Flank wear Lim et al. (1993a) argue, generally causes an increase in the cutting force and the interfacial temperature, leading normally to dimensional inaccuracy in the workpieces machined and to vibration which makes the cutting operation less efficient. It has been observed that under conditions of flank wear during cutting, forces tend to increase with increase in tool wear.

6.7.5.2 Coated BT42 HSS

The two figures of 6.25 and 6.26 show the force vs. average flank wear for coated BT42 HSS insert for cutting speeds of 10 m/min and 30 m/min. respectively. The feed rate of 0.15 mm/rev was used and the rake angle of 6^{o} , flank angle 5^{o} , depth of cut of 2 mm, nose radius of 0.8 mm with dry cut were used. (See appendix 1 tables A1.5 to A1.8 for test conditions).

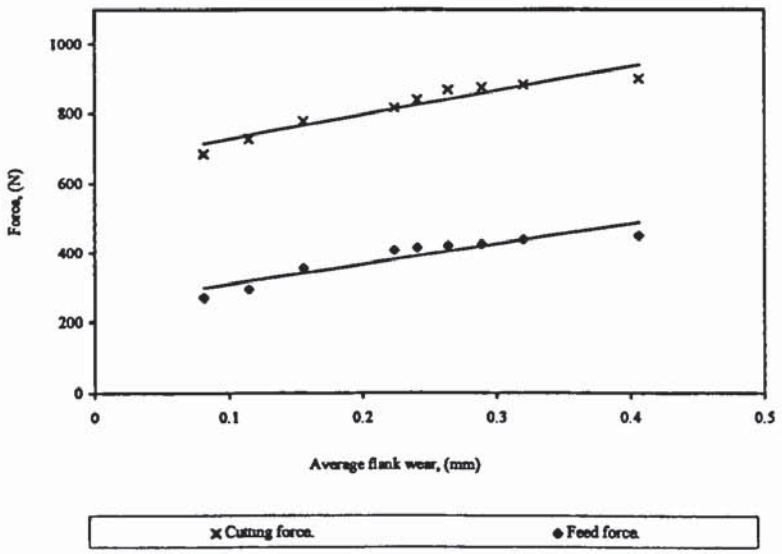

Figure 6.25. Force *vs*. average flank wear for coated BT42 HSS insert, at cutting speed of 10/min., with 2 mm DOC, 6 & 5 deg. rake & flank angles, 0.4 mm nose radius, feed rate 0.15 mm/rev., dry cut.

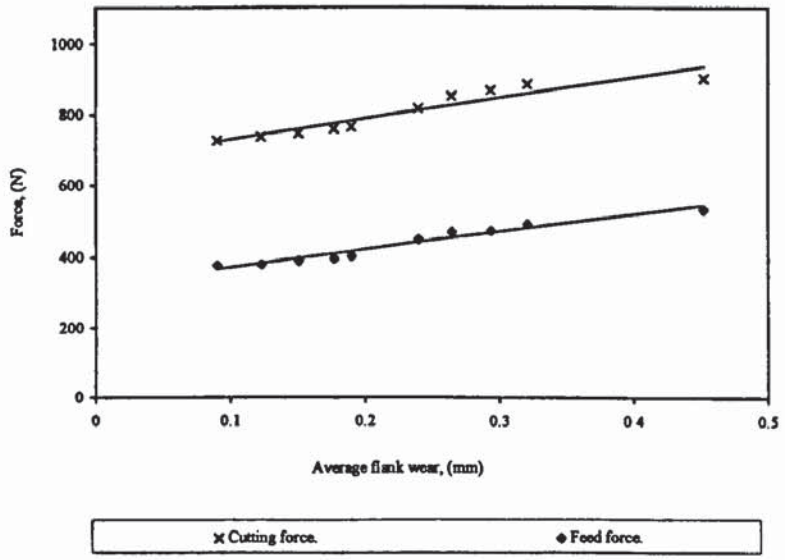

Figure 6.26. Force *vs*. average flank wear for coated BT42 HSS insert, at cutting speed of 30/min., with 2 mm DOC, 6 & 5 deg. rake & flank angles, 0.4 mm nose radius, feed rate 0.15 mm/rev., dry cut.

For the two graphs the increase in average flank wear can be seen to increase both the cutting and feed forces. Both graphs are very similar, which means one can say that under these similar test conditions similar wear mechanisms are acting.

The increase in feed force with wear is highly dependent upon the cutting conditions.

6.8 SEM PHOTOGRAPHS AND DISCUSSION

6.8.1 General Tool Wear

In this figure 6.27, a general view of the cutting edge and flank face, of the tool material BT42 HSS, is shown and it is evident that there is breakage on the cutting edge. The cutting speed was 10 m/min.

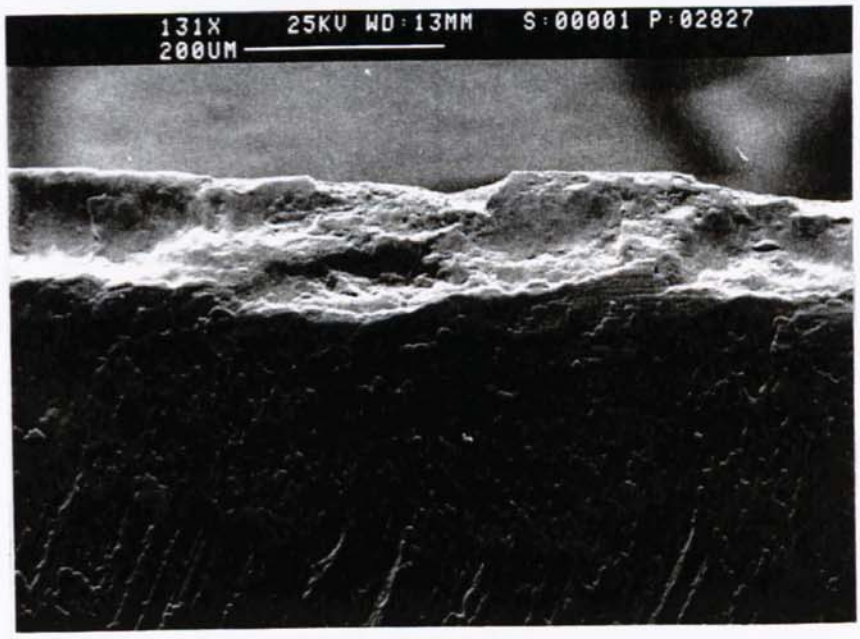

Figure 6.27 Uncoated BT42 HSS, cutting speed 10 m/min, rake angle 6°, flank angle 5°, and feed rate 0.15 mm/rev.

A general view of the cutting edge of M2 HSS can be seen if figure 6.28. The cutting speed used for this test was 20 m/min. In the SEM figure the cutting edge can be seen to have been chipped out.

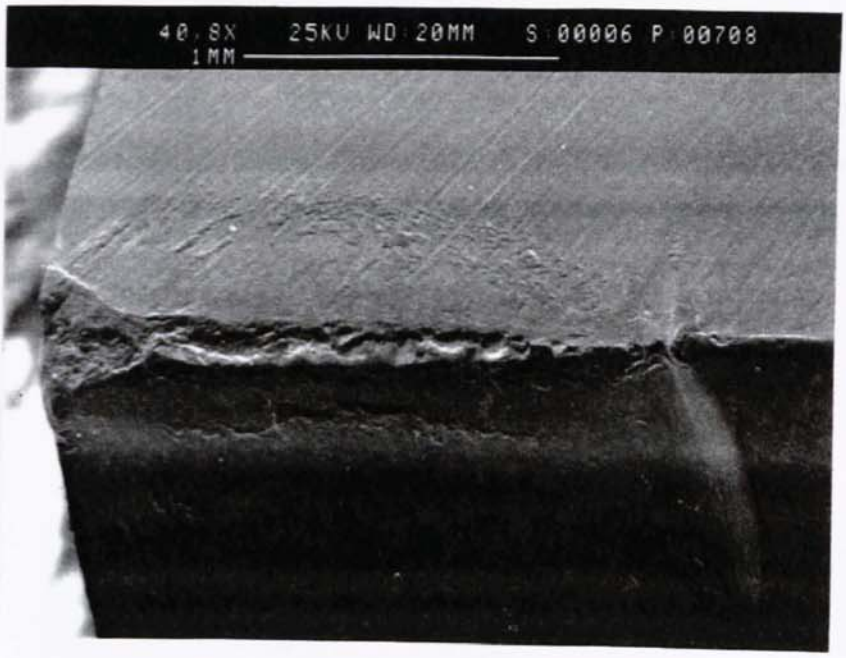

Figure 6.28 M2 HSS, cutting speed 20 m/min, rake angle 5°, flank angle 10°, and feed rate 0.15 mm/rev.

6.8.2 Build-up Edge

The material adhering to the flank and cutting edge of M2 HSS at the cutting speed of 20 m/min can be seen in figure 6.29. It can also be seen that by having the material which is adhered to the flank wear, the flank wear may be difficult to measure.

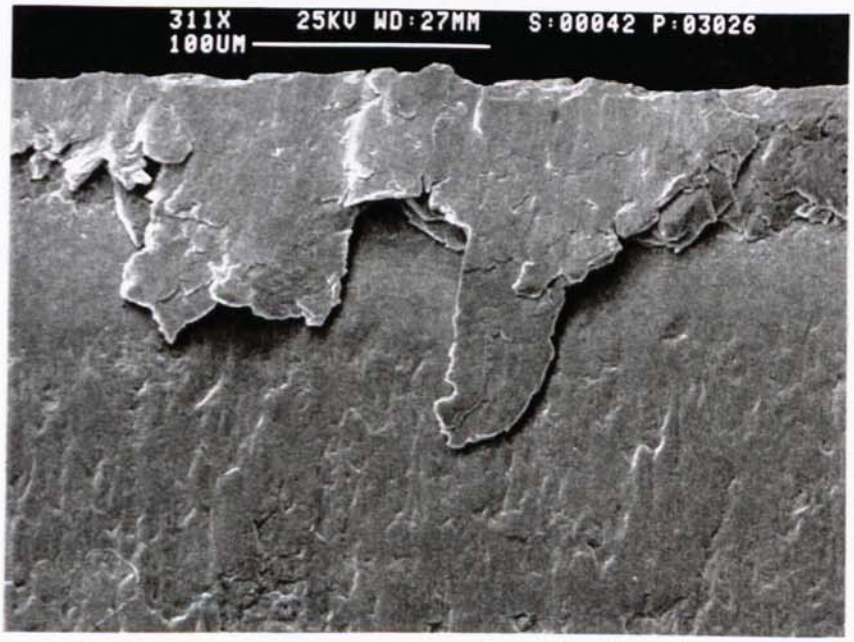

Figure 6.29 M2 HSS, cutting speed 20 m/min, rake angle -6°, flank angle 10°, and feed rate 0.15 mm/rev.

Figure 6.30 shows M2 HSS at the cutting speed of 10 m/min. The tool can be seen to have a BUE adhering to the cutting edge and flank wear. The BUE is adhered very strongly to the cutting edge, which is a fact well known that at low speed and the BUE is hard to dismantle. The BUE, as Boothroyd et al. (1989) suggest, begins to act as a cutting edge and performs the cutting action itself.

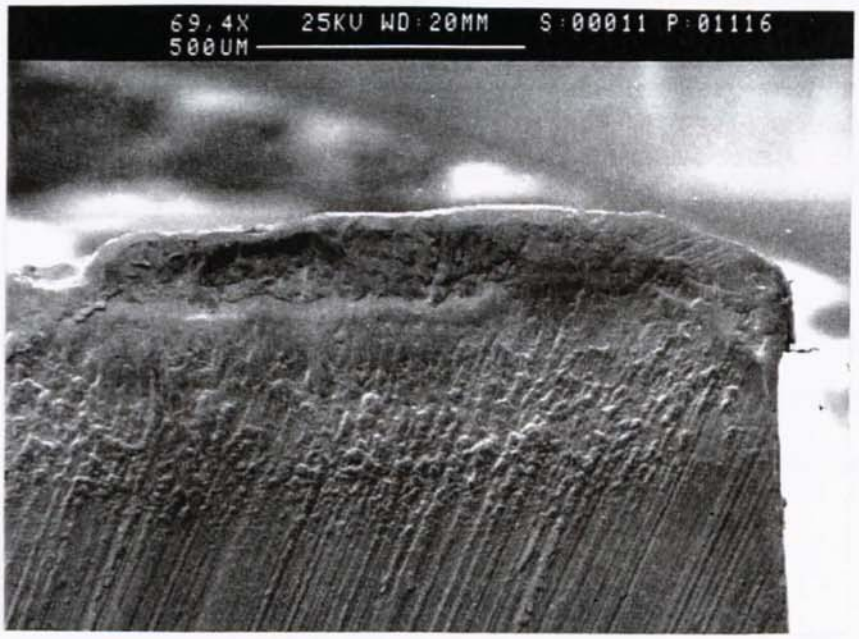

Figure 6.30 M2 HSS, cutting speed 10 m/min, rake angle 15°, flank angle 6°, and feed rate 0.15 mm/rev.

At magnification 173X, the BUE on the tool can be seen more clearly in figure 6.31. Speed 30 m/min was used to cut M2 HSS. The BUE is weaker, not so strongly adhered as in figure 6.30.

It is starting to be dismantled and when it is dismantled the fragments from the BUE will flow with the chip by adhering to the chip surface. The chip surface with the adhered BUE can be seen in figure 6.32.

Figure 6.31 M2 HSS, cutting speed 30 m/min, rake angle 10°, flank angle 5°, and feed rate 0.15 mm/rev.

Figure 6.32 shows the chip surface of M2 HSS with fragments from the BUE adhered to it. The speed used in this test which produced this chip was 40 m/min. The fragment of BUE has caused a groove as a result of being to the chip underside before being released, and hence flow away with the chip.

Figure 6.32 M2 HSS, cutting speed 40 m/min, rake angle -6°, flank angle 5°, and feed rate 0.15 mm/rev.

6.8.3 Chips

Figure 6.33 shows the surface of the chip under a magnification of 47.8X. The cutting speed to machine the M2 HSS was 10 m/min. It is seen here that a coarse surface on the chip is produced.

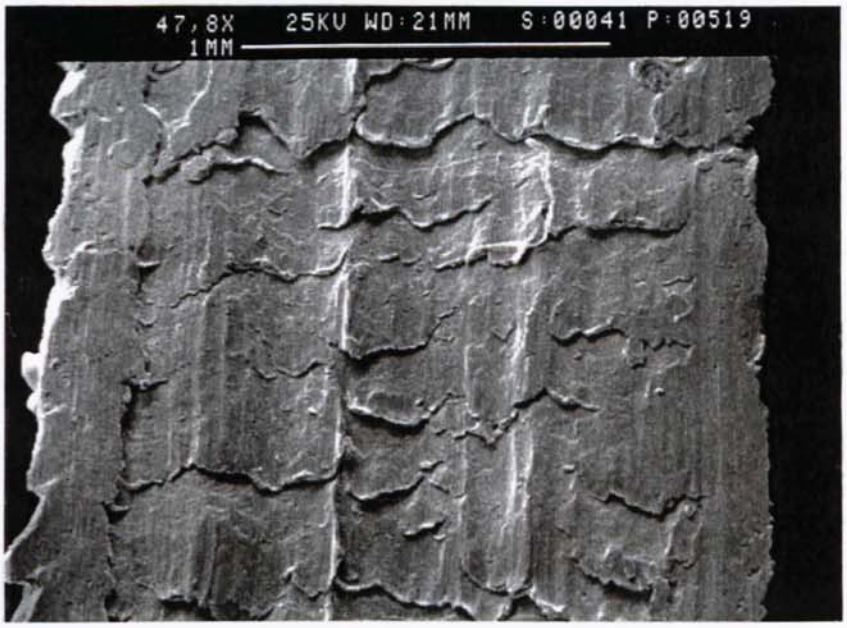

Figure 6.33 M2 HSS, cutting speed 10 m/min, rake angle 6°, flank angle 5°, and feed rate 0.15 mm/rev.

At cutting speed 20 m/min for cutting M2 HSS, figure 6.34, the chip surface can be seen to still be coarse but it also has some smoothness than the figure 6.33 with the speed of 10 m/min. The magnification in this figure is 43.9X.

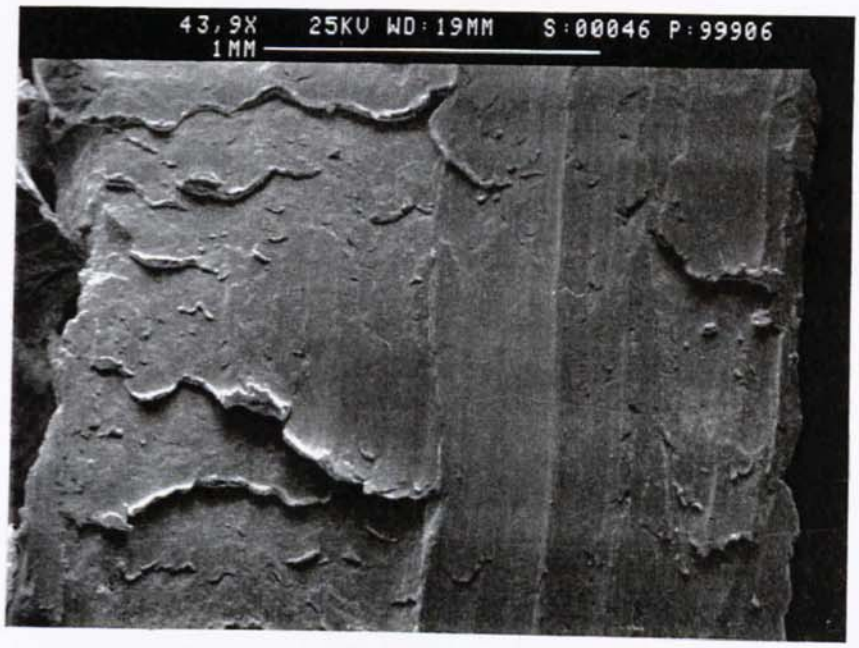

Figure 6.34 M2 HSS, cutting speed 20 m/min, rake angle 6°, flank angle 5°, and feed rate 0.15 mm/rev.

The surface of the chip in figure 6.35, at magnification 39.3X is shown to be smoother than figure 6.34. The speed used here to cut M2 HSS was 30 m/min.

Figure 6.35 M2 HSS, cutting speed 30 m/min, rake angle 6°, flank angle 5°, and feed rate 0.15 mm/rev.

Figure 6.36 is shown at magnification 41.7X. Here a speed of 40 m/min was used to machine M2 HSS. This is the smoothest out of the four figures (6.33, 6.34 and 6.35). This is due to the temperature of the cutting. The higher the temperature the hotter the chip, and therefore the softer the material of the chip in which case the material is smoother. Therefore the smoothest surface would be at 40 m/min since the higher the speed the higher the temperature.

Figure 6.36 M2 HSS, cutting speed 40 m/min, rake angle 6°, flank angle 5°, and feed rate 0.15 mm/rev.

6.8.4 Wear Mechanisms

Figure 6.37 shows the flank face of BT42 HSS at the cutting speed of 20 m/min. The wear mechanism appears to be adhesive wear.

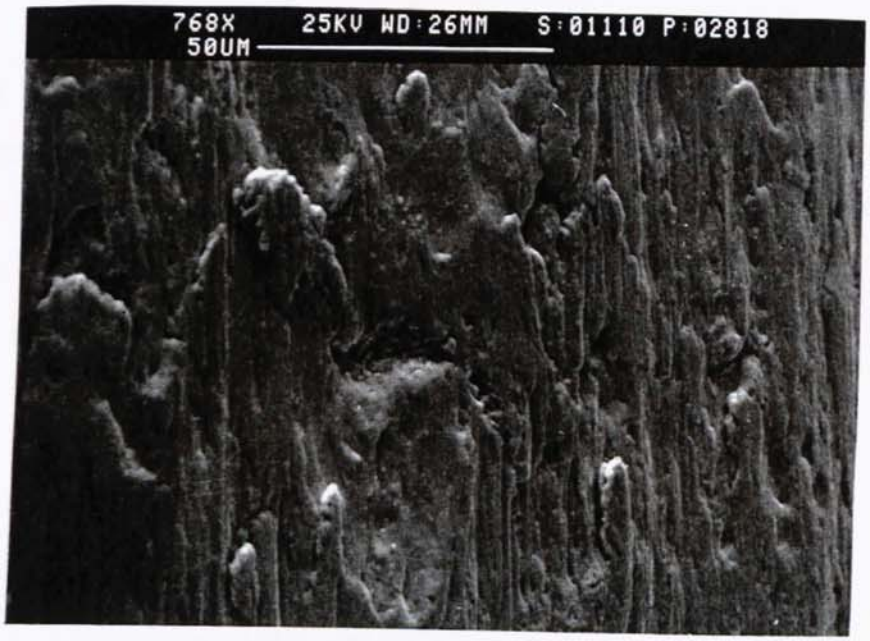

Figure 6.37 Uncoated BT42 HSS, cutting speed 20 m/min, rake angle 6°, flank angle 5°, and feed rate 0.15 mm/rev.

Figure 6.38 shows BT42 HSS at cutting speed 30 m/min. The wear mechanism is a combination of adhesion and abrasion. Also a closer examination of the figure reveals crack near the cutting edge.

Figure 6.38 Uncoated BT42 HSS, cutting speed 30 m/min, rake angle 6°, flank angle 5°, and feed rate 0.15 mm/rev.

At the speed of 40 m/min M2 HSS was cut and the figure 6.39 shows, at magnification of 89.1X, that plastic deformation seems to occur near the nose. The wear scars have a generally smooth appearance with a fine rippled surface consisting of shallow grooves running parallel to the direction of chip flow. This type of surface has been observed by other workers, and it is consistent with the mechanism proposed by Brandt (1986) as superficial plastic deformation.

Figure 6.39 M2 HSS, cutting speed 20 m/min, rake angle -6°, flank angle 5°, and feed rate 0.15 mm/rev.

Figure 6.40 shows M2 HSS at the speed of 20 m/min. It can be seen that one wear mechanism seems to be acting in this figure. One can see at the top of the figure adhesive wear is showing.

Figure 6.40 M2 HSS, cutting speed 20 m/min, rake angle 10°, flank angle 10°, and feed rate 0.15 mm/rev.

In figure 6.41 one can see that the dominant wear mechanism on the flank face seems to be adhesion wear. The tool material M2 HSS was cut at a speed of 20 m/min.

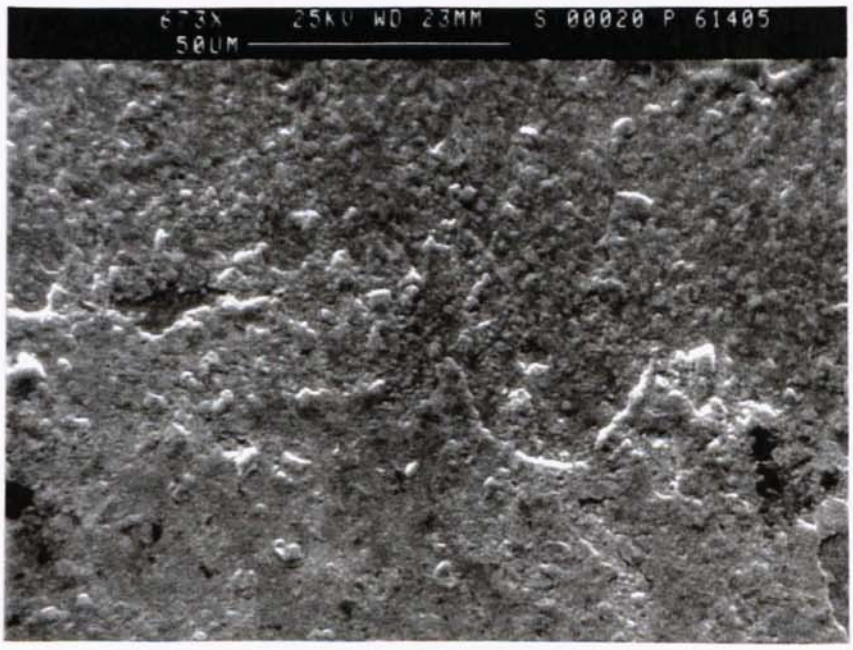

Figure 6.41 M2 HSS, cutting speed 20 m/min, rake angle 10°, flank angle 15°, and feed rate 0.15 mm/rev.

Figure 6.42 shows the tool material M2 HSS cutting at a speed of 10 m/min. There can be seen more than one wear mechanism may be at work here; adhesion and abrasion. Both these wear mechanisms can be seen of the flank face.

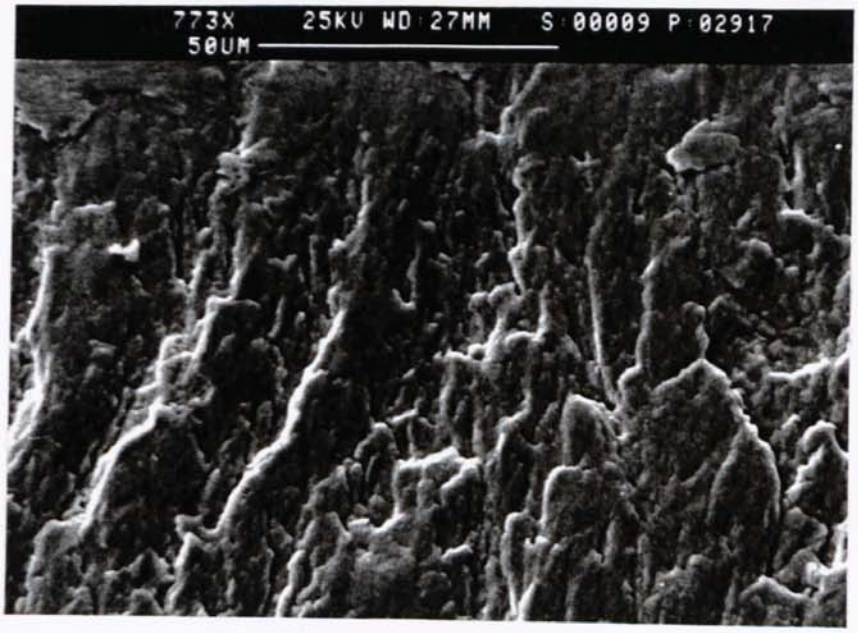

Figure 6.42 M2 HSS, cutting speed 10 m/min, rake angle 10°, flank angle 10°, and feed rate 0.15 mm/rev.

The dominant wear mechanism shown on the flank face in figure 6.43 seems to be adhesion wear, but abrasion can also be seen. The speed used is 10 m/min to cut M2 HSS.

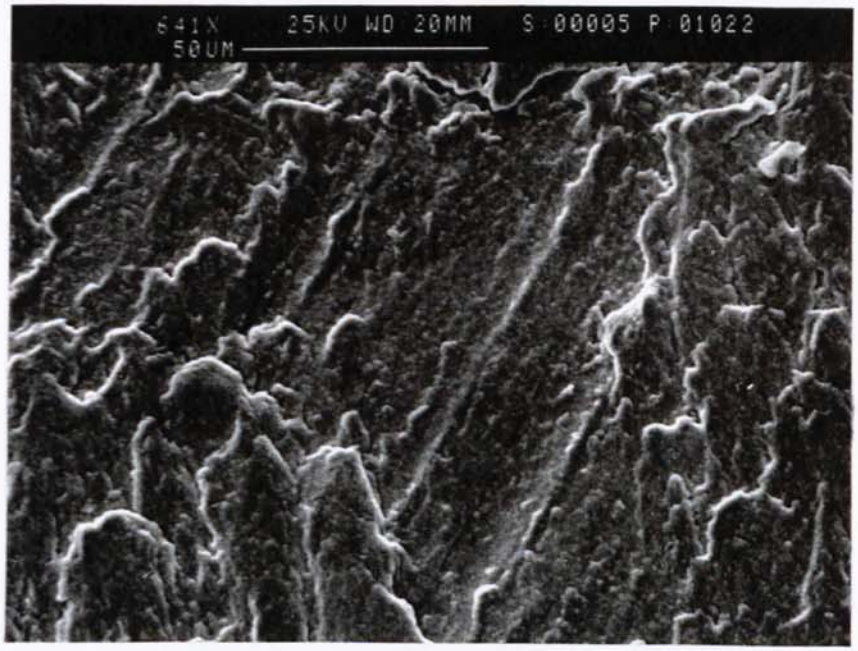

Figure 6.43 M2 HSS, cutting speed 20 m/min, rake angle 6°, flank angle 10°, and feed rate 0.15 mm/rev.

Figure 6.44 shows M2 HSS cut at speed 20 m/min. It can be seen that there is wear on the flank face, and the dominant wear mechanism suggested for being responsible for the wear is abrasion.

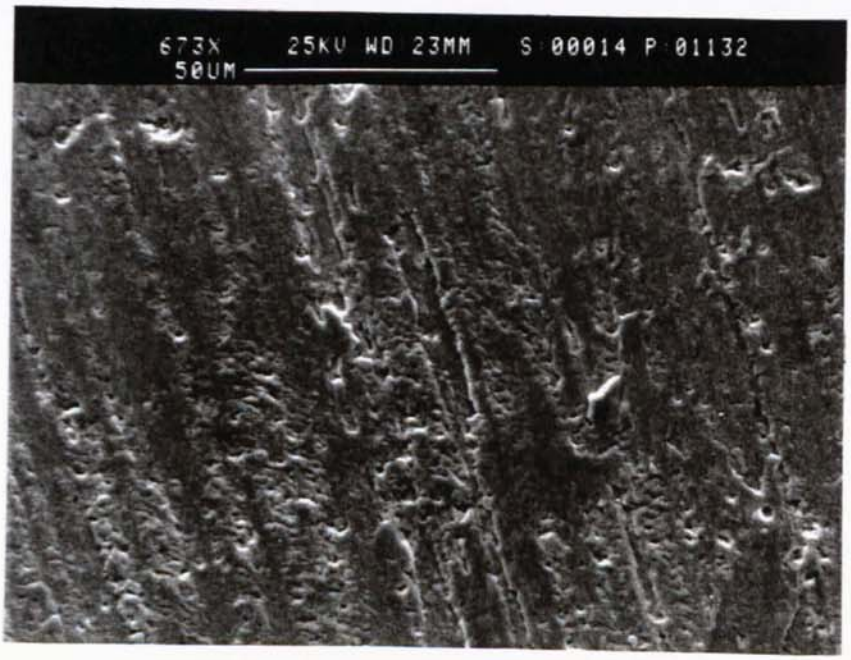

Figure 6.44 M2 HSS, cutting speed 20 m/min, rake angle 10°, flank angle 5°, and feed rate 0.15 mm/rev.

It can clearly be seen that in figure 6.45 diffusion wear is the dominant wear mechanism. This can be seen with the smoother surface that the M2 HSS tool material seems to have when cut at the speed of 40 m/min.

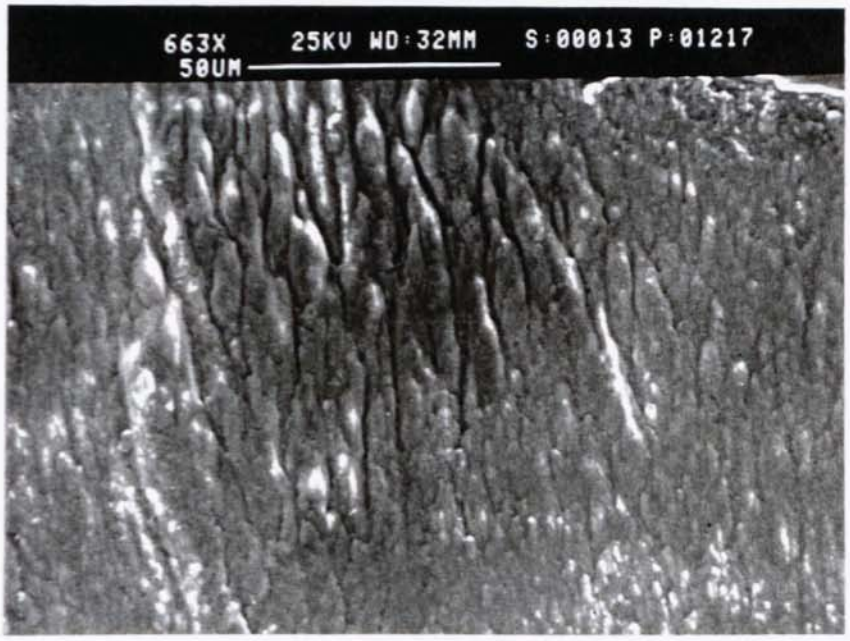

Figure 6.45 M2 HSS, cutting speed 40 m/min, rake angle 10°, flank angle 10°, and feed rate 0.15 mm/rev.

The figure 6.46 shows M2 HSS cutting at the speed of 30 m/min. It can be seen that micro-chipping occurs close to the cutting edge, and a crack can also be seen along the cutting edge. This chipping and cracking will eventually lead to catastrophic failure of the tool.

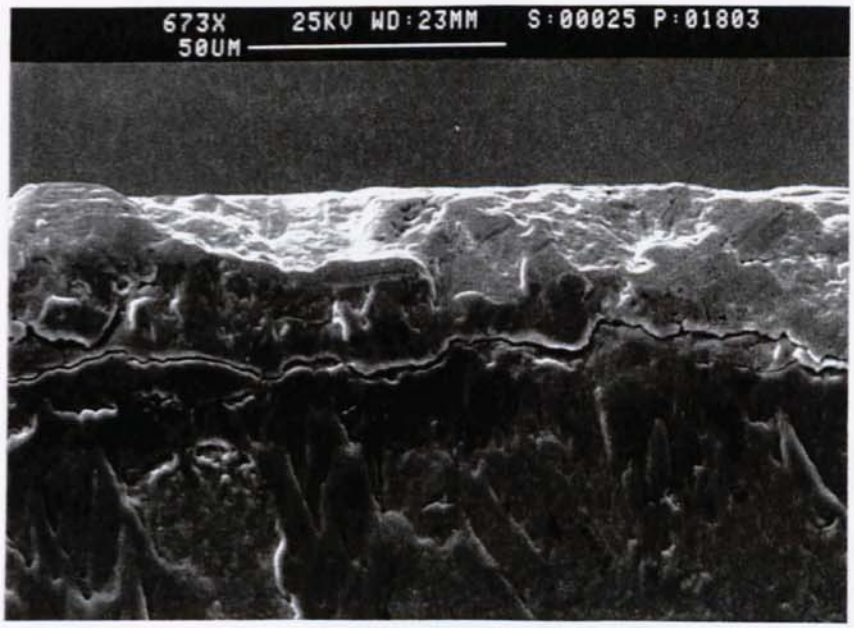

Figure 6.46 M2 HSS, cutting speed 30 m/min, rake angle 30°, flank angle 5°, and feed rate 0.15 mm/rev.

6.8.5 Catastrophic Failure

Figure 6.47 shows catastrophic failure of the tool which has occurred in the tool nose and flank face after the tool has been cutting for sometime. The general wear of the flank and cutting edge can be seen on the worn M2 HSS at the speed of 30 m/min.

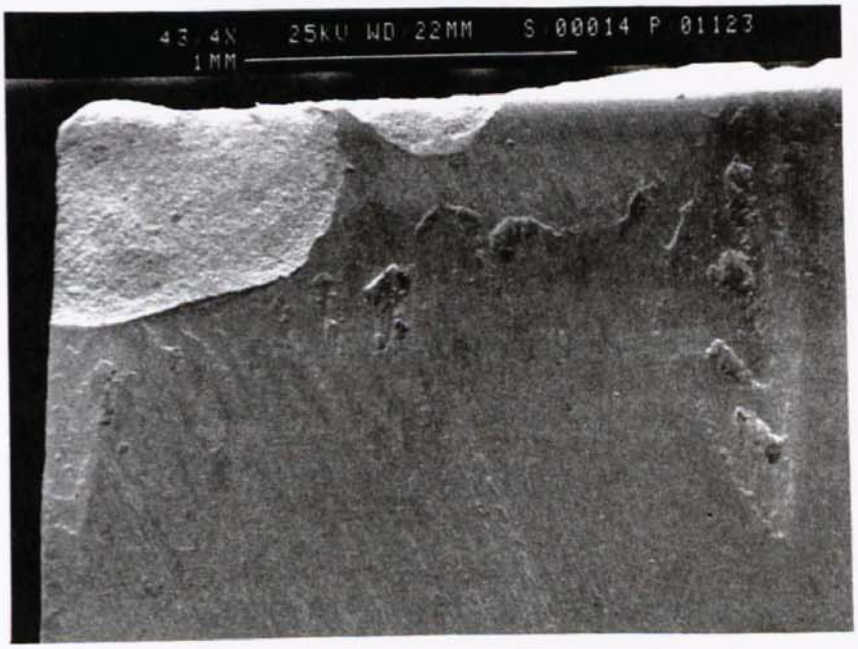

Figure 6.47 M2 HSS, cutting speed 30 m/min, rake angle 10°, flank angle 5°, and feed rate 0.15 mm/rev.

Figure 6.48 at magnification 38.8X shows M2 HSS cut at speed of 40 m/min. Here a general view of crater wear is seen. When the tool has been used to cut after sometime, catastrophic failure occurs. The damage can be seen near the nose radius.

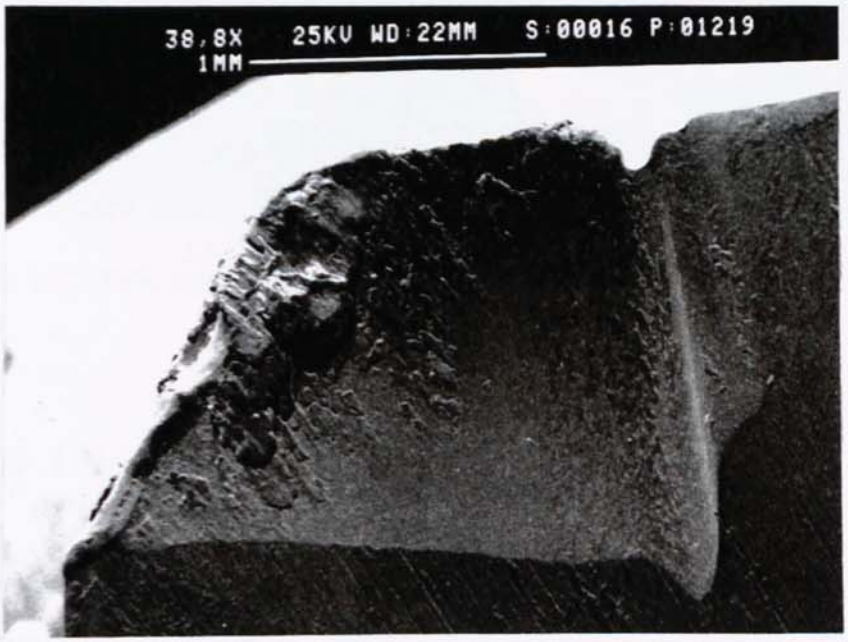

Figure 6.48 M2 HSS, cutting speed 40 m/min, rake angle 10°, flank angle 5°, and feed rate 0.15 mm/rev.

Figure 6.49 shows M2 HSS cut at the speed of 40 m/min at magnification 20.1X. Catastrophic failure occurs at once near the nose. This happened because the speed was too high for the condition used, and therefore the tool was burned out.

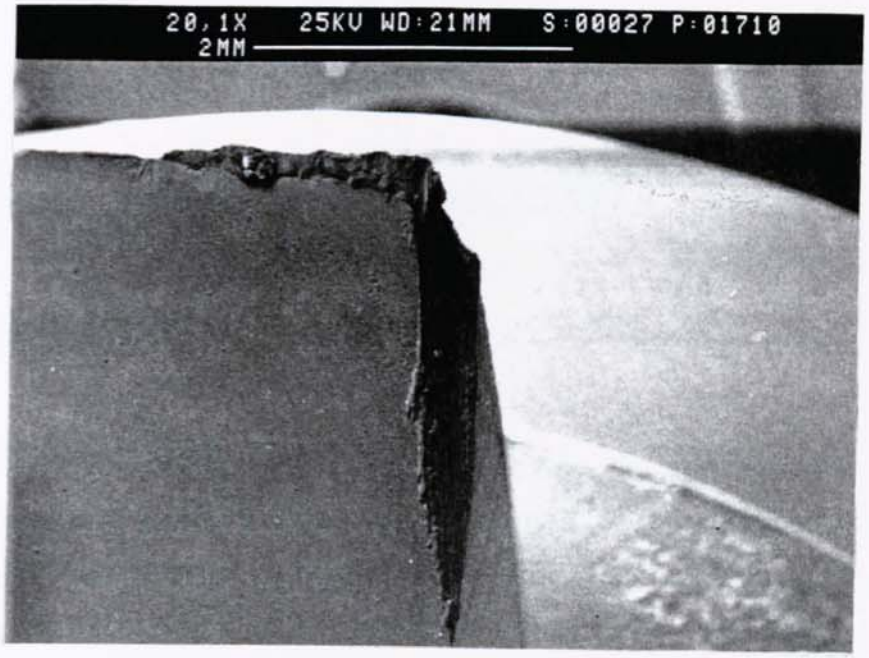

Figure 6.49 M2 HSS, cutting speed 40 m/min, rake angle 30°, flank angle 5°, and feed rate 0.15 mm/rev.

6.9 CONCLUSION

In concluding this section, it can be commented that measuring cutting forces is one of the most commonly used techniques in detecting tool failure. However, the mechanisms for causing tool wear and failure have a complex relationship with cutting forces. For example, the relationship of cutting forces and tool wear is dependent upon the properties of the materials of the cutting tool and workpiece, as well as the variation of other cutting conditions. From the SEM photographs one can see that the different wear mechanisms are acting at the different stages in the tool's life, for instance, at the low cutting speeds adhesion wear seem to be the dominant wear mechanism and as the speed is increased, abrasion wear becomes more dominant and finally, diffusion wear seems to be the dominant wear mechanism at the higher cutting speeds. This can be seen discussed in more details in chapter 8, where it is shown that the temperature influences the wear mechanisms that are acting during the different stages of the tool life.

In chapter 9 it is seen that a predictive force model for turning that was developed by Taibi (1994) was used for the results obtained in this work and that is shown in this chapter.

Chapter 7

FORCES IN DRILLING

7.1 INTRODUCTION

The study of drilling force has been an interesting topic and there are many results obtained from both experimental and theoretical approaches. This chapter deals with the examination of the experimental results obtained for the forces in drilling, and as in the previous chapter, although forces were dealt with in Chapter 2, this chapter looks at forces in more detail which relate to the material in this chapter. Measurements methods for the forces can be seen in chapter 4 and figure 4.5 shows the dynamometer attachment to the Bridgeport machine centre for force measurement.

The thrust, torque and power in drilling are important machining performance characteristics required for improvements in machine tool and drill designs as well as selection of optimum cutting conditions. The total power expended during the drilling process consists of the rotational power and feed power (Chandrashekhar et al. 1990).

The thrust and torque analyses can be developed by considering the two distinct regions of the drill, - the lip region and the chisel edge region.

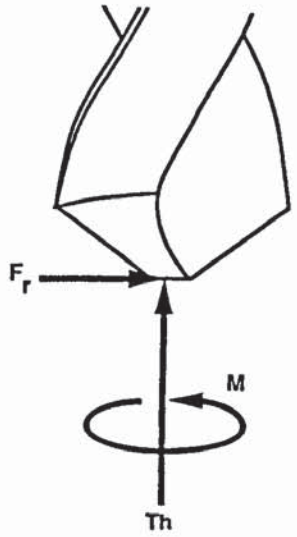

Figure 7.1 Forces in Drilling (Stephenson et al. 1997)

The Drilling Torque was defined by Webb (1990) as the summation of three components. The first is the torque required by the drill cutting edges in performing their metal removal operation. The second is the friction force between the drill shaft and the hole sides. The third is the friction force between the swarf material contained within the drill flute and the hole sides.

The Drilling Thrust is the summation of two components. The first is the thrust required by the cutting edges in performing their metal removal operation. The second is the thrust generated by the drill point or flank faces due to their lack of a positive cutting clearance towards the centre of the drill point (Webb 1990). The thrust force in drilling is the force that acts in the direction of the hole axis. If this force is excessive, it can cause the drill to break or bend. The thrust force depends on factors such as the strength of the workpiece material, feed, rotational speed, cutting fluids, drill diameter, and drill geometry.

Twist drills are unique amongst all metal cutting tools, both in their geometry and their method of operation. The most prominent feature of their geometry consists of the double helical flutes which allow the formation of the two cutting lips. The flutes are defined by their contour and the lead of the helix. The helix angle increases with radius, and its peripheral value is commonly used to specify drills.

7.2 TOOL REGIONS AND FORCES

7.2.1 Cutting Lip

Oxford (1955) thought that the shape of the drill flute should be such that the cutting lip will be a straight line. More torque and, therefore, more power are required when the lip is either concave or convex than if straight. If the lip is concave, a compression force is set up within the chip, and, conversely, if convex, a tensile force is set up, in addition to

a force outward between the chip and the wall of the hole. These forces increase the friction between the chip and the cutting lip, increase the force required to separate the chip from the work, and impede the flow of the chip up the flute. Anything which constrains the chip, either during or after formation, increases the power required, in turn increasing the heat to be dissipated, and impairing the performance of the drill.

Watson (1985a) originally developed a drilling model for the cutting lip region, assuming that a pilot hole removes the region that would be machined by the chisel edge portion of the drill, and that the material being machined by each lip can be considered as a number of individual elements.

The previous model assumed a series of elements across the cutting lip and underestimated the torque and thrust, Watson (1985b) modified it in order to account for the necessary integrity of the chip. Because the integral chip flows initially as a unit in one direction and is rotating about a point, there must be a linear variation in the chip velocity across the lip. This variation in chip velocity effects the shear angle across the lip, effectively reducing the range from that calculated series of elements.

7.2.2 Chisel Edge

Watson (1985c) published a series of papers detailing the development of a drilling analysis. The model was fairly successful in accounting for the torque and thrust components developed at the drill lips but less so when it applied to the torque and thrust developed at the chisel edge.

However apart from the work of Oxford, and Bera and Bhattacharyya, the chisel edge has received very little attention in many of the drilling studies. Most researchers have acknowledged the complex action of the chisel edge but apart from likening it to an extrusion process, they have chosen to eliminate its effect by using a pilot hole of diameter equal to the chisel edge width (Watson 1985c).

The chisel edge plays an important role in the overall performance of a drill since it contributes some 50-60% of the total thrust, according to Williams (1973) and is instrumental in controlling hole size. Therefore it must be considered in any study of the mechanics of the drilling process.

As mentioned, the torque contribution from the chisel edge would be expected to be small and this was confirmed by the results, produced by Watson (1985d), which show that it is generally less than the experimental variation in the torque results for the total drill. In a later section the thrust contribution of the chisel edge will be considered in more detail.

There is evidence to suggest that the main cutting edge contributes approx. 85% of the total torque and approx. 40% of the total thrust developed by a drill. Analysis by Williams shows that from this theoretical study, the chisel edge makes a negligible contribution to the total torque while the main cutting edge appears to account for about 60% of the total thrust (Williams 1973).

7.3 TOOL GEOMETRY

The geometry of the drill affects the drilling torque, thrust force, radial forces and power consumption amongst other things. Some brief information concerning the forces in drilling can be seen in chapter 2. (See appendix 2 for terms and definitions).

7.3.1 Tool Angles

On the cutting lip, the cutting action is an oblique machining process with the rake and inclination angles and the cutting velocity varying across the edge.

7.3.1.1 Point Angle

Watson's (1985d) experimental results and trend lines for both the full drill and cutting lip tests showed the influence of point angle on thrust, together with the chisel edge component.

Watson (1985a) predicted that there is a gradual increase in the predicted thrust as the point angle is increased, while only a minor variation in the predicted torque is indicated for the same point angle change. Experimentally there was a gradual increase in thrust and a reasonable decrease in torque as the point angle is increased. The variation of the contributing components of extrusion, cutting and wear with point angle, where it will be seen that the peak in the cutting thrust occurs at the half point angle for which the wear is zero.

Rubenstein (1991b) found that as the point angle is increased, the torque decreases, while the thrust force increases. This is also confirmed by Galloway (Rubenstein 1991b) when drilling steel and cast iron workpieces with all but the smallest (1/16 in diameter) drills.

The situation, however, is not as simple as appears at first sight since, in addition to the explicit dependence of the torque and thrust components, the torque and thrust forces generated at the lips, there is implicit dependence of the chisel edge components on the point angle, that is, both torque and thrust force generated at the chisel edge depend on point angle. It has been well established that as the rake angle of a cutting tool decreases and becomes more negative, the pressure between the workpiece and the rake face increases resulting in the BUE becoming larger.

Consequently, as the point angle increases, i.e., as the rake angle at the chisel edge becomes more negative, both torque and thrust force generated at the chisel edge will increase. Thus, as far as the thrust force is concerns, both the thrust force generated at the lips and at the chisel edge will increase as the point angle increases and hence the thrust force may be expected to increase with point angle invariably. (This analysis is

based on the assumption that the removal process is quasi-orthogonal. The removal process ceases to be quasi-orthogonal when the drill diameter becomes sufficiently small).

In contrast, a different situation is obtained in the case of the torque in that, while the component of the torque force generated at the cutting lips decreases, the component of the torque force generated at the chisel edge increases with increase in the point angle. These considerations explain the different behaviour found by Galloway (Rubenstein 1991b) when drilling titanium alloy workpiece. There it was found that not only the thrust force but also the torque increases as the point angle increased. No explanation was offered other than to suggest that it might be attributable to the tendency for chips produced from this workpiece 'to weld to the drill and hole surfaces'; in other words, to the fact that this workpiece material manifests high adhesion. This is precisely the material property which would enhance BUE formation at the chisel edge thereby causing the component of the torque force at the chisel edge to increase as the point angle increases. If Rubenstein (1991b) argues, as is apparently the case in his experiments, the increase in the torque force at the chisel edge outweighs the decrease in the torque force at the lips, then the behaviour noted when drilling the titanium alloy workpiece is explained.

No explanation is given to the behaviour observed with drills of a larger diameter, where an increase in the point angle caused the thrust force to decrease when the 1/16 in diameter drill was used by Galloway (Rubenstein 1991b).

7.3.1.2 Helix Angle

Rubenstein (1991b) reports that when all other geometrical features of the drill remaining unchanged, an increase in helix produces an increase in the normal rake angle and this, in turn, causes the shear plane angle to increase. This results in a decrease in the torque and thrust forces at the lips, and consequently, a reduction in both the torque and the thrust force.

For any drill with a specified helix angle at the periphery, the static rake angles are directly influenced by point angle and the dynamic rake angles by both point and feed angles.

Shaw et al. (1957) state it should not be inferred that drill helix angle is of negligible influence. For some work materials and operating conditions the helix angle is of prime importance in facilitating removal of chips from the hole.

The findings of Narasimha's et al. (1987) investigation is proposed as a probable basis for the traditional popularity of a 28 - 30 degrees helix angle for drills. The investigation looks at the influence of helix angle on the coupling effect in turn, the influence this coupling has on the static characteristics of a drill. First of all the drastic effect that helix angle has on drill torsional stiffness is clearly shown. This confirms Kronenberg's observations on twisted profiles (Narasimha et al. 1987). The pure torsional stiffness of drills is maximised for a helix angle around 28. Also, owing to the coupling effect, the same value of helix angle results in the largest increase in torsional stiffness under thrust (which simulates drilling conditions).

7.3.1.3 Rake Angle

Williams (1973) argues that along the main cutting edges the rake angles vary in magnitude from the outer corner to the chisel edge corner.

And according to Chandrachekhar (1990) that since the rake angle is dependent on the radius, the expression for the total axial force is derived by summing up the axial force due to infinitely many small regions along the cutting edges.

King (1985) argues that on the conventional twist drill, the rake angle decreases toward the drill centre and approaches large negative values. Thus, while the outer edge produces a smooth chip, the inner edge does not. The material under the chisel edge is subjected to deformation by displacement. Therefore, the chisel edge creates a great thrust force.

Oxford (1955) argues that there are no conclusive data regarding the influence of effective rake angle on drill torque.

7.3.1.4 Relief Angle

Watson (1985a) suggests that since the relief angle on the cutting lip is comparable to the clearance angle on a single point cutting tool, it is expected that any changes of this angle will produce only a slight change in the experimental torque and thrust. Variation of the relief angles, however, produce a minor change in the side rake angle and hence in the normal rake angle through a change in the angle, so that it is to be expected that there will be a slight change in the predicted torque and thrust when varied.

There are very slight increases in the predicted torque and thrust when the secondary relief angle is increased with the primary angle kept constant, and that there is a slightly greater increase in the predicted thrust and only a very small increase in the predicted torque when the primary angle is increased with the secondary angle kept constant.

In a later paper, Watson (1985d) argues that the two relief surfaces generate the chisel edge of a bevel ground drill and consequently a change in either or both of the relief angles with or without a change in the point angle will affect the geometry of the rake and clearance surfaces of the chisel edge. When either relief angles is increased, there is an increase in the radius to the edge of the cutting region and an increase in the cutting thrust.

Webb (1990) argues that extensive hole and drill geometry measurement was also made by Galloway. He examined relief and feed angles along the drill cutting lips, the difference giving the effective clearance. Both these values vary across the drill lips and chisel. Optimum penetration rate is described as the which gives an even distribution of wear along the cutting edge. Too high a penetration rate was seen to cause accelerated wear of the corners. Too low a penetration rate reached a point of sudden rise in both torque and thrust due to wear. Both changes led to a reduction in the number of inches depth of material drilled over an 'optimum' penetration rate (Williams 1973).

7.3.1.5 Clearance Angle

To calculate the clearance angle around its periphery Billan and McGoldrick, according to Webb (1990), made an attempt to calculate the cutting clearance across the flank face and make no allowance for drill feed. Ignoring feed reduces the value of the analysis because, of the two major forces in drilling, torque and thrust. The thrust may be attributed to the absence of cutting clearance not at the periphery but towards the centre of the drill flank face (Webb, 1990).

7.3.2 Radius

Williams (1973) argues that the torque decreases with the reduction in drill radius, while the elemental thrust increases with decreasing radius. The extrusion process at the chisel edge is negligible for drill torque but not for drill thrust since the resultant force in the extrusion operation is directed predominantly along the drill axis and the mean radius associated with the chisel edge will be small.

Shaw et al. (1957) point that the resultant torque force need not act at the midpoint of the radius of a drill and in general it will not.

7.3.3 Diameter

Watson (1985a) argues that both torque predictions decrease nearly linearly, while the negative slope of the thrust/pilot hole diameter decreases as the pilot hole diameter increases.

The results obtained by Watson indicate that torque shows a parabolic variation with pilot diameter. Thrust results show that the area near the web contributes a very large proportion of the total thrust.

7.3.4 Web Thickness

The cross section profile of a standard drill is anti-symmetric Narasimha et al. (1987) suggest, and its varies significantly due to the increasing web thickness along the fluted portion. In addition, the fluted portion is thoroughly non-prismatic due to the helix, and has a back taper.

Thick webs considerably increase the cutting force according to Radford (1980). The web thickness increases as the drill is progressively shortened by grinding, and hence the forces acting on an old drill are considerably greater than those acting on a new one unless the web is thinned.

The web thickness of the drill is found to influence thrust and torque significantly, but as Shaw et al. (1957) show that the influence of helix angle is found to be relatively unimportant. Shaw et al. (1957) argue that if the web thickness is doubled, the total torque is increased by about 22% with the chisel edge contributing about 38% of the total. While the partition of torque is independent of feed, the percentage of thrust due to the web increases with decreasing feed owing to the constant extrusion component.

Spur and Masuha (Narasimha et al. 1987) found that indiscriminate increase of web thickness results in a decrease in torsional stiffness. This can be well explained on the basis of the coupling effect. An increase in web thickness decreases the torque-thrust interaction, which means the benefit of the stiffening action of thrust is lost. This leads to a lower torsional stiffness.

The effect of increasing the drill-web thickness. Here, the effective rake angle is higher and more uniform at every point with the heavy-web drill although the normal rake is lower (or more negative) than that of the regular-design drill (Oxford 1955). The heavy-web drill has been found to have higher effective rake angles than regular-design drills but it does have the disadvantage of longer chisel edge which requires higher thrust forces and somewhat increased torque (Oxford 1955).

7.4 CUTTING CONDITIONS

7.4.1 Cutting Speed

Watson (1985a) argues that as the rotational speed is increased, the torque and thrust, both predicted and experimental, decrease in a similar fashion to that obtained for orthogonal and oblique machining tests, with the thrust curves decreasing more rapidly than the torque curves.

The full drill tests to confirm the chisel edge model that incorporated wear, extrusion and cutting regimes revealed that, in contradiction to previous information, variation of the cutting speed does produce a great change in the thrust (Watson 1985d). The thrust initially decreased as the rotational speed increase, (which was expected) then increased quite sharply to a maximum, (the unexpected part) and then began to decrease again as the speed further increases (Watson, 1985d).

However, since the drill geometry at any radius is not affected by a variation in the rotational speed (the cutting conditions at any radius are unchanged except for a change in the cutting velocity) the bevel ground form of the drill can not be responsible for the sharp increase in the thrust with increase in the cutting speed. It therefore appears that the response must be a function of the work material.

Because the thrust is a function of the shear flow stress, Watson (1985d) suggests that the observed change in thrust with increase in cutting speed is related to a variation in the shear flow stress with cutting speed. When the shear flow stress increases and then decreases as the temperature increases in a comparable way to the change in thrust with cutting speed, the response is referred to as dynamic strain ageing or blue brittleness.

If during machining the shear plane temperature then fell within the blue brittle range there would be an increase in the thrust for the reasons described above. Further increases in speed would increase the temperature more until the conditions were above the dynamic strain ageing range.

A range of drilling speeds and feeds were used by Morin et al. (1995). Torque, thrust and flank wear were correlated with depth drilled. The cutting speed has no significant effect, as expected. These results are in general agreement with those of Monaghan and O'Reilley (Morin 1995) for spindle speed, where torque is seen to increase with feed rate, but diverge from their observations which show a decreasing torque with increasing feed rate.

7.4.2 Cutting Feed

The results are in marked contrast with those presented by Monaghan and O'Reilly who show thrust forces decreasing with increasing feed rate for HSS drills, but are in general agreement with their results for carbide drills, and the work of Jawaid who also used carbide drills in their tests (Morin et al. 1995).

It was found by Watson (1985a) that as the feed increases the rate of increase in torque and thrust decreases. Varying the feed produces an effect on both the torque and thrust for the experimental and predicted results similar to that observed in metal cutting with single point cutting tools, in that the ratio of cutting force to undeformed chip thickness (comparable to specific pressure) decreases as the undeformed chip thickness is increased. In the drilling case, the slopes of the torque/feed and thrust/feed curves for the experimental and predicted values decrease as the feed is increased.

Since the radii to the edges of the extrusion and cutting areas increase as the feed increases for a given combination of point and relief angles, it is to be expected that the cutting and extrusion components of the thrust will also increase as the feed increases. The cutting and extrusion components of thrust are nearly quadratic functions of the feed because of the near linear increase in thrust per unit edge length with undeformed chip thickness and the linear increase in the length of cutting and extrusion action with feed. The region of the chisel edge contributing to the wear process extends from the edge of the cutting region to the chisel edge corner and this wear region decreases as the feed increases. The wear thrust initially increases with feed because of the increase in thrust per unit edge length with undeformed chip thickness while the length of the edge

is decreasing, and eventually the decreasing length of the edge causes the wear thrust to decrease to zero (Watson 1985d).

It is found, by Schmidt et al. (1949) that this shear angle increases considerably with increasing feed. As a result the average temperature rise resulting from deformation on the shear angle increases with increasing feed that the average chip temperature decreases with increasing feed. On the other hand, it is evident that with a heavy feed the chip is pressed against the tool face with greater force than with a light feed. As a result, more frictional heat is generated at the chip-tool interface at high feeds than at low. It is for this reason that the chip-tool interface temperature increases with increasing feed in spite of the fact that the average chip temperature decreases.

To obtain repeatable data, Shaw et al. (1957) argue, it was necessary to condition the drills by first drilling one or two holes at a high feed. This removed any grinding burrs which might remain on the drills and give misleading results at low feeds.

As a result of the 3-dimensional nature of drilling operations, the over-all specific cutting energy is found to vary with the product of feed and diameter, rather than the feed alone as in turning (Shaw et al. 1957).

The significance of exponents is that they give information about the change in torque and thrust with changing diameter of the drill and changing feed. The torque increases 74% when the feed is doubled and 250% when the diameter is doubled. The thrust, however, is much less affected by a change in diameter of the drill than the torque - 75 - 80% when the feed is doubled (Shaw et al. 1957).

In analysing the thrust data Levy et al. (1976a) observed that there is negligible effect of cutting speed on thrust (generally 10% or less) for a constant feed rate. With the torque, the effect of increasing the cutting speed at a constant feed rate was to occasionally increase the torque but more generally either to decrease of have no effect on it. In analysing the sensitivity of the thrust to differences in machinability, the magnitude of differences in the thrust increases as the feed rate increases.

The slope of the thrust force vs. feed rate relationships decreases for steels of increasing machinability. This implies that the relative influence of increasing feed rate on increases in drill thrust is less significant for more machinable steel grade, i.e., for very machinable steels, the thrust force does not increase as rapidly with increases in feed rate as that for less machinable steels (Levy et al. 1976a).

7.4.3 Cutting Fluid

Gilbert states (Schmidt 1949) that torque and thrust dynamometers have shown there is little change in torque or thrust when using water as a cutting fluid in this type of drilling. While Merchant (Schmidt 1949) had demonstrated that under certain conditions plain water can be fairly effective cutting fluid in reducing tool forces and power consumption, i.e., heat generation. This is particularly true at very low speeds (Schmidt et al. 1949).

7.5 TOOL WEAR

As in other cutting tools, the most practical parameter is the amount of wear at a certain point of the drill tip, which may be assumed to be related to the cutting force. This force has 2 primary components, the axial force and moment, and one secondary component, the radial force. The latter is apparently more important from the viewpoint of the sought criterion, (a positive criterion was sought for the stage at which resharpening would be necessary and economically justified), since the radial force is produced by geometrical differences between the drill lips which are unquestionably a major factor in the service life of the tool (Ehrenreich et al. 1971).

Using a simple model, Subramanian and Cook obtained relationships between drill flank wear on the one hand and thrust force and torque of the other (Thangaraj et al. 1988). Thangaraj et al. (1988) argue that if the hardness of the work material is a constant, the thrust force will increase linearly with flank wear under a given set of

cutting conditions. However, in practice, fluctuations in the hardness cause random variations in the thrust force under normal drilling conditions.

Thangaraj's et al. (1988) state that the results in their experiment indicate the gradual increase of the thrust force level as the tool wears and the relatively rapid increase in the failure region. By contrast, a substantial increase in the thrust force itself was observed only when the outer corner wear was around 1.46 mm.

High temperature conditions at the outer corner of the drill lead to greater wear which in turn leads to still higher temperatures. This cyclic process results in a rapid increase in the local temperature and thereby a significant reduction in the yield strength of the material. This causes local welding of the outer corner to the hole surface. As the drill is fed at a constant rate, higher forces are exerted to overcome the resistance due to local welding. Under the influence of the high stresses caused by the high forces, shear fracture of the drill material occurs. This leads to a sharp decrease in the forces exerted by the drill on the work material.

Experimental evidence emphasises the correlation between thrust force and outer corner wear; it is suggested that the sharp spikes in the thrust force that are observed under failure conditions are caused by a macroscopic stick-slip phenomenon (Thangaraj et al. 1988).

According to Morin et al. (1995) after initial penetration of the point of the drill, thrust and torque were essentially constant with depth, consistent with the fact that there was no measurable wear in this case. The specific cutting energy in turn is taken to be directly proportional to the Brinell hardness for classical materials and is expected to increase due to any wear of other dulling of the drill. That it does increase with wear is confirmed by the increase of torque with depth drilled, i.e., with wear.

Measurements were made by Morin et al. (1995) of thrust, torque and flank wear for several feed rates and drill speeds. Speed had no significant effect on wear or on drilling forces. Flank wear proceeded linearly with depth of material drilled, or with the total

distance passed by the lip or cutting edge of the drill. A linear relation between both thrust and torque against flank wear was observed, so that either thrust or torque may be measured to give an indication of wear of the drill. The linear relation between torque and wear of the drill implies a linear variation of specific energy with flank wear.

Morin et al. (1995) argue that given the linearity of the relation between wear, torque and thrust against depth, it follows that a linear relation exists, to the same degree of approximation, between torque and thrust and flank wear. As a result of tool wear, drilling torque and thrust forces increased with depth drilled. The rate of increase becomes nearly linear after about 10 mm depth drilled.

The total torque and thrust developed by a drill arises from two main sources, the main cutting edges and the chisel edge. The action of the drill lands does contribute to the overall torque value but until both lands wear appreciably this force is small and can be neglected.

7.6 EXPERIMENTAL RESULTS AND DISCUSSION

More details about the experimental methods and equipment can be seen discussed in chapter 4. Test conditions can be seen in appendix 1, tables A1.10 to A1.12.

7.6.1 Forces in the new tool

The figures following; figure 7.2 to figure 7.5 show the results obtained when testing new drills.

7.6.1.1 9 mm diameter standard helix drill

Figures 7.2 and 7.3 show thrust vs cutting speed and torque vs cutting speed respectively. The tool material used is M2 HSS 9 mm drills for cutting speeds 354, 707 and 1061 rpm at dry cut. (See appendix 1 tables A1.10 to A1.12).

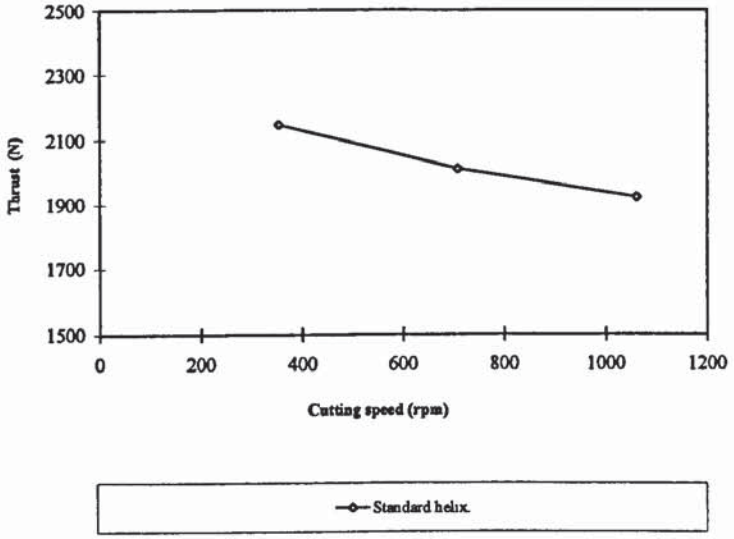

Figure 7.2. Thrust vs. cutting speed for 9 mm diameter M2 HSS, dry cut.

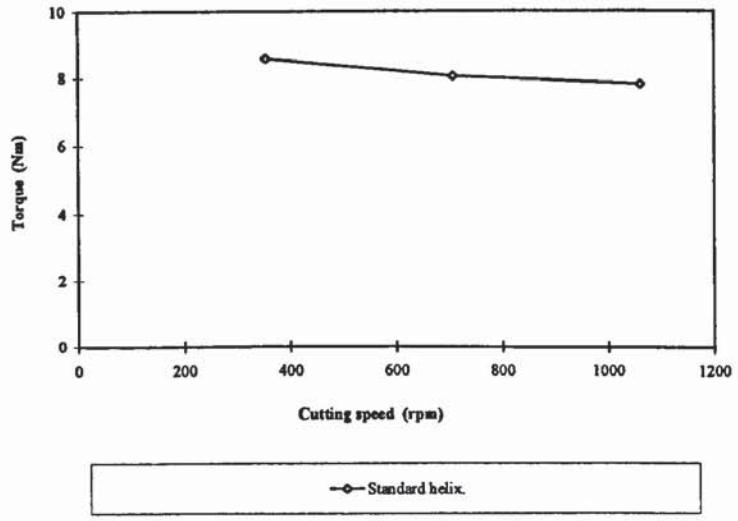

Figure 7.3. Torque *vs*. cutting speed for 9 mm diameter M2 HSS, dry cut.

In both figures it can be seen that by increasing the speed, both thrust and torque decrease. This decrease in the forces is due to the temperature because as the speed increases so does the temperature and therefore the forces decrease due to the softening of the material. Watson (1985a) argues that as the rotational speed is increased, the torque and thrust, decrease which is expected.

7.6.1.2 13 mm diameter, slow, standard and fast helix drill

Figures 7.4 and 7.5 show thrust vs cutting speed and torque vs cutting speed respectively. The drills used were M2 HSS 13 mm drills at slow, standard and fast helix. The speeds were 244, 490 and 735 rpm at dry conditions, and only 2 mm was cut in each lip from the corner. (See appendix 1 tables A1.10 to A1.12).

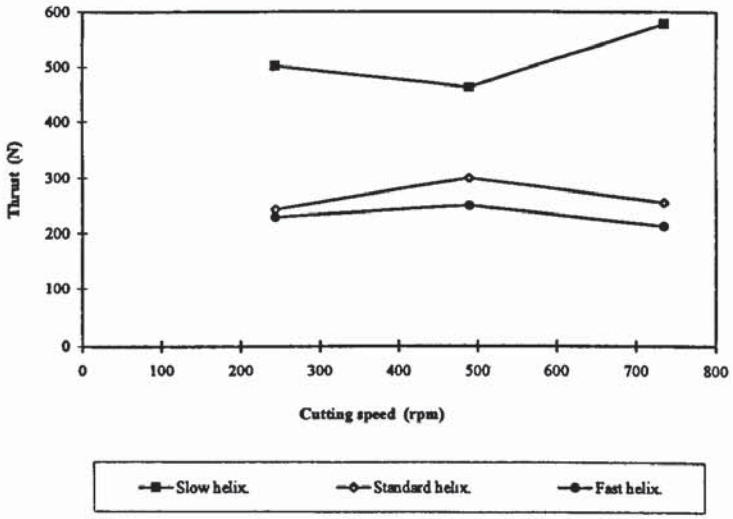

Figure 7.4. Thrust *vs*. cutting speed for 13 mm diameter M2 HSS, 2 mm cut each lip, dry cut.

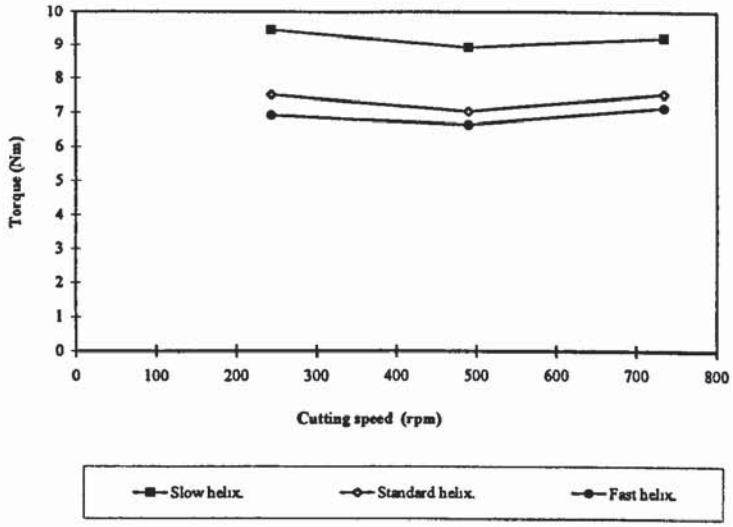

Figure 7.5 Torque *vs*. cutting speed for 13 mm diameter M2 HSS, 2 mm cut each lip, dry cut.

In both graphs it is seen that for the slow helix drill the thrust and torque forces are higher than the standard and fast helix drills. The standard and fast helix drills are similar but still for the standard helix the thrust and torque forces are marginally higher than the fast helix. Again as in figures 7.2 and 7.3 the forces decrease as the speed is increased.

When comparing the three different helix for both figures, one can see that the effect of the helix angle on temperature. That is the slower the helix angle then it takes longer to get rid of the chip, which means that it has more contact with the chip, which has higher temperature and which effects wear mechanism, as can be seen in figures 7.20, 7.21, 7.22, 7.23 and 7.24, and therefore affect the forces.

Rubenstein (1991a) reports that as the helix angle increases both the torque and thrust decrease. According to Shaw et al. (1957) it is seen that torque and thrust decrease slightly with increases helix angle. The helix angle is of prime importance in facilitating removal of chips from the hole.

7.6.2 Effect of wear on tool forces

The figures 7.6 to 7.11 show the results for the tests carried out with drills that have wear. (See appendix 1 tables A1.10 to A1.12).

Practical testing of drills identified the need to enumerate in detail the individual cutting geometry of a particular twist drill. Webb (1990) proposes a new solution to the complex geometry of the twist drill form and therefore offers mathematical predictability. The dynamic instability of the drill cutting process is then superimposed on this basic drill geometry. Webb (1990), in his thesis, explains a new and simple method which, with the use of a personal computer, is able to put accurate figures to the problem of drill geometry. Some of the calculations used in these tests were calculated using Webb's software.

7.6.2.1 9 mm diameter standard helix drill

In figures 7.6 and 7.7, the graphs show torque vs. lip wear 1 mm away from the corner, and thrust vs. lip wear 1 mm away from the corner respectively. The tool material used was 9 mm diameter drill M2 HSS standard helix at dry cut. Three different cutting speeds were used 354, 707, and 1061 rpm with three feeds: 112, 226, and 340 mm/rev respectively. The cut was made 1 mm away from the corner in order to use it as a standard for measuring the speed, rake and flank angles. (See appendix 1 tables A1.10 to A1.12).

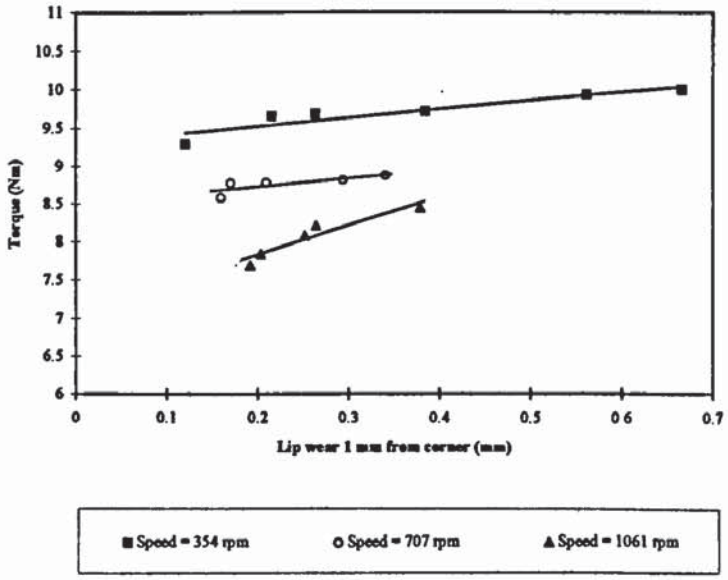

Figure 7.6 Torque vs. lip wear for 9 mm diameter standard helix M2 HSS, dry cut.

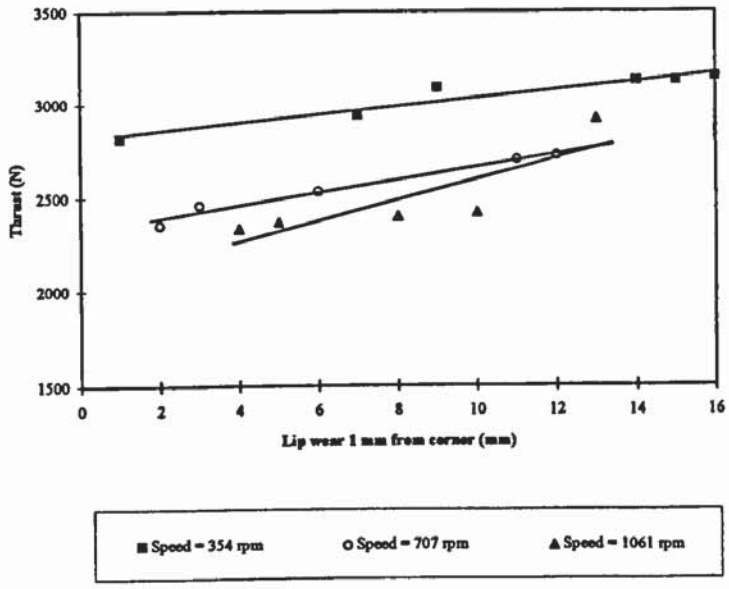

Figure 7.7 Thrust *vs*. lip wear for 9 mm diameter standard helix M2 HSS, dry cut.

Cutting speed, rake and flank angles, were calculated (by using the Webb (1990) model), 1 mm away from the corner. Approximately the rake angle was 23°, flank angle 12.5° , and at this point the speed, 1 mm away from the corner is 275, 550, 825 rpm for the three speeds used in these tests: 354, 707, 1061 rpm respectively.

It can be shown from both the graphs that the lower the cutting speed the higher the torque and thrust forces. One can also see the increase in the lip wear which produces increases in the torque and thrust.

Even though for all speeds the torque and thrust forces increase as wear increases, with the high speeds the torque and thrust increase more steeply and rapidly, while for the two other speeds of 707 and 354 rpm the increase in the torque and thrust forces are more steady.

A reason for this is with the increase in wear the temperature increases, and therefore the material becomes softer and therefore needs less force at higher speeds to machine the material. As Morin et al. (1995) show that as a result of tool wear, drilling torque and thrust forces increased. More on temperature and its effect on wear mechanisms can be seen in the next chapter where it is discussed in more details.

7.6.2.2 13 mm diameter slow, standard and fast helix drill

The figures 7.8 and 7.9 show torque vs. average lip wear (only 2 mm cut each lip from corner) and thrust vs. average lip wear (only 2 mm cut each lip from corner). The tool material used is 13 mm M2 HSS drill with slow, standard, and fast helix. The rake angle for the slow helix (by using the Webb (1990) model) is in the range of 6° to 11° and the average is approximately 8.5°. For the standard helix (by using the Webb (1990) model) is in the range of 23.5° to 33° and the average is approximately 28.5°. And for the fast helix (by using the Webb (1990) model) is in the range of 32.5° to 43° and the average is approximately 38°. The range of the speed, for all the helix angles, is from a minimum of 170 rpm to a maximum of 244 rpm. The feed rate is 78 mm/rev, and the flank angle is in the range of 11.5° to 8.5° with an approximate average of 10°. (See appendix 1 tables A1.10 to A1.12).

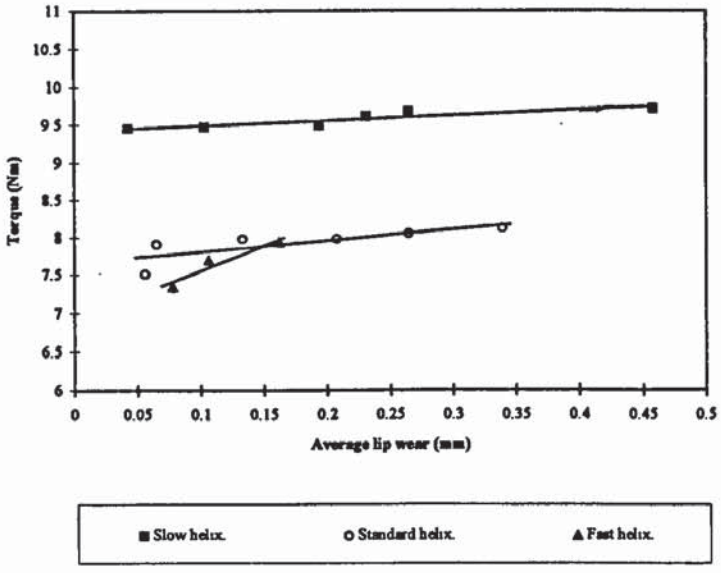

Figure 7.8 Torque vs. lip wear for 13 mm diameter M2 HSS, 2 mm cut each lip, at speed 244 rpm, dry cut.

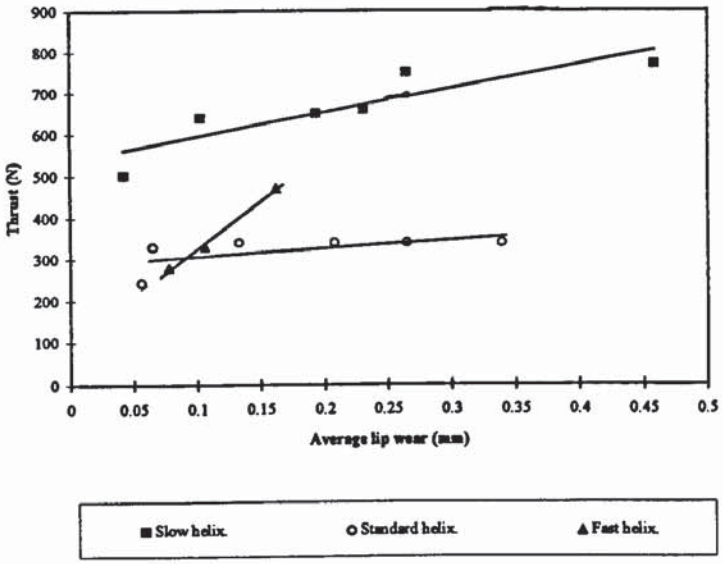

Figure 7.9 Thrust vs. lip wear for 13 mm diameter M2 HSS, 2 mm cut each lip, at speed 244 rpm, dry cut.

It can be seen from the figures that the highest torque and thrust occur with the slow helix angle, and it can also be seen the fast helix angle the tool fails quicker, as can be seen in figure 7.25 of catastrophic failure. This is caused due to the tool geometries and it can be seen that the standard helix angle is best compared to the other two and this has the lowest torque and thrust.

The reason for this is that at slow speed the torque is higher because of the chip, it is slower to exit. At fast speeds the chips leave faster and because the tool geometry (rake angle) also affects, this causes the tool failure.

Standard helix is seen to be in between the slow and fast, as is the rake angle and the flank angle. The fast helix has a steeper and more rapid increase than the slow and standard, they have more steady increase.

The figures 7.10 and 7.11 show torque vs. average lip wear (only 2 mm cut each lip from corner) and thrust vs. average lip wear (only 2 mm cut each lip from corner) respectively. The tool material used is 13 mm M2 HSS drill with slow, standard, and fast helix. The rake angle for the slow helix (by using the Webb (1990) model) is in the range of 5.5° to 10.5° and the average is approximately 8°. For the standard helix (by

using the Webb (1990) model) is in the range of 24.5° to 34° and the average is approximately 29°. And for the fast helix (by using the Webb (1990) model) is in the range of 34° to 44.5° and the average is approximately 39°. The range of the speed, for all the helix angles, is from a minimum of 340 rpm to a maximum of 490 rpm. The feed rate is 78 mm/rev, and the flank angle is in the range of 11.5° to 8.5° with an approximate average of 10°. The cutting speeds in these figures are higher than the previous figures (7.8 and 7.9).

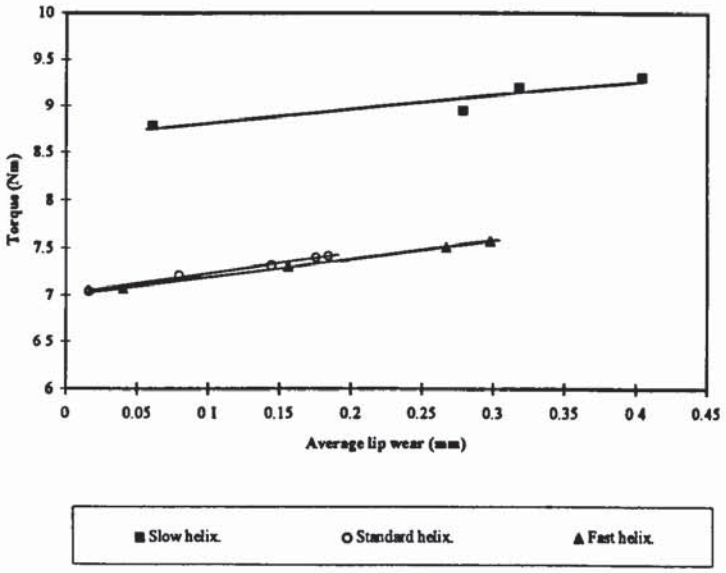

Figure 7.10 Torque *vs*. lip wear for 13 mm diameter M2 HSS, 2 mm cut each lip, at speed 490 rpm, dry cut.

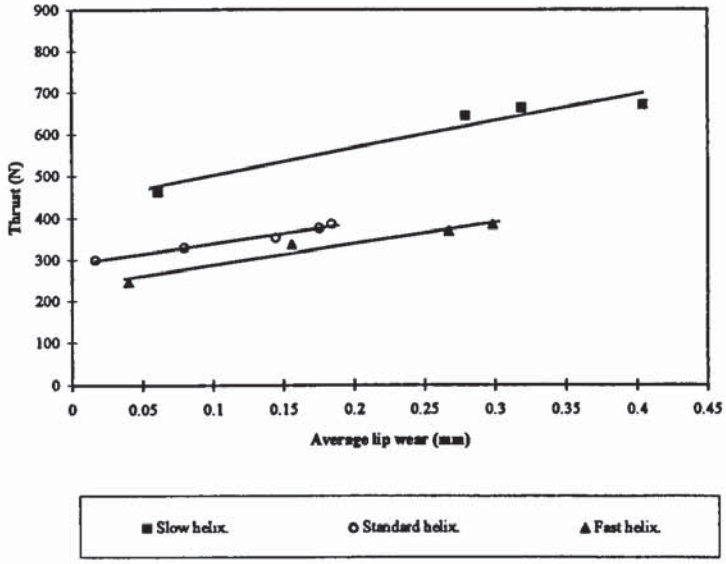

Figure 7.11 Thrust *vs*. lip wear for 13 mm diameter M2 HSS, 2 mm cut each lip, at speed 490 rpm, dry cut.

In both figures it can be seen that as the average lip wear increases the torque and thrust increase. It can also be seen that the slow helix angle has the highest forces (thrust and torque), and the standard and fast helix are very similar. Even though the standard is a little higher compared to the fast helix. This can be put down because the rake angle is lower at the slow helix and this causes higher forces.

Also the at slow helix angle, the chip is exiting the system slower, as compared to the other two, that is, standard and fast helix angles, and this causes higher forces (thrust and torque).

7.7 SEM PHOTOGRAPHS AND DISCUSSION

7.7.1 General Tool Wear

Chisel wear can be seen in figure 7.12 when using the 9 mm diameter M2 HSS drill, and where the cutting speed was 354 rpm.

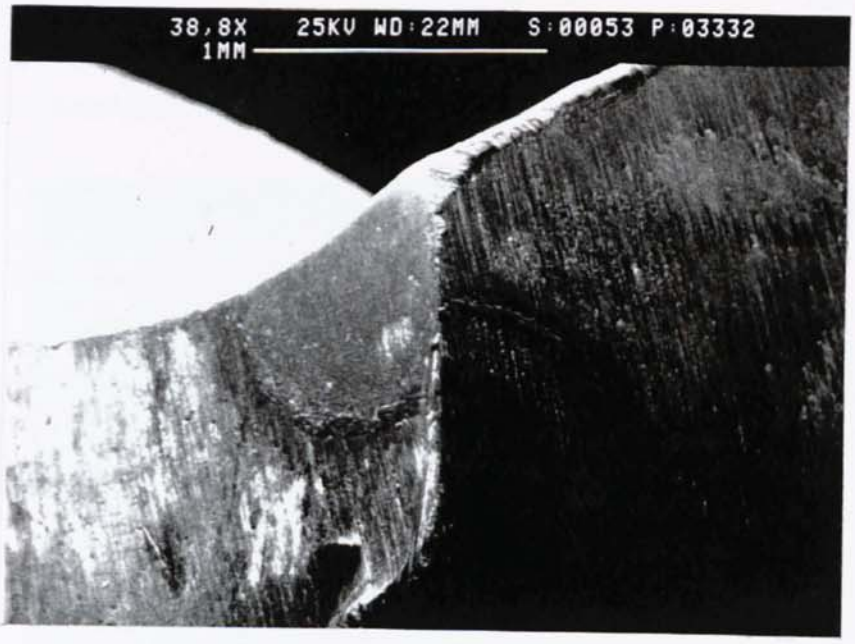

Figure 7.12 9 mm diameter M2 HSS drill, cutting speed 354 rpm.

Figure 7.13 shows 13 mm diameter M2 HSS standard helix drill with the speed of 244 rpm. Here the cutting lip can be seen and a micro-chip in the cutting lips can be seen and also outer corner wear. The wear mechanism seems to be adhesion wear.

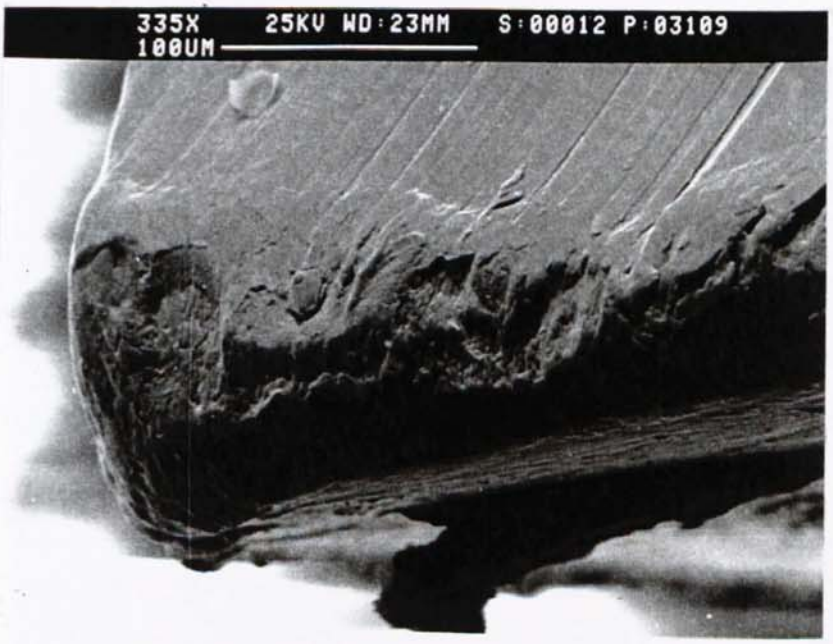

Figure 7.13 13 mm diameter M2 HSS standard helix drill, cutting speed 244 rpm.

Figure 7.14 shows 13 mm diameter M2 HSS standard helix drill at a speed of 490 rpm. This is a general view of the flank wear. Also it is a general view showing possibly two wear mechanisms; adhesion and abrasion.

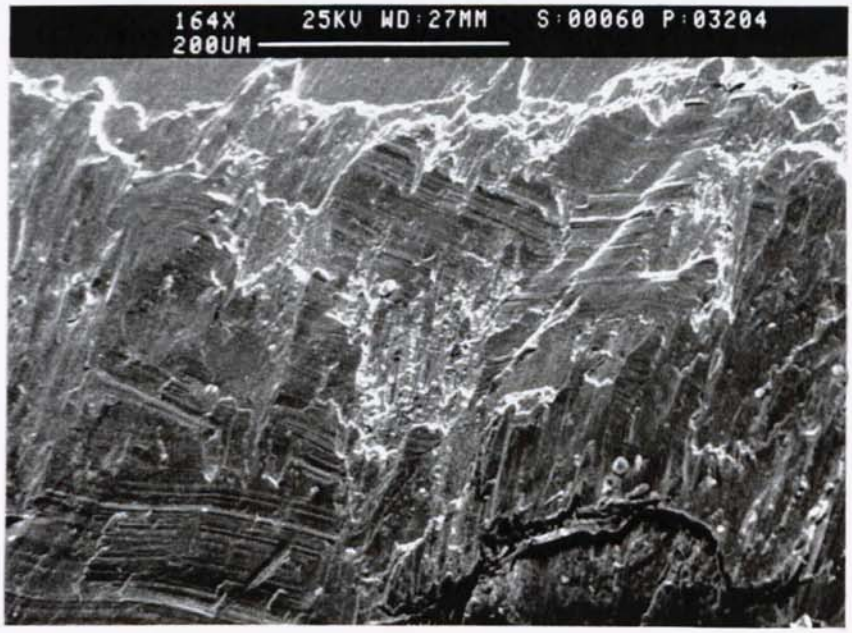

Figure 7.14 13 mm diameter M2 HSS standard helix drill, cutting speed 490 rpm.

A general view of flank wear, corner wear and land wear can be seen in figure 7.15 of the 13 mm diameter standard helix drill at a speed of 490 rpm. In this figure it can be seen that the lip was cut 2 mm only from the corner.

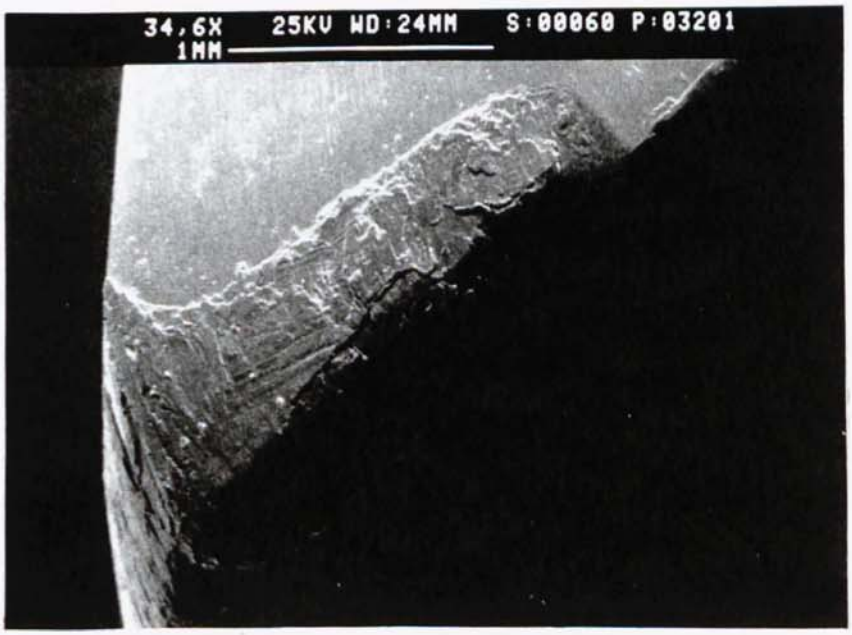

Figure 7.15 13 mm diameter M2 HSS standard helix drill, cutting speed 490 rpm.

Figure 7.16 shows 13 mm diameter M2 HSS slow helix drill with wear in the lip. At a speed of 735 flank wear, land wear and corner side wear can be seen. The damage on the cutting lip can be seen, also the work material is seen accumulated on the rake face.

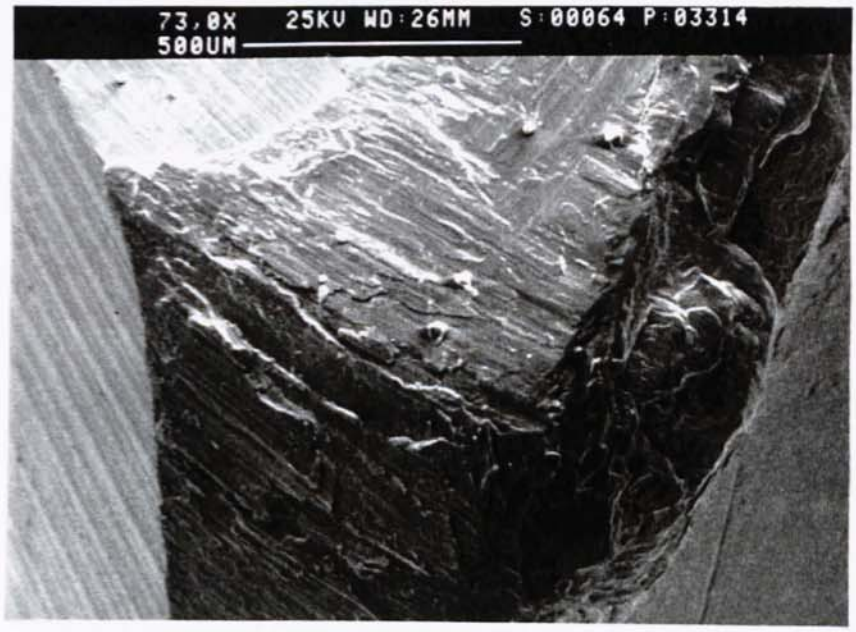

Figure 7.16 13 mm diameter M2 HSS slow helix drill, cutting speed 735 rpm.

7.8.2 Build-up Edge

This figure 7.17 shows 9 mm diameter M2 HSS drill with corner wear in the drill. BUE can also be seen at a speed of 354 rpm.

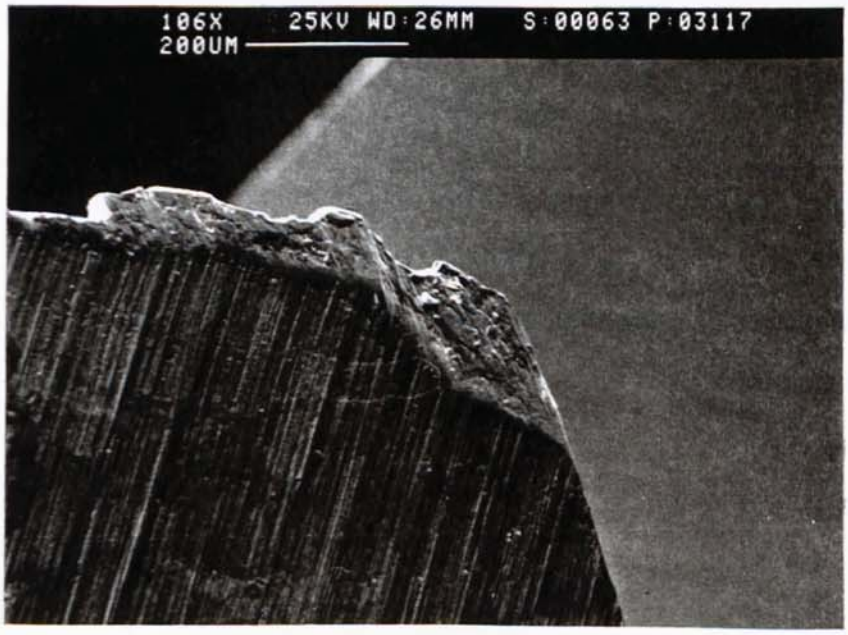

Figure 7.17 9 mm diameter M2 HSS drill, cutting speed 354 rpm.

7.7.3 Chips

The 13 mm diameter standard helix drill can be seen in figure 7.18. The figure shows the underside surface of the chip. The surface of the chip is seen to be coarse which usually occurs with low speed.

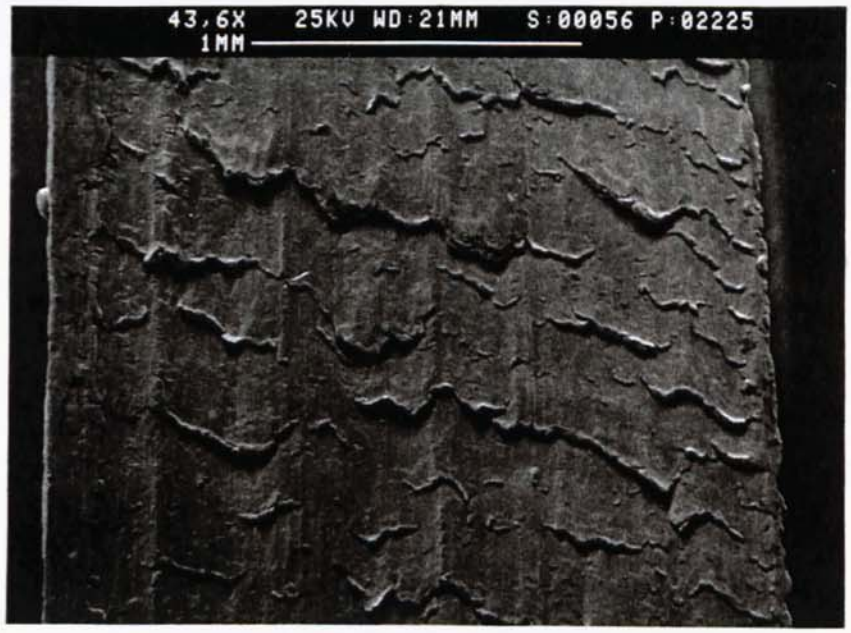

Figure 7.18 13 mm diameter M2 HSS standard helix drill, cutting speed 244 rpm.

The figure, 7.19, shows the underside surface of the chip of the 13 mm diameter M2 HSS standard helix drill, at speed 490 rpm. This can be seen to be smoother than figure 7.18, this is due to the high speed. The higher the speed the higher the temperature and therefore the surface of the chip becomes softer with the high temperature and therefore smoother.

Figure 7.19 13 mm diameter M2 HSS standard helix drill, cutting speed 490 rpm.

7.7.4 Wear Mechanism

This figure 7.20 at magnification 672X shows the 13 mm diameter M2 HSS standard helix drill. The predominant wear mechanism that seems to be operational is adhesion wear, although a little abrasion wear can also be seen.

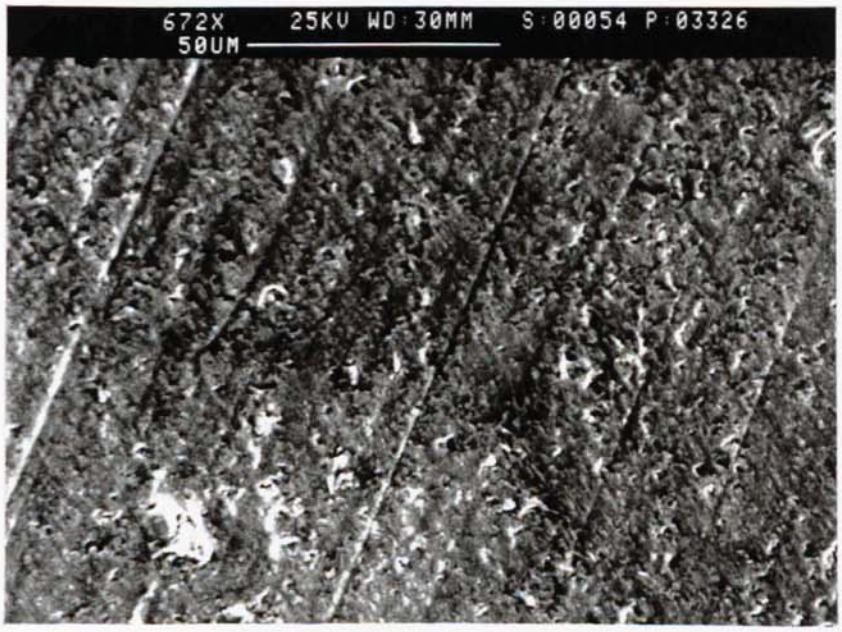

Figure 7.20 13 mm diameter M2 HSS standard helix drill, cutting speed 244 rpm.

The figure 7.21 shows the 13 mm diameter M2 HSS fast helix drill with a speed of 244 rpm. Two wear mechanism can be seen here; adhesive at the bottom of the figure and abrasive at the top of the figure.

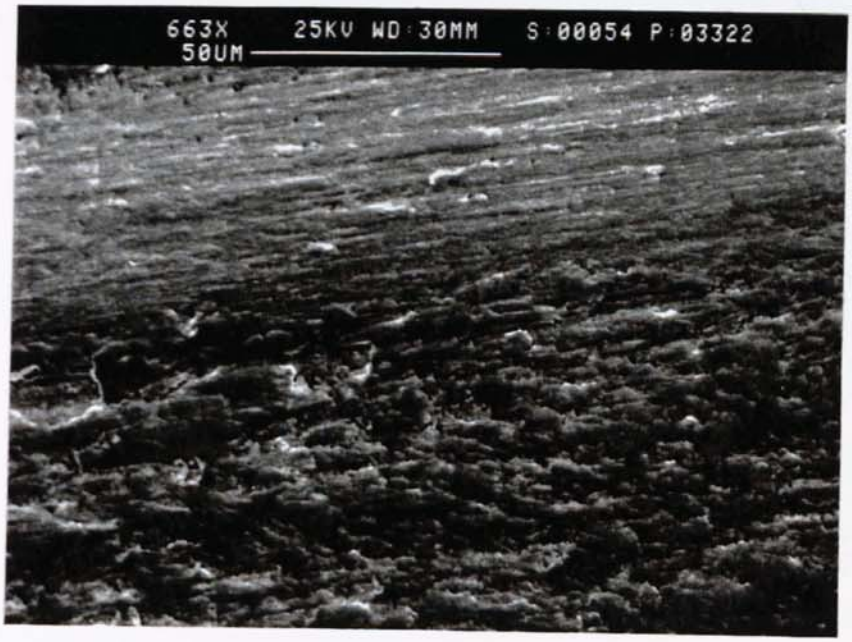

Figure 7.21 13 mm diameter M2 HSS fast helix drill, cutting speed 244 rpm.

Figure 7.22 shows 13 mm diameter M2 HSS slow helix drill at a speed of 490 rpm. The predominant wear mechanism that seems to be responsible with the wear is abrasion wear.

Figure 7.22 13 mm diameter M2 HSS slow helix drill, cutting speed 490 rpm.

Figure 7.23 shows 13 mm diameter M2 HSS standard helix at speed of 490 rpm. The predominant wear mechanism here again seems to be abrasion wear.

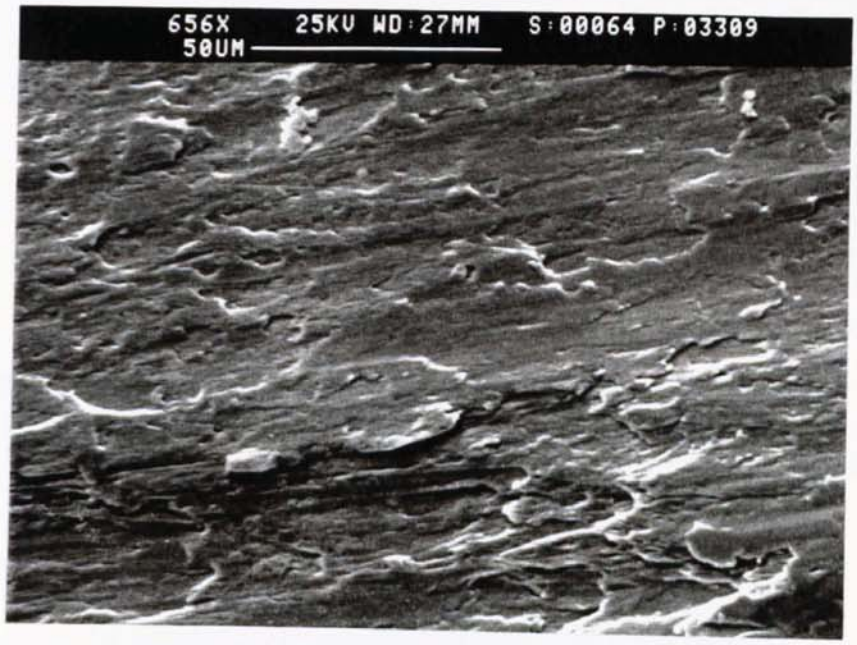

Figure 7.23 13 mm diameter M2 HSS standard helix drill, cutting speed 490 rpm.

Two wear mechanism can be seen in figure 7.24, of the 13 mm diameter M2 HSS slow helix drill at a speed of 735 rpm. Adhesive and possibly diffusive wear. The smoothness is a common sight of this condition.

Figure 7.24 13 mm diameter M2 HSS slow helix drill, cutting speed 735 rpm.

7.7.5 Catastrophic Failure

This figure 7.25 shows a general view of the lip of the 13 mm diameter M2 HSS fast helix drill with a speed of 735 rpm. Wear in the flank is seen and the drill can be seen chipped out on the side of the land, in other words catastrophic failure has occurred, which is due to cutting with high speed.

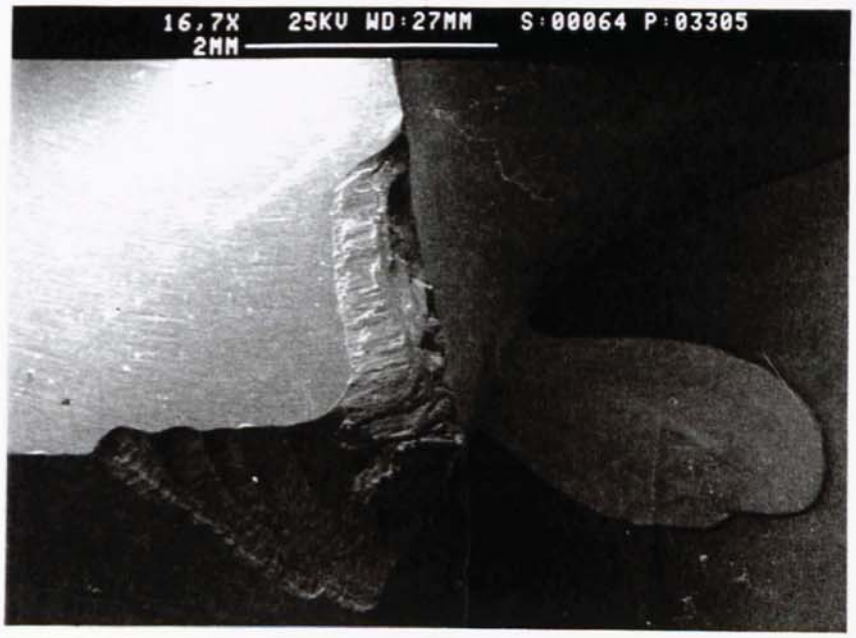

Figure 7.25 13 mm diameter M2 HSS fast helix drill, cutting speed 735 rpm.

7.8 CONCLUSION

Cutting force control for drilling processes has not yet been studied as vigorously as for the turning process. In the design and application of metal-cutting tools it is useful to be able to predict the forces which act upon a tool or the power required under a given set of operating conditions.

Although an ordinary twist drill operates in essentially the same way as a simple single point tool, it is extremely complex geometrically. When only the lips of a drill are used to cut a tubular test bar the action is similar to machining with a single-point tool and therefore can be considered related to machining accomplished in planer, lathe, and many milling-machine operations.

Compared to these removal processes, drilling is manifestly more complex in that the tool geometry and the tool obliquity change along the cutting edge. The angle of inclination increases and the rake angle decreases as the lip is transversed from the margin towards the web. In the absence of such a model, there is no basis on which analytical expressions for the torque and thrust force can be derived.

It was shown in this chapter that the forces have a similar effect on the drilling operation as they did in single point turning. It was seen that the wear mechanisms as in the previous chapter acted at the different stages of the tool life. It was also shown that temperature has an effect on the wear mechanisms. This influence that the temperature has is discussed in more detail in the next chapter with the illustrations of the results that were obtained from tests carried out in this work. It can also be seen in chapter 10 that a force predictive model that was for turning is extrapolated to drilling.

Chapter 8

TEMPERATURE IN TURNING AND DRILLING

8.1 INTRODUCTION

Cutting temperatures are of interest because they affect machining performance. The tool temperature is one of the fundamental parameters to measure the behaviour of wearing tools. This chapter will look at the various methods used by other investigators to measure temperature, as well as the technique used in this research. It will also look how temperature is generated and the factors that affect it. The results of the tests in this work in turning and in drilling will be discussed and analysed.

The fact that the machining temperature has a critical influence on tool wear and tool life has been well recognised since the work of Taylor (1907). Temperature influences many factors including the tool geometry, forces (as seen in chapters 6 and 7) and tool wear.

In addition to its influence on the various tool wear mechanisms, temperature is also important when determining the behaviour of the material in the chip formation process. It is, therefore, important to understand the factors which influence the generation of heat, the flow of heat and the temperature distribution in the tool and work material.

8.2 HEAT GENERATION

Practically all of the energy expanded in cutting metal is converted into heat. The heat generated during machining is due to mainly three sources: plastic deformation in the primary and secondary zones, and friction on the chip-tool interface and on the workpiece-tool interface.

Temperatures in the primary deformation zone, where the bulk of the deformation involved in chip formation occurs, influence the mechanical properties of the work material and thus the cutting forces. Temperatures on the rake face of the tool have a strong influence on tool life. As temperatures in this area increase, the tool softens and either wears more rapidly through abrasion or deforms plastically itself. In some cases constituents of the tool material diffuse into the chip or react chemically with the cutting fluid or chip, leading ultimately to tool failure. Stephenson et al. (1997) argue that since cutting temperatures increase with the cutting speed, temperature-activated tool wear mechanisms limit maximum cutting speeds for many tool-work material combinations. Finally, temperatures on the relief face of the tool affect the finish and metallurgical state of the machined surface. Moderate levels of these temperatures induce residual stresses in the machined surface due to differential thermal contraction, while high levels may leave a burned or hardened layer on the machined part.

8.2.1 Factors Affecting Cutting Temperatures

Cutting speed and feed rates have an influence on the temperature in that by increasing the cutting speed the rate of heat generation in the cutting zone increases. Increasing the feed rate also increases heat generation and cutting temperatures.

Other parameters such as the depth of cut and the rake angle, also influence cutting temperatures; changes in these parameters which increase the cutting force normally slightly increase cutting temperatures.

Material properties also strongly influence cutting temperatures. Cutting temperatures are higher for harder work materials because cutting forces and thus energy dissipation are increased. For materials of similar hardness, cutting temperatures increase with ductility, since more ductile materials can absorb more energy through plastic deformation.

Thermal properties of the work material which influence cutting temperatures include the thermal conductivity and heat capacity. Temperatures generally decrease as these

parameters increase, since an increase implies that heat is more readily conducted away through the workpiece or that the temperature increases more slowly for a given heat input. Increasing the thermal conductivity and heat capacity of the tool material also reduces temperatures, although, as Stephenson argues, the effect does not appear to be as marked as for the work material (Stephenson et al. 1997). This must surely be due to the reduced heat sink capacity of the tool since it is not an integral part of the tool holder and therefore a weakness in the heat transfer chain. Factors of this kind, i.e., tool size, geometry etc. are similar factors which lead to the differences which were found in this work and which is discussed throughout the chapter. Factors affecting heat sink capacity such as for example bar size might be expected to play a part and this would be demonstrated later in the chapter.

8.3 SCOPE OF VARIOUS TECHNIQUES

Considerable effort has been made in the past to determine the temperature in the tool, chips and workpiece because the cutting temperature is one of the most important factors contributing to the mechanism of the cutting process. Kato et al. (1996) argue that in particular, the determination of the temperature distribution in a tool, not the average tool-chip interface temperature, is essential for studying the tool-wear mechanism with a high degree of confidence. Several methods of measuring cutting temperatures have been developed. Particular methods generally yield only limited information on the complete temperature distribution.

8.3.1 Tool-Work Thermocouple Method

Cutting temperatures are most commonly measured using thermocouple techniques and the most widely used method is the tool-work thermocouple method which as Barrow (1973) states was first developed in the 1920s almost simultaneously by Gottwein, Herbert and Shore.

This method uses the tool and workpiece as the elements of a thermocouple. In this technique the electromotive force (emf) generated at the junction between the workpiece and tool is taken as a measure of the temperatures in the region. The hot junction is the interface between the tool and the workpiece, and the cold junction is formed by the remote sections of the tool and workpiece, which must be connected electrically and held at a constant reference temperature. It is important when using this technique to insulate the thermocouple circuit from the machine and to use the same circuit when calibrating the thermocouple.

Boothroyd et al. (1989) state that the tool-work thermocouple method is limited because it gives no indication of the distribution of temperature along the tool rake face. There are a number of sources of error in using the tool-work thermocouple. In particular, the tool and work materials are not ideal elements for a thermocouple. Consequently, the emf tends to be low and the emf/temperature calibration non-linear. The tool-work thermocouple must be calibrated against a standard thermocouple. Each tool and workpiece material combination must be calibrated separately. In addition, it is unlikely that the emf determined with a stationary tool, used for calibration, is the same as that obtained for an equivalent temperature during cutting when the work material is being severely strained.

Despite these difficulties, the tool-work thermocouple method has a number of advantages. Stephenson et al. (1997) show that the results are repeatable and correlate well with tool wear for carbide and high speed steel tools. The measurements also show good time response, making the method suitable for measuring temperatures in thermally transient processes such as milling and for monitoring temperatures as an indication of tool wear. The instrumentation required can also be built into the machine tool and operated reliably without constant readjustment.

Leshock et al. (1997) investigated the tool-chip interface with flank and crater wear to determine the effect of tool face temperature on these tool wear mechanisms by using this technique. Also by using this technique, Zakaria et al. (1975) measured the cutting temperature by sensing on-line.

Methods similar to the tool-work thermocouple technique include those in which insulated wires are embedded in the tool or workpiece (Stephenson et al. 1997). In the first case the hot junction is formed at the point of contact between the workpiece and the wire embedded in the tool; in the second case, the hot junction is formed when the tool cuts through the wire. In either case, the cold junction is formed in the same manner as in the tool-work thermocouple method. Agapiou et al. (1994) show that if the wire material is properly selected (e.g. a copper wire for a tungsten carbide tool), the thermoelectric power of the circuit can be increased, improving the signal-to-noise ratio of the measurement. Stephenson et al. (1997) argue that their chief disadvantages are that they require careful calibration and tedious specimen preparation and data reduction. In the case of when embedded in the workpiece, the time required for the tool and wire to come to thermal equilibrium also limits the maximum cutting speed which can be used.

Conventional thermocouples can be embedded in the tool or workpiece to map temperature distributions. This approach has not been widely applied because of the extensive specimen preparation required. Since temperature gradients near the cutting zone are steep, its accuracy is limited by the placement accuracy of the thermocouples, according to Stephenson et al. (1997). The resolution and accuracy of the measurements are also limited by the bead size of the thermocouple, by the difficulty of obtaining good thermal contact between the thermocouple bead and specimen, and by the fact that the temperature field is disturbed by the presence of the holes required to insert the thermocouple. In most cases the embedded wire methods will yield more accurate results with less effort.

Conventional thermocouples can also be used to measure temperatures at points in the tool remote from the cutting zone. An advantage of this method is that the required thermocouples can be built into the toolholder, making the method attractive for routine measurements and process monitoring.

8.3.2 Metallurgical Methods

Metallic tool materials often undergo metallurgical transformations or hardness changes which can be correlated to temperature. Trent (1991) states that much more information about temperature distribution near the cutting edge of tools may be obtained by using the tool itself to monitor the temperature. The room-temperature hardness of hardened steel decreases after reheating, and the loss in hardness is related to the temperature and time of heating. These changes provide an effective means of determining temperature distributions in the tool during cutting.

Microhardness measurements on tools after cutting can be used to determine constant temperature contours in the tool and the structural changes can be observed by optical and electron microscopy. Trent (1991), in his experiments, showed the structures within the regions and with the temperature corresponding to each structure. Also, he demonstrated how the light area in the centre of the heat-affected region has been above 900 °C. But the microhardness technique is time-consuming and requires very accurate hardness measurements, and the structural change method requires experience in interpretation of structures but, where it can be used, it is as accurate and much more rapid. In conjunction with metallographic studies of the interface, important information can be gained which is lost using microhardness alone.

This method, according to Boothroyd et al. (1989), had been used to study temperature distributions in high-speed steel lathe tools and drills. The main limitations of this method of temperature estimation is that it can be used only within the range of cutting conditions suitable for high-speed steels and when relatively high temperatures are generated.

8.3.3 Radiation Techniques

Cutting temperatures can also be estimated by measuring the infrared radiation emitted from the cutting zone. This method was first applied by Schwerd (Stephenson et al. 1997) and further developed by Kramer (Barrow 1973). They developed a total radiation

pyrometer for determining the temperature distribution at the surfaces of the tool and workpiece.

Several workers attempted to overcome the problem of access to the chip tool interface by scanning through holes drilled either in the workpiece or tool. These include Reichenback who measured both shear plane and relief face temperatures, Chao et al and Bornhoefer and Pahlitzsch measuring the temperature distribution on the flank face of a cutting tool. In both cases the flank face was scanned through the workpiece. Lenz (Stephenson et al. 1997) and Prins (1971) measured the temperature at the rake face with a radiation pyrometer. In both cases there is considerable interference of the contact zone which must influence the heat flow and the resulting temperatures. In addition it is difficult to calibrate the pyrometers precisely, since there are problems in simulating the emissivity of either the chip or tool surface.

In an attempt to eliminate these problems, Boothroyd et al. (1989) used infra-red photography to obtain temperature distributions in the chip, tool and workpiece by taking full-field infrared photographs of the cutting zone in low speed experiments. Infrared measurements are limited to exposed surfaces and cannot be used to directly measure temperatures in the interior of the chip. The signal-to-noise ratio of measurements from many areas of the cutting zone is limited by the fact that the chip is normally much hotter than other areas and dominated the infrared signal, obscuring other nearby features. Finally, it is necessary to estimate the emissivity of the target (which is often difficult because it varies with both the temperature and the surface finish) to convert measured infrared intensities to temperatures. Because of these limitations infrared measurements are difficult to perform accurately and often do not produce repeatable results.

Young (1996) used the non-contact infrared thermographic technique to investigate the cutting temperature during chip formation which has shown a clear relationship between the measured chip-back temperatures and the tool-chip interface temperatures.

8.3.4 Thermo-chemical Reactions

Temperature distributions can also be estimated by coating specimens with thermosensitive paints. The technique depends on the fact that paints change their colours at a certain temperature. This colour change phenomenon, although a chemical reaction, is much dependent on the heating conditions such as the heating rate and the heating duration. The application of the technique is limited to measurements made under strictly controlled heating conditions. The technique can result in serious errors especially in cases where the change in temperature is as rapid as that which generally occurs in cutting tools. While most researchers, including Schallboch and Lang, Bickel and Widner, and Vieregge have only measured the temperature of the accessible tool surface by this technique (Barrow 1973), Okushima and Shimoda (Kato et al. 1996) measured the temperature distribution within a tool. They designed a special split-tool and were able to measure the temperature in the vicinity of the cutting edge because the paint, sandwiched between the two halves of the split-tool, was protected from being scraped off by chips.

Kato et al. (1996) developed a technique to estimate the temperature utilising the physical phenomenon of melting instead of the chemical reaction of the paints. The principle of the method is based upon the fact that the fine powder of a material melts at a certain sharp and determinable melting point and that the border between melted zone and unmelted indicates an isotherm. Consequently, several lines obtained using various materials showed the temperature distribution in a tool. However, the thermal response in this technique is poor because the powder forms a thick layer and does not establish a close contact with the tool surface.

Another new method that was used by Kato et al. (1996) to measure the temperature distribution in cutting tools was the PVD (physically vapor deposited) method. A thin PVD film deposited on a cutting tool is used as a thermal sensor. Various films of different materials, that is, indium, bismuth, lead, tellurium, antimony and germanium, are deposited to determine the location of a multiplicity of isotherms at different temperatures. It is confirmed that the boundary between the melted film zone and the

unmelted film zone showed the isotherm directly and clearly. This method is also found to be very sensitive and applicable to any tool material as well as to a very small area.

Other techniques include one used by Schmidt et al. (1949) where the object of his investigation was to determine the amount of heat which goes into the workpiece, chips, and drill at different cutting speeds and feeds. The total heat, the heat in the chips, and the heat in the drill were measured separately in a calorimeter. Water at room temperature was measured into the calorimeter and the water-temperature readings were taken immediately before and after cutting. The total heat was measured by performing the drilling operation with the workpiece, chips, and tool submerged in water. The heat in the tool was determined by cutting an identical test bar dry by dropping the tool into the calorimeter immediately upon completion of cutting. Heat in the chips was obtained by noting the temperature rise of the calorimeter and water into which only the chips were permitted to fall.

8.3.5 Finite Element Approach

Many investigators have contributed to the theoretical analysis and experimental measurement of metal cutting temperature distributions as reviewed in the previous section. Further improvements in temperature estimates became possible by the use of the finite element method.

The use of the finite element method for calculating machining temperature distributions was first described in 1974 by Tay, Stevenson, and De Val Davis (Stevenson et al. 1983). The main advantage of these models was they predicted complete temperature distributions rather than average temperatures over one or two surfaces. The input requirements, however, made them difficult to apply accurately to a broad set of cutting conditions.

Tay's original model, and later Muraka's et al. (1979) model required measured cutting forces, chip properties, tool-chip contact lengths, and work material velocity distributions to predict temperatures. Subsequent researchers simplified Tay's model

and eliminated the need for measured velocity fields, so that temperature distributions could be based on cutting force and chip property inputs equivalent to those used in the simpler analytical models. Since this information is predicted by the more complete models of the cutting mechanics, these analyses are suitable for use in coupled force and temperature models such as those reported by Oxley, Usui, and Strenkowski and Moon (Stephenson et al. 1997).

The classical finite element method, with a few measured temperatures at arbitrary points given as boundary conditions, provides a powerful tool for determining the isotherms. However, the boundary conditions for convection and radiation heat transfer cannot be easily included in the mathematical model. Mansour et al. (1973) presented a quasi-finite element model for the determination of steady-state thermal fields in a tool-chip-workpiece system. The approach accounts for all the three modes of heat transformation: conduction, convection and radiation. Only a few temperature measurements, at certain discrete points in the continuum, are needed as boundary conditions.

It is difficult to assess the accuracy of finite element temperature models because the temperature distributions they predict cannot be easily measured. In some cases calculated temperatures are presented without any experimental comparison. and in others, calculations are compared with limited point temperature measurements. The lack of comprehensive comparisons with experiments is of concern because many physical and numerical assumptions are required to carry out calculations.

The tool temperature in turning and the drilling operations has been experimentally studied in this work by using thermocouple embedded in the tool which was chosen not because it is the most recommended and it gives good results in a short interval, and because of its ease in implementation after it has been calibrated, and its low cost. In the turning operation, two thermocouples were used in different positions on the tool as can be seen in figure 8.2, as well as further illustration in figure 8.3 and 8.4. In the drilling operation the position of the thermocouple can be seen in figure 8.5, and further illustration can also be seen in figure 8.6.

8.4 EXPERIMENTAL WORK

8.4.1 Temperature Measurement Technique

As mentioned above, in this research the technique that was used for measuring the temperature was by using the thermocouple wire embedded in the tool. More details on experimental methods and equipment can be seen in chapter 4 in figure 4.7.

In the turning operation, the tool used was uncoated BT42 HSS. The tool was in the form of a triangle with a nose radius of 4 mm with the specifications of TPUN 16 03 04 according to the manufacturers of Kennametal. Two locations were used to place the thermocouples. For thermocouple number one, a groove was cut in the tool as shown in figures 8.1 by using Electrical Discharge Machining (EDM).

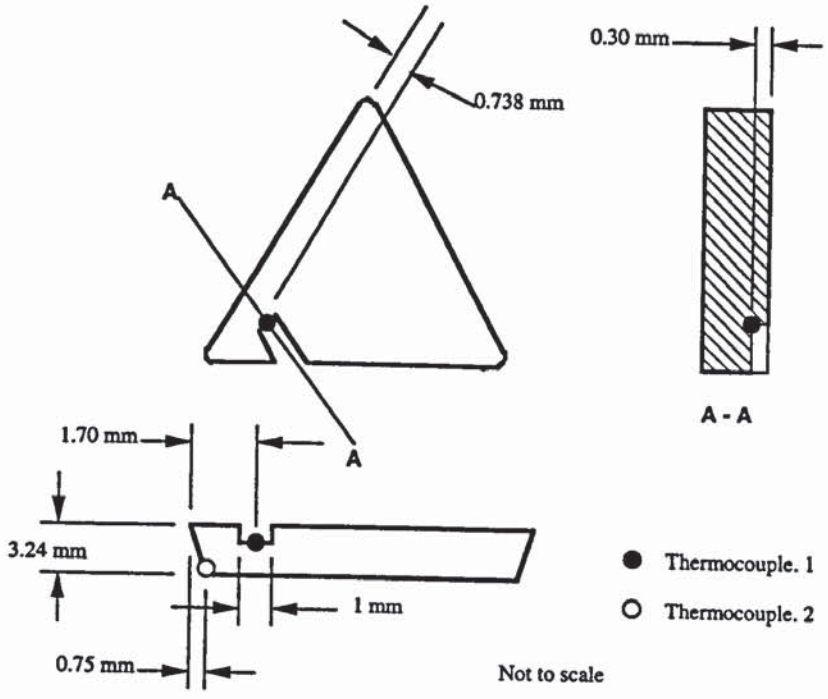

Figure 8.1 Thermocouple positions in the tool for the turning operation

The groove was made in the rake face and the thermocouple wire was placed in the groove near the cutting edge as seen in figure 8.2. The groove was then filled with silver dag in order to further enhance conduction. What some researchers have attempted

before is to drill a hole and place the thermocouple. However, this technique does not have the advantage that the groove technique has where the position of the thermocouple can be seen and the where one can also see that contact has been made with the tool.

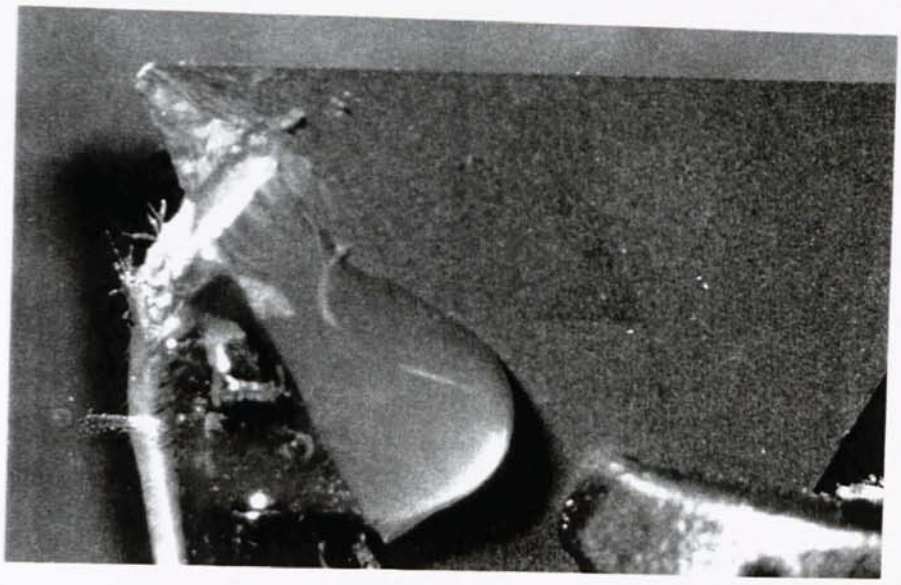

Figure 8.2 Illustration of thermocouple one embedded in the groove

The second thermocouple was placed under the tool as seen in figure 8.1 and 8.3.

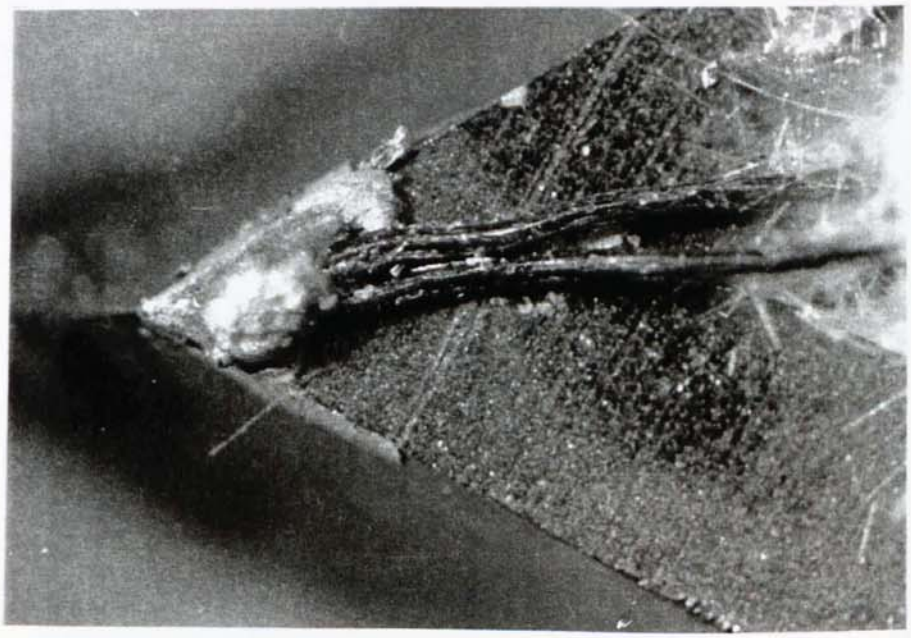

Figure 8.3 Illustration of thermocouple two under the tool

The procedure that was followed in the drilling operation was to embed two thermocouples in the drill, routing them through the oil holes of pressure-fed drills as seen in figure 8.4 and figure 8.5. The drill used was ADX 8 mm diameter uncoated HSS standard helix. The tests were performed while the workpiece rotated and the drill was stationary.

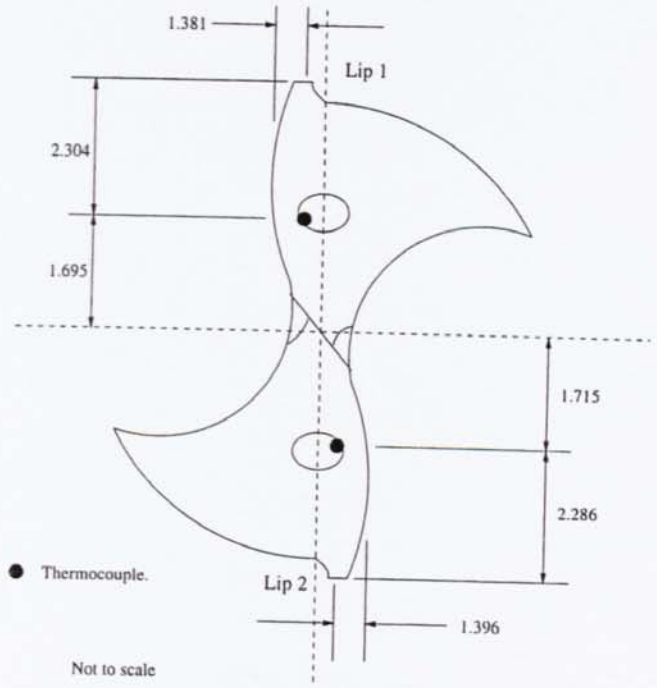

Figure 8.4 Thermocouple position through the oil hole of a drill

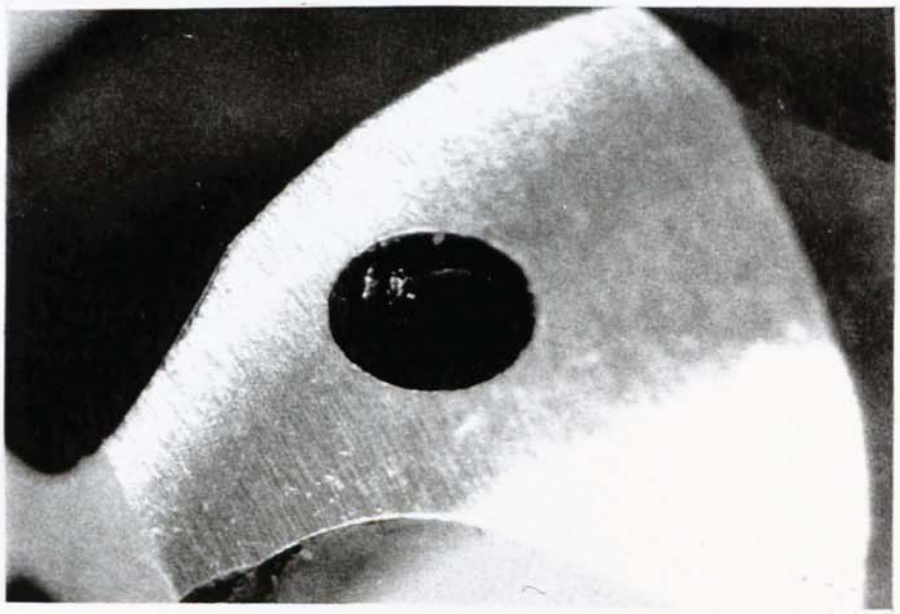

Figure 8.5 Illustration of the thermocouple in the oil hole

8.4.2 Chemical Analysis and Calculation Techniques

Another system which was used in this work, and which may be used when cutting steel at low speed is to calculate the temperature of the chip surface. This is an approach which can give alternative information on temperature effects in relation to the chip. This can be carried out by analysing the surface of the chip and calculating the amount of oxide iron and free iron on the surface (that is, percentage of oxide iron ratio to the percentage of free iron ratio). More details can be seen in chapter 4.

The technique used to undertake this analysis is called X-ray Photoelectron Spectroscopy (XPS). In this technique photoelectrons are produced from the atoms near to the surface of the chip by irradiating the sample with monochromatic X-rays. Measurement of the photoelectron energy enables the identification of elements on the surface from hi upwards. The chemical state of those elements can be found by measurement of small shifts in the primary photoelectron lines. Concentration can be determined from the peak intensities with a knowledge of relative sensitivity factor.

This technique was chosen in order to further prove the bar diameter effect on the temperature which will be discussed later in the chapter.

8.5 EXPERIMENTAL RESULTS

8.5.1 Turning

Table 8.1 shows the sets of results obtained for the maximum temperature for the two thermocouples in the two different locations as shown in figures 8.1, 8.2 and 8.3. The test time was 15 seconds for both sets of tests seen in the table; one set of tests was carried out for the tool with the new tip and the other for the tool with wear. (See test conditions in appendix 1 tables A1.13 to A1.19).

Temperature (°C)							
set of test	new tip (1)		worn tip (1)		new tip (2)		worn tip (2)
Speed (m/min)	t/c (1)	t/c (2)	t/c (1)	t/c (2)	t/c (1)	t/c (2)	t/c (2)
10	166.25	113.25	215.5	122	186.5	114.5	141
20	214.5	149.5	269.25	156.5	218.5	146.75	177
30	249.25	171.25	311.25	183.75	228.5	171.5	225.75
40	331.75	220.75	345.5	228.5	255.25	196	311.5

Table 8.1 Temperature in Turning.

8.5.1.1 New Tool

Figure 8.6 shows the tool temperature vs. cutting time for the new tool. The tool material BT42 uncoated HSS, with a feed rate of 0.15 mm/rev., nose radius 0.4 mm dry cut. The cutting speeds were 10, 20, 30 and 40 m/min. It can be seen from the graph that the temperature increases as the speed is increased. The graph also shows that within approximately 3.5 seconds of cutting the temperature has reached steady state. (See test conditions in appendix 1 tables A1.13 to A1.16).

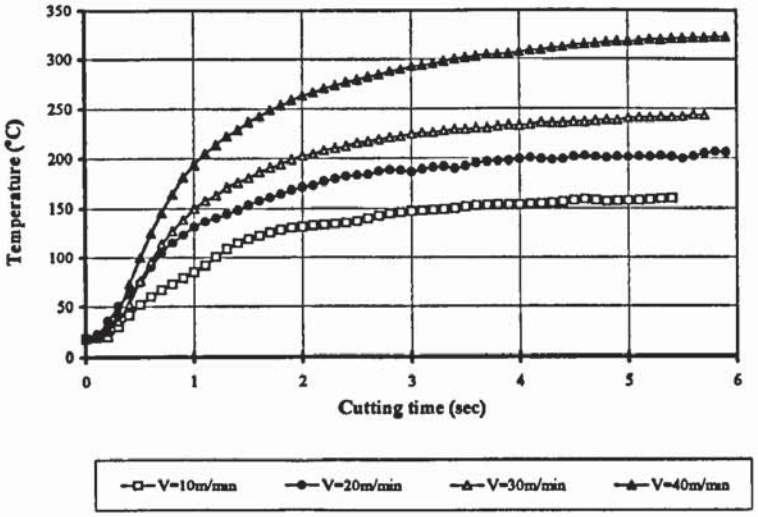

Figure 8.6. Tool temperature *vs*. cutting time, tool material is BT42 uncoated with 2 mm DOC, 6 & 5 deg. rake & flank angles, nose radius 0.4 mm, feed rate 0.15 mm/rev., dry cut. Thermocouple (1).

In figure 8.7 a new tool is tested. The graph shows that as the speed increases the temperature increases. It is shown that it takes about 0.5 second at the beginning before there is any difference in temperature between the four speeds and it takes longer than thermocouple 1, as shown in figures 8.1, 8.2 and 8.3, for the temperature to reach steady state, which is in approximately 4 seconds.

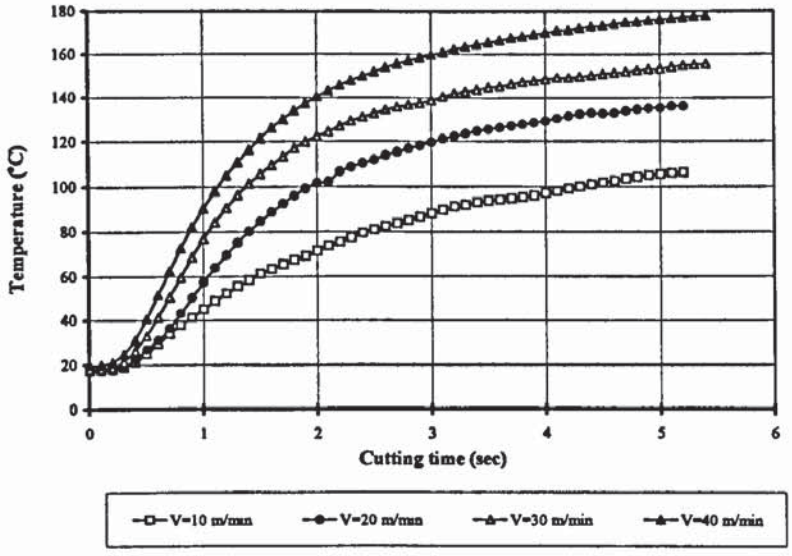

Figure 8.7. Tool temperature *vs*. cutting time, tool material is BT42 uncoated with 2 mm DOC, 6 & 5 deg. rake & flank angles, nose radius 0.4 mm, feed rate 0.15 mm/rev., dry cut. Thermocouple (2).

8.5.1.2 Worn Tool

The results seen in graph 8.8 are for worn tool and the tool material is as above. The graph shows tool temperature against cutting time, with flank wear 0.177 mm maximum, 0.118 mm average, 0.299 mm notch wear, 0.243 mm nose wear, and depth of rake face wear of 0.1 mm. Again the temperature can be seen to increase by increasing the cutting speed, and the cutting temperature increasing with wear as compared with graph 8.6. The cutting speed being again the same as the above. Again here the steady state temperature is reached in approximately 3 seconds. (See test conditions in appendix 1 table A1.17).

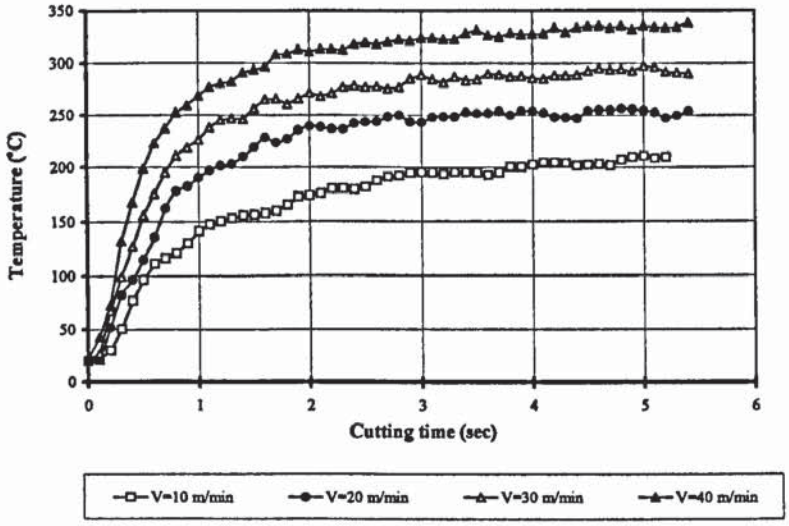

Figure 8.8. Tool temperature vs. cutting time, tool material is BT42 uncoated with 2 mm DOC, 6 & 5 deg. rake & flank angles, nose radius 0.4 mm, feed rate 0.15 mm/rev., dry cut.with flank wear: 0.177 mm max., 0.118 mm av., 0.299 mm notch wear and 0.243 mm nose wear, and depth of rake face wear 0.1 mm. Thermocouple (1).

Figure 8.9 shows the results for the tool which has wear in the flank and rake angle. The graph shows that the temperature is higher than in graph 8.7, and again it takes about 0.5 second before there is a difference in temperature between the four speeds. It also takes approximately 4 seconds for the temperature to reach steady state.

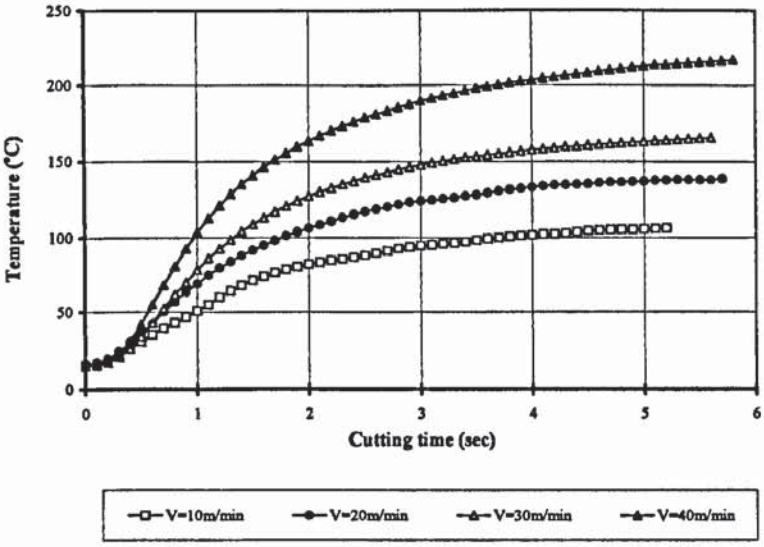

Figure 8.9. Tool temperature vs. cutting time, tool material is BT42 uncoated with 2 mm DOC, 6 & 5 deg. rake & flank angles, nose radius 0.4 mm, feed rate 0.15 mm/rev., dry cut.with flank wear: 0.177 mm max., 0.118 mm av., 0.299 mm notch wear and 0.243 mm nose wear, and depth of rake face wear 0.1 mm. Thermocouple (2).

In both graph 8.6 and 8.8 the results are shown from thermocouple 1 which is nearer to the cutting edge and therefore is recording a higher temperature. The diagrams of thermocouple 1 are shown in figure 8.1 and 8.2 above.

Graphs 8.7 and 8.9 show the results for thermocouple 2 which is under the tool and can be seen above in figure 8.1 and 8.3. Again the tool material used for both is BT42 uncoated HSS. Both graphs show tool temperature vs. cutting time and the cutting speeds used are 10, 20, 30 and 40m/min.

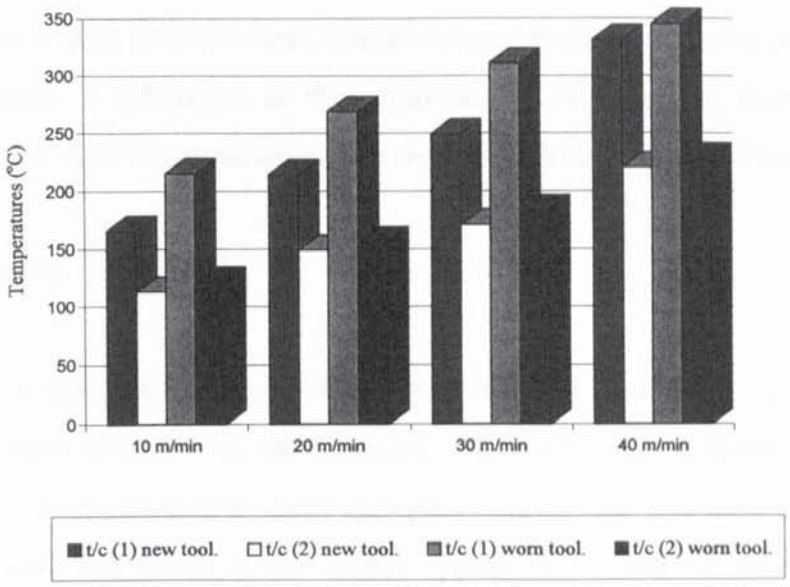

Figure 8.10. Tool temperature *vs* . cutting speed, tool material is BT42 uncoated with 2 mm DOC, 6 & 5 deg. rake & flank angles, nose radius 0.4 mm, feed rate 0.15 mm/rev., dry cut.

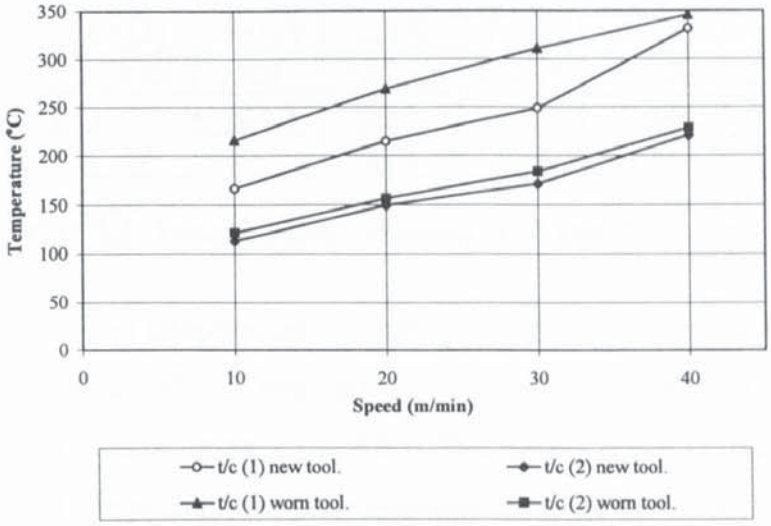

Figure 8.11. Tool temperature *vs* . cutting speed, tool material is BT42 uncoated with 2 mm DOC, 6 & 5 deg. rake & flank angles, nose radius 0.4 mm, feed rate 0.15 mm/rev., dry cut.

Figures 8.10 and 8.11 show the graph of temperature vs. cutting speed (after 15 seconds of cutting). From both graphs it can be seen that the two thermocouples are at different locations as shown in figures 8.1, 8.2 and 8.3. One set of the tests is for the tool with the new tip and the other is for the tool with wear.

From the graphs it is seen how the wear affects the temperature. Also the position of the thermocouples make a difference in the temperature; even though there is a small distance between the two thermocouples there is a large difference in the temperature.

8.5.1.3 Bar Diameter

The results of the temperature tests for the four different speeds 10, 20, 30 and 40 m/min.) and the three different bar diameters (31, 53 and 75 mm) is shown in table 8.2. For the speeds of 10 and 20 m/min. thermocouples were used at two locations as seen in figures 8.1, 8.2 and 8.3, while at the higher speeds of 30 and 40 m/min. only one thermocouple was used; the second thermocouple as seen in figure 8.3, as seen in figure 8.1 and 8.3. (See test conditions in appendix 1 tables A1.18 to A1.19).

Bar diameter	Cutting Speed (m/min)							
	10		20		20		30	40
	t/c (1)	t/c (2)	t/c (1)	t/c (2)	t/c (1)	t/c (2)	t/c (2)	t/c (2)
31	173.5	139.25	231	193.25	214.75	185.25	228.75	318
53	165.5	131.5	223.5	184	-	180	218	272.75
75	159.25	129	-	173	-	177	215.75	265

Table 8.2 Temperature variation with bar diameter.

Graph 8.12 shows the tool temperature vs. cutting time for tool material BT42 uncoated HSS with a nose radius of 0.4 mm dry cut. The results here are obtained from thermocouple two as seen in figure 8.1 and 8.3. The cutting speed is fixed at 20 m/min. and the feed rate at 0.15 rev/min., the only variation being the bar diameter at 31 mm, 53 mm, and 75 mm.

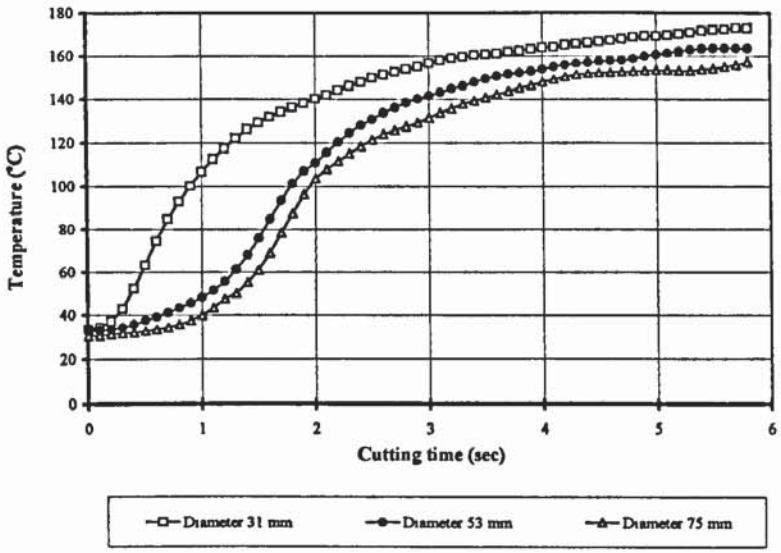

Figure 8.12. Tool temperature *vs*. cutting time, tool material is BT42 uncoated with 2 mm DOC, 6 & 5 deg. rake & flank angles, nose radius 0.4 mm, feed rate 0.15 mm/rev., dry cut. Thermocouple (2).

As can be seen clearly from the graph, the highest temperature is at diameter 31 mm as compared to the other 2 diameters, and then the next highest is at 53 mm diameter then at 75 mm diameter. Therefore the smaller the bar diameter the higher the temperature and the larger the bar diameter the lower the temperature. It took approximately 0.5 second before any response was recorded for the temperature. For the 31 mm diameter it took about 3 seconds for the temperature to reach steady state, while for diameters 53 mm and 75 mm it took about 4 seconds. All the results are recorded from thermocouple two as seen in figure 8.3.

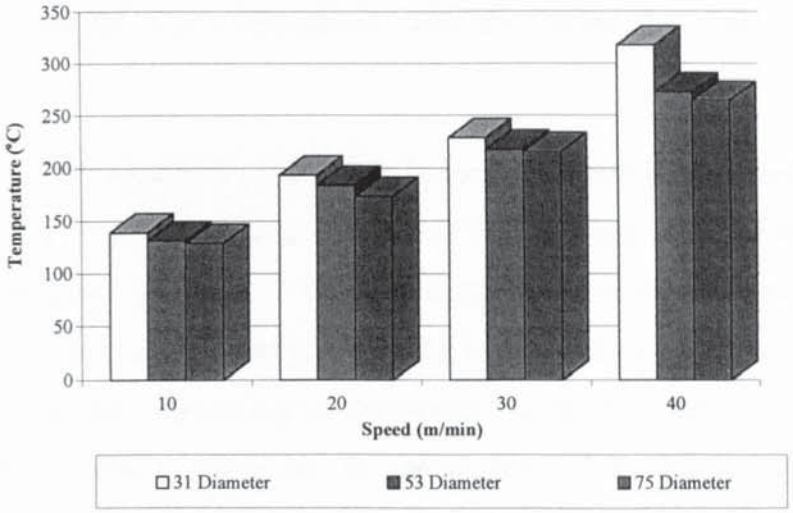

Figure 8.13. Tool temperature vs. cutting speed, tool material is BT42 uncoated with 2 mm DOC, 6 & 5 deg. rake & flank angles, nose radius 0.4 mm, feed rate 0.15 mm/rev., dry cut. Thermocouple (2).

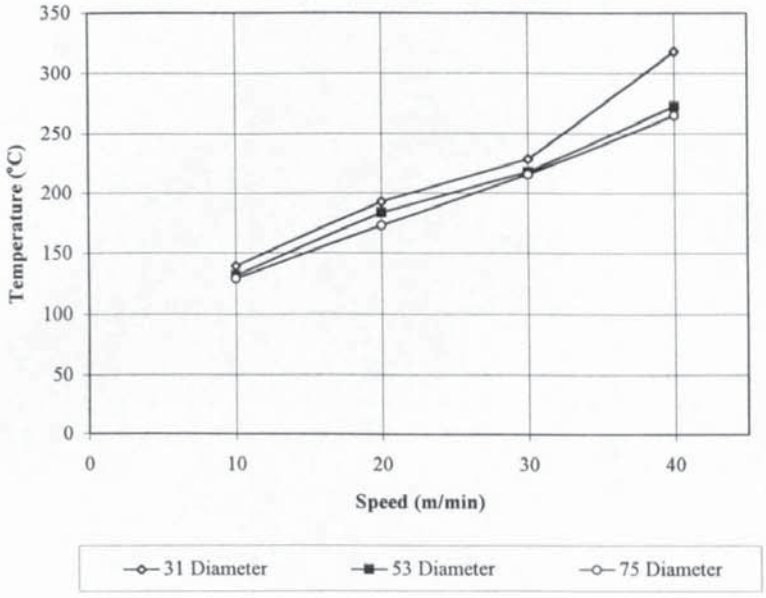

Figure 8.14. Tool temperature vs. cutting speed, tool material is BT42 uncoated with 2 mm DOC, 6 & 5 deg. rake & flank angles, nose radius 0.4 mm, feed rate 0.15 mm/rev., dry cut. Thermocouple (2).

Both the results for graphs 8.13 and 8.14 have also been obtained, (after 15 seconds of cutting), from thermocouple two as above, which is shown in figure 8.3. The tool material used was uncoated BT42 HSS with nose radius 0.4 mm. Four different cutting speeds (10, 20, 30 and 40 m/min.) and three different bar diameters (31, 53 and 75 mm)

were used. For all the four speeds, in both graphs, it is seen that the smaller the bar diameter the higher the temperature, and the larger the diameter the lower the temperature.

In figure 8.15 a photograph of the chip is seen. The test was carried out by using the cutting speed of 20 m/min. And a feed rate of 0.15 mm/rev. with the same bar with three different diameters (31, 53 and 75 mm). It can be seen from figure 8.15 (a) the chip colour is brownish-purple, from (b) the chip is dark straw, and from (c) the chip colour is not noticeable, the same as that of the workpiece material, that is, no change in colour. According to the colour of the chip, the temperature of the chip in (a) is higher than that in (b), and the temperature in (b) is higher than that in (c) which have bar diameters of 31, 53 and 75 mm respectively.

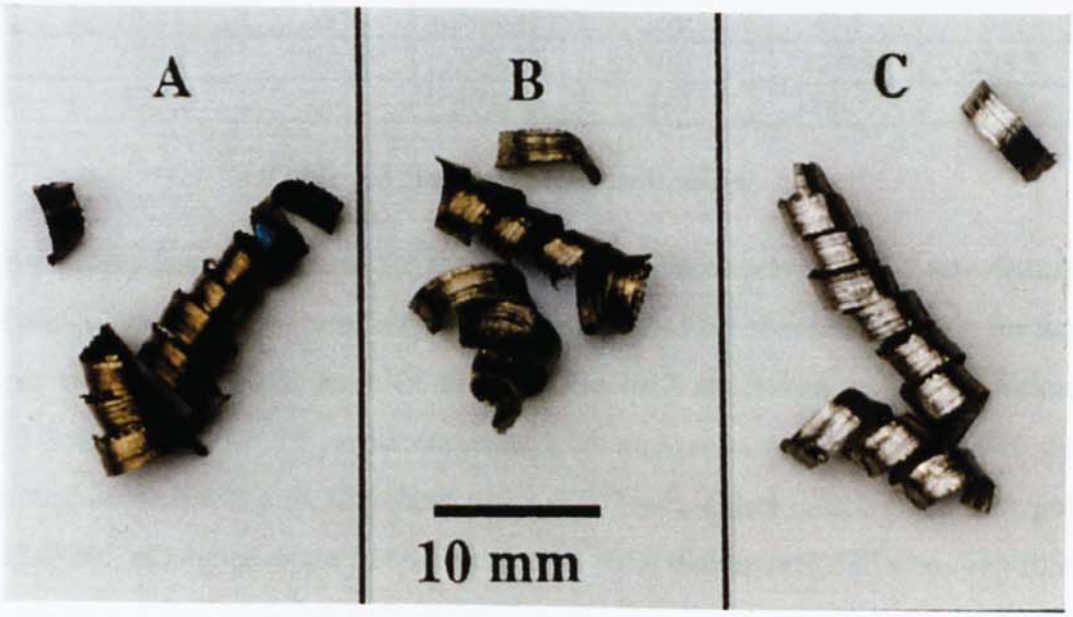

Figure 8.15 Photograph of chip colour with varying bar diameter: (a) 31 mm, (b) 53 mm and (c) 75 mm.

Therefore, for a given rate of energy input the heat is dissipated in a proportionate manner to the tool, the workpiece and the chip. The rate of dissipation of heat to the workpiece is influenced by size (diameter) since the heat sink capacity is affected. Also this reduction puts a greater burden on the tool and chip as heat dissipaters. The consequence being that the tool temperature rises and the chip shows similar evidence.

8.5.2 Drilling

The tool material used for the following tests is M2 HSS standard helix drills. In table 8.3 the maximum temperature in the drilling operation is seen in both lips with the test time of 15 seconds. Two thermocouples were used; one in each lip. Three different speeds (310, 700 and 900 rpm) and three different feed rates of 78, 156, and 234 mm/min respectively, were used. The table shows the results obtained from the drill tests under three different conditions: the first is for the new drill, the second is for the drill with wear, and the third is for the new drill of 2 mm cut only. (See test conditions in appendix 1 tables A1.20 to A1.25).

Temperature (°C)						
set of test	2 mm cut only		new drill		worn drill	
Speed (rpm)	Lip (1)	Lip (2)	Lip (1)	Lip (2)	Lip (1)	Lip (2)
310	163.25	165	202.25	199	314	211
700	259.25	254.5	304.75	302	323.5	323.5
900	275.5	274	353.75	349	383.75	377

Table 8.3 Temperature in Drilling.

Table 8.4 shows four sets of tests for the temperature. Three sets are for 8 mm diameter drill of which two sets have two thermocouples, the third set of results is again for the 8 mm drill with one thermocouple in the lip. The drill specifications are as follows: standard helix angle 32° 25`, drill diameter 8.05 mm, relative lip height 0.049 mm, cutting land width 0.898 mm, flute land width 6.372 mm, chisel length 1.638 mm, point angle 124° 20`, clearance angle 31° 04`, and total point clearance 0.335 mm. The fourth set is with an 8.5 mm diameter drill which is worn (this was performed as a trial before the rest of the tests took place).

Temperature (°C)						
set of test	8 mm new drill		8 mm new drill		8 mm new drill	8.5 mm worn drill
Speed (rpm)	Lip (1)	Lip (2)	Lip (1)	Lip (2)	one lip only	one lip only
310	209.5	208.5	213.2	208	207	200.25
700	308.75	311	319	318.5	309	401.75
900	374	366	364.5	360	358	513

Table 8.4 Temperature for 8 mm diameter drill.

8.5.2.1 New Drill

Graph 8.16 shows tool temperature vs. cutting time for tool material M2 HSS standard helix angle drill with 8 mm diameter, using a new tool at dry cut. Three different speeds of 310, 700 and 900 rpm, three different feed rates of 78, 156, and 234 mm/min respectively, and two thermocouples at each cutting lip were used which can be seen in figures 8.4 and 8.5 above. (See test conditions in appendix 1 tables A1.20 to A1.22).

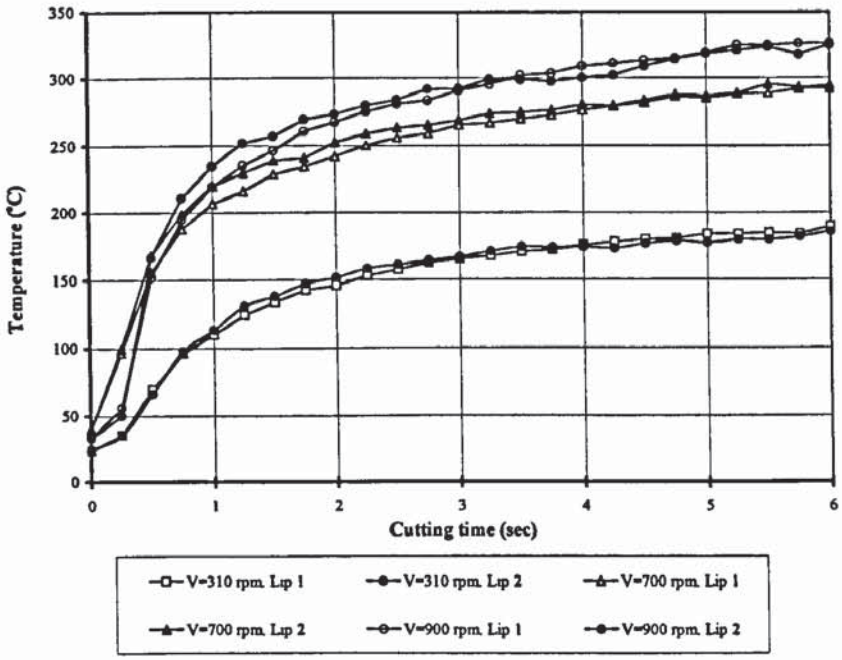

Figure 8.16. Tool temperature *vs*. cutting time, tool material is M2 HSS, standard helix angle drill 8 mm diameter resharpened, dry cut.

From the graph it can be seen that the higher the cutting speed then the higher the temperature. The highest temperature was reached for speed 900 rpm, the 700 rpm and the lowest for the cutting speed of 310 rpm. It can also be seen from the graph that the difference in temperature between the 310 rpm cutting speed and the other two speeds of 700 and 900 rpm is quite notable. It is seen from the graph that the two cutting lip temperatures are extremely close. It can be seen that approximately 3 seconds were taken for the temperature to reach steady state.

8.5.2.2 Worn Drill

The tool temperature vs. cutting time results for the drill, as above in figure 8.16, but with wear can be seen in graph 8.17. The flank wear was 0.138 and 0.132 mm maximum, 0.051 and 0.72 mm average, the corner wear was 0.139 and 0.158 mm. Again the same three different speeds as above were used and two thermocouples; one for each cutting lip were used. Again it can be seen that the temperature reaches steady state in approximately 3 seconds. (See test conditions in appendix 1 tables A1.23 to A1.24).

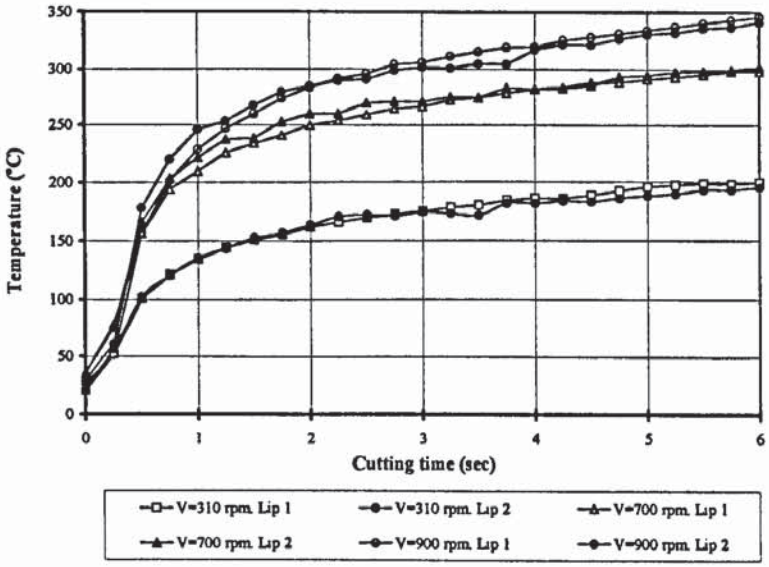

Figure 8.17. Tool temperature *vs*. cutting time, with flank wear: (0.138 and 0.132) mm max.,(0.051 and .072) mm av., (0.139 and .158) mm corner wear, standard helix angle drill 8.0 mm diameter resharpened, dry cut.

From this graph, it is seen that the temperature for all the three cutting speeds (310, 700 and 900 rpm) are higher when compared to graph 8.16, with the highest temperature at cutting speed 900 rpm and the lowest at the cutting speed of 310 rpm. Again, from the graph, it can be seen that the temperatures for both cutting lips are very similar.

8.5.2.3 Lip cutting 2 mm only

The graph in figure 8.18 shows the tool temperature vs. cutting time for the drill and two thermocouples in each cutting lip as above. But in this case, each lip cuts 2 mm only. Three different speeds (310, 700 and 900 rpm) and three different feed rates (78, 156, and 234 mm/min respectively,) were used. As expected the temperature is much lower then when the lip cuts all the way as shown in the two previous graphs of 8.16 and 8.17. But again the higher the cutting speed then the higher the temperature, and the temperature for the cutting speed of 310 rpm is lower as compared to the two other cutting speeds of 700 and 900 rpm. Once again as in the above results, the temperature in the two cutting lips are almost the same. It also takes approximately 3 seconds for the temperature to reach steady state. (See test conditions in appendix 1 table A1.25).

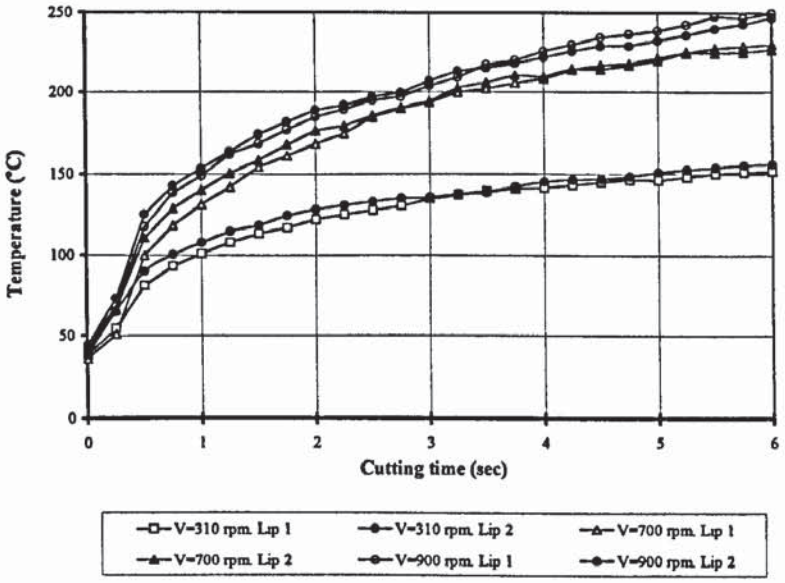

Figure 8.18. Tool temperature *vs*. cutting time,each lip cuts 2 mm only, tool material is M2 HSS, standard helix angle drill 8.0 mm diameter resharpened, dry cut.

In figures 8.19 and 8.20 three different cutting speeds (310, 700 and 900 rpm) and three different feed rates of 78, 156, and 234 mm/min respectively, (after 15 seconds of cutting). Three tests were carried out: the first with the new drill, the second with the worn drill and the third with the drill of 2 mm cut only for each lip, and two thermocouples were used, one on each lip.

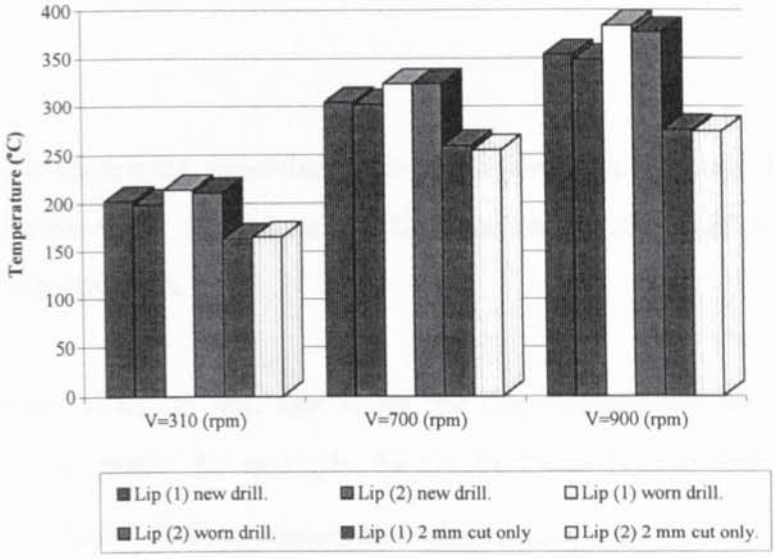

Figure 8.19. Tool temperature *vs*. cutting speed,each lip cuts 2 mm only, tool material is M2 HSS, standard helix angle drill 8.0 mm diameter resharpened, dry cut.

From the graphs in figure 8.19 and 8.20, it can be easily seen that the worn drill has the highest temperature, then the new drill and then, as expected, the lowest temperature was for the drill with 2 mm cut only.

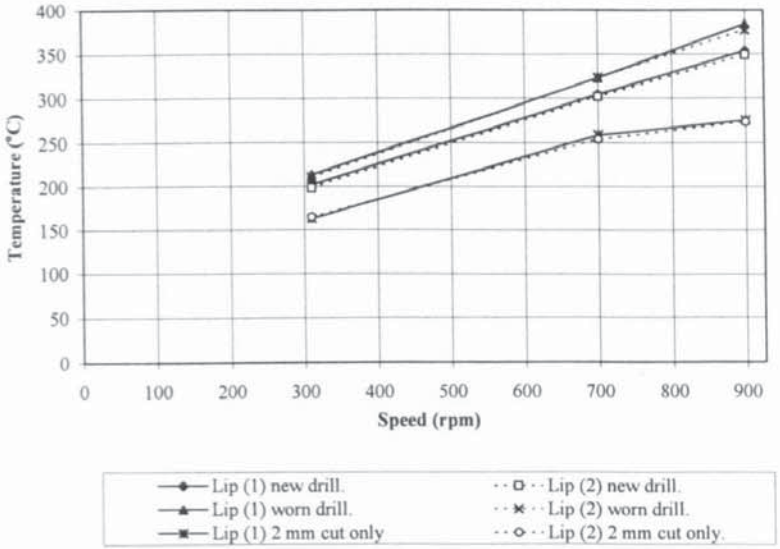

Figure 8.20. Tool temperature *vs*. cutting speed,each lip cuts 2 mm only, tool material is M2 HSS, standard helix angle drill 8.0 mm diameter resharpened, dry cut.

In these sets of tests for both graphs, for the two thermocouples that were used, one in each lip, the temperatures in both lips were very close.

8.5.3 Analysation and Calculation of Oxide Iron and Free Iron Content

The section below shows the procedure that was undertaken in order to calculate the ratio of concentration of the oxide iron and free iron on the chip surface. See chapter 4 for discussion on the method.

In general, the type of oxide iron that is on the chip surface can be found from the binding energy of the graph, for example, Fe_2O_3, Fe_3O_4 or FeO at 710.8 eV, 710.4 eV and 709 eV respectively. This is temperature dependent, therefore at 270°C the oxide found is Fe_2O_3, at 270°C - 540 °C the oxide iron is Fe_3O_4, and from 540 °C on the oxide iron is FeO.

Figure 8.21 shows the components of the Fe 2p peak, representing the oxide iron and metallic iron on the chip surface. The example used in the graph displays the findings from the test with the cutting conditions of 53 mm bar diameter, 20 m/min. speed, and 0.15 mm/rev. feed rate.

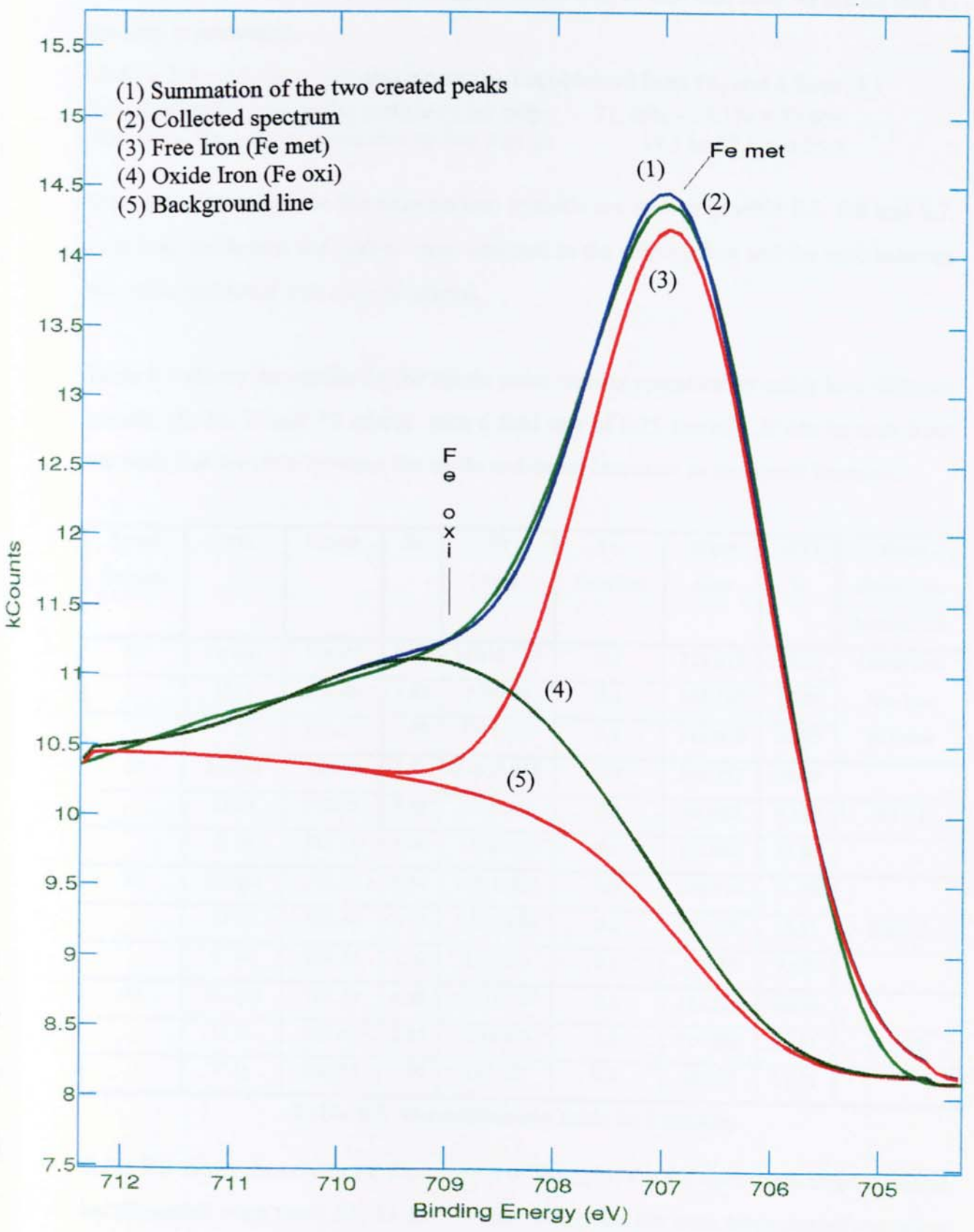

Figure 8.21 shows the synthetic of Fe peak

As seen in table 8.6, the percentage of the oxide iron which was found to be Fe_3O_4, is 18.81. Below is a model of calculating the oxide iron to free iron ratio on the surface of the chip is presented:

18.81 x 3/4 = 14.1% (in which case the 3 is obtained from Fe_3 and 4 from O_4)
To calculate the iron on the surface of the chip: 71.76% - 14.1% = 57.6%
Therefore, the ratio of oxide iron to free iron is: 14.1 to 57.6 = 0.25:1

Quantification tables for the chip surface analysis are shown in table 8.5, 8.6 and 8.7. Free iron, oxide iron and carbon were analysed in the chip surface and the ratio between the oxide and metal was also calculated.

Table 8.5 shows the results for the single point turning operation by using four different speeds: 10, 20, 30 and 40 m/min. with a feed rate of 0.15 rev/min. It can be seen from the table that the ratio between the oxide and metal increases as the speed increases.

Speed (m/min)	Peak	Centre	SF	Pk Area	Tx. Function	Norm Area	(AT) %	Ratio Oxide iron: metallic iron
10	Fe 2p3	706.95	6.50	11630.713	0.2	213.013	25.57	Oxide iron
	O 1s	530.09	2.85	2539.89	0.2	103.160	12.38	too low
	C 1s	284.61	1.00	4595.327	0.1	516.618	62.03	to count
20	Fe 2p3	705.67	6.50	27620.998	0.2	505.753	69.88	
	O 1s	528.81	2.85	1625.266	0.2	66.000	9.119	0.1 : 1
	C 1s	283.31	1.00	1352.113	0.1	151.988	21.00	
30	Fe 2p3	707.22	6.50	29816.924	0.2	546.116	71.76	
	O 1s	530.48	2.85	3525.380	0.2	143.194	18.81	0.25 : 1
	C 1s	284.56	1.00	637.636	0.1	71.684	9.420	
40	Fe 2p3	709.29	6.50	22716.717	0.2	416.229	50.46	
	O 1s	529.66	2.85	7740.444	0.2	314.366	38.11	3.1 : 1
	C 1s	284.65	1.00	837.327	0.1	94.135	11.41	

Table 8.5 Quantification table in Turning.

Table 8.6 shows the results for the analysis of the chips for the tests when three different bar diameters were used: 31, 53 and 75 mm, otherwise the tests were carried out using the same bar and the same test conditions. In this table it is seen that the ratio between the oxide and metal increases when the size of the bar diameters becomes smaller.

Bar diameter	Peak	Centre	SF	Pk Area	Tx. Fu-nction	Norm Area	(AT) %	Ratio Oxide iron: metallic iron
31	Fe 2p3	706.68	6.50	17363.914	0.2	318.000	44.41	
	O 1s	529.95	2.85	2880.150	0.2	116.978	16.33	0.37 : 1
	C 1s	284.61	1.00	2499.998	0.1	281.056	39.25	
53	Fe 2p3	707.00	6.50	22836.246	0.2	418.243	55.64	
	O 1s	530.26	2.85	1150.644	0.2	46.735	6.217	0.17 : 1
	C 1s	284.65	1.00	2550.225	0.1	286.703	38.14	
75	Fe 2p3	707.00	6.50	15168.441	0.2	277.809	74.59	
	O 1s	530.27	2.85	1564.098	0.2	63.529	17.05	0.09 : 1
	C 1s	284.68	1.00	276.580	0.1	31.094	8.349	

Table 8.6 Quantification table with bar diameter.

The results for the analyses of the chip surface for the drilling operation can be seen in table 8.7. The tests carried here used three different speeds: 310, 700 and 900 rpm and a feed rate of 0.15 mm/rev. In this table, as in table 8.5, it is seen that the ratio between the oxide and metal increases as the speed is increased.

Speed (rpm)	Peak	Centre	SF	Pk Area	Tx. Function	Norm Area	(AT) %	Ratio Oxide iron: metallic iron
310	Fe 2p3	709.29	6.50	18076.891	0.2	331.216	46.35	
	O 1s	529.66	2.85	5619.361	0.2	228.222	31.93	2.2 : 1
	C 1s	284.65	1.00	1379.878	0.1	155.130	21.71	
700	Fe 2p3	709.29	6.50	30420.811	0.2	557.388	50.20	
	O 1s	529.66	2.85	11663.531	0.2	473.696	42.66	5.5 : 1
	C 1s	284.65	1.00	703.381	0.1	79.076	7.123	
900	Fe 2p3	709.29	6.50	4366.602	0.2	80.007	7.925	metallic iron
	O 1s	530.29	2.85	1977.941	0.2	80.338	7.958	too low
	C 1s	284.56	1.00	7554.021	0.1	849.238	84.11	to count

Table 8.7 Quantification table in Drilling.

The findings confirm that the chip is running at a higher temperature with decreased bar diameter in turning. This therefore proves the fact that bar diameter affects the temperature and therefore the wear mechanisms.

8.6 DISCUSSION AND COMMENTS

One intention of the tests carried out was to examine the temperature effect on the tools used in this experiment. The temperature, as mentioned before in this chapter, is an important factor and one of its effects on tool is wear. As well as examining the effects that the temperature has on the tool and its wear, a comparison is made between the two operations of turning and drilling where the similar test conditions were used for both in order to determine the similarities and differences that occur during both operations.

8.6.1 Turning

In order to determine the effect of existing tool flank wear on the temperature, two different tools were used under similar cutting conditions: the first tool was a new tool with no flank wear, whereas, in the other one, a flank wear land was introduced before the test was performed.

It was observed that during the turning operation, for both the new tool and the tool with wear that the temperature increases with an increase in cutting speed. This case is as anticipated, since the heat produced in the cutting process is mainly due to the sources of plastic deformation, and friction between the tool and chip, and the tool and workpiece. At higher cutting speeds heat is being supplied to the tool at a faster rate. Even though the chip carries away a larger proportion of the cutting energy at higher speeds. The time available for this heat to be dissipated from the tool is reduced hence the temperature on the rake and clearance faces rise.

When examining the difference between the tests that were carried out with the new tool and the tool with wear, it is clearly seen that when the tool has some wear the temperature is higher than that in the new tool. This is demonstrated in figures 8.6 to 8.9. This outcome is as expected since due to the wear area, contact between the tool and workpiece has been increased. Also since the cutting edge of the worn tool is not as sharp, therefore this leads to more friction between the tool and the workpiece.

Increased cutting tool and workpiece temperatures greatly influence tool wear. It is, therefore, concluded that as the temperature increases, the flank wear increases too. This observation is in agreement with the experimental results of Barnes et al (1995) and Young (1996). However, these findings oppose the results of Leshock et al. (1997), where the average interface temperature as measured by the tool-chip thermocouple was not found to increase with an increase in flank wear.

In turning, as stated above, two thermocouples were used, placed in two different positions of the tool. It was established by figures 8.10 and 8.11 that the temperature results from thermocouple one are much higher than those of thermocouple two. This can easily be resolved by the fact that thermocouple one was placed nearer the cutting edge than thermocouple two. The tool temperature varies according to the position of the thermocouple and as expected the temperature decreases with increasing distance from the cutting edge. Thermocouple one was placed closer to the heat source, hence the difference in temperature between the two thermocouples.

The bar diameter was used, in the turning operation, in order to examine its effect on the tool temperature, which has not previously been considered. A single bar was used under the same conditions excluding the difference in the bar diameters.

The results clearly demonstrated (figures 8.12 - 8.14) that bar diameter does have an effect on temperature. The tool with the smallest bar diameter of 31 mm had the highest temperature and as follows with the largest bar diameter of 75 mm had the lowest temperature.

The reason for this result can be explained due to temperature distribution in the bar diameter. An interesting comparison can be made with DeVries et al (1968) where the effect of the workpiece size, or heat sink, was investigated in drilling by employing several different drill diameters. The results show an increase in the drill flank temperature as the workpiece size decreases. Also the temperature decreases more at the drill periphery than at other locations on the drill flank as the workpiece size increases.

This indicates that the heat sink has a significant effect on the drill flank temperature distribution especially in the area near the drill periphery.

During the tests of bar diameter, the chips were examined and as illustrated in figure 8.15 they further prove that the change in the bar diameter size does affect the temperature. To eliminate the effect of wear on the experiment, the same test conditions were used with the same bar, only the bar diameter differed.

Trent (1991) states that the most obvious indication of temperature of steel chips is their colour. The chip is seen to change colour a few seconds after leaving the tool. As stated in section 8.5.1.3, figure 8.15 (a) shows the colour of the chip which indicates a temperature of approximately 260 °C, (b) approximately 240 °C, and in (c) which is less than 230 °C.

An innovative technique was used to demonstrate that by calculating the ratio of oxide iron to free iron in the surface of the chip then temperature can be estimated. This idea only works when machining steel at low speed. From tables 8.5 - 8.7 it is seen that the higher the speed the higher the temperature and this can also be seen when the ratio of the oxide iron is higher than that of the free iron. Therefore, it has been shown that the higher the speed the higher the ratio of oxide iron and evidently as proven the higher the speed the higher the temperature. These results resemble those of Trent (1991), where he demonstrates these temper colours are caused by a thin layer of oxide on the steel surface and indicate a temperature of the order of 250 to 350°C .

8.6.2 Drilling

In the drilling operation, as in the turning one, the higher the speed the higher the temperature. It was noticed that although the temperature at the speed of 310 rpm was much lower than that at the speeds of 700 and 900 rpm, the difference between the speed of 310 and 700 rpm was much greater than that between 700 and 900 rpm as seen in figure 8.16. The reason for this increase in temperature is again due to the fact that an increase in the cutting speed increases the rate at which energy is dissipated through plastic deformation and friction, and thus the rate of heat generation in the cutting zone.

Agapiou et al. (1990a) pointed out that a sharp tool with adequate clearance, has the friction limited to a line along the cutting edge or drill lip, and therefore the frictional heat sources due to tool wear on the flank and margin can be neglected.

In drilling the temperature in the two lips are very similar and the difference is negligible, therefore there is no lip height variation. This was of course due to both thermocouple being placed in similar positions in the oil hole.

It is clearly illustrated in figure 8.20 which is when the cut was only 2 mm in each lip, the temperature in the lips is much lower than that of the full cut. The cause is the area of plastic deformation is much smaller to that of the full cut, therefore less energy is converted to heat, and so there is less friction area between the tool and the chip, and the tool and the workpiece. Also the drill rake angles are greater at the outer corner of the cutting lips and therefore cutting efficiency is better than at the point nearer the inner corner of the lip when the rake angle is towards the negative.

The results of the tests show that the temperature reaches a steady state in an average of about 2-5 seconds in both turning and drilling and under all test conditions used. When examining similar works it is found that the results of these tests seem to fall in between many of them. For example, at one extreme DeVries et al (1968) found that it took 60 seconds for the temperature to reach steady state, Agapiou et al. (1990b) took 30 seconds, while Redford et al. (1976) state that the steady state condition is reached in 20

seconds. On the other hand, Leshock et al. (1997) results demonstrate that the steady state conditions is reached in 0.33 seconds and according to Levy et al (1976b) it took 1.5-2 minutes for the temperature in their test results to reach steady state.

It is therefore found that the results of the tests carried out in this work seem to fall in the midst of all the above quoted works. The reason for this difference in the results is possibly because the attainment of steady state conditions depends upon the efficiency of the heat transfer routes and the timing depends upon the sitting of the thermocouples. Thus, one would expect the thermocouple closest to the heat source (the cutting zone) to reach steady state quicker than one sited farther away even if all other conditions were equal.

However, an interesting contrast to these is Agapiou's et al. (1990b) view that drilling differs from some other processes in that a steady state is never established; tool temperatures simply increase with hole depth.

The results also showed that the tool temperature at the cutting edge rises extremely rapidly in a few seconds immediately after the cutting starts, and then rises rather gradually with the cutting time. The gradual rise in the tool temperature is caused by the fact that the workpiece is heated by the cutting heat conducted to it and that it takes some time for the cutting energy to flow into the whole cutting tool. For this reason it takes a long time before the temperature distribution acquires a strictly steady condition over the whole insert.

8.6.3 Turning and Drilling

As can be seen from the above both the turning and the drilling operations have many similarities, for example, in both cases an increase in the cutting speed causes an increase in temperature. Also with a higher temperature flank wear increases.

When examining the similarities and differences that occur between the two operations of turning and drilling in terms of the recorded temperatures, it is shown quite easily that

and as one expected the drill temperatures are higher when compared to the turning operation. This is the case even when very similar conditions, work materials, tool materials are used, and even in this test when the position of the thermocouples in the turning operation is closer to the heat generating area than that in the one in drilling.

Some of the reasons as to why this is the case is due to the fact in the drilling the operation is internal, that is it is carried out inside the hole. The area is almost closed, and therefore the temperature tends to take longer to cooling as compared to turning. The turning operation is external and there is an air cooling effect to the operation, which therefore makes the tip cool much quicker.

Other reasons as to why the temperature is higher in the drilling operation as compared to turning is due to the chip. Under most normal cutting conditions, the largest part of the work is done is in forming the chip at the shear plane, and that most of this generated heat is passed into the chip. Heat may be lost from the body of the chip by conduction into the tool through the contact area. The temperature of the chip can affect the performance of the tool only as long as the chip remains in contact; the heat remaining in the chip after it breaks contact is carried out of the system, while a small but variable percentage is conducted into the workpiece and raises its temperature. In drilling, the chips absorb much of the cutting energy in the form of heat, and are produced in a confined space and remain in contact with the tool for a relatively long time. In turning, unlike the drilling, as soon as the chip has been dismantled from the secondary zone, there is no further contact between the tool and the chip.

The heat conducted into the chip is greatest some way up the rake face, and this results in eventual crater wear occurring in the tool at this position. This is not the only form of wear that is produced: just as serious are the flank wear that occurs on the clearance face of the tool and the other wear mechanisms. The elevated tool temperature causes effects of crater wear, and this was traditionally attributed to the heat generated at the interface between the tool and workpiece by means of friction and its conversion to heat energy.

In order to make similar conditions in turning and drilling operations, the speed and the feed have to be double in the drilling as compared to the turning, because of the two lips. By doing this, the drill will have heat in two different places (two lips), and therefore the loss of temperature is slower than in the turning operation which has only one area heated rather than two.

Therefore, the mechanisms and routes of heat dissipation whose efficiency determines the proportions of heat carried away by the tool, by workpiece and by chip, and therefore the temperature distribution and the maximum temperature achieved - it is this which was found to have a strong influence upon the differences between turning and drilling.

It was mentioned earlier that the heat sink has a significant effect on the drill flank temperature, this relates to a direct comparison with DeVries's (1968) work in that both works support the point about factors influencing temperature and the influence can arise in two ways:

- Changes in energy input (increase in speed). The proportions of heat energy carried by the various routes (tool, workpiece, chip) might be expected to remain much the same but the system operates at higher temperatures which reflect the increased demand.

- Changes in the efficiency of energy transmission via a particular route. Changes in the heat sink capacity of a particular route puts pressure on the others and again temperatures increase.

8.7 CONCLUSIONS

It seems that for the different techniques used in measuring the temperature, the average temperature along the tool rake face is most accurately measured using the tool-work thermocouple method, provided the materials involved permit its use. Tool-work thermocouple measurements are relatively easy to perform and yield repeatable results, the temperature distributions along the tool rake or relief faces can be measured

accurately by cutting through an insulated wire, by metallographic methods, or by mounting and infrared sensor inside the workpiece or measuring the infrared intensity through a pre-drilled hole. These methods are much more tedious to perform, which makes them difficult to apply in broad studies over wide ranges of cutting conditions.

Temperatures within the deformation zones of the chip are much more difficult to measure. The only suitable methods are those using embedded thermocouples or full-field infrared sensors. These approaches are tedious to apply and often do not yield repeatable results.

In this study tool temperature in the turning and the drilling operations has been experimentally studied using thermocouples embedded in the tools. Knowledge of the tool temperature can be used to better understand and control the underlying machining process.

The cutting temperature readily reacts to instantaneous changes in the cutting conditions. And as has been demonstrated in the above tests, cutting speed has the largest influence on the temperature, in that as the cutting speed increases so does the temperature.

The tool temperature is also seen to increase rapidly, which is due to a sudden breakdown of the sharp cutting edge; this is followed by a slight increase in the temperature with increasing uniform wear, and then by acceleration after a critical wear value has been reached. The temperature is seen to reach steady state between 2-5 seconds.

The study also presented the analysis of the relationship between tool wear and temperature where it appears that tool wear has an effect on temperature. Also a high temperature level is most likely to lead to increased tool wear. Young (1996) also mirrors these results by finding by showing that tool wear to be strongly temperature dependent, a fact which has been well recognised since the work of Taylor (1907). It was therefore concluded that due to flank wear the temperature increases.

It was also concluded that the temperature in the drilling operation is higher than that in the turning operation when similar conditions were used. This was due to the difference in the way the cutting was carried out as well as how the chip had an effect on transmitting some heat while leaving the tool. Thermal conditions in drilling differ significantly from those of turning. The chip is formed at the bottom of the hole and remains in contact with the drill over a comparatively long distance, which increases by the fact that the drill point moves slowly into the portion of the work material being heated by chip formation; in turning, the work material approaching the cutting edge is generally cooler. The cutting speed varies across the lip of the drill, so that temperatures are highest near the outer corner or margin of the drill, and temperature-activated margin wear often limits maximum spindle speeds.

The temperature distribution on the surface of the tools is one of the most important parameters determining the cutting performance and tool life, and is closely related to the wear mechanism, including adhesion, diffusion, abrasion, oxidation etc. Abrasion wear is prominent in the low speed range and as the speed increases, adhesive wear becomes the dominant wear mechanism, while the effect of abrasion diminishes.

Tool temperature is a very important parameter in the analysis of metal cutting. It was shown in this chapter that temperature has a great influence on most factors of machining. Perhaps the greatest influence it has is on the wear mechanisms, in terms of which mechanism will occur at what stage of the tool's life due to the temperature. All this was discussed in the above chapter and will also be further discussed in the next two chapters of 9 and 10 of the force prediction models in turning and drilling.

It is evident from the above that a knowledge of cutting temperature is essential when studying most metal cutting problems and it is not surprising, therefore, that considerable efforts have been made to assess cutting temperatures by both experimental and theoretical means.

Chapter 9

EXAMINATION OF A REPRESENTATIVE PREDICTIVE APPROACH IN TURNING

9.1 INTRODUCTION

In chapter 3 it was seen and concluded that predictive approaches were very important to investigate as they provided solid basis to the subject of tool wear. On the same line, it is worthwhile to explore other issues concerning metal cutting such as forces. In chapter 6 it was concluded that a representative predictive approach in turning is feasible to examine as this chapter will show. Investigations of this type lead to a deeper understanding of the whole topic and allows researchers to build up on already existing theories to widen their scope and comprehension of predictive equations and models.

Due to the complexity of the phenomenon of tool wear in metal cutting no researcher has yet managed to produce a comprehensive model/theory although much effort has been developed to that end. Some published work, particularly that based on the relationship between wear and cutting forces is considered in this chapter. In particular the work of Taibi (1994) will be considered and his model tested against results obtained during this research. This particular model and the reasoning behind its selection for test purposes will be considered in more detail in section 9.3.

Analyses of cutting tool wear have traditionally emphasised flank wear more than crater wear, and the reason is the more direct influence that flank wear has on the quality of the product. Flank wear results in changes in the mechanics of cutting process, tendency to chatter and changes in the dimensions of the product. Henceforth because it is the deciding factor in most cases, the study will be confined to the study of flank wear on the machining process.

Therefore, an important point of this chapter is to show that attempts at modelling of wear have:

- to recognise the type of wear predominating,
- to encompass all major, relevant parameters influencing the mechanism,
- to set limits on the range of conditions to which the model might be expected to be applicable.

Also, it is shown here how the use or extension of other models is difficult because:
- replication of actual test conditions and results can be difficult and the model compromised where the model overlooks influencing factors, such as bar diameter which were discussed in more details in chapter 8, which reduce the value of a model for practical use, and
- attempts to extend a model can also be difficult without an understanding of the wear mechanisms at which it was originally targeted.

9.2 TOOL WEAR MODELLING BASED ON FORCE VARIATION WITH WEAR

In chapter 3, prediction literature was examined in relation to tool wear. In this section tool wear modelling based on force variation with tool wear is assessed to give a background and highlight strengths and weaknesses of previous models.

Force generation is a significant characteristic of mechanical systems and processes, such as spindle systems and machining processes. Owing to the great advance of computers and sensing technologies today, quantitative and detailed studies of forces of complicated mechanical systems and processes become possible.

The first two papers that are examined, of Merchant (1945a, b) and Wallace et al. (1964), look at modelling using tool forces. The rest of the papers look at tool force modelling while taking tool wear into account. Factors considered here include the data required to achieve a result and the complexity of the equations. It is also necessary to evaluate the balance between adequate information to achieve a reasonable estimation and the complexity or simplicity of the equations.

Merchant's (1945a) paper has been the foundation of the analysis of forces in turning and including his follow up paper (Merchant 1945b), which looks into plasticity conditions. His purpose was to set forth certain original findings in regard to the mechanics and physics of the various aspects of the metal cutting process.

The analysis presented is limited to the case of orthogonal cutting, with a tool having a single straight cutting edge and a plane face, and to a continuous chip without built-up edge. This type of chip is produced when machining steel with sintered carbide type of tool materials. But this analysis has also been found to give good approximation to a continuous chip with BUE.

In the first paper Merchant (1945a) presented relationships which make possible the analysis of an orthogonal cutting process in terms of basic mechanical quantities, from measurements of forces on the tool and the geometry of chip formation. However, it is evident that the force system controls the geometry of chip formation in a manner dictated by those physical properties of the work material which determine its plastic behaviour. The results of an initial theoretical and experimental study of plasticity conditions in cutting, to determine the relationship between forces and geometry, serve as the basis for this second paper. Merchant stated that the study is by no means complete, but does result in a good first approximation. The analysis is again limited, in theory at least, to orthogonal cutting with a tool having a single straight cutting edge and a plane face, and generating a continuous chip without BUE, as in the previous paper.

The force system acting in the case of orthogonal cutting with a continuous chip without BUE, was discussed in chapter 6, and shown in figure 6.3. The important force relationships derivable from the geometry of this figure are:

$$\mu = \frac{F}{N} = \tan\tau = \left(\frac{F_t + F_c \tan\alpha}{F_c - F_t \tan\alpha}\right)$$

$$F = F_t \cos\alpha + F_c \sin\alpha$$

$$F_s = F_c \cos\Phi - F_t \sin\Phi$$

$$S_n = \frac{F_s}{A_s} = \frac{\left(F_c \sin\Phi\cos\Phi - F_t \sin^2\Phi\right)}{A_0}$$

$$S_n = \frac{F_n}{A_s} = S_s \tan\left(\Phi + \tau - \alpha\right)$$

$$W_f = \frac{F}{A_c}$$

$$W_s = S_s \varepsilon$$

$$W_c = W_s + W_f$$

where μ is equal to the coefficient of friction between chip and tool, S_s is equal to the mean shear stress on shear plane, A_s is equal to the area of shear plane which is equal to $A_0 / \sin\Phi$, and S_n is equal to the mean compressive or normal stress on shear plane, W_f is equal to the work dissipated in friction per unit volume of metal removed, W_s is equal to the work dissipated in shear per unit volume of metal removed, ε is equal to shearing strain undergone by chip which is equal to $\cot\Phi + \tan\left(\Phi - \alpha\right)$ and W_c is equal to total work dissipated in cutting per unit volume of metal removed.

The physical properties governing the plastic behaviour of the work material evidently determine what value the shear angle, Φ, will assume for any given value of the angle $\tau - \alpha$ in the figure (figure 6.3, chapter 6). According to the principle of minimum energy, the angle Φ will assume such a value as to make the total work done in cutting a minimum. Since the force component F_c, the cutting force, is alone responsible for the total work done in cutting per unit distance travelled by the tool, it follows that, for any given value of angle $\tau - \alpha$, the angle Φ will assume such a value as to make F_c a

minimum. This principle will be employed in determining the plasticity conditions for the cutting process.

From the geometry of figure 6.3 (chapter 6) it can be seen that :

$$F_c = R\cos(\tau - \alpha)$$
$$= F_s \cos(\tau - \alpha) / \cos(\Phi + \tau - \alpha)$$

But

$$F_s = S_s A_0 / \sin\Phi$$

Therefore

$$F_c = S_s A_0 \cos(\tau - \alpha) / \sin\Phi\cos(\Phi + \tau - \alpha)$$

The simple plasticity condition is represented by:

$$2\Phi + \tau - \alpha = C$$

where C is equal to $arc\cot k$. This appears to offer a degree of approximation sufficiently accurate for many practical cases in the cutting of metals, in spite of the fact that in formulating this condition no account has been taken of the effect of plastic strain, rate of shear, and the resulting temperature rise at the shear plane.

The introduction of the plasticity condition into the force equations makes it possible to analyse with good accuracy the force system as well as the geometry of chip formation, in an orthogonal cutting process, from measurements of the chip geometry alone. No force measurements during the operation are necessary. However, in order to do this, the values of S_0 and k (S_0 is the shear strength of the metal under zero compressive stress, and is roughly equal to one-half the tensile strength, at high values of strain, and the constant k represents the slope of the shear strength vs. compressive curve) for the material being cut must be known. The only method which the present investigation offers for determining these constants is initial cutting tests on the material, with measurement of both forces and chip geometry.

Merchant's goal was the analysis of forces, stresses and strains, velocities, energy distribution etc. to the extent that the design and control of similar systems were to be handled on anything other than an empirical basis. Even though no experimental values were shown in comparison with the theory, it was merely stated that the results were reasonable.

Wallace et al. (1964) look at the tool forces and tool-chip friction in turning. The results show that two mechanisms of friction exist on the chip-tool interface: the first over part of the contact area between chip and tool 'sliding' friction occurs which the coefficient of friction is constant, and the second, over the remainder of contact, 'sticking' friction occurs in which the frictional stress remains constant and independent of normal pressure. Friction affects both rate of wear and power required. However, in the study only continuous chip formation is considered and it is concerned primarily with the frictional behaviour on the rake face.

It is assumed that the resultant force acting on a cutting tool is distributed over both the tool rake face and the tool nose as seen in figure 9.1. To permit an examination of the frictional behaviour between chip and tool rake face it is necessary to determine experimentally the component of the resultant tool force which acts on the rake face only.

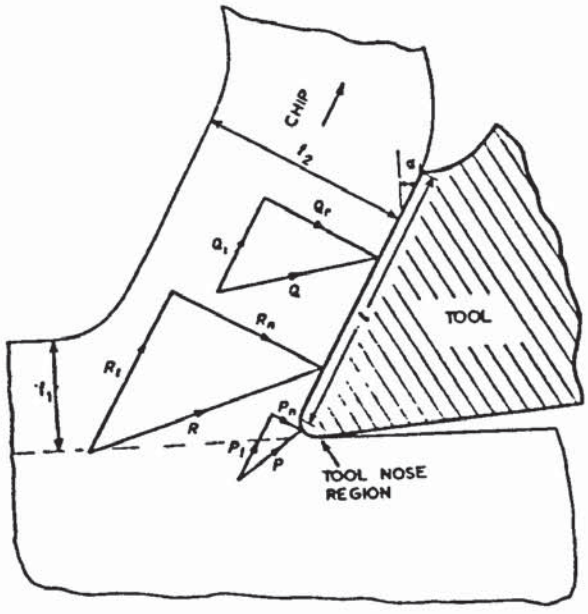

Figure 9.1 Tool Force Diagram (Wallace et al. 1964)

Equation 1 states that

$$\vec{R} = \vec{P} + \vec{Q} \qquad \text{Eq 1}$$

where R if the resultant tool force, P is the force acting on the tool nose, and Q is the force acting on the rake face.

Hence,

$R_n = P_n + Q_n$

$R_t = P_t + Q_t$

where the suffixes n and t denote components normal and tangential to the rake face respectively.

The proposed method of finding Q under given conditions is first to find P as the limit of R when Q approaches zero, and then to obtain Q from equation 1. Therefore as $Q \to 0$

$$R_n \to P_n \qquad \text{Eq 2}$$
$$R_t \to P_t$$

provided that P remains constant as $Q \to 0$.

The mean coefficient of friction between chip and tool in metal cutting has been found to be variable, depending for given condition on:

- The normal stress distribution on the rake face,
- The shear strength of the chip material in contact with the rake face, and
- The coefficient of sliding friction between the two materials.

Wallace et al.'s (1964) paper was found to be an in depth study of the varying friction types active on the rake face, whereas the force element was not analysed in such detail and no derivations were proposed as to the prediction of these. The forces were purely measured in an experimental environment.

In their paper, McAdams et al. (1961) encompass the area of forces on a worn cutting tool and the implications of tool wear in metal cutting.

The assumptions for the analysis are as follows:

- Continuous chip, and variation of rake as the result of crater wear on the tool face or a built-up edge on the tool tip is ignored.
- As the tool wears, a wear land develops on the tool flank, so that the worn tool makes an area of contact with the new work surface.
- Tool mounting is ideally rigid, so that deflections resulting from the applied forces do not need to be taken into account.

The simplistic Merchant analysis of forces is discarded as unrealistic except on the early life of the tool. According to McAdams et al. (1961) a more realistic model is proposed in which the vertical force is made up of the two vertical components of the forces on the shear plane and on the wear land.

The tool is ideally sharp, as seen in figure 9.2, in that it presents a line contact with the new work surface. The vertical force F_V is the same as the feed force, and the horizontal force F_H on the shear plane is the same as the cutting force.

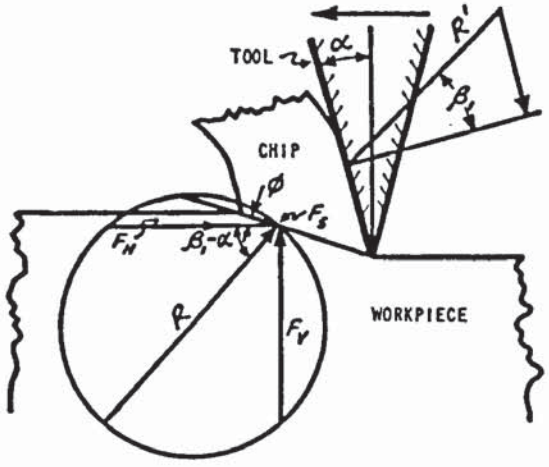

Figure 9.2 Forces in a non-wearing tool (McAdams et al. 1961)

A more realistic picture is that of a worn tool, as seen in figure 9.3, where the feed force acting on the tool is shared between the shear plane and the wear land:

$$F_V = F_{VS} + F_{VW}$$

Feed force = Vertical force on shear plane + Vertical force on wear land

Therefore,

$F_{VS} = F_V - F_{VW}$

and, for a worn tool, the vertical force F_{VS} on the shear plane is less than the applied feed force F_V.

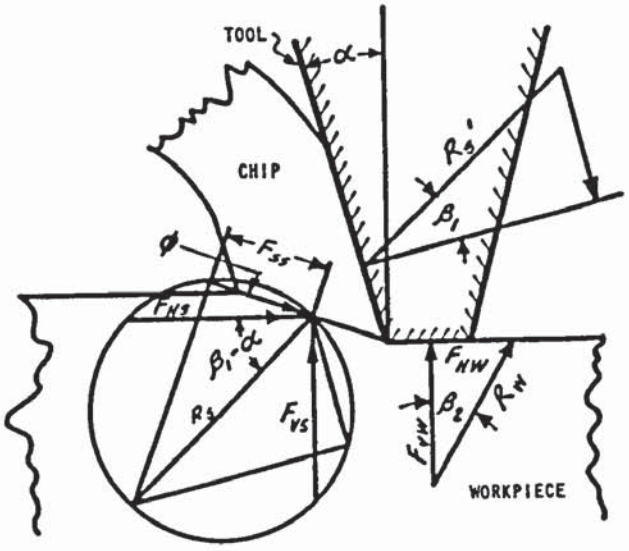

Figure 9.3 Forces on a tool subjected to wear (McAdams et al. 1961)

It was found that when rake angle, friction angle and shear angle are assumed constant then tool depth of cut is proportional to that part of the feed force acting on the shear plane. The paper proposes that at constant applied feed force the depth of cut is a linear function of the area of the flank wear land. Also, the feed force increases as a linear function of the area of the wear land, provided the shear stress remains constant and the welded fraction of the real contact area does not change.

Elanayar et al. (1996) investigated the aspect of forces on a worn tool. Although linear empirical relations between flank wear and cutting forces have been observed, no models for ploughing forces can be formulated unless the edge forces are isolated from the measured ones. The difficulty in monitoring of tool wear based on cutting force

would be greatly reduced if the forces due to the cutting edge could be adequately modelled. In addition, the edge forces are known to contribute to the cutting process damping and hence to the stability of machine tools. The objective of this work is to develop modelling methods to separate the ploughing component of cutting forces from total measured forces. Since edge forces are affected by the geometry of a cutting edge, specifically flank wear, a model of the ploughing process is developed.

Assumptions used in this model include:
- Temperature increase due to flank wear negligible compared to that due to shearing. Flank wear is assumed to have a negligible effect on the shear angle.
- Ploughing forces associated with a fresh tool are of relatively smaller magnitude compared to total forces, or even to ploughing forces associated with a worn tool.

According to Stern et al. (1993) the interest in formulating a comprehensive set of equations able to predict the wear and machining forces as a function of the machining parameters and workpiece materials is evident, but at this point such equations are limited. Some attempts to relate flank wear to machining forces have been made; Koren et al. (1986) presents the following equation:

$$F = F_0 + tC_W W$$

where

F = machining force (feed, thrust or cutting)

F_0 = initial machining force (with sharp tool)

t = depth of cut

C_W = constant for the machining parameters

W = flank wear

One can see that the general assumption is that the forces vary linearly with the wear and depth of cut. However, C_W is obtained by the linearization of the secondary zone of the wear curve. But Stern states that the assumption that the machining force pattern follows the tool life curve, however, is not well sustained in this study. Stern's results show that the allowable wear is already reached in the primary zone of the wear curve

where linearization may lead to significant error. The constant C_W is not easily obtained because it includes many other interactions with the cutting parameters that may not display a linear behaviour. The process of obtaining C_W would be essentially experimental and limited in use.

Common characteristics of flank wear/cutting forces models are the assumption that machining force patterns follow the tool life curve and that the allowable flank wear used in the research is often much greater than that allowable in an industrial environment.

Although the first attempt to model the machining process was made by Merchant in 1945, the focus of the research during the last decade or so is upon the establishment of a predictive theory or analytical system which enables prediction of aspects of the cutting performance such as chip formation, cutting forces, cutting temperature, tool wear and surface finish, rather than the development of theories of a descriptive nature which only explain the mechanism of metal cutting phenomena. In other words, metal cutting theories need to be developed in order to be utilised for practical machine shop problems such as the determination of optimum conditions for a given operation, and to obtain this analytical prediction is needed.

One of the main reasons there is so much variety in tool wear modelling is that few modelling efforts have been under way for a long time. Each author typically focuses on the wear phenomena in which he is interested, and these are almost invariably different from those studied by others. In most cases, neither these researchers who initially proposed a model, nor their colleagues or successors have continued a particular modelling process to maturity.

In the next section an attempt is made to fit the results obtained from the test carried out in this research to the model of Taibi of force in turning. Taibi, a previous research student at Aston University who completed his research in 1994, attempted to produce a model for predicting the forces in turning, which could be used over a much wider range of machining conditions than had been previously attempted. Therefore, the choice

seemed to be strengthened by the fact that Taibi had used the same equipment, material and laboratory conditions as was available for this research, in which case one can eliminate taking account of these factors when analysing the results.

9.3 TAIBI'S MODEL

Taibi stated that the most widely used methods for wear monitoring in turning are based on the analysis of machining forces. One aim of his work was to develop a model covering a wide range of cutting conditions in the steady state and dynamic conditions.

The thesis, according to Taibi, presented an approach to cutting dynamics during turning based upon the mechanism of deformation of work material around the tool nose known as 'ploughing'. Starting from the shearing process in the cutting zone and accounting for 'ploughing', new mathematical models relating turning force components to cutting conditions, tool geometry and tool vibration are developed. These models were developed separately for steady state and for oscillatory turning with new and worn tools.

Experimental results were used to determine mathematical functions expressing the parameters introduced by the steady state model in the case of a new tool. The form of these functions are of general validity though their coefficients are dependent on work and tool materials. Good agreement was achieved between experimental and predicted forces.

9.3.1 Taibi's Equation

Taibi showed that the forces acting on the tool during turning result from the shearing and the ploughing process. The forces due to the shearing process are applied upon the upper surface of the tool (rake face) and are named throughout as rake forces. While the forces due to the ploughing process are applied around the tool nose and along the

clearance face are named ploughing forces. Taibi adapted Merchant's equations and presented the equations as seen below.

The measured force components (F_x and F_z) are the resultant of both the force components occurring upon the rake (F_{xs} and F_{zs}) as well as along the flank of the tool and around the nose (P_x and P_z). These are as follows:

$$F_x = \frac{wC_s S_0 k}{\sin(\phi)(\cos(\phi) - C_s \sin(\phi))} + \frac{1}{2}\frac{P_s w \zeta^2}{\tan(\gamma)}$$

$$F_z = \frac{wS_0 k}{\sin(\phi)(\cos(\phi) - C_s \sin(\phi))} + \frac{1}{2}\frac{P_s w \zeta^2}{\tan(\gamma)}\tan(\tau - \gamma)$$

F_x = Turning force component in the feed direction

F_z = Turning force component in the mean cutting direction

w = depth of cut

C_s = Rake forces ratio

S_0 = Undeformed chip thickness

k = mean shear stress

P_s = Ploughing factor

ζ = Depth of tool penetration

ϕ = Shear angle

γ = Flank angle of the cutting edge

τ = Equivalent mean friction angle along the flank face of the tool

It was proposed by Taibi that the turning force components could be fully described by the shear angle ϕ, the mean shear stress k, the rake forces ratio C_s, the depth of tool penetration ζ and the ploughing forces ratio C_P as dependent parameter. These parameters are strongly influenced by rake angle α, chip thickness S_0, cutting speed V and flank angle γ. The temperature effect was taken into account by Taibi through the

introduction of the independent parameters S_0 and V upon the mean shear stress and mean friction angle β and τ.

In this model, other properties are excluded on the basis that the tool and the work materials enter the chip formation process in so many ways that the possibility of substituting other materials, as can often be done in heat transfer and fluid mechanics problems, seems to be too remote. That is to say that the correlation of the machining results of lead, for example, with those of steel seems, at least for the time being, not feasible. Therefore, considering more properties of the tool and work materials will complicate the solution, possibly, without gaining much more generality. This investigation is confined to the case of orthogonal dry cutting of an unpreheated workpiece with new edge and hence properties of the cutting fluid, initial workpiece temperature are all excluded. However, as will be shown further on, the material properties can be introduced as a proportionality coefficient in the mean shear stress k and in the ploughing factor P_s.

The mean friction angle was found by:

$$\tau = \tan^{-1}(\mu)$$

The equations used for chip thickness ratio, r, and rake forces ratio, C_s are as shown:

$$C_s = C_{s0} + C_{s1}\sin(\alpha)$$

$$r = r0 + r_1\sin(\alpha)$$

where C_{s0} and $r0$ are the intercepts of the C_s and r respectively, while C_{s1} and r_1 are the slopes of the $C_s - \sin(\alpha)$ and $r - \sin(\alpha)$ linear relationships respectively.

The numerical fitting of the experimental data, by Taibi, resulted in the following expressions for the intercepts and slopes:

$$C_{s0} = [1 S_0] \begin{bmatrix} 0.74 & -0.07 & -0.01 \\ 547.50 & -343.30 & 48.30 \end{bmatrix} \begin{bmatrix} 1 \\ 0.6V \\ (0.6V)^2 \end{bmatrix}$$

$$C_{s1} = [1 S_0] \begin{bmatrix} -0.99 & 0.10 & -0.03 \\ -866.20 & -365.30 & 334.70 \end{bmatrix} \begin{bmatrix} 1 \\ 0.6V \\ (0.6V)^2 \end{bmatrix}$$

$$r_0 = [1 S_0] \begin{bmatrix} 0.09 & 0.01 \\ 449.00 & 279.40 \end{bmatrix} \begin{bmatrix} 1 \\ 0.6V \end{bmatrix}$$

$$r_1 = [1 S_0] \begin{bmatrix} 0.19 & -0.35 & 0.39 & -0.06 \\ -540.90 & 4759.70 & -3256.50 & 438.80 \end{bmatrix} \begin{bmatrix} 1 \\ 0.6V \\ (0.6V)^2 \\ (0.6V)^3 \end{bmatrix}$$

where S_0 is in m/rev and V in m/s.

The above expressions provide the effect of the steady state cutting conditions upon the chip thickness ratio and the rake forces ratio and henceforth provide the variation of the mean friction angle on the rake of the tool and the shear angle.

The expression for mean shear stress was found in a similar fashion, by Taibi, and yielded:

$$k = \begin{bmatrix} 1 & 1000S_0 & 0.6V & (0.6V)^2 \end{bmatrix} \begin{bmatrix} 66.02 & 353.41 \\ 585.31 & -477.14 \\ 117.48 & -227.29 \\ -17.22 & 35.57 \end{bmatrix} \begin{bmatrix} 1 \\ \sin(\alpha) \end{bmatrix}$$

where S_0 is in m/rev and V in m/s.

It is found that the tool penetration as well as the mean friction coefficient along the flank are linear functions with the tool rake angle and thus can be represented by:

$$\zeta = \zeta_0 + \zeta_1 \sin(\alpha)$$
$$\mu f = \mu f 0 + \mu f 1 \sin(\alpha)$$

where ζ_0 and $\mu f 0$ are the intercepts of ζ and μf respectively and, ζ_1 and $\mu f 1$ are the slopes of the $\zeta - \sin(\alpha)$ and $\mu f - \sin(\alpha)$.

ζ_0 and $\mu f 0$ are the depth of the tool penetration and the mean friction angle along the tool flank for a tool with nil rake angle.

This investigation has shown the possibility of machining forces during turning by considering both the contact between the tool and the chip along the rake and the deformation around the tool nose and along the flank of the tool. The former action is attributed to the shearing process and the latter to the ploughing mechanism.

The theoretical analysis has led to establish a new theoretical relationships for the turning force components where new parameters controlling the cutting force are introduced to include the effect of the tool size. Experimental data was obtained from turning tube in orthogonal conditions and used to yield an analytical expression of the rake force ratio, the uncut chip thickness ratio, the mean shear stress, the depth of the tool penetration and the mean friction coefficient on the flank of the tool.

Moreover, the model was used to predict the turning force over a wide range of the cutting conditions when machining different work materials using different tool geometries and the following conclusions were drawn:

- Good prediction of the forces is obtained for bar turning of different materials when a hardness factor is introduced.

- The model also provides a good prediction of the turning force when negative rake angle tools are used to cut a tubular workpiece and best prediction is obtained for high speeds and low feeds.

A direct consequence of the findings of this investigations is that the steady state coefficients for a particular work and tool geometry can be established over a wide range of the cutting conditions from a relatively small number of the machining tests.

9.4 APPLICATION OF AUTHOR'S RESULTS TO TAIBI'S EQUATION

To ensure the validity of the prediction model, which relates to the unworn tool, from Taibi, it was tested against some results using an identical set up by the author. The experimental equipment and measurement techniques were fully described in chapter 4 of the experimental methods.

9.4.1 Verification of the Model

The aim of the following section is to use the same cutting conditions as those used for determining the model coefficients and compare the predicted and the experimentally measured turning forces so that the quality of the fitting for the different parameters will be highlighted.

The measured and the model predicted turning force results are shown in figures 9.4 to 9.7 for the tool materials with a new cutting edge, the forces were recorded within the first 3 seconds of machining, in order to minimise wear.

In figures 9.4 and 9.5, uncoated BT42 HSS was used with a depth of cut of 2 mm, rake angle of 6°, flank angle of 5° and nose radius of 0.4 mm. In figure 9.4 the feed rate was 0.18 mm/rev while in figure 9.5 the feed rate was 0.15 mm/rev.

Figure 9.4 shows the graph of forces vs. cutting speed. The range of cutting speeds used were 10, 20, 30, 40, 50, 60 and 70 m/min. It can be seen from the graph that for the cutting speeds of 30, 40 and 50 m/min, both the experimental and predicted results of the cutting force are similar. But at the low cutting speeds of 10 and 20 m/min there is a difference between them. At the very high speeds of 60 and 70 m/min the difference between the experimental results of the cutting force and the predicted results is increasing. One reason for this is due to the early catastrophic failure of the tool.

As for the feed force, for the cutting speeds of 10, 20, 30, 40 and 50 m/min. both the experimental and predicted results are quite similar, while at the higher cutting speeds of 60 and 70 m/min the experimental results of the feed force is higher than the predicted ones. Again this is due to the accelerated failure of the tool.

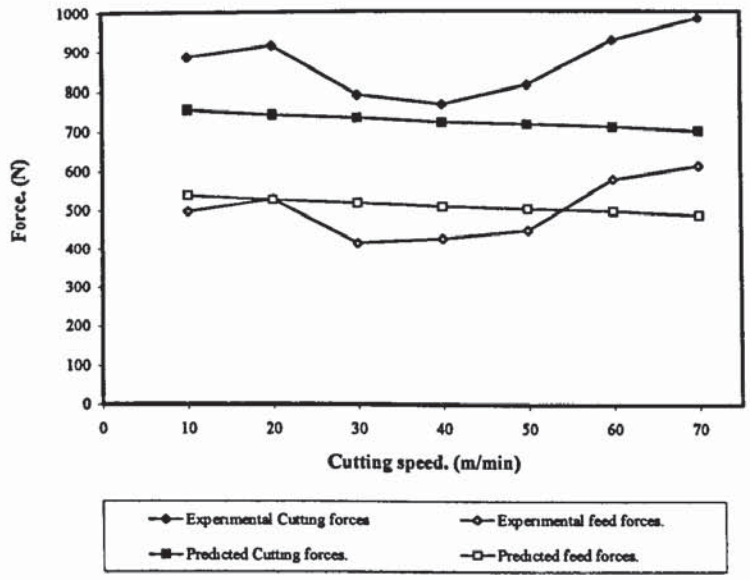

Figure 9.4 Force vs. cutting speed for uncoated BT42 HSS insert, with 2 mm DOC, 6 & 5 deg. rake & flank angles, 0.4 mm nose radius, 0.18 mm/rev. feed rate, dry cut.

In figure 9.5 of forces vs. cutting speed, the range of cutting speeds were 10, 20, 30, 40, 50 and 60 m/min, again the experimental and predicted results of the cutting and feed forces can be seen to be close, especially that of the feed force. At all the speeds of 10, 20, 30, 40 and 50 m/min the results are all quite alike. But at the high cutting speed of 60 m/min, the failure of the tool is accelerated, and this can be seen for both the cutting and feed force.

The percentage difference between the experimental and predicted values for the cutting force for the cutting speed of 10 m/min is 11%, for the cutting speed of 20 m/min it is 10%, for 30 m/min it is 6% and at 40 m/min the difference percentage is 13%. For the feed force the percentage difference between the experimental and predicted values for the cutting speed of 10 m/min it is 0.21%, for 20 m/min it is 8%, for 30 m/min it is 6% and for 40 m/min it is 0.22%. This will be discussed in more detail and it will be shown how this relates to the drilling results in chapter 11 in the discussion.

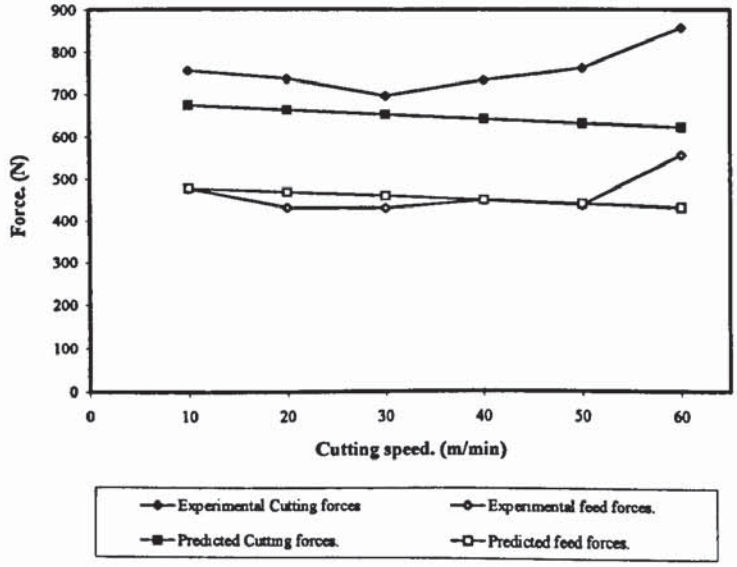

Figure 9.5 Force vs. cutting speed for uncoated BT42 HSS insert, with 2 mm DOC, 6 & 5 deg. rake & flank angles, 0.4 mm nose radius, 0.15 mm/rev. feed rate, dry cut.

In figures 9.6 and 9.7 the tool material used is M2 HSS with a feed rate of 0.18 mm/rev, rake angle of 15° , flank angle of 8° , and nose radius 0. The depth of cut for figure 9.6 was 2 mm and for figure 9.7 it was 1 mm.

In figure 9.6 the graph is forces vs. cutting speed for the cutting speeds of 10, 20, 30 and 40 m/min. The experimental and predicted results for both the cutting force and feed force are again quite similar except at the cutting speed of 40 m/min where the experimental results of the cutting forces declines compared to the predicted one. A reason for this is that the tool is chipped out and the conditions for the tool are quite high.

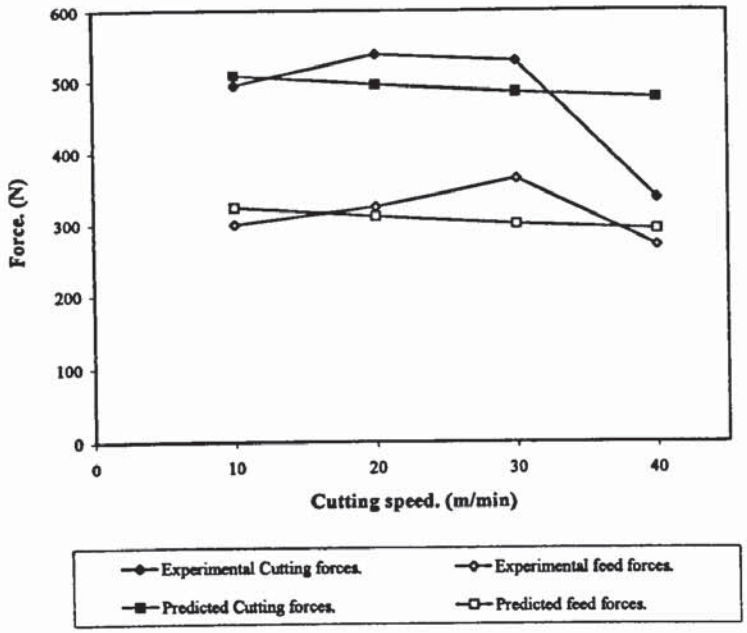

Figure 9.6 Force *vs*. cutting speed for M2 HSS billet. with 2 mm DOC, 15 & 8 deg. rake & flank angles, 0.18 mm/rev. feed rate, dry cut.

The graph of forces vs. cutting speed is shown in figure 9.7 for the cutting speeds of 10, 20, 30 and 40 m/min. At the cutting speed of 10 m/min the experimental and predicted results for the cutting force are a little different, at 20 m/min the results are similar and at 30 and 40 m/min the results are different again. While for the feed force, at the cutting speed of 10 m/min the experimental and predicted results are similar, at the cutting speeds of 20 and 30 m/min the results are a little different and again at the cutting speed of 40 m/min the results are similar. In this case, as in the other cases when the results differ it is due to the different wear mechanisms that are acting at different cutting speeds which effect the forces.

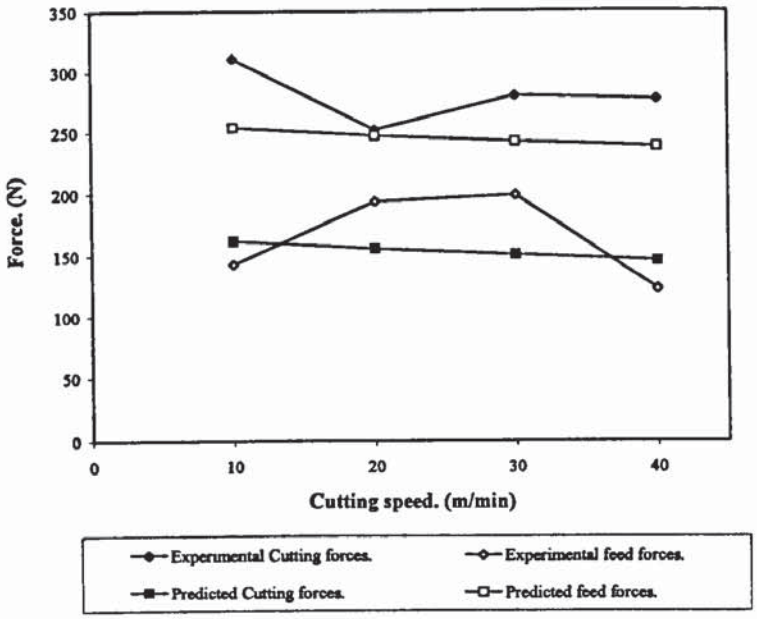

Figure 9.7 Force *vs*. cutting speed for M2 HSS billet. with 1 mm DOC, 15 & 8 deg. rake & flank angles, 0.18 mm/rev. feed rate, dry cut.

In all the graphs, both the experimental and predicted results were quite similar. But when the gap between the experimental and predicted results began to increase, it was mainly due to the accelerated and catastrophic failure of the tool, or due to different wear mechanisms acting on the tool. This increase usually occurred in the higher cutting speeds which is due to the rise in temperature as was illustrated in chapter 8 and which will be discussed further in the discussion chapter 11.

Overall, regarding the validity of the sharp edge Taibi model, the results obtained in this work give quite a good fit.

9.5 VALIDATION OF TAIBI'S MODEL WITH VARIATION OF ANGLES

Taibi's model covers rake angles, flank angles etc. The following section takes three different rake angle and flank angle combination as an example to demonstrate the validation of the model using different angle combinations.

Figures 9.8, 9.9 and 9.10 show the graphs of forces vs. cutting speed for M2 HSS billet at four different cutting speeds: 10, 20, 30 and 40 m/min. All tests were carried out using new tool with 2 mm depth of cut, 0.15 mm/rev. feed rate and 0 nose radius at dry cut. The only variations between the three figures are the rake and flank angle variations. Again as in the previous figures in this section the forces were recorded within the first 3 seconds of machining in order to minimise the wear.

In figure 9.8, both the rake and the flank angles were 6°. In this graph it can be seen that both experimental and predicted values for both feed and cutting forces are very similar. It is seen that as the cutting speed increases the forces decrease, except for the cutting speed of 40 m/min where the forces increase slightly.

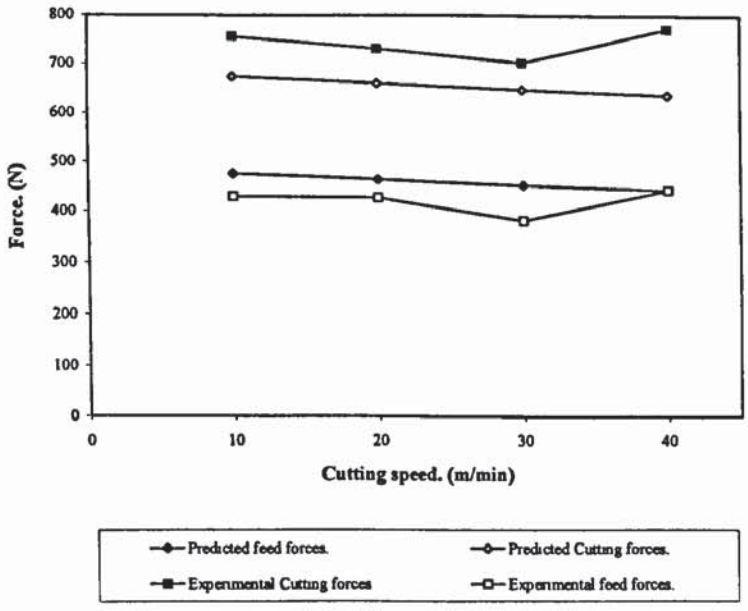

Figure 9.8. Force *vs*. cutting speed for M2 HSS billet, with 2 mm DOC, 6 deg. rake & flank angles, 0.15 mm/rev. feed rate, dry cut.

Figure 9.9 shows the graph with a rake angle of 10° and a flank angle of 5°. Again in this graph as the cutting speed increases the forces decrease and also for both the experimental and predicted values for both cutting and feed forces are quite similar for all the four cutting speeds.

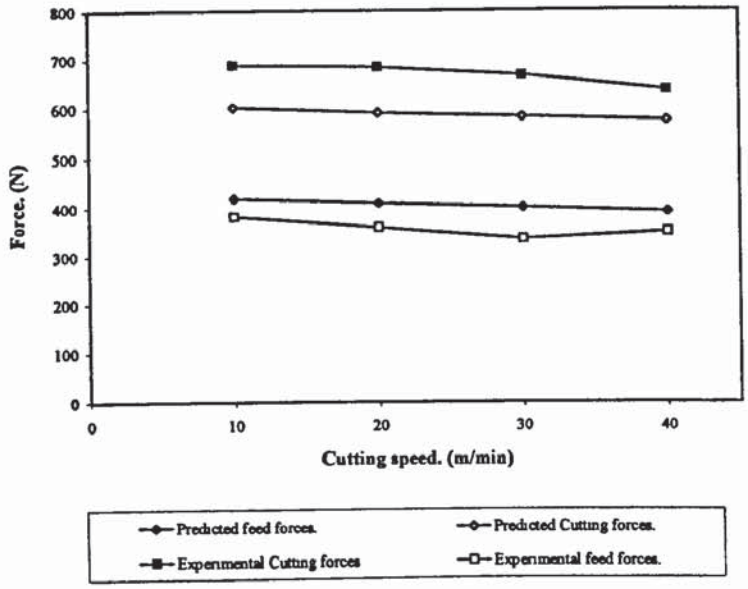

Figure 9.9. Force *vs*. cutting speed for M2 HSS billet, with 2 mm DOC, 10 & 5 deg. rake & flank angles, 0.15 mm/rev. feed rate, dry cut.

In figure 9.10, the rake angle used was -6° and the flank angle 5°. In this graph it can be seen that at the cutting speed of 10 m/min the experimental values are similar to the predicted values for both the cutting and feed forces. At the cutting speed of 20 m/min the values of the forces decrease immensely but only slightly in the predicted values. This decrease is possible due to the wear mechanism acting for that cutting speed which will be illustrated in section 9.6.1 of this chapter.

At the cutting speeds of 30 and 40 m/min the forces began to increase again for the experimental values, but the predicted values began to decrease, this is due to tool failure.

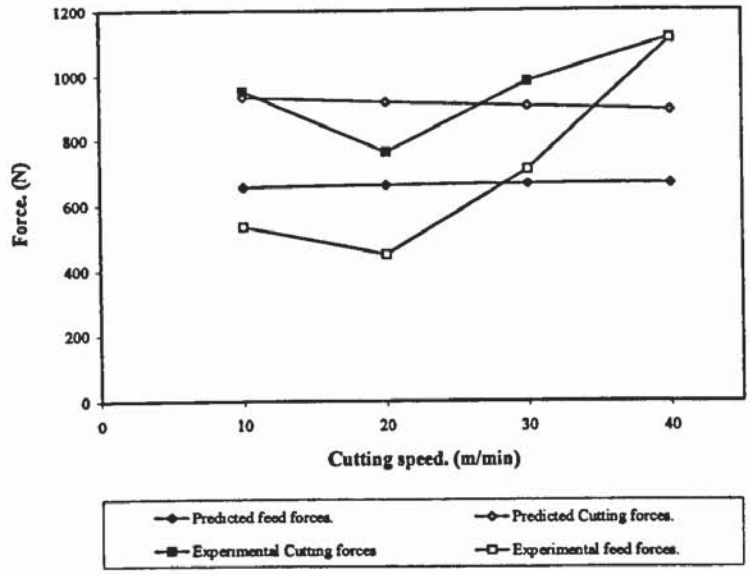

Figure 9.10. Force *vs* . cutting speed for M2 HSS billet, with 2 mm DOC, -6 & 5 deg. rake & flank angles, 0.15 mm/rev. feed rate, dry cut.

As expected from this graph the forces are higher than in the previous two graphs, which is attributed to the negative value of the rake angle. These figures illustrate that the Taibi model was successful with the variation of rake and flank angles. A more detailed discussion of the effects of the angles on the forces took place in chapter 6.

In testing Taibi's model against the results obtained in this work it was demonstrated that it works moderately well, that is it works when tried by an independent investigator which is not usually the case with predictive models.

9.6 EXTENSION OF TAIBI MODEL TO WORN TOOLS

Taibi developed a model for force prediction in single point turning with a new tool. But as the cutting process progresses, the tool edge is subject to range of failure possibilities and its life is limited. Taibi extended his model to include the effect of flank wear. The following section illustrates Taibi's extended model with flank wear.

In the case of cutting with worn flank the turning force components can be expressed as:

$$F_x = \frac{wC_s S_0 k}{\sin(\phi)(\cos(\phi) - C_s \sin(\phi))} + wP_s\zeta\left\{Wf + \frac{1}{2}\frac{\zeta}{\tan(\gamma)}\right\}$$

$$F_z = \frac{wS_0 k}{\sin(\phi)(\cos(\phi) - C_s \sin(\phi))} + wP_s\zeta\left\{Wf\tan(\tau) + \frac{1}{2}\frac{\zeta}{\tan(\gamma)}\tan(\tau - \gamma)\right\}$$

Wf = Average width of the flank wear land in the central part of the active cutting edge.

These equations show that turning force components are increasing linearly with flank wear Wf, and that the force introduced by the worn surface increases more rapidly in feed direction than in cutting direction and this force is proportional to depth of tool penetration, depth of cut and to the specific ploughing factor. Moreover, the ratio of the vertical to the horizontal components of the ploughing force introduced by flank wear is equal to the equivalent friction coefficient along the worn area.

The present ploughing model expresses the turning force acting upon worn tool in terms of dependent and independent parameters.

9.6.1 Verification of the Model

A series of cutting tests at various conditions and various tool flank wear levels were carried out and experimental results are compared with model predicted forces.

In figures 9.11 to 9.16, the experimental and predicted forces are presented versus flank wear for the investigated cutting conditions.

In figures 9.11, 9.12, 9.13 and 9.14 the tool material used was uncoated BT42 HSS insert with the cutting speeds of 10, 20, 30 and 40 m/min respectively. The feed rate is 0.15 mm/rev, the rake angle 6°, the flank angle 5°, the depth of cut is 2 mm and the nose radius is 0.4 mm.

Figure 9.11 shows the graph of forces vs. average flank wear. It shows that with increasing wear the forces increase. In the case of the cutting forces, both the experimental and the predicted results are close. While for the feed force, the experimental and predicted results are quite different.

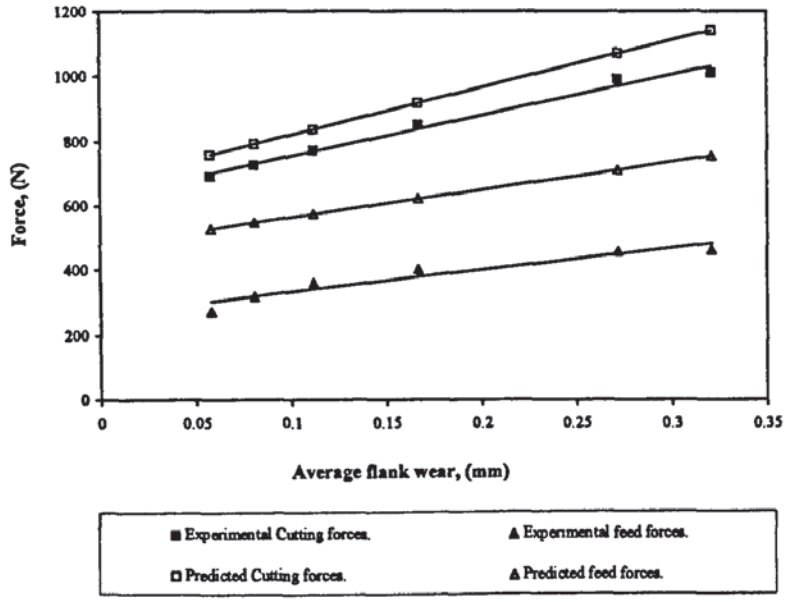

Figure 9.11 Force *vs* . Average flank wear for uncoated BT42 HSS insert, at 10 m/min cutting speed, with 2mm DOC, 6 &5 deg. rake & flank angles, 0.4 mm nose radius, 0.15 mm/rev. feed rate, dry cut.

Figure 9.12 shows the graph of forces vs. average flank wear and in this graph both the experimental and predicted results of the cutting force are almost the same, while for the feed force the results are close, and especially when the wear is increasing the results are closer together. This is due to the different wear mechanisms acting at different levels of the wear scar.

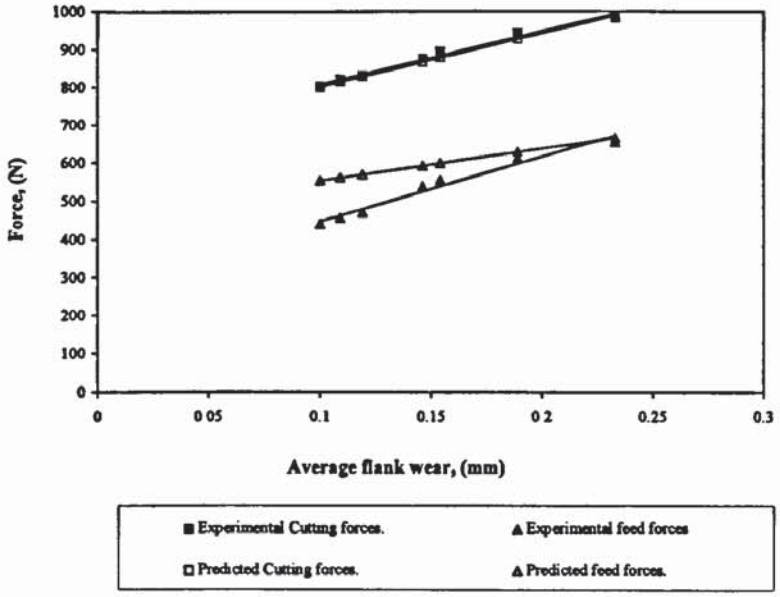

Figure 9.12 Force *vs*. Average flank wear for uncoated BT42 HSS insert, at 20 m/min cutting speed, with 2mm DOC, 6 &5 deg. rake & flank angles, 0.4 mm nose radius, 0.15 mm/rev. feed rate, dry cut.

Figures 9.13 and 9.14 again show the graphs of forces vs. average flank wear. For both the experimental and predicted results of the cutting forces and the feed forces there is a difference.

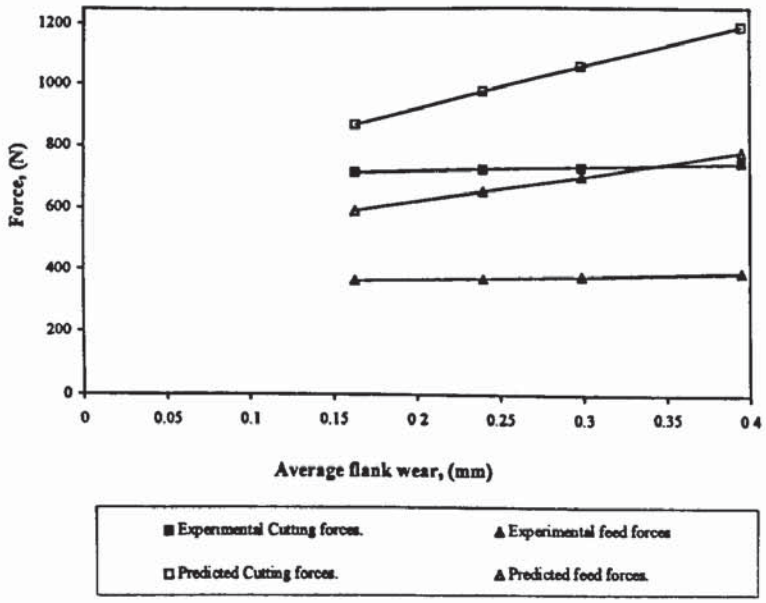

Figure 9.13 Force *vs*. Average flank wear for uncoated BT42 HSS insert, at 30 m/min cutting speed, with 2mm DOC, 6 &5 deg. rake & flank angles, 0.4 mm nose radius, 0.15 mm/rev. feed rate, dry cut.

The difference in the experimental and predicted results in both the forces is caused by the different wear mechanism acting, which the predicted equation did not take account

of. The reason being that it is difficult to take account of the predominant wear mechanism.

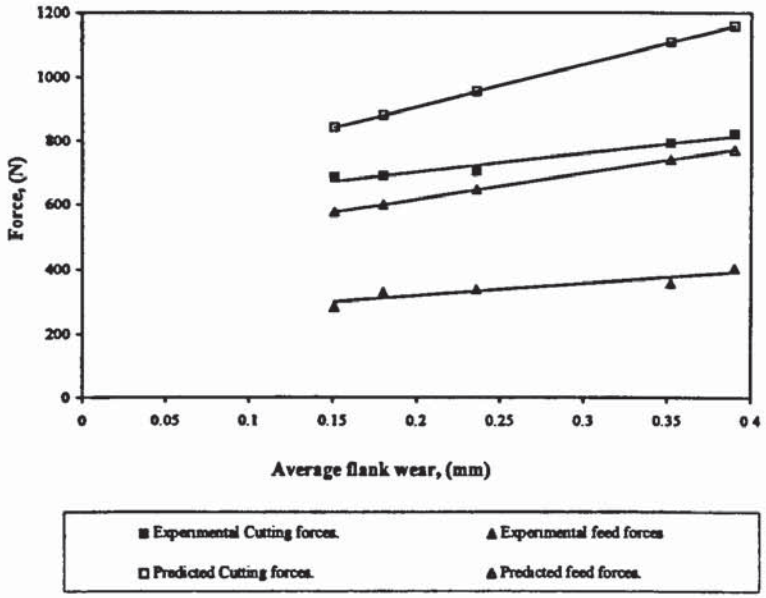

Figure 9.14 Force *vs*. Average flank wear for uncoated BT42 HSS insert, at 40 m/min cutting speed, with 2mm DOC, 6 &5 deg. rake & flank angles, 0.4 mm nose radius, 0.15 mm/rev. feed rate, dry cut.

In figures 9.15 and 9.16 the tool material used was coated BT42 HSS insert with the cutting speeds of 10 and 30 m/min. The feed rate is 0.15 mm/rev, the rake angle 6°, the flank angle 5°, the depth of cut is 2 mm and the nose radius is 0.8 mm.

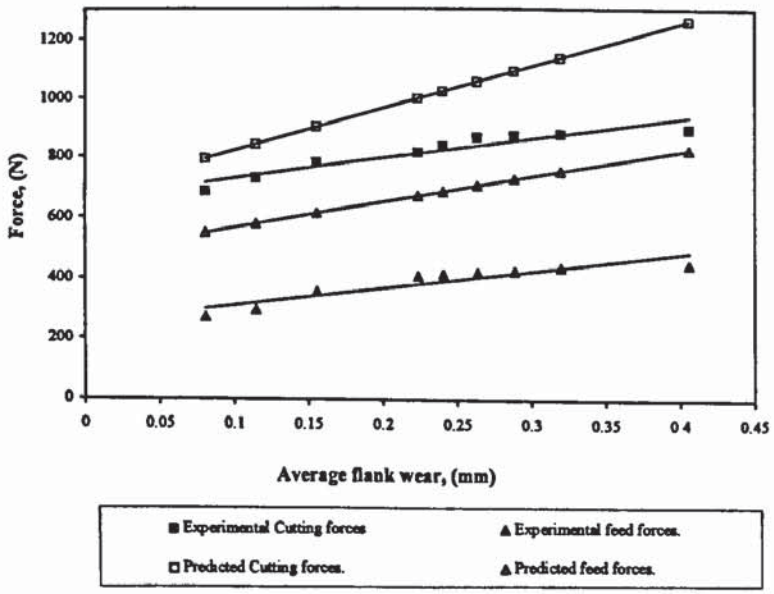

Figure 9.15 Force *vs*. Average flank wear for coated BT42 HSS insert, at 10 m/min cutting speed, with 2mm DOC, 6 &5 deg. rake & flank angles, 0.8 mm nose radius, 0.15 mm/rev. feed rate, dry cut.

Figures 9.15 and 9.16 show the graphs of forces vs. average flank wear. It can be seen in both graphs that as the wear scar increases, both the difference in the experimental and predicted results of both the cutting forces and the feed forces increases. Once again, the is due to the different wear mechanism acting. It is seen that at low cutting speed the experimental and predicted results of the cutting force is very close but when the wear scar is high then difference is greater between the two results.

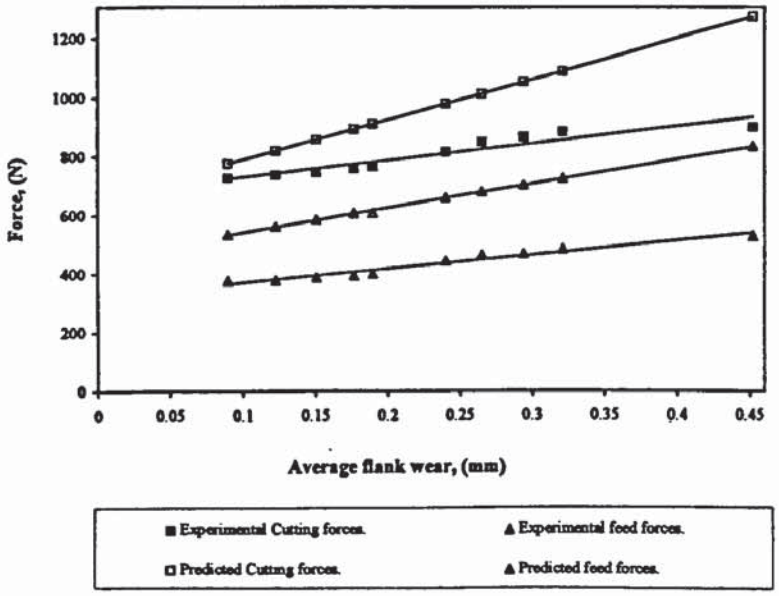

Figure 9.16 Force *vs*. Average flank wear for coated BT42 HSS insert, at 30 m/min cutting speed, with 2mm DOC, 6 &5 deg. rake & flank angles, 0.8 mm nose radius, 0.15 mm/rev. feed rate, dry cut.

In all the graphs, both the experimental and predicted results were similar when compared to the results for the unworn tool. The experimental and predicted results of the tests, for both cutting and feed forces, in the lower cutting speeds seemed closer than those performed at higher cutting speeds. The increase in cutting speeds increases the temperature, as discussed in chapter 8, which in turn leads to different wear mechanisms acting, as shown in the figure. This point is interesting as Taibi assumed that his approach was not influenced by wear mechanism but only by wear damage. This issue will be further discussed in chapter 11 of the discussion.

The results obtained at the lower cutting speeds gave a better fit to those at higher cutting speeds. This is probably caused by the increase in temperature as the cutting speed is increased as pointed out in the results in chapter 8, and also shown in the

temperature chapter that an increase in temperature leads to further tool wear. Increase in speed and therefore in temperature lead to different wear mechanisms acting on the tool at the different stages. This fact is also demonstrated by Barth (1985) and Hastings et al (1976) in figures 2.16 and 2.17 respectively in chapter 2, where it was shown that different wear mechanisms act as the temperature increases.

Considering that Taibi assumed wear mechanisms did not influence his model then one must consider if that was the case then the results of this work should have given a good fit to the Taibi model of worn tools. But since they did not, then probably one can only explain this by different wear mechanisms acting at different stages.

It can therefore be concluded that, overall, regarding the validity of the worn tool Taibi model, the results did not give quite a good fit.

This last set of figures, 9.11 to 9.16, demonstrated that by using Taibi's force model with wear, the results from the tests performed in this work did not fit in the model. It is the proposition here that this is due to the different wear mechanisms acting and that since Taibi did not take account of the wear mechanisms as he assumed they do not influence his model then that was the cause of the failure of the model when wear was added to the model. This is demonstrated in the following figures.

Figures 9.17 and 9.18 show the graphs of average flank wear vs. cutting time. Similar test conditions were used in both, 2 mm depth of cut, 6° rake angle, 5° flank angle, 0.4 mm nose radius and 0.15 mm/rev. feed rate.

The tool material in figure 9.17 is uncoated BT42 HSS insert machined at four different cutting speeds: 10, 20, 30 and 40 m/min. From this graph it can be seen that the lower the cutting speed, the longer the steady state stage is. For example, at the cutting speeds of 10 and 20 m/min, the wear mechanisms acting are for the steady state stage. The tool when cut at the speed of 10 m/min, it has a longer tool life. At the cutting speeds of 30 and 40 m/min, it can be seen that the steady state stage is short and that the wear rate is quite fast and the tool life is shorter.

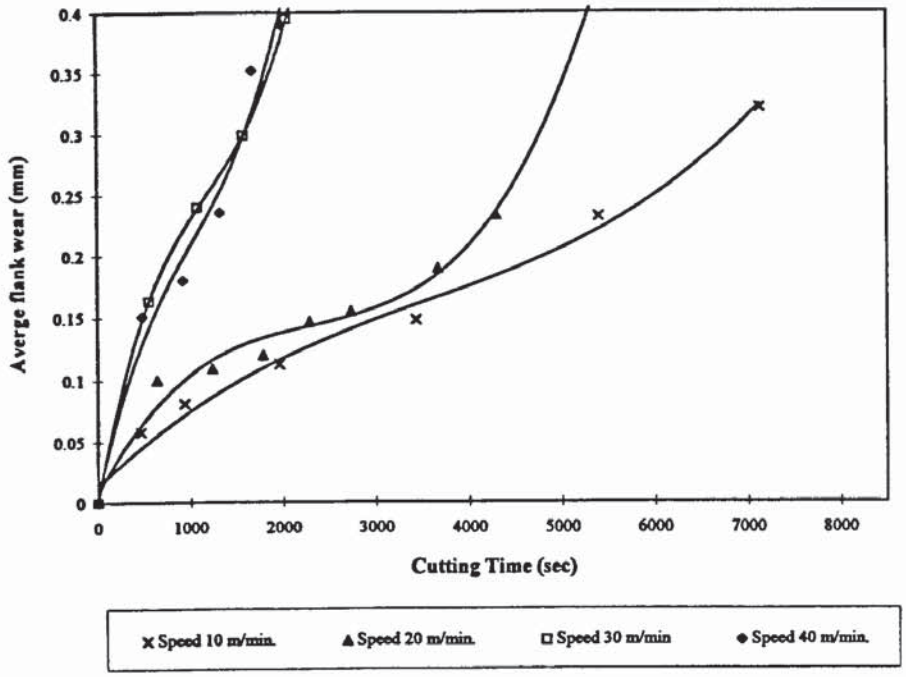

Figure 9.17 Average flank wear vs. Cutting time for uncoated BT42 HSS insert, with 2mm DOC, 6 &5 deg. rake & flank angles, 0.4 mm nose radius, 0.15 mm/rev. feed rate, dry cut.

In figure 9.18, the tool material used is coated BT42 HSS insert for the cutting speeds of 10 and 30 m/min. Again it can be seen here that when the cutting speeds of 10 and 30 m/min are compared, at 10 m/min the tool wear rate and the steady state stage are longer. This is due to different wear mechanisms acting at the two different cutting speeds. The different wear mechanisms can be seen in the SEM photographs in chapter 6, where in figure 6.37 the cutting speed is 20 m/min and the wear mechanism is adhesion and in figure 6.38 the cutting speed is 30 m/min and the wear mechanism is a combination on adhesion and abrasion.

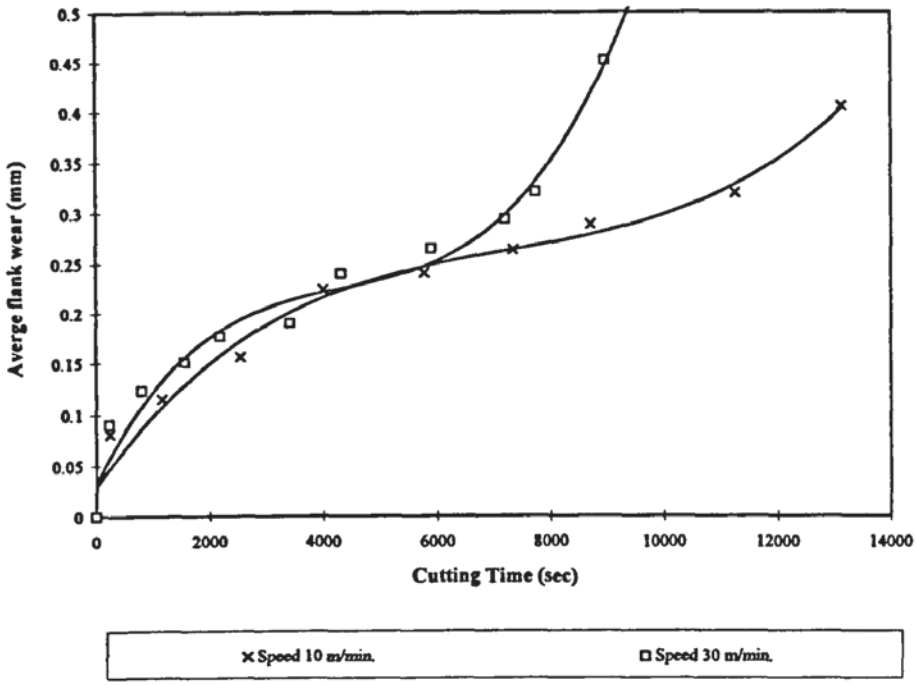

Figure 9.18 Average flank wear *vs*. Cutting time for coated BT42 HSS insert, with 2mm DOC, 6 &5 deg. rake & flank angles, 0.4 mm nose radius, 0.15 mm/rev. feed rate, dry cut.

Figures 9.17 and 9.18 showed average flank wear vs. time to demonstrate linearity and non-linearity as an indication of the different wear mechanisms that are working at the different cutting speeds. As was discussed in chapter 2, where Hoglund (1976) argued that in general at low cutting speeds, it is considered that adhesion and abrasion wear are the main wear mechanisms of flank wear in the steady state region, and that diffusion wear increases in the accelerated wear region when temperature increases. This can also be seen in the figures mentioned above of 2.16 and 2.17 in chapter 2.

Despite the promising start with the model for the sharp tool, the adaptation to wear phenomena is less successful. This reinforces the 'complex phenomenon' aspect of the wear process and the implication that a wear term in an equation which is supposed to universally cover a spectrum of machining conditions over which the predominant wear phenomena can change is optimistic.

9.7 EFFECT OF ANGLE VARIATION ON WEAR

The following section shows the effect of tool angle variation on wear. The results of the tests with the angle variations are shown in figures 9.19 to 9.25. In all the graphs there was a presence of BUE, which started to act as the cutting edge and therefore protect the wear on the flank. As discussed in chapter 2, Boothroyd (1989) had argued that a stable BUE protects the tool surface from wear and performs the cutting action itself. Due to this the tool life was long for cutting. Although the tests were performed in the cutting speeds of 10 to 40 m/min., in this section only a representative sample is shown for the cutting speed of 20 m/min. This is due to the fact that the results of the tests are enormous and one is unable to present all of them in this work. The cutting speed of 20 m/min was chosen as it is the speed in the middle range of the sample. All the tests results shown are for the tool material M2 HSS and where the depth of cut is at 2 mm and the feed rate at 0.15 mm/rev.

In figures 9.19 to 9.21 the graphs show the effect of variation in the rake angle with a fixed flank angle on flank wear.

Figure 9.19 shows the graph of average flank wear vs cutting time. The flank angle was fixed at 5° while the rake angle was varied at 6, 10, 30 and -6°.

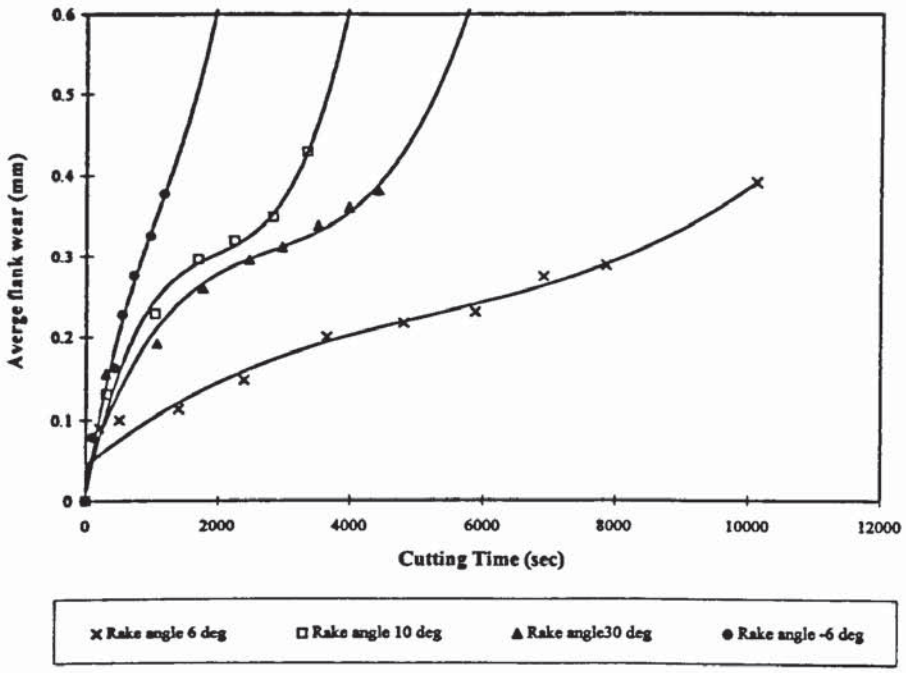

Figure 9.19 Average flank wear vs. Cutting time for M2 HSS, with fixed flank angle at 5 deg, variable rake angles, 2mm DOC, 0.15 mm/rev. feed rate, dry cut.

Figure 9.20 shows the graph of average flank wear vs cutting time. The flank angle was fixed at 10° while the rake angle was varied at 6, 10, 30 and -6°.

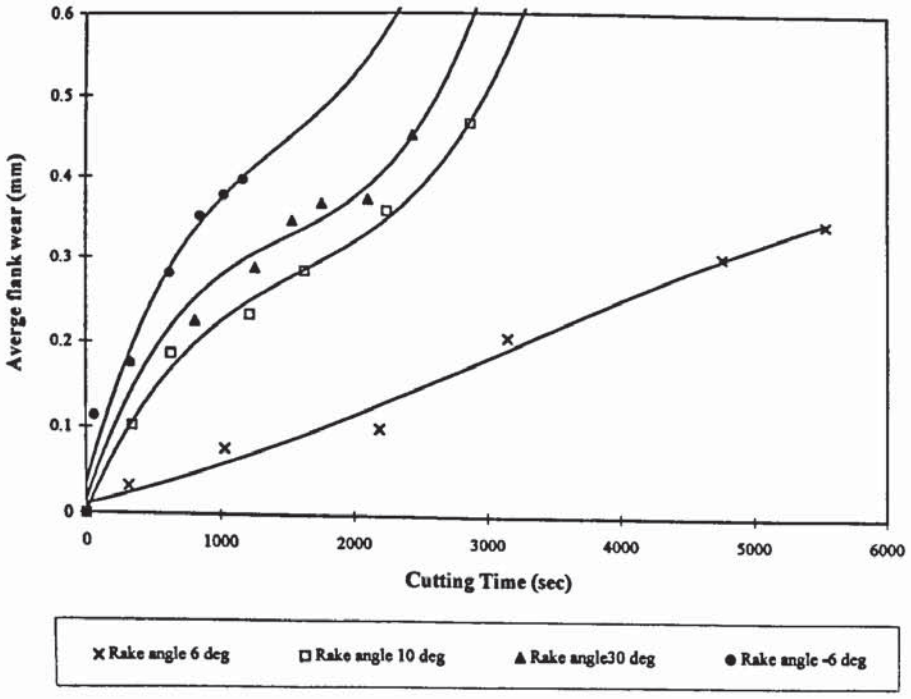

Figure 9.20 Average flank wear vs. Cutting time for M2 HSS, with fixed flank angle at 10 deg, variable rake angles, 2mm DOC, 0.15 mm/rev. feed rate, dry cut.

Figure 9.21 shows the graph of average flank wear vs cutting time. The flank angle was fixed at 15° while the rake angle was varied at 6, 10, 30 and -6°.

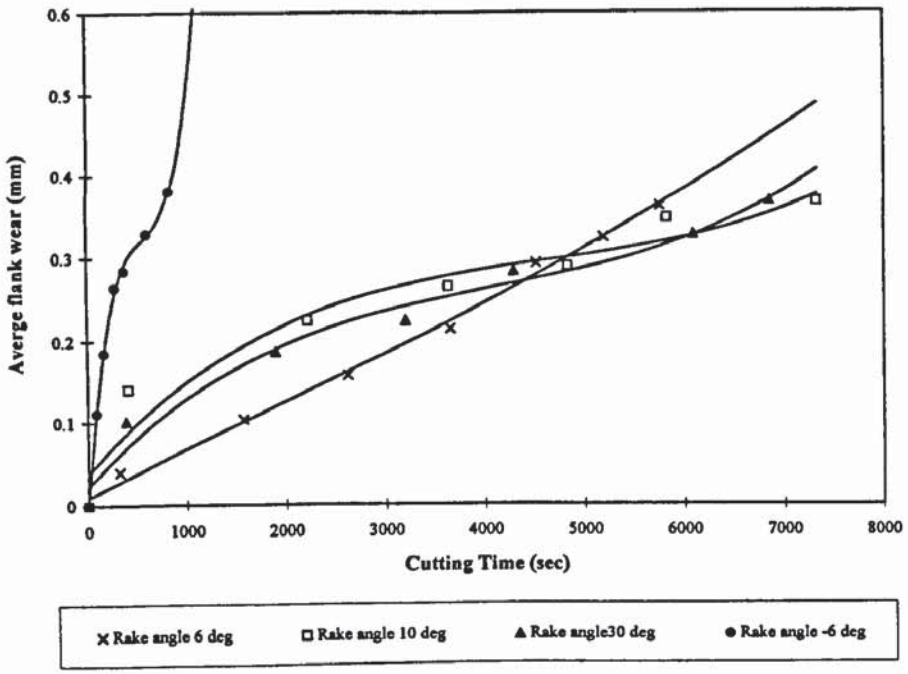

Figure 9.21 Average flank wear vs. Cutting time for M2 HSS, with fixed flank angle at 15 deg, variable rake angles, 2mm DOC, 0.15 mm/rev. feed rate, dry cut.

From the above figures it can be seen that when the rake angle is negative, then the tool life is the shortest as compared to the other three positive rake angles. It is also seen that the wear rate for this negative angle is faster as compared to the other three. Overall by looking at the cutting time one can see that for the flank angle of 15°, the tool life is the longest then the flank angle of 5° and 10° respectively.

Figures 9.22 to 9.25 show the graphs where the rake angle was fixed and the flank angle varied.

In figure 9.22 the graph showing average flank wear vs cutting time is shown when the rake angle is fixed at 6° and the flank angle is variable between 5, 10 and 15°.

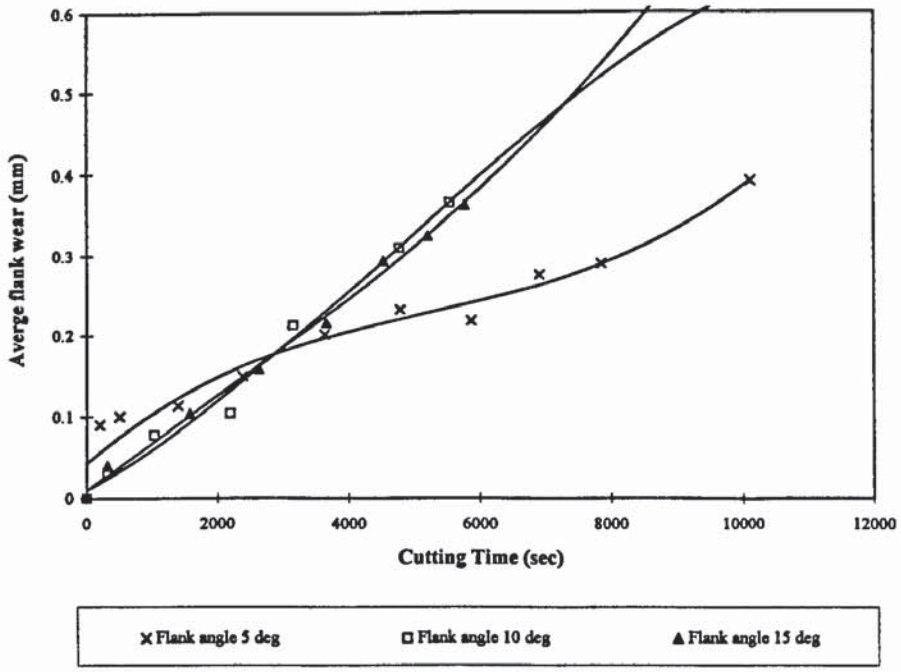

Figure 9.22 Average flank wear vs. Cutting time for M2 HSS, with fixed rake angle at 6 deg, variable flank angles, 2mm DOC, 0.15 mm/rev. feed rate, dry cut.

In figure 9.23 the graph showing average flank wear vs cutting time is shown when the rake angle is fixed at 10° and the flank angle is variable between 5, 10 and 15°.

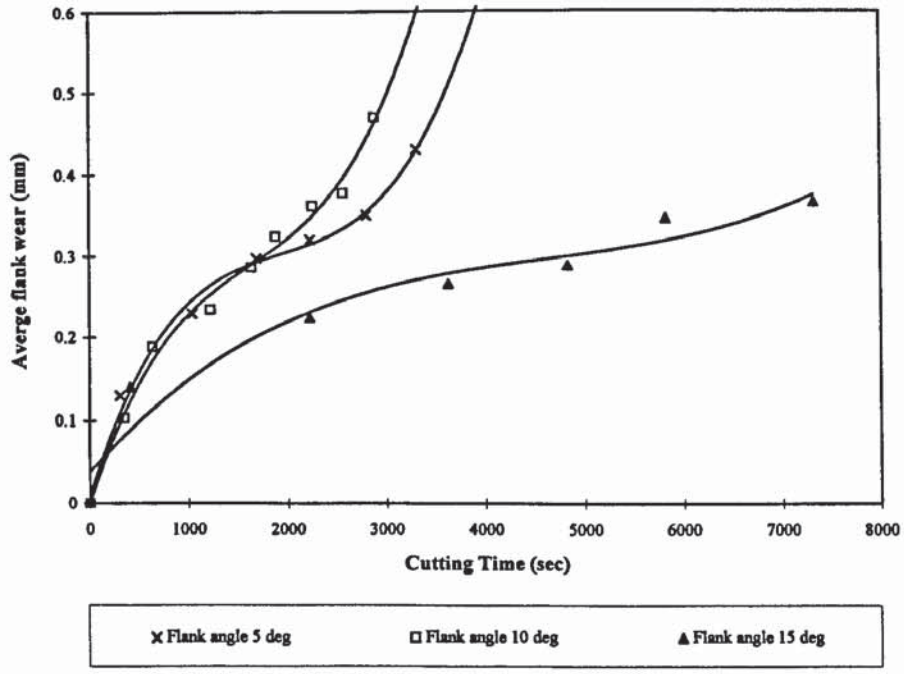

Figure 9.23 Average flank wear vs. Cutting time for M2 HSS, with fixed rake angle at 10 deg, variable flank angles, 2mm DOC, 0.15 mm/rev. feed rate, dry cut.

In figure 9.24 the graph showing average flank wear vs cutting time is shown when the rake angle is fixed at 30° and the flank angle is variable between 5, 10 and 15°.

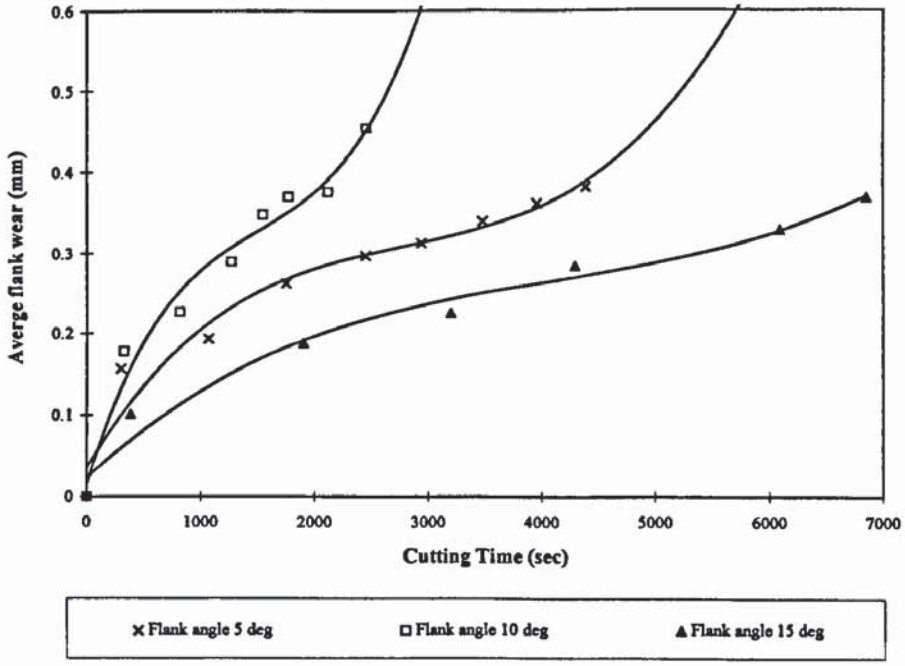

Figure 9.24 Average flank wear vs. Cutting time for M2 HSS, with fixed rake angle at 30 deg, variable flank angles, 2mm DOC, 0.15 mm/rev. feed rate, dry cut.

In figure 9.25 the graph showing average flank wear vs cutting time is shown when the rake angle is fixed at -6^{o} and the flank angle is variable between 5, 10 and 15^{o}.

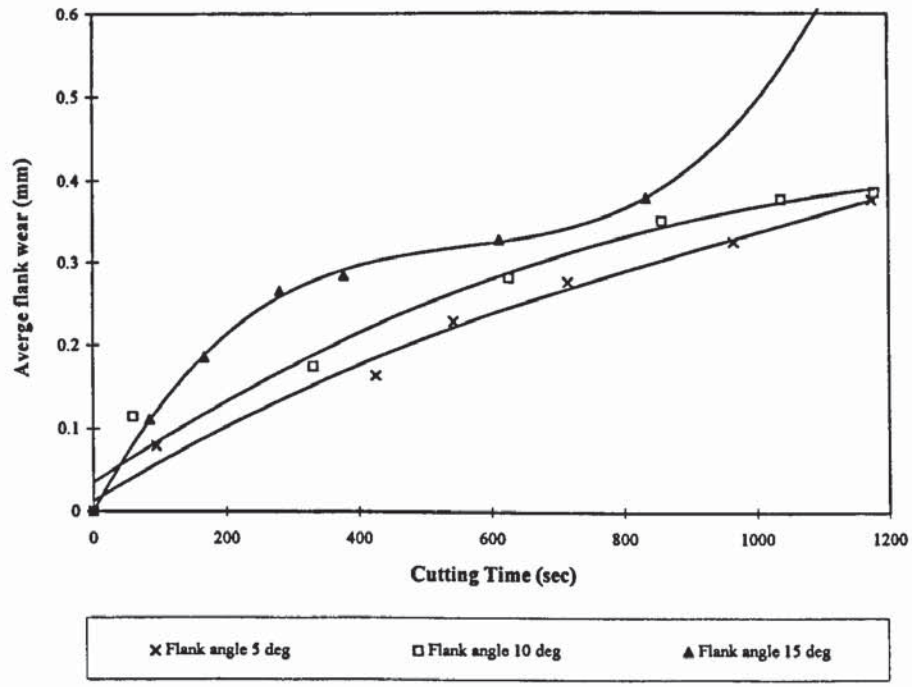

Figure 9.25 Average flank wear vs. Cutting time for M2 HSS, with fixed rake angle at -6 deg, variable flank angles, 2mm DOC, 0.15 mm/rev. feed rate, dry cut.

From graphs 9.22 to 9.25 it is seen, and as expected, the shortest tool life is when the rake angle is -6°, it is by far shorter when compared to the other three angles. The tool life for the other three angles are the shortest for 30°, then 10° then 6°.

As pointed out earlier with the previous set of results for the effect of variation of angles, it is seen that the negative rake angle shortens the tool life and the wear rate is increased faster then when the rake angle is larger. An increase in rake, as Boothroyd (1989) states, usually leads to an improvement in cutting conditions, and a longer tool life is therefore expected. However, when the tool rake is large, the cutting edge is mechanically weak, resulting in higher wear rates and shorter tool life.

According to Trent (1991), tool forces usually rise as the tool is worn, as the clearance angle is destroyed and the area of contact on the clearance face is increased by flank wear.

9.8 CONCLUSION

This chapter attempted to use the model developed by Taibi for the forces in the turning process by substituting the results with those obtained in this research.

It was found that both the experimental and predicted results gave a good fit for the model of unworn tools in turning, in both cutting and feed forces. But for the model of worn tools, the experimental and predicted results did not give a good fit for both the cutting and feed forces.

It was also shown that with a variation of the tool angles, that is rake and flank, a moderate fit was given between the experimental and predicted results.

As will be discussed further in the conclusion of chapter 10 and the final discussion in chapter 11, it is believed that the reason for Taibi's force model with wear does not work is because wear mechanisms were not taken account of. It has been explained

throughout this chapter that increasing the cutting speed, increases the temperature and therefore the wear rate. At the different cutting speeds and temperatures different wear mechanisms act, and this was shown here in graphs 9.17 and 9.18. It is therefore important to take account for any wear mechanisms.

It is well known, in actual tool wear, that several different wear mechanisms, such as adhesion, abrasion, diffusion, oxidation, fatigue, fracture and superficial plastic flow can operate simultaneously in a given situation. Determining the dominant mechanism is always a problem.

It was shown that with a variation of the tool angles, where the rake angle was varied and the flank angle was fixed, and also where the rake angle was fixed and the flank angle was varied, a moderate fit was given between the experimental and predicted results. The graphs with the variation of tool angles (as in the above) and wear, it was seen that wear rates are greater in the latter than the former for the same wedge angle.

In conclusion, however, the tool wear is increasing as the cutting progresses and the rate of its increase is affected by the cutting conditions, the cutting configuration and work material. Henceforth, if a model for machining control is needed to be developed, this model needs to take account for tool wear.

Finally, no single universal equation or extensively accepted theory has been developed to fully explain the many types of wear behaviour and to successfully build wear models. The scattered selection of parameters in wear equations shows that each wear model focuses on a very small part of the wear process. However, it also indicates that many wear modellers have tried to understand wear and to build models from their own academic perspective.

This will be discussed further in chapter 11, the discussion chapter. It was therefore decided to continue with the drilling model.

Chapter 10

EXAMINATION OF A REPRESENTATIVE PREDICTIVE APPROACH IN DRILLING

10.1 INTRODUCTION

As in the previous chapter, chapters 3 and 7 concluded that there is a need for predictive approaches in order to expand our comprehension of the metal cutting process and the various cutting conditions involved in the process. In order to be able to adopt an efficient cutting process and cutting conditions the research has been undertaken in this area.

Although drilling theories exist, they tend to have been developed, in general, in isolation from turning theory, without a complete knowledge of drill geometry, and where wear is considered this limits the work, hence the paucity of literature in drilling on this aspect.

It is the intention of this section to apply Taibi's (1994) force model for turning to the drilling operation by combining it with a model of predicting drill geometry developed by Webb (1990). Webb, a previous research student at Aston University developed a geometric model which proposes a new solution to the complex geometry of the twist drill which offers equivalent numerical information about any drill form and therefore offers mathematical predictability. The dynamic instability of the drill cutting process is then superimposed on this basic drill geometry. Webb's geometric model has shown very good agreement with measurements on sectioned drills and is used by a drill company for designing new drills. More details are given in section 10.4 as to how the Taibi model was adapted for drilling and combined with Webb's model for the purpose of this work.

As in the previous chapter, the model was tested in conditions where the tool is both sharp and worn. The use of high speed steel as the testing tool in the turning section (chapter 9) also allowed direct comparison with the drilling results.

10.2 TOOL WEAR MODELLING BASED ON FORCE VARIATION WITH WEAR IN DRILLING

Although Taibi's model will be adapted for the drilling operation, it seems relevant to look at the work that has been done before. A range of papers that attempted to develop models or equations using forces, and in some also wear, have been selected to be assessed, in order to demonstrate their limitations in terms of the usage of various cutting conditions as opposed to Taibi's model. Again, as in the previous chapter, the arrangement deals with the papers that deal with the modelling of the tool forces first and then those papers that also deal with tool wear and its effects on the models.

Compared to these removal processes (shaping, planing, turning, and broaching), drilling is manifestly more complex in that the tool geometry and the tool obliquity change along the cutting edge, as can be seen in figure 2.7 chapter 2, and figure 10.1. Rubenstein (1991a) argued that, in view of this complexity, it is not surprising that little progress has been made in the search for a theoretical model of the chip formation process in drilling. However, when Rubenstein (1991a) made the following statement, it should be noted that the Webb model had not been developed yet. Rubenstein (1991b) continued to argue that in the absence of such a model, there is no basis on which analytical expressions for the torque and thrust force can be derived. Instead empirical, or at least, semi-empirical expressions have been obtained which, because of the lack of an underlying model, offer no a priori insight into the origin of the indices and coefficients appearing in these expressions nor can the dependence of these latter on drill geometry or on removal parameters be predicted.

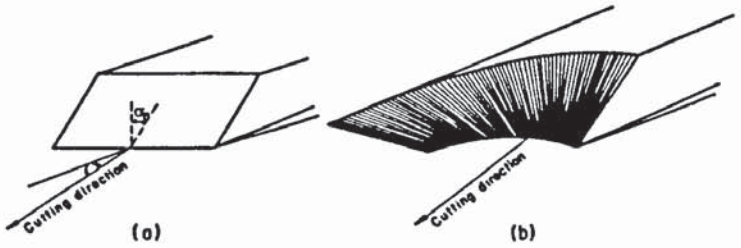

Figure 10.1 A Schematic representation of the form that a single edge would require in order to simulate the removal process (a) in oblique cutting (b) at the lip in twist drilling (Rubenstein 1991a)

An idea of the complexity of the semi-empirical expressions for the torque, M and thrust force, F, arising in drilling can be gained by examining the formulae obtained by Shaw et al. (1957) via dimensional analysis.

According to Shaw et al. (1957) the problem of computing the torque and thrust developed on a drill is approached from dimensional reasoning and the rules of cutting force development in two-dimensional cutting. General equations are derived for torque and thrust and found to be in good agreement with experimental data obtained by use of a drill dynamometer.

In the design and application of metal cutting tools it is useful to be able to predict the forces which act upon a tool of the power required under a given set of operating conditions. For the analysis of drill torque, Shaw et al (1957) begin by performing a dimensional analysis on a drill of given geometry drilling a given material. The pertinent variables shown below with their units (F stands for force and L for length). All other quantities are considered constant.

M = drill torque (FL)

f = feed (L)

d = drill diameter (L)

c = length of chisel edge (L)

H_B = work hardness (FL^{-2})

s = mean spacing of imperfections (L)

All metals contain imperfections which decrease their strength from the large theoretical value corresponding to a perfect metal lattice to the value actually observed in an engineering structure.

If all the variables of interest in the above variations are included, it follows that

$$M = \psi_1[H_B, c, f, d, s]$$

where ψ_1 represents some function of the variables with brackets.

According to Shaw et al. (1957), the drilling process can be divided into two parts; i.e., the action of the cutting edges and the action of the chisel edge at the centre of the drill. The cutting edges act in a manner similar to the two-dimensional tool, but the material at the centre of the drill (cylindrical column of diameter equal the chisel edge length, c) is removed by a very complex process. This action at the chisel edge may be considered to be in part a cutting operation and in part an extrusion operation. When evaluating the total torque or thrust on a drill, three components should then be considered (Shaw et al., 1957):

1- The value associated with the cutting process along the lips of the drill.
2- The values associated with the cutting process at the chisel edge.
3- The value associated with the extrusion process at the chisel edge.

The third item will be negligible for drill torque but not for drill thrust since the resultant force in the extrusion operation will be directed predominately along the drill axis and the mean radius associated with the chisel edge will be small. Thus the total torque on a drill may be expressed

$$M = M_l + M_c$$

where M_l is the torque due to cutting at drill lips and M_c is the torque due to cutting along the chisel edge.

A similar operation may be performed on the drill thrust

T = drill thrust (F)

The thrust on a drill will consist of three components

$$T = T_l + T_c + T_e$$

where T_l and T_c are the thrust due to cutting along lip and chisel edge, respectively, and T_e is the component of thrust due to chisel-edge extrusion.

Subsequently, attempts have been made to derive values for the torque and thrust force by assuming an oblique cutting model of the chip formation processes occurring at a series of elements of the drill lips and of the chisel edge. An original analysis by Armarego and Cheng (Shaw et al. 1957) met with mixed success but later, a more successful model was advanced. In this, relevant values of the chip thickness ratio, the shear stress acting along the shear plane and the rake face 'friction' angle were obtained from orthogonal cutting tests performed at several cutting speeds with a variety of tool rake angles and the values of these parameters were used to estimate the force and torque contributions originating at the individual elements. Summing these elemental components gave the computed values of the torque and thrust generated when drilling a steel and an aluminium alloy workpiece and, in general, these proved to be within 20% of the measured values.

More recently, Watson (1985a,b,c,d) published a series of papers detailing the development of a drilling analysis. The model was fairly successful in accounting for the torque and thrust components developed at the drill lips but less so when it was applied to the torque and thrust developed at the chisel edge.

In his first paper, Watson (1985a) developed a drilling model for the cutting lip region, as seen in figure 10.2, assuming that a pilot hole removes the region that would be machined by the chisel edge portion of the drill, and that the material being machined by each lip can be considered as a number of individual elements. Experimental drilling results when drilling with a pilot hole are found to differ significantly from the cutting lip drilling model predictions.

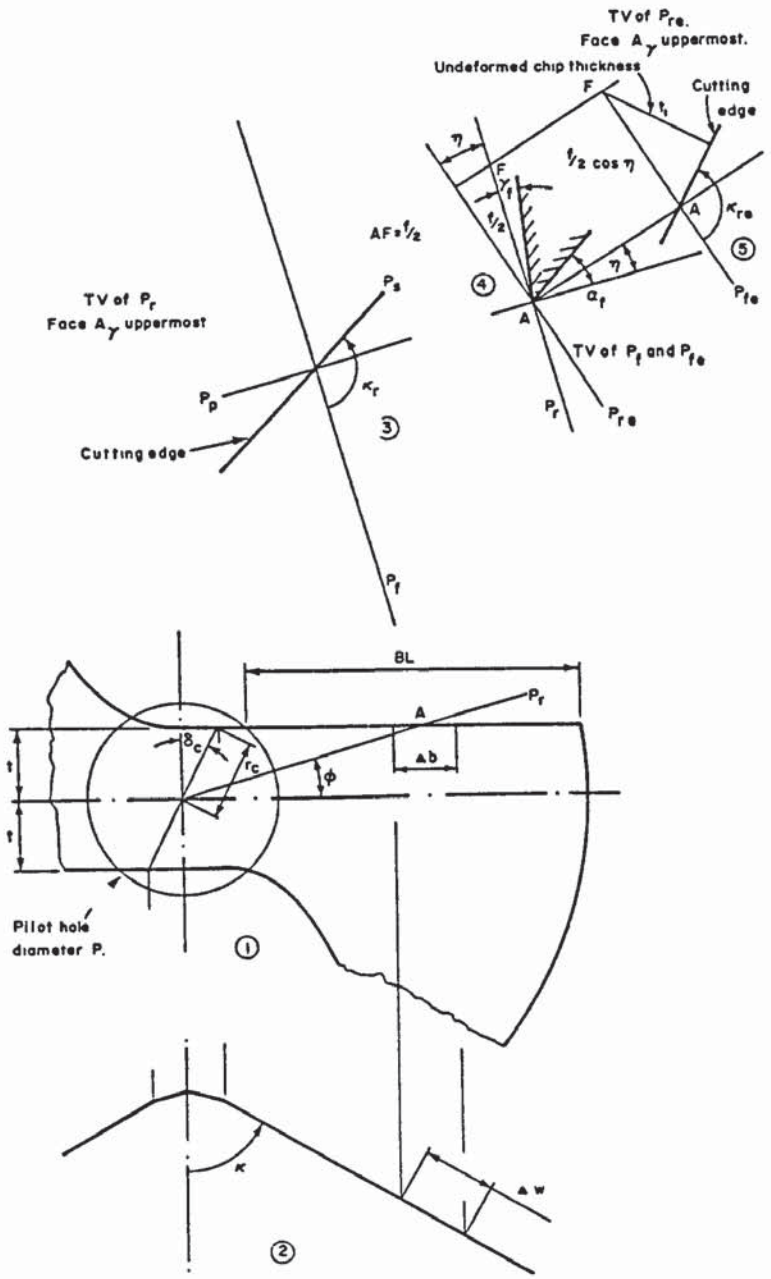

Figure 10.2 Geometric arrangements for cutting lip model (Watson 1985a)

The friction force in the rake face and parallel to the cutting edge, F_f, given by

$$F_f = \sin \lambda_n \tan \eta_c \sqrt{\left(F'^2_C + F'^2_T\right)}$$

where λ_n is the friction angle, and η_c is the chip flow angle. The exact definitions of F'^2_C and F'^2_T are only described as the cutting forces.

The increments of thrust and torque for the element are:

$$\delta TH = \left(\left(F'_C \sin\lambda_{se} - F_f \cos\lambda_{se}\right)\cos k_{re} + F'_T \sin k_{re}\right)\cos\eta + \left(F'_C \cos\lambda_{se} + F_f \sin\lambda_{se}\right)\sin\eta$$

and

$$\delta TQ = \frac{\rho D}{2}\left\{\left(F'_C \cos\lambda_{se} + F_f \sin\lambda_{se}\right)\cos\eta - \left(\left(F'_C \sin\lambda_{se} - F_f \cos\lambda_{se}\right)\cos k_{re} + F'_T \sin k_{re}\right)\sin\eta \right\}$$

where

λ_{se} is the working cutting edge inclination

k_{re} is the working cutting edge angle

η is feed angle

δTH is thrust

δTQ is torque

ρ is pilot hole diameter

D is drill diameter

These are the increments of thrust and torque on an element of one lip of the drill, so that the total thrust and total torque on the cutting lips of a drill from pilot hole edge to the outside diameter will be

$$TH = 2\sum \delta TH$$

and

$$TQ = 2\sum \delta TQ$$

In conclusion, the experimental torque and thrust results were greater (often more than 50% greater) than the predicted values, and consequently the bases of the predictive model must be questioned.

In the second paper (Watson 1985b) the model is modified to take account for the observed integrity of the chip, (i.e. the chip being one piece instead of a series of individual elements). The revised modified model is said to take account of the variation of most of the drill and process variables.

The friction force in the rake face and parallel to the cutting edge, F_f, now becomes

$$F_f = \sin\lambda_n \tan\eta_{cc} \sqrt{F'^2_C + F'^2_T}$$

where η_{cc} is the common chip flow angle for the elements.

The respective equations for incremental thrust and total thrust from the first paper are still used in the computer model. However, the modifications due yield two new unknowns ρ_s (0.2) and η_{cc} (-35°), which are chosen so that they give good agreement between predicted and experimental results. The results after the modifications do give good agreement, it was not felt that there was due justification or explanation given for the choice of the above factors.

In the third paper (Watson 1985c) the chisel edge is then considered, as seen in figure 10.3, and a drilling model is advanced for this region. The contributions from the chisel edge region and the cutting lips are added to obtain the total torque and thrust for the drill.

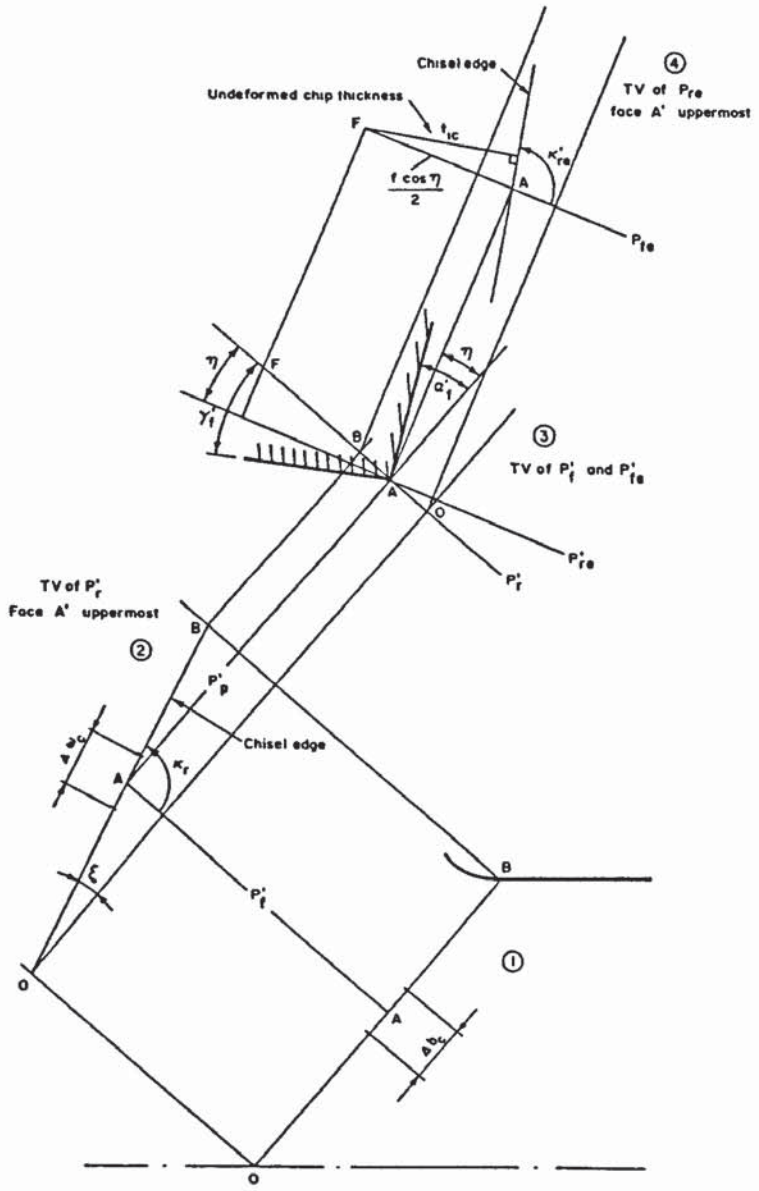

Figure 10.3 Geometric arrangements for cutting on chisel edge (Watson 1985c)

The axial thrust TH_W and the torque TQ_w for this region is

$$TH_W = 2\sum \delta TH_W$$

and

$$TQ_W = 2\sum \delta TQ_W$$

where δ is the chisel angle, summed over the elements for which the wear model is appropriate.

The analysis here does not contain extremely complex maths, but does lose the reader constantly as there is not sufficient explanation as to how each step is taken and where all the terms come from.

Finally, in the fourth paper (Watson 1985d), the predicted values from the previous paper are compared with values obtained when drilling without a pilot hole; however the correspondence between these predicted values and the experimental results for the full drill is not as good as the correspondence between the experimental and predicted results for the cutting lip portion alone. The temperature effects were taken into account and the variation with drilling speed, this was said to give similar values to those observed. Even though this was so, there was some unexpected effects from the unsteady heat transfer in the material from the heat sources on the drill.

The extrusion and wear processes at the chisel edge, though not making a large contribution to the thrust, are probably very significant heat sources for the chisel edge region. This was given as an area for further research and development of the model.

While the model developed for the cutting lip yielded results that correspond reasonably well with experimental results, the variable speed results for the chisel edge have revealed that the unsteady heat transfer in the material to be machined form the heat sources on the cutting regions on the drill, and particularly those on the chisel edge, has to be incorporated into the drilling model before reasonable predictions for the chisel edge can be made.

Rubenstein (1991a) showed that computation of the torque and thrust components, in accordance with the model proposed by Wiriyacosol and Armarego in 1979, was performed on computer and proved to be relatively complex so that, as an alternative, the authors proposed more tractable, empirical expressions for the torque and the thrust force as functions of drill geometry and feed. For 1020 steel the expressions were:

$$M = 1.821 \times 10^{5} f^{0.661} d^{2.004} \left(\frac{w}{d}\right)^{0.113} (2p)^{-0.226} \delta_0^{-0.263} \psi^{-0.177}$$

and

$$F = 3.635 \times 10^3 f^{0.546} d^{1.027} \left(\frac{w}{d}\right)^{0.279} (2p)^{0.518} \delta_0^{-0.210} \psi^{0.05}$$

Rubenstein stated that the measure of our lack of progress in formulating a model on a fundamental understanding of the mechanics of drilling can be gained from the realisation that, although offering a more comprehensive response to the influence of drill geometry parameters, these expressions are no different in form from those advanced as early as 1909 when, for example, the formulae

$$M = C_1 f^{0.7} d^{1.8}$$

$$F = C_2 f^{0.6} d^{0.7}$$

were proposed for drilling steel by Smith and Poliakoff.

d = drill diameter

c = chisel edge length

w = web thickness

p = semi-point angle

δ_0 = helix angle at the outer diameter of the lip

ψ = chisel edge angle

f = feed

M, F = torque and thrust force, respectively

Using a simple model, Subramanian et al. (1977) obtained relationships between flank wear on the one hand and thrust force and torque on the other. They are in the general form:

$$T_f = H_B(P + Qw)$$

where T_f is the thrust force or torque, H_B is hardness of the work material, P and Q are constants (dependent on drill diameter, feed per revolution and radius of the cutting edge) and w is the flank wear.

The equation illustrates the correlation between thrust force and drill wear. If the hardness of the work material is a constant, the thrust force will increase linearly with flank wear under any given set of cutting conditions. However, in practice, fluctuations in the hardness cause random variations in the thrust force under normal drilling conditions.

Morin et al. (1995) investigated the effect of drill wear on cutting forces in the drilling of metal matrix composites (MMC). Holes were drilled in aluminium alloy as well as in a particle-reinforced MMC. HSS drills were used, and measurements were made of thrust (normal force), torque and flank wear for several feed rates and drill speeds. It was found that when drilling Duralcan with unworn tools, both torque and thrust varied with feed rate raised to the power 0.81 as for classical materials. When flank wear V_b became significant, torque and thrust varied linearly with V_b and with $f^{0.8}$ but no empirical relation with physically meaningful parameters was found to fit the thrust data.

The model derived by Shaw et al. (1957) was used for fitting by Morin et al (1995). In this model, torque M is related to feed rate f through

$$M = Af^{1-a} \qquad \text{Eq 1}$$

The relation is based on the fact that, on purely geometrical considerations, the mean specific cutting energy if related to torque through

$$\bar{u} = \frac{8M}{fd^2} \qquad \text{Eq 2}$$

where d is drill diameter. For classical materials it is observed that, very nearly, the mean specific cutting energy depends on feed through

$$\bar{u} \propto (fd)^{-a} \qquad \text{Eq 3}$$

where the exponent a is typically close to 0.2. Equating the two expressions now gives equation 1, which, with the commonly observed value of a, becomes

$$M = Af^{0.8} \qquad \text{Eq 4}$$

The equation is expected to be independent of cutting speed over a 'normal' range of cutting speeds. The constant A is a function of drill diameter and geometry and is directly proportional to. The specific cutting energy $\bar{u}$ in turn is taken to be directly proportional to the Brinell hardness for classical materials and is expected to increase due to any wear or other dulling of the drill. That $\bar{u}$ does in fact increase with wear is confirmed when calculated using equation 2 and is plotted against V_b.

First, the case where $V_b = 0$ is considered, i.e., at zero depth. Taking the zero depth intercepts of the torque vs. depth curves, and data obtained for the 6061 aluminium, the regression equation

$$M = 13.1f^{0.88} \qquad \text{Eq 5}$$

is obtained for Duralcan, and

$M = 12.6f^{1.15}$

is obtained for the 6061 alloy. Cutting speed has no significant effect, as expected. The agreement with Shaw is good, considering a certain amount of scatter in the results.

Secondly, the case where there is wear of the drill is considered. If the constant A is directly proportional to $\bar{u}$, it must vary linearly with flank wear, V_b, in accord with the

observations where torque, and hence $\bar{u}$, is seen to be directly proportional to V_b. The constant A in equation 1 must therefore be replaced with a linear function of V_b. When this is done, the regression equation

$$M = (7.71 + 22.09V_b)f^{0.81} \qquad \text{Eq 6}$$

is obtained with a correlation of $R^2 = 0.994$, shows the fit obtained. In spite of apparently very good correlation coefficient, it is clear that equation 6 can not be extrapolated to $V_b = 0$ to give the same results as equation 5. Thus, although the Shaw relation holds with Duralcan for a sharp drill, it must be modified when there is wear.

As for torque, thrust may also be analysed in terms of the classical work of Shaw and Oxford. They predict a dependence of thrust against feed rate of

$$N = Af^{0.8} + B \qquad \text{Eq 7}$$

where again A and B depend on specific cutting energy of drill geometry. B is positive and typically much smaller than the term $Af^{0.8}$.

Again when considering a situation for no wear, the results of fitting data from measurements of thrust vs. feed rate fit quite well to the equation

$$N = 2849f^{0.81} \qquad \text{Eq 8}$$

When considering the case where there is wear of the drill. An attempt to fit their data to equation 7, with the constants A and B again replaced by linear functions of V_b. because of the observed linearity of thrust with flank wear. That is, the equation

$$N = (a + bV_b)f^n + (c + dV_b) \qquad \text{Eq 9}$$

is taken as a model. As a variation of this, the parameters c and d may be set to zero, so that the equation resembles equation 8, i.e.

$$N = (a + bV_b) f^n \qquad \text{Eq 10}$$

other variations are possible.

Using obtained results with $n = 0.81$ to resemble equation 8, the regression equation

$$N = (3475 + 80.58V_b) f^{0.81} \qquad \text{Eq 11}$$

with correlation coefficient $R^2 = 0.9262$ is found. Systematic deviations from the observed results are observed, and the extrapolation to $V_b = 0$ is unsatisfactory.

If a regression analysis is done using equation 9 as a model, with all five parameters allowed to float, the regression equation

$$N = (12676 + 17878V_b) f^{0.10} - (10609 + 13686V_b) \qquad \text{Eq 12}$$

is found, with correlation coefficient $R^2 = 0.9997$.

Morin et al (1995) reported that the fit is now very good, which is perhaps not surprising since there are five free parameters, however, neither the exponent 0.10 nor the negative second term are acceptable on physical grounds.

No equation of the general form of equation 7 was found which fit the observations with physically acceptable regression values for the adjustable parameters. Thus again, while the Shaw equation fits well for the no-wear situation, modifications will be required when there is significant wear of the drill. Therefore, predictions of drill torque and thrust forces must be modified to account for drill wear, the precise modifications required have not been determined by Morin et al (1995).

As can be seen from this section, there are quite a few papers on the topic of drill torque and thrust prediction and even some on drill force prediction and wear. The purpose of these models is to reduce the amount of testing normally required to develop or improve a cutting process. Perhaps the most interesting is that there are drill force prediction models which are accurate and therefore that can be used for force prediction. But, it

must be stated at this point that, taking for example Morin's paper which was produced in 1995, this was not available when Taibi (1994) was doing his research at Aston University and therefore had to attempt to devise his own approach. One of the many reasons why Taibi was chosen as opposed to the other models, is that even though he does not mention temperature in his model, he uses a coefficient, which reflect temperature because he bases them on a series of tests. Taibi takes account of virtually all parameters, certainly more than anyone else had taken account of, by virtue of this coefficient he employed. Therefore this research is a continued development from Taibi's model and for reasons stated earlier in chapter 9.

10.3 EXTRAPOLATION FROM TURNING OPERATION TO DRILLING

For some considerable time the manufacturing industry, in conjunction with tooling manufacturers, has been studying the wear of cutting tools in an endeavour to be able to reliably predict tool life in drilling.

From the earliest tool life experiments by Taylor (1907) numerous tool life studies have been carried out mainly in the turning mode and the process is reasonably well understood, though it can be perceived that there is still plenty of scope for further work.

However, there has not been anything like the same volume of work carried out to study drilling tool life or wear processes, and where this work has been undertaken often the emphasis is on flank and crater wear which are the measurements normally recorded for turning experiments. Cherry (1961) pointed out that the cutting action at the edge of any cutting tool has considerable similarity, and a wear surfaces on common tool due to tool motion can be shown in figure 10.4 (Alden Kendall 1989), and the behaviour when turning can be a guide for other processes.

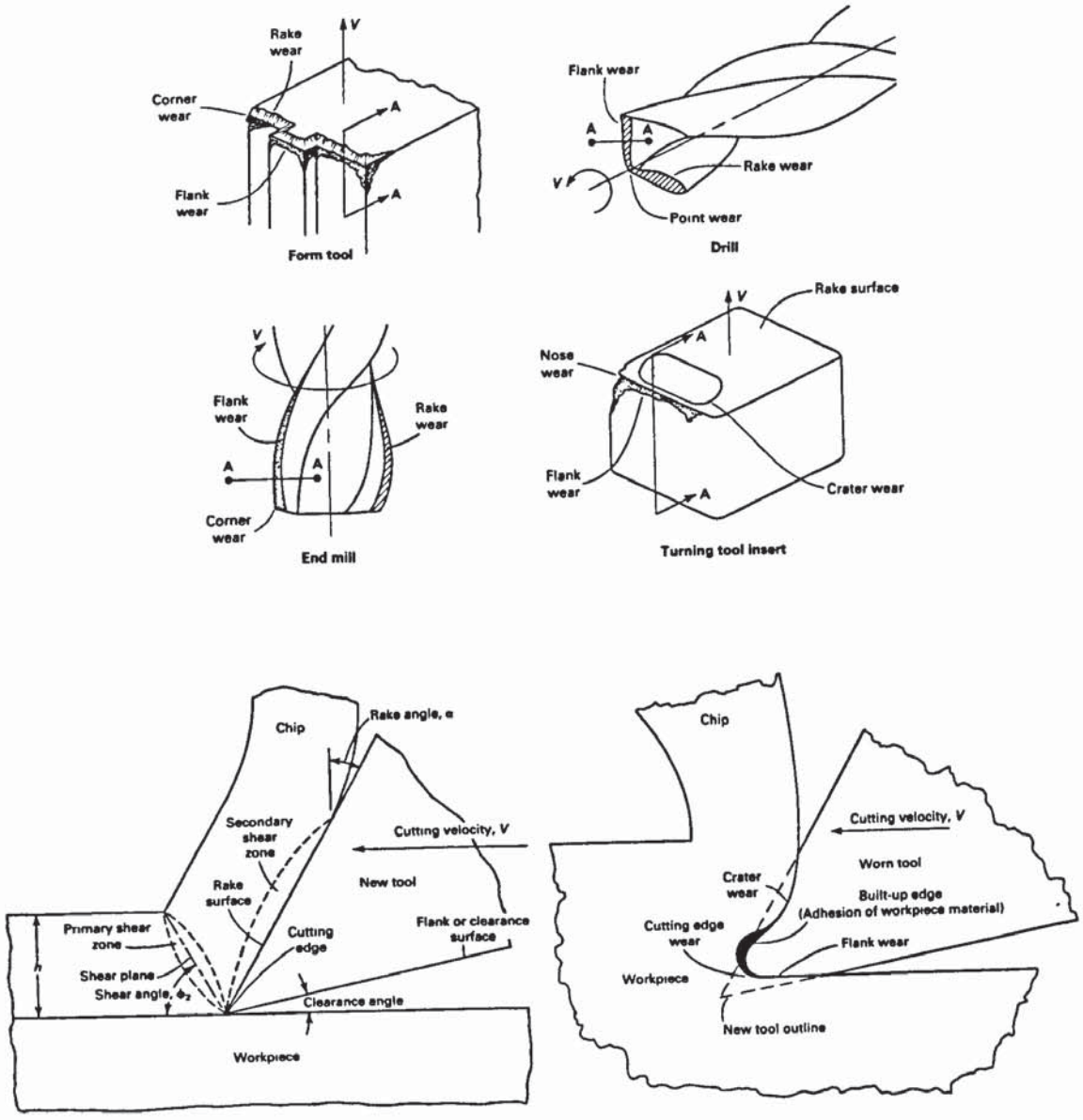

Figure 10.4 Wear surfaces on common tool due to the tool motion (Alden Kendall 1989)

In any study of metal cutting processes, realistic models are required which can be used as a basis for the prediction of cutting forces. In this respect numerous papers are available for orthogonal turning and this work has been extended to oblique turning. Both the orthogonal and oblique cutting theory have been used to develop models of the drilling process. If the effect of the chisel edge can be isolated in testing then these turning models should show a degree of similarity to the work on the drilling process.

Subramanian and Cook (1977) used a simplified model together with empirically derived constants to derive expressions for the thrust and torque. In their expressions values for the average flank wear were incorporated, however, no account was taken of the wear at the outer corner, and as pointed out by Williams (1974) this factor must be inclined in the latter stages of drill life.

Before attempting to develop a wear/geometry relationship for the drilling process, it was necessary to look at the observations and developments of previous research. It was found that a great deal of research had been undertaken towards the prediction of drill-life in general.

In the literature available on drill wear and drill life prediction, there was no detailed reference to the dependence upon geometry. This is perhaps a consequence of the difficulties involved in developing any relationship concerning drill geometry and that most research is undertaken in the interests of industry (to enable the prediction of tool changes and subsequently reduce machine downtime).

10.4 EXTRAPOLATION OF TURNING FORCE MODEL TO DRILLING

The aim here is to use Taibi's developed model for prediction of forces in turning for the prediction of the forces in drilling. Since Taibi's model covered a wide variety of cutting conditions, and was used for the turning operation then it would be a natural progression to use it for the drilling in order to be able to do straight comparisons.

In order to calculate the forces in drilling, Taibi's force model in turning, and Webb's geometric model in drilling were combined and used by the author of this work to enable the calculation of the forces across the lip of the drill, an example of which will be demonstrated in the section below.

CO-ORDINATES OF POINTS ON CUTTING LIP OF DRILL

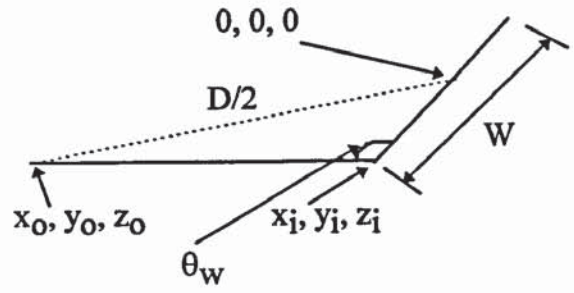

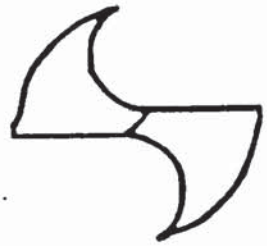

VIEW ALONG AXIS OF DRILL

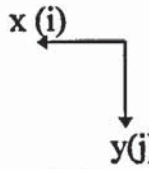

x-y plane defines x-section of the drill.

D = drill diameter
W = chisel length
θ_W = chisel angle

x_i, y_i, z_i = co-ordinates of inner corner of drill lip
x_o, y_o, z_o = co-ordinates of outer corner of drill lip
0, 0, 0 = co-ordinates of centre of drill

R_L = length of drill lip
P = point angel of drill

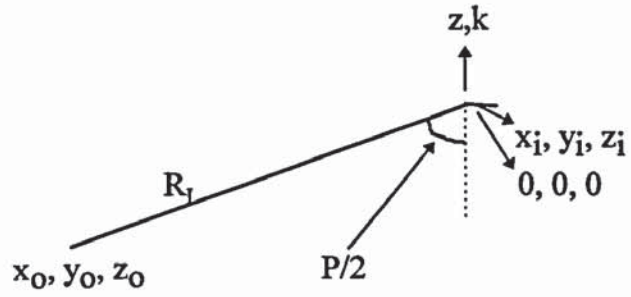

VIEW DRILL AXIS

z axis (k unit vector) indicates direction of drill axis in the force direction.

CALCULATION OF CO-ORDINATES OF ANY POINT ON DRILL LIP

$$\left.\begin{aligned} x_i &= \frac{W}{2}\sin\theta_W \\ y_i &= \frac{W}{2}\cos\theta_W \\ z_i &= 0 \end{aligned}\right\} \text{ co-ords of inner corner}$$

$$R_L = \left[\left[\frac{D^2}{2} - y_i^{\,2}\right]^{\frac{1}{2}} - x_i\right]\frac{1}{\sin\left(\frac{P}{2}\right)}$$ } lip length

$$x_0 = \left[\left(\frac{D}{2}\right)^2 - y_i^{\,2}\right]^{\frac{1}{2}}$$

$$y_0 = y_i$$

$$z_0 = -(x_0 - x_i)\cot\frac{P}{2}$$

} CO-ORDS OF OUTER CORNER

CALCULATION OF CO-ORDS OF <u>ANY</u> POINT ON DRILL LIP

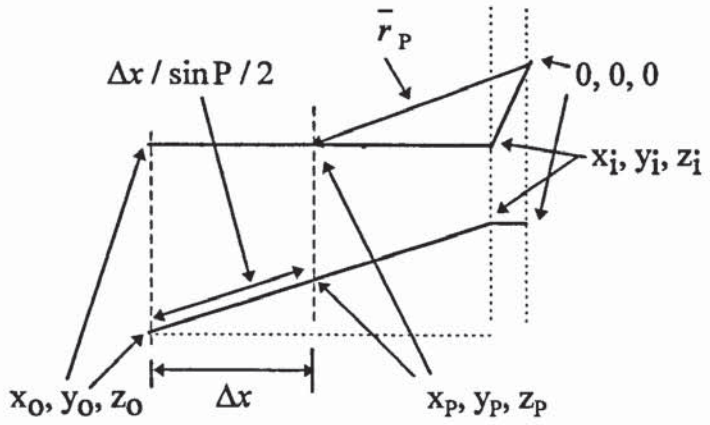

$$x_p = x_0 - \Delta x$$

$$y_p = y_i$$

$$z_p = -\left[z_0 - \Delta x \cot\frac{P}{2}\right]$$

Calculation of velocity at any point on lip (of drill)

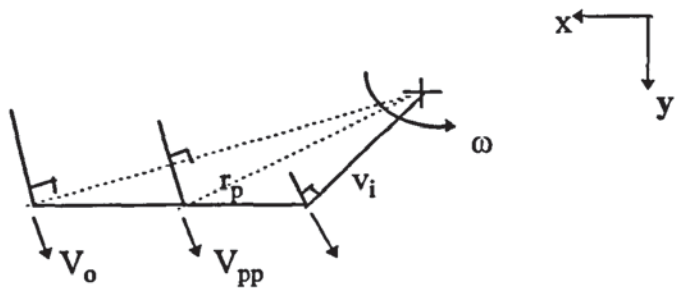

Using vector cross product

In x-y plane

$$\overline{V_{pp}} = \left[\overline{\omega} \times \overline{r_p}\right]$$
$$= \omega k \times \left(x_p i + y_p j + z_p k\right)$$
$$= \left(\omega \cdot x_p \cdot j\right) + \omega \cdot y_p(-i)$$

R.H.S. rule

In z direction

$$\overline{V_{pp_z}} = fNK = +\frac{f\omega}{2\Pi}k$$

f = feed/rev., N = rev/sec., K = direction

Total velocity of any point on lip

$$\overline{V_{pp}} = -\omega y_p(i) + \omega x_p(j) + \frac{f\omega}{2\Pi}(k)$$

Note:must ensure all units are compatible

Magnitude of $V_{pp} = \omega\left[{y_p}^2 + {x_p}^2 + \frac{f^2}{4\Pi^2}\right]^{\frac{1}{2}}$ (PYTHAGORAS)

Calculation of unit vectors of direction for lip, cutting force, feed force.

- Direction of approach of material at any point relative to the cutting lip $\bar{u}$

$$\overline{V_{pp}} = V_{pp} \cdot \bar{u}$$

$$\therefore \bar{u} = \frac{\overline{V_{pp}}}{V_{pp}}$$

$$\bar{u} = \frac{\omega y_p}{V_{pp}} \cdot (i) - \frac{\omega x_p}{V_{pp}} (j) - \frac{f\omega}{2\Pi \cdot V_{pp}} (k)$$

- Direction along cutting lip u_ε

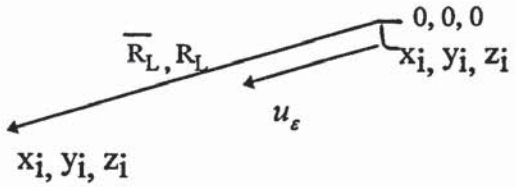

$$\overline{R_L} = R_L \cdot \bar{u}_\varepsilon$$

$$\bar{u}_\varepsilon = \frac{\overline{R_L}}{R_L}$$

$$= \frac{(x_0 - x_i)}{R_L} i + \frac{(y_0 - y_i)}{R_L} j - \frac{(z_0 - z_i)}{R_L} k$$

$$= \frac{(x_0 - x_i)}{R_L} i + \overset{y_0 = y_i}{0} - \frac{z_0}{R_L} k$$

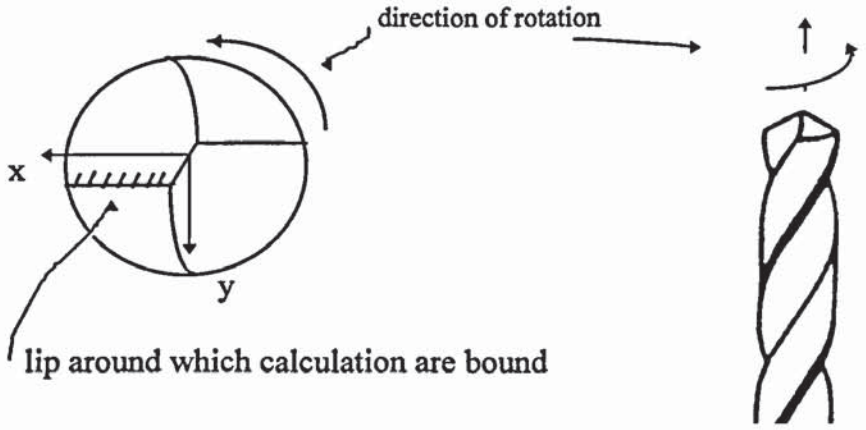

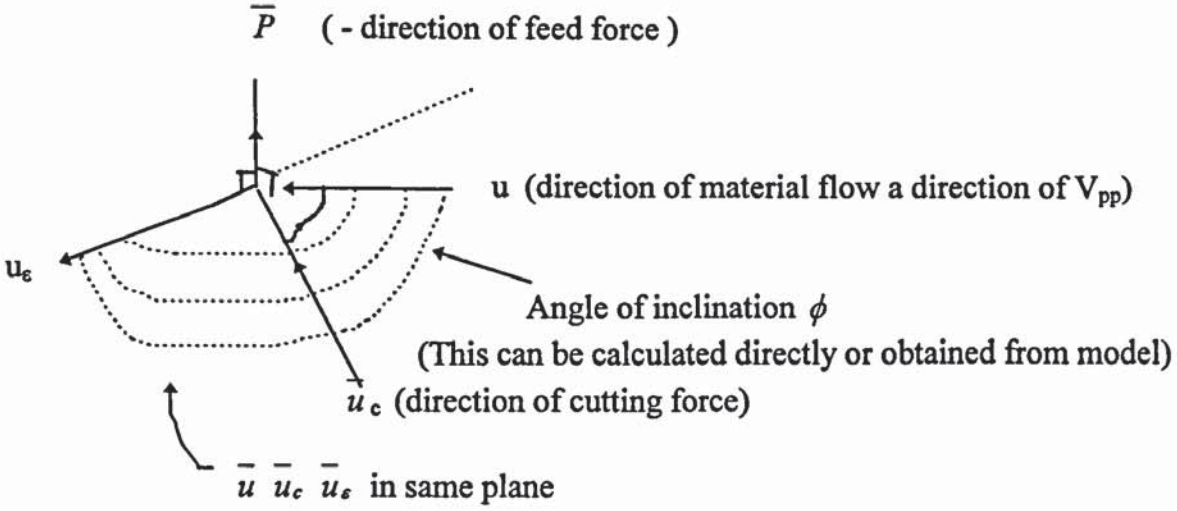

From above picture

$\bar{u} \cdot \bar{u}_\varepsilon = \sin\phi$

- Direction of cutting force $\perp$ to lip at any point $(\bar{u}_C)$

Direction of feed force $\perp$ $(\bar{P})$

Assume $\bar{u}_C = \cos\theta_{xc} i + \cos\theta_{yC} j + \cos\theta_{zC} k$

$\bar{P} = \cos\theta_{xp} i + \cos\theta_{yp} j + \cos\theta_{zp} k$

$\bar{P}$ can be found from the cross product

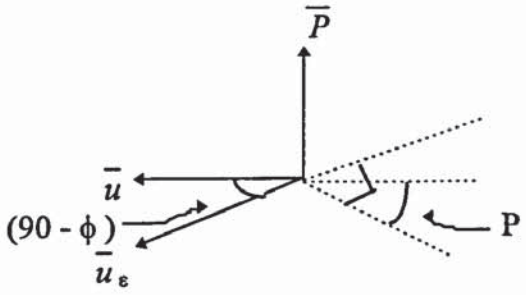

$$\overline{u} \times \overline{u}_\varepsilon = \overline{P}\sin(90-\phi)$$
$$= \cos\theta \cdot \overline{P}$$

$$\begin{vmatrix} i & j & u \\ u_x & u_y & u_z \\ u_{\varepsilon x} & u_{\varepsilon y} & u_{\varepsilon z} \end{vmatrix} = \left[P_x i + P_y j + P_z u\right]\cos\theta$$

Thus

$$+\left(u_{\varepsilon z} \cdot u_y - u_{\varepsilon y} \cdot u_z\right) \cdot \frac{1}{\cos\phi} = P_x$$

$$-\left(u_{\varepsilon z} . u_x - u_{\varepsilon x} \cdot u_z\right) \cdot \frac{1}{\cos\phi} = P_y$$

$$+\left(u_{\varepsilon y} \cdot u_x - u_{\varepsilon x} \cdot u_y\right) \cdot \frac{1}{\cos\phi} = P_z$$

$\overline{u}_C$ can be found from the cross product

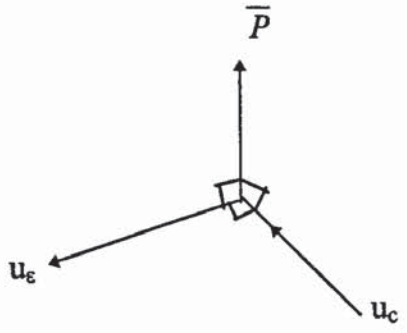

$$\bar{u}_e \times \bar{P} = \bar{u}_C$$

$$\begin{vmatrix} i & j & u \\ u_{ex} & u_{ey} & u_{ez} \\ P_x & P_y & P_z \end{vmatrix} = u_{Cx} i + u_{Cy} j + u_{Cz} \bar{u}$$

$$+\left[P_z \cdot u_{ey} - P_y \cdot u_{ez}\right] = u_{Cx}$$

$$-\left[P_z \cdot u_{ex} - P_x \cdot u_{ez}\right] = u_{Cy}$$

$$+\left[P_y \cdot u_{ex} - P_x \cdot u_{ey}\right] = u_{Cz}$$

Estimation of Thrust on the drill

The calculation embodied in the following is carried out for every incremental element of the drill lip considered. The resulting values are summed and multiplied by 2 to yield total thrust due to cutting lips.

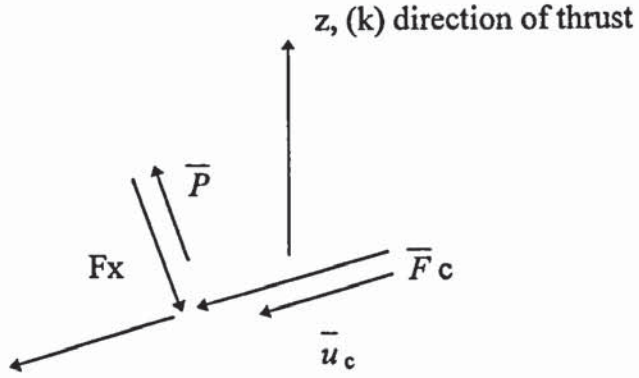

F_z = *cutting force*
F_x = *feed force*
} per unit of cutting lip length

R = friction force on lip per unit of cutting lip length

R defined as = $u\left[F_z^2 + F_x^2\right]^{\frac{1}{2}}$

Fz, Fx are calculated from TAIBI EQUATIONS

Contribution to thrust dT = thrust per unit of lip length
T = the total thrust attributed to a given sector of the lip

$i \cdot k$, $j \cdot k = 0$
only $k \cdot k$ yields

$$dT = \left[F_z + F_x + \overline{R}\right] \cdot \left[\overline{K}\right]$$

$$= \left[F_z \cdot \cos\theta_{zc} K - F_x \cos\theta_{zp} K + R\cos\theta_{u\varepsilon} u\right] . \overline{u}$$

$$= \left[F_z \cdot \cos\theta_{zc} - F_x \cos\theta_{zp} + R\cos\theta_{u\varepsilon}\right]$$

Estimation of torque on the drill

As for thrust the calculation embodied in the following is carried out for each incremental element of the drill lip under consideration. The resulting values are summed and multiplied by 2 to yield total torque due to the engagement of the lips.

If dM is the torque/unit length
M = the total torque attributed to a given sector of the lip

$$d\overline{M} = \overline{r}_p \times \left[\overline{F}_z + \overline{F}_x + \overline{R}\right]$$

$\overline{r}_p$ = position from origin on drill axis @ centre of chisel to the mean point of the unit length under consideration.

Outcome will be the form

$$d\overline{M} = dM_x i + dM_y j + dM_z k$$

$dM_x i$ and $dM_y j$ - These two are cancelled by the equal and opposite on the other lip.
$\therefore$ Only dM_z need be calculated

$$dM = \left[\begin{vmatrix} x_p & y_p \\ F_z\cos\theta_{xc} & F_z\cos\theta_{yc} \end{vmatrix} + \begin{vmatrix} x_p & y_p \\ F_x\left(-\cos\theta_{xp}\right) & F_x\left(-\cos\theta_{yp}\right) \end{vmatrix} + \begin{vmatrix} x_p & y_p \\ R\cos\theta_{x\varepsilon} & R\cos\theta_{y\varepsilon} \end{vmatrix}\right.$$

This is the form of expansion embodied in the spreadsheet.

The adaptation to the estimation of thrust and torque was based on consideration of the lips alone to avoid introducing the need to consider extrusion effects associated with the chisel and thus have to go outside the Taibi model.

The final equations used for calculating the drill thrust and torque are shown below.

Estimation of the thrust per unit length of lip is:

$$dT = \left[F_z + F_x + \overline{R}\right] \cdot \left[\overline{K}\right]$$

$$= \left[F_z \cdot \cos\theta_{zc} K - F_x \cos\theta_{zp} K + R\cos\theta_{u\alpha} u\right].\overline{u}$$

$$= \left[F_z \cdot \cos\theta_{zc} - F_x \cos\theta_{zp} + R\cos\theta_{u\alpha}\right]$$

Estimation of the torque per unit length of lip is:

$$dM = \left[\begin{vmatrix} x_p & y_p \\ F_z\cos\theta_{xc} & F_z\cos\theta_{yc} \end{vmatrix} + \begin{vmatrix} x_p & y_p \\ F_x\left(-\cos\theta_{xp}\right) & F_x\left(-\cos\theta_{yp}\right) \end{vmatrix} + \begin{vmatrix} x_p & y_p \\ R\cos\theta_{x\delta} & R\cos\theta_{y\delta} \end{vmatrix}\right.$$

Therefore as demonstrated above, by using the Taibi model, elements of the lip are used to work out the force components, and using the Webb model to supply the information with the Taibi model and aggregating the two to develop the thrust and torque. In order to do that, one has to develop from the geometric model the angles of movement or the angles where these cutting forces took place because one has to aggregate them to get the thrust, or torque and so on. Taibi's model was put onto a spreadsheet and used as the section below demonstrates. The analysis which showed the development of the drill model as used in the final analysis utilising force results from Taibi estimation model.

10.4.1 Validity of the Drilling Model

As stated earlier the model that was developed by Taibi for the prediction of forces in single point turning was used to attempt to obtain a fit for the forces generated in drilling. The drill size used was 13 mm as it so happened that work was going on on that drill size for Dormer's the suppliers of the tool material. The reason for the 2 mm cut on the 13 mm drill was due to the difficulties of allowing for chisel effects, and in order to keep as close as possible to the turning conditions where the depth of cut was 2 mm. The following section attempts to compare the results obtained in the predictions with those obtained in the experiments.

Figures 10.5 and 10.6 show the results obtained for the forces during experiments and the predicted results for a new tool. The drill used was 13 mm diameter M2 HSS with three different helix angles: slow, standard and fast. For the cutting speed of 244 rpm, a feed rate of 78 mm/min was used, for 490 rpm a feed rate of 156 mm/min was used and for the cutting speed of 735 rpm a feed rate of 234 mm/min was used, and in all the tests only 2 mm was cut in each lip from the corner.

Figure 10.5 shows the graph of thrust vs. cutting speed for the three different angles (slow, standard and fast). The graph is a comparison of experimental and predicted results, and it can be seen that the results are quite good, in fact better than those of the single point turning.

The slow helix angle produced very similar results for all the three different speeds, and in fact, there was only about 3% difference between the experimental and predicted results. With the standard helix angle, the results were fair for all the three speeds and the percentage difference between the experimental and predicted values was about 14%. The results for the fast helix angle were more improved as those obtained for the standard helix but not than the ones obtained for the slow helix angle, the percentage difference being 6%. This will be discussed further and related to single point turning in the discussion chapter 11.

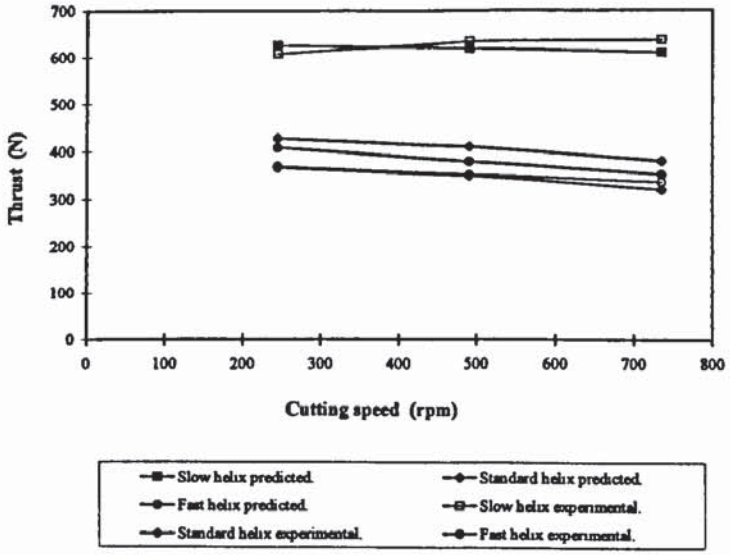

Figure 10.5 Thrust *vs*. cutting speed for 13 mm diameter M2 HSS, 2 mm cut each lip, dry cut.

Figure 10.6 shows the graph for torque vs. cutting speed for a tool with new edge. As can be seen, the results are quite different between those obtained experimentally and those obtained by prediction. For the slow helix angle, a similarity can be seen in that the torque values were high for both the experimental and predicted results when compared to the other two helix angles. For the standard and fast helix angles, the torque values were closer together for both the experimental and predicted values.

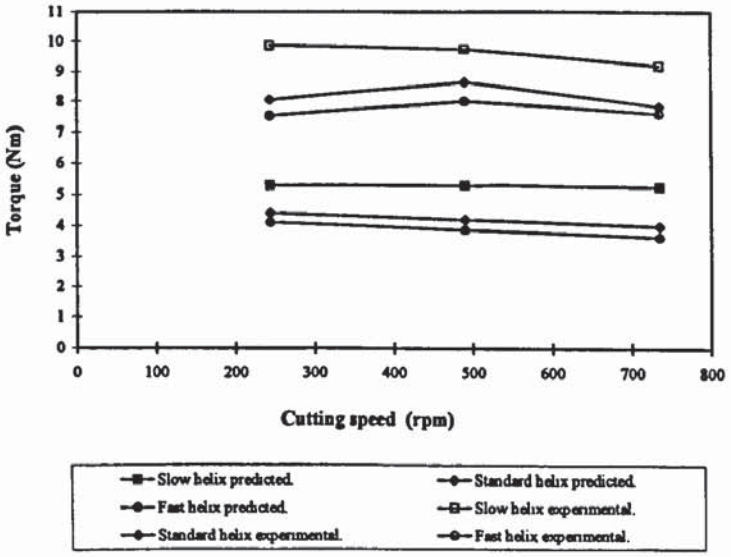

Figure 10.6 Torque *vs*. cutting speed for 13 mm diameter M2 HSS, 2 mm cut each lip, dry cut.

The percentage difference for all the nine results (that is, for all three helix angles and for all the three cutting speeds) is quite high, it varies between 43% and 52%. As in the previous figures, the similarities between single point turning and drilling will be discussed further in chapter 11 of the discussion.

The thrust for both the experimental and predicted results was quite close together for all the three cutting speeds, but for the torque, the experimental and predicted results were not so close for all the three cutting speeds. The percentage difference, as can be seen, is very little and this can be compared to the results of the turning, and as stated above will be discussed in more details in the discussion. But, it can be seen that the results give a good fit overall.

10.5 VALIDITY OF WEAR MODELS

In figures 10.7, 10.8 and 10.9 the graphs show thrust vs. average lip wear for the three different helix angles for a new tool. The differences between the three figures is the cutting speeds in which the tests were performed. The cutting speeds used were 244, 490 and 735 rpm for figures 10.7, 10.8 and 10.9 respectively.

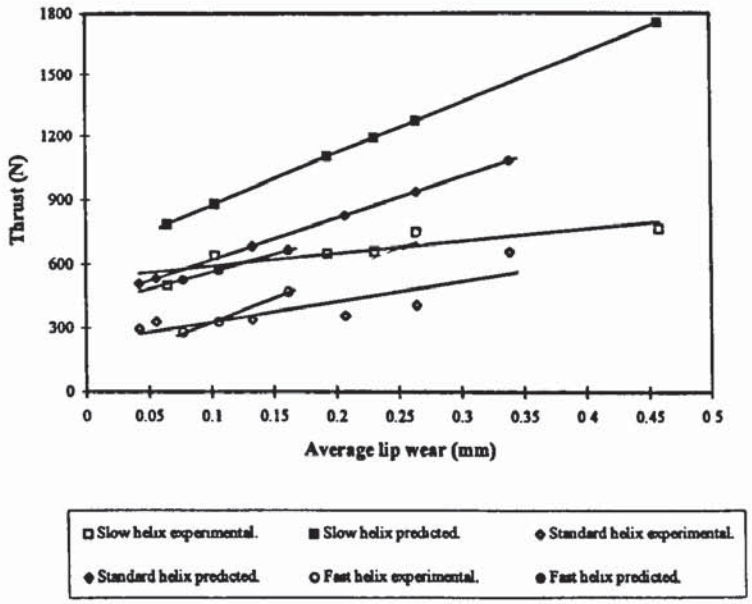

Figure 10.7 Thrust *vs*. lip wear for 13 mm diameter M2 HSS, at speed 244 rpm, feed rate 78 mm/min., 2 mm cut each lip, dry cut.

As can be seen in all the three figures that as the average lip wear increases so does the thrust force. A further discussion will take place to discuss the effect of wear in the discussion chapter 11.

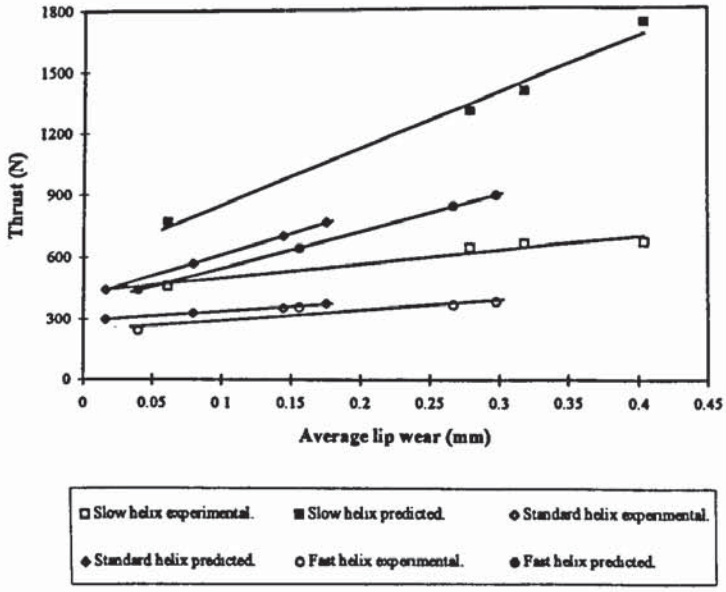

Figure 10.8Thrust *vs*. lip wear for 13 mm diameter M2 HSS, at speed 490 rpm, feed rate 156 mm/min., 2 mm cut each lip, dry cut.

It is also seen that the predicted values for slow helix angle, in all the three graphs, is the highest, the standard helix angle is the next highest value, although it is quite similar to the fast helix angle. This situation is also observed for the experimental values for all the three helix angles.

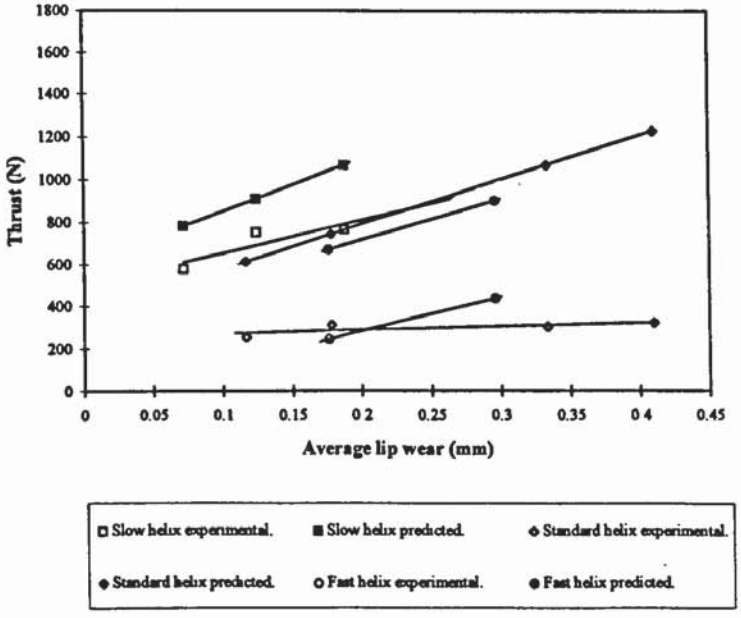

Figure 10.9 Thrust *vs*. lip wear for 13 mm diameter M2 HSS, at speed 735 rpm, feed rate 234 mm/min., 2 mm cut each lip, dry cut.

Figures 10.10, 10.11 and 10.12 show the graphs with the exact same conditions as the previous three graphs (figures 10.7, 10.8 and 10.9) but these following three figures are for torque vs. average lip wear. Again as for the previous three graphs the cutting speeds used are 244, 490 and 735 rpm for figures 10.10, 10.11 and 10.12 respectively.

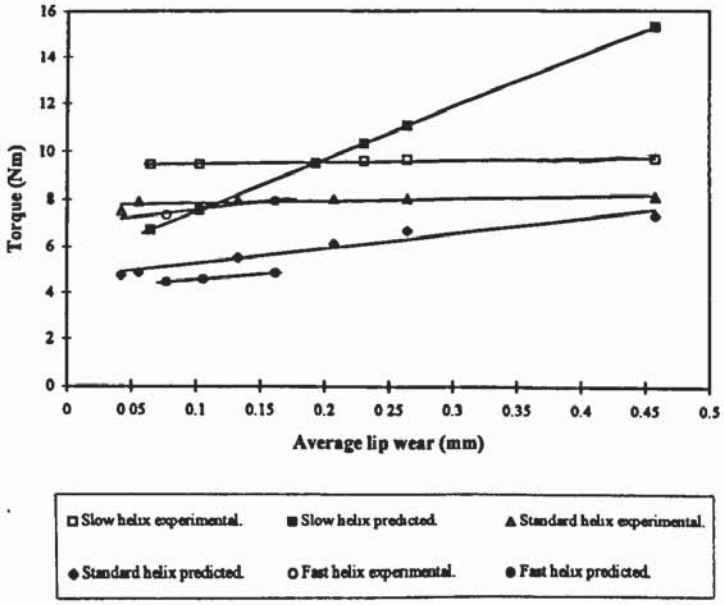

Figure 10.10 Torque *vs*. lip wear for 13 mm diameter M2 HSS, at speed 244 rpm, feed rate 78 mm/min., 2 mm cut each lip, dry cut.

In these figures it is shown that for both the experimental and predicted results that as the average lip wear increases the torque increases, but the between the experimental and predicted results no similarity is shown.

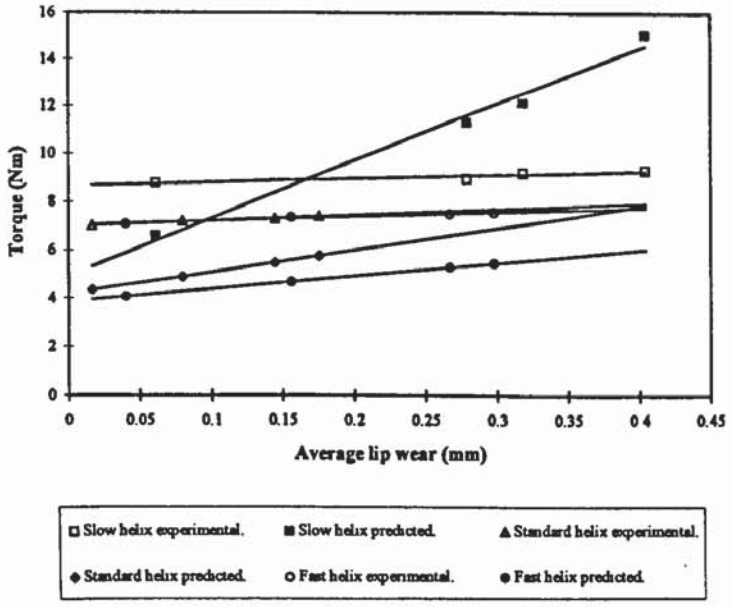

Figure 10.11 Torque *vs*. lip wear for 13 mm diameter M2 HSS, at speed 490 rpm, feed rate 156 mm/min., 2 mm cut each lip, dry cut.

From the graph it is seen that the predicted results are higher than the experimental ones but also the experimental and predicted results do not show similarity between them.

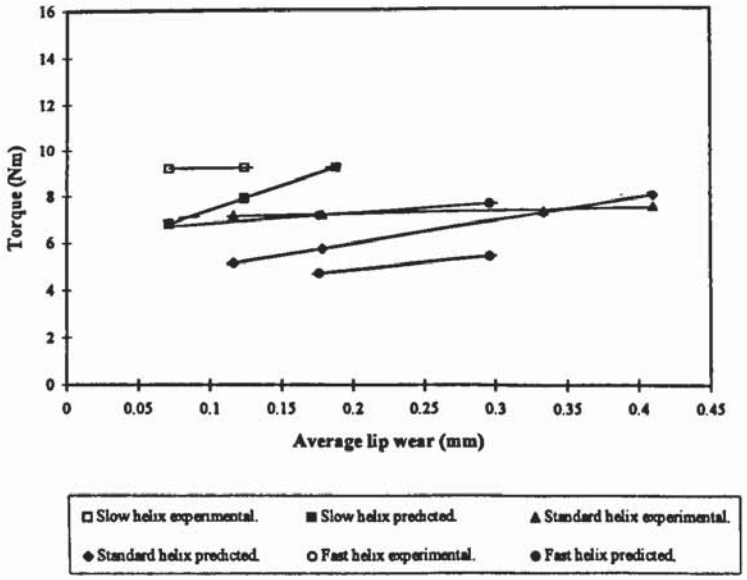

Figure 10.12 Torque *vs* . lip wear for 13 mm diameter M2 HSS, at speed 735 rpm, feed rate 234 mm/min., 2 mm cut each lip, dry cut.

As can be seen from these figures, the torque values increase with the increase in average lip wear.

In all the graphs it is shown how the results of both the thrust and torque differ for the experimental and predicted values. This is the case for all the three cutting speeds used. It can be seen that the results for the thrust and torque do not fit when lip wear exists. As in the previous chapter, the role the wear mechanisms play is important. As discussed in chapter 8, when the speed is increased so is the temperature and in turn the wear. Also as in turning, different wear mechanisms act in different conditions and hence the change in circumstances.

Figure 10.13 is used here as an example to show the effect of cutting speed on wear rate. The graph shows average lip wear vs. number of holes for 13 mm diameter M2 HSS slow helix angle drill. Three different cutting speeds were used 244, 490 and 735 rpm with the feed rates of 75, 156, and 235 mm/min respectively.

It is seen in the graph that at the lower cutting speed of 244 rpm, the steady state region is longer than at the other two cutting speeds of 490 and 735 rpm. It is also seen that by increasing the cutting speed the tool life is shortened, and this is caused by the wear rate increasing and different wear mechanisms acting. The tool life can be seen being the longest at the lowest cutting speed of 244 rpm, then at the cutting speed of 490 and the shortest tool life is at the highest cutting speed of 735 rpm. This is caused by the high cutting speed which in turn causes the temperature to rise and therefore different wear mechanisms to act. The different wear mechanisms can be seen in the SEM photographs in chapter 7. Figure 7.20 at cutting speed 244 rpm shows adhesion wear, figure 7.23 at cutting speed of 490 rpm shows abrasion wear, while in figure 7.24, diffusion wear is seen at cutting speed 735 rpm.

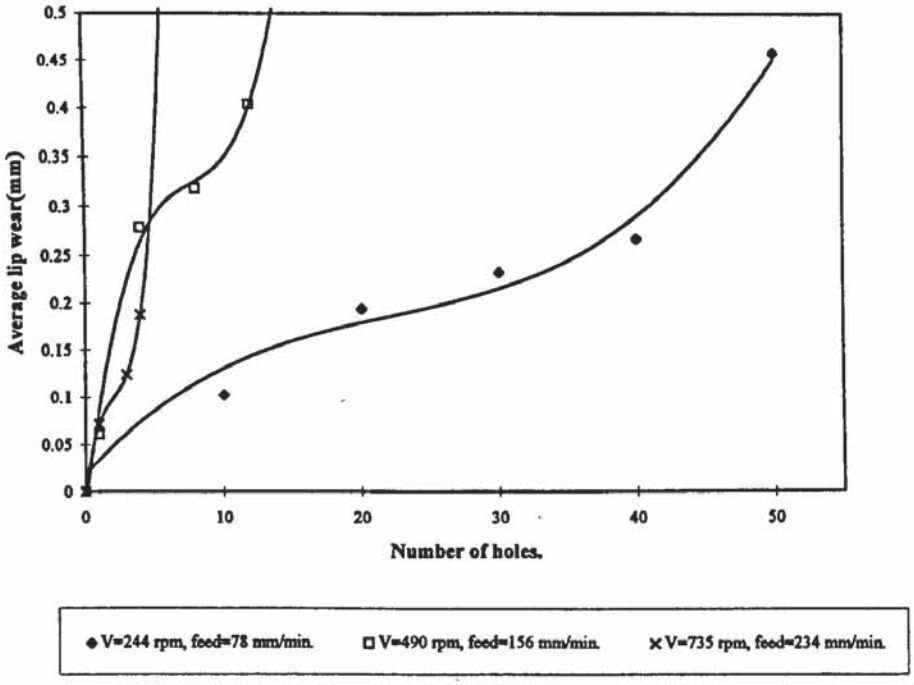

Figure 10.13 Average lip wear *vs*. Number of holes for 13 mm diameter M2 HSS, slow helix angle, 2 mm cut each lip, dry cut.

The result that is seen in figure 10.13 is similar when compared to the results of figures 9.17 and 9.18 in turning, where as explained different wear mechanisms act at different stages of the tool life.

10.6 CONCLUSION

In the first instance it was interesting to establish the basic processes of turning and then drilling as a more complex natural progression from the former. Then it was decided which factors influenced the cutting force under ideal circumstances and thereafter consider influences that occur in 'real life' situations. Finally it was necessary to look at the appropriateness of extrapolating the results to drilling by examining the success/failure of these predictions.

In conclusion to both chapters 9 and 10, it is found that Taibi's equation fits quite well with the results of the tests in this work for forces in the turning and drilling operations. But when wear was added the agreement was not good.

This situation reflects that of Morin et al. (1995) where it was attempted to fit their results with the model of Shaw and Oxford. It was shown that there was a good fit for the predictions of drill torque and thrust forces but not for the predictions for drill torque and thrust forces with wear.

The work in this thesis took a further step by taking the Taibi turning model and extrapolating it to drilling. But as mentioned earlier it produced better fit for the drill thrust forces than the torque forces, and it did not produce a good fit for drill torque and thrust forces with wear.

Morin et al. (1995) provided no explanation for this, only that predictions for drill torque and thrust forces must be modified to account for drill wear. A suggestion in this work is the reason as to why the predictions models for forces for both turning and drilling did not work with wear is due to the influence and effects of the various wear mechanisms that are acting on the tool.

As discussed previously in chapter 8, wear mechanisms are affected by the cutting speed. The higher the cutting speed, the higher the temperature. In turn this influences the forces on the tool. Temperature also has a great influence on the wear mechanisms.

It is therefore suggested here that as mentioned earlier in chapter 9, that although Taibi attempted to produce a model which could be used over a wide range of machining conditions, his theory only took account of wear damage and made the implicit assumption that the mechanisms causing it are not important despite the fact that wear surface condition is a factor in his analysis.

But a belief in this work is that the reason why the prediction model does not work when wear is added is due to the different wear mechanisms acting on the tool. Prediction models have to take account of the wear mechanisms at play since they alter the wear rate and wear scar.

Also the proposition here is that the mechanics of the turning and drilling processes are the same and one might therefore speculate that it might be possible to extrapolate theory from one process to the other. It was shown that the results in both turning and drilling were similar. This was highlighted by the similarity in the percentage difference between experimental and predicted values in both the turning and drilling operations, as can be seen from figure 9.5 in chapter 9 and figures 10.5 and 10.6 in this chapter.

The similarity in the turning and the drilling processes was also seen when figures 9.17 and 9.18 in chapter 9 for turning and figure 10.13 in chapter 10 for drilling were compared. It shows that in both processes as the cutting speed increases so does the temperature and in turn the wear rate, as seen in chapter 8 for the temperature measurements. In both processes it is seen how different wear mechanisms act at the different stages of the tool life, and that in both the reactions are similar in that at the lower cutting speeds usually abrasion and adhesion wear mechanisms take place where the graph gives a linear fit, and at the higher cutting speed diffusion wear mechanism begins to take place where the graph fit becomes non-linear.

Whilst the mechanics might be the same, as soon as temperature becomes significant the different heat flow path efficiencies relating to geometry differences etc. will lead to

difference. Therefore 'new tool' results might be expected to be capable of calculation from the same basic theory but wear results not.

One major difference is the rate at which heat may be dissipated through the tool. In turning the heat only has one way to go and that is through the tool, but in drilling a large part of the heat may be transferred through the job. This may lead to less heat build-up through the drill, however, there will be far greater temperatures at the extruding interface of the drill, as was discussed in more detail in chapter 8. This will be further discussed in the next chapter of the discussion. Therefore, although all the factors affecting wear are the same their contribution to the efficiency of the individual heat flow path is the critical factor.

Therefore, as it was shown in this chapter, that by substituting results from one research to another it is possible to get good fits but of course one must take into account that in both researches the same equipment and material were used, it therefore facilitates this process. When adding, for example, wear to the equation the fit was not good for both the process that the model was originally developed for and for drilling.

As for extrapolating information from one process to another, it was shown that for the force results with the new drill the fit was not bad but with the force results of the worn tool there was no fit. This demonstrates that the mechanics of the process is the same, the difference is that when the process is entering a situation where wear is a factor, then temperature becomes important, and temperature is dependent entirely on how much energy is getting in, and how efficiently it is being removed, and the influence of geometry and the kinematics of the system. All of these influence the heat flow path so that if one is to predict anything in drilling from turning, one expects it to be something in the new tool before one obtains efficient objectives.

It is therefore clear that this area needs further work and in more details in order to be able to use equations for all actions in a process, and for different processes.

Chapter 11

DISCUSSION

11.1 INTRODUCTION

At the beginning of this study a number of objectives were set out and throughout the work these objectives were put to the test. In this chapter the discussion is grouped under headings on the original objectives that were set to discuss how the work set out to achieve these objectives.

The broad purpose of this research was to look at wear and wear mechanisms, over a range of cutting conditions, for example, cutting temperatures, forces, cutting speeds, tool geometry, tool wear etc., in the cutting operations of single point turning and drilling. By understanding these, one is able to compare the similarities and differences of these two operations and therefore investigate this comparability with the existing theories. The tool material used for the tests in both the turning and drilling operations was HSS and similar work materials were used in order to eliminate differences due to the materials used.

It was also the intention of this work to look at and examine prediction models, their limitations and the difficulties in their replication.

11.2 LITERATURE SURVEY

An explicit literature survey was undertaken from 1907 (the Taylor tool life equation) to the present in order to obtain a clear and fundamental understanding of wear, wear in cutting and the cutting processes where wear has been and is being studied. This was intended give a better understanding of the extrapolation of information, theories, and models from one machining operation to another.

The survey covered literature on tool geometry, wear sites, wear mechanisms and tool life criterias for both single point turning and drilling. It also covered literature which examined the relationship between temperature and wear, and the interaction between tool geometry, tool and workpiece materials and cutting conditions in the context of that relationship. Literature on the influencing factors on physical conditions, such as build-up edge, surface roughness, chip formation and lubrication, at the contact interfaces of tool and workpiece were also examined.

The survey was conclusive and it was found that research in wear has been the subject of investigation for a very long time, and although there have been many theories put forward by different researchers, there seems to be a general agreement on the basics of most theories on what influences wear and wear mechanisms. However, agreement has not been reached on theories in terms of tool life equations of modelling in general.

11.3 TOOL LIFE EQUATIONS

The development of quantitative methods for predicting tool life has long been a goal of metal cutting research since tool life has a strong economic impact in production operations.

It is the intention of this work to present a critique of researchers in wear prediction that their predictions are limited because they generally fail to properly identify the nature of wear mechanisms operative in the range of their study. Also they fail to identify, or they lump together, factors having a significant influence on wear.

In order to achieve this an examination of tool life equations and wear, that relate to different conditions, in single point turning and drilling was undertaken in chapter 3. It was found that, like in many areas of this research where drilling is concerned, that there has not been much investigation by researchers and therefore there were not many or even sufficient tool life equations in that area. One can see from the proportion of the two sections in the chapter, that drilling has not been researched like single point turning in terms of tool life equations in relation to tool wear. As mentioned earlier one reason

for this could be due to the complexity of the drill geometry across the lip, effect of temperature variation through the lip, variation in angles and cutting speed etc. But also what has been researched, is very simple when compared with the single point turning.

Apart from the complexity of the tool geometry in drilling, and as mentioned before, the lack of standards in the drilling operation detracts researchers from attempting to undertake investigations in drilling. Lack of standards, as pointed out by Singpurwalla et al. (1966) can cause problems in that drill life can mean different things to different researchers. There are no standards so it is the case where every researcher set out their own criterias in a manner they see fit.

Some of the papers in chapter 3 included Jalili et al. (1991) who examined four variables: speed, feed, drill diameter and work material hardness and encountered difficulties in attempting to develop a statistical model to predict tool life, due to the large number of variables involved. They conclude that in terms of tool management, their tool life equations provides the basis for a simple cutting time tool management system, and that through the use of a real-time torque/thrust monitoring system, one may use the torque/thrust models as tool management guides for either wear or tool breakage. However, Subramanian et al. (1977) argue that tool life and tool wear are closely related, and it is the extent of wear on the tool that determines whether a tool has reached the limit of its economical life or not. Drill life varies greatly but there has been very limited testing under 'industrial' conditions.

Many equations similar to those discussed in this section have been proposed by researchers. Simple tool life equations are useful mainly for comparative purposes, for example, for ranking the general machining performance of insert grades. Taylor (1907) tool life tests performed according to defined standards are also useful in ensuring results from different sources are consistent. Tool life predictions based on these relations, as Stephenson et al. (1997) point out are generally not quantitatively reliable as the empirical constants are estimated from tool life tests in which tool life is assumed to have ended when a specified level of flank wear is reached. In practice, tools are not

used when the part's dimension, form accuracy, or surface finish is out of tolerance. A variety of mechanisms other than flank wear may produce such conditions.

Many researchers attempted to formulate different kinds of equations to do with a variety of conditions, but so far each equation seems to be incomplete. It is yet to be seen that an equation includes all factors that are concerned with machining.

The investigation in chapter 3 did not show that any of the tool life equations had been related to different wear mechanisms, or even geometry. Therefore, on the basis of that evidence more research must be carried out in this area in order for any reliable equations to be taken into account when considering tool life equations and tool wear.

It is the proposition to clarify how the identification of wear factors should be approached, for example,

- temperature in the cutting zone is the definitive parameter which influences wear mechanisms and rate of wear,
- temperature is determined by the imbalance between heat input and the efficiency of heat extraction by chip, tool and workpiece,
- that the parameters which influence this efficiency can be defined,
- that any theory would have to recognise these and either include them of limit itself to situations in which they were fixed,
- that this would ensure that any attempt to replicate theory is properly informed.

A range of activity which would examine this proposition, making the point by attempting the cross referencing of two processes, turning and drilling was undertaken.

11.4 TURNING AND DRILLING OPERATIONS

It was discovered throughout this thesis that most work up to date concerning cutting operations has been performed in turning, specifically in single point turning. While drilling on the other hand, has been the least investigated as Stephenson et al. (1997) pointed out, due to its extremely complex tool geometry. This was demonstrated in

chapter 3 of wear prediction models, and other prediction models, as in forces, as seen in chapters 6 and 7, and also in setting standards as shown in chapter 5.

Twist drills are unique amongst all metal cutting tools, both in their geometry and their method of operation. The most prominent feature of their geometry consists of the double helical flutes which allow the formation of the two cutting lips. The flutes are defined by their contour and the lead of the helix. The helix angle increases with radius, and its peripheral value is commonly used to specify drills.

Although an ordinary twist drill operates in essentially the same was as a simple single point tool, it is extremely complex geometrically. When only the lips of a drill are used to cut a tubular test bar the action is similar to machining with a single-point tool and therefore can be considered related to machining accomplished in planer, lathe, and many milling-machine operations.

Compared to these removal processes, drilling is manifestly more complex in that the tool geometry and the tool obliquity change along the cutting edge. The angle of inclination increases and the rake angle decreases as the lip is transversed from the margin towards the web. In the absence of such a model, there is no basis on which analytical expressions for the torque and thrust force can be derived. More details about the tool geometries can be seen in chapter 2.

At an early stage of the investigation it became apparent that standards (International and British) for tool life testing in drilling, as compared to turning, were non existent. This was also confirmed by several sources including British Standards Institution, Bert Howarth (Application and Design Engineer) of Dormer Tools Ltd., and Stephenson et al. (1997) and a possible reason for this was due to the complexity of the drilling operation. The existence of standards is extremely important and this was illustrated throughout this investigation but specifically in chapter 5.

Standards are important in that they contain recommendations which can be used by industrial researchers, as well as manufacturing and industrial units etc. These

recommendations in turn unify procedures so that reliability and comparability of theories, procedures and results are increased. The need of standards are also needed to define the sites of tool wear and its measurement, as well as procedures for measurements.

In performing the tests in this work, one of the drill wear measurements that were taken were 1 mm and 2 mm from the corner in order to determine exactly the position of the where the wear is, as well as to perceive the exact cutting conditions such as cutting speed, angles etc. and to measure the exact point every time. More details can be seen in chapter 4 concerning the experimental conditions.

The points above are important so that when a research is being carried out, by using for example, international standards, then this would eliminate matters that would effect the results of the research if standards were not used. This was illustrated in the chapters of tool wear models (chapter 3), and the predictive force models (chapters 9 and 10), where it was shown that when developing models or equations, it is important to be talking about the same thing, that is, angles, wear, sites etc. If not then that may be one reason why equations and models do not work when carried out by different researchers.

11.5 CUTTING FORCES

It was shown in chapters 6 and 7 that knowledge of the cutting forces in turning and drilling is essential in the manufacturing and design of machine tools. It is needed for various measurements including the working out of power requirements and determining tool geometries. The cutting forces vary with the tool angles, and accurate measurements of these forces would be a helpful factor in optimising tool design.

Cutting force control for drilling processes has not yet been studied as vigorously as for the turning process. In the design and application of metal-cutting tools it is useful to be able to predict the forces which act upon a tool or the power required under a given set of operating conditions. This can now be accomplished for single point cutting tools.

In single point turning, in both oblique and orthogonal cutting conditions, the cutting force generated by the bar's rotation is the largest force and it varies in magnitude depending upon whether a positively or negatively-inclined insert is used. Negatively inclined inserts, as pointed out by Smith (1991), produce strong blunt edge, and therefore produce higher forces. The feed force is determined by the feedrate, in that if it is increased then this will produce a higher feed force, but not in isolation, since it will also lead to increases in the cutting force. The radial force is usually assigned to the plan approach angle: as this increases, so will the radial force, and the nose radius of the insert will also produce a small radial force.

It was determined that at the low cutting speed a BUE adheres to the cutting edge, as can be seen in figure 6.30, and it starts to act as a cutting edge as Boothroyd et al. (1989) pointed out. As the cutting speed increases the BUE becomes weaker and begins to dismantle, as seen in figure 6.31. The fragments from the BUE then flow with the chip adhering to the chip surface as seen in figure 6.32.

It was found that the highest torque and thrust occur with the slow helix angle, and it can also be seen the fast helix angle the tool fails quicker where catastrophic failure can be seen in figure 7.25. This is caused due to the tool geometries and it can be seen that the standard helix angle is best compared to the other two and this has the lowest torque and thrust. Rubenstein (1991b) reports that an increase in helix produces an increase in the normal rake angle and this, in turn, causes the shear plane angle to increase. This results in a decrease in the torque and thrust forces at the lips, and consequently, a reduction in both the torque and the thrust force.

In the SEM figures one can see that the chip surface can also be related to the cutting speed. In figure 6.33 at the cutting speed of 10/min, it is seen that the chip surface is coarse, while in figure 6.35 at the cutting speed of 30 m/min and in figure 6.36 at the cutting speed of 40 m/min, the chip surface is seen to become smoother. The same is seen in chapter 7 for drilling, in figure 7.18 at the low cutting speed of 244 rpm the surface of the chip is seen to be coarse, then as the speed increases to 490 rpm the chip surface is seen to be smoother. Therefore the higher the temperature the smoother the

chip surface and this is due to the metal becoming softer with the higher temperature and therefore smoother.

In drilling, as in the turning, the thrust, torque and power are important machining performance characteristics which are required for improvements in machine tool and drill designs as well as selection of optimum cutting conditions. The thrust and torque analyses can be developed by considering the two distinct regions of the drill, - the lip region and the chisel edge region. The thrust force in drilling is the force that acts in the direction of the hole axis. If this force is excessive, it can cause the drill to break or bend. The thrust force depends on factors such as the strength of the workpiece material, feed, rotational speed, cutting fluids, drill diameter, and drill geometry.

It was found that both in turning and drilling the cutting speed decreases the forces. Watson (1985a,b,c,d) argued that as the rotational speed in increases both torque and thrust decrease, in a similar manner to that obtained in oblique and orthogonal machining. In chapter 7 of the drilling forces it was shown in figure 7.4 and 7.5 that the forces decrease as the cutting speed increases.

The helix angle also has an effect on the temperature, the slower the helix angle the longer it takes to get rid of the chip, and the more contact with the chip the higher the temperature and which affects the wear mechanisms and this can be seen in figures 7.20 to 7.24. of chapter 7.

As discussed throughout the thesis, the different wear mechanisms are related to the different cutting speeds. This is shown in chapter 6 where in figure 6.42 at the cutting speed of 10 m/min, both the wear mechanisms of adhesion and abrasion can be seen, and at 20 m/min the wear mechanism of abrasion can be seen in figure 6.44. Also at the cutting speed of 40 m/min, as seen in figure 6.45, the diffusion wear mechanism is seen.

In comparison to this, in chapter 7, at the low cutting speed of 244 rpm the wear mechanism of adhesion is seen to be predominant in figure 7.20, and a little of the abrasive wear is beginning to show. While at the cutting speed of 490 rpm abrasion

wear is seen in figure 7.23. In figure 7.24 at the cutting speed of 735 rpm diffusion wear can be seen.

The SEM photographs seem to show a pattern in terms of the type of wear mechanism and how they are related to cutting speed. This can also be related to the temperature which will be discussed more later in this chapter. It was already mentioned that the cutting speed decreases forces, but it also increases the temperature.

11.6 CUTTING TEMPERATURE

Cutting temperatures are of interest because they affect machining performance. Knowledge of the tool temperature can be used to better understand and control the underlying machining process. The tool temperature is one of the fundamental parameters to measure the behaviour of wearing tools. The investigation looked at the various methods used by other investigators to measure temperature: tool-work thermocouple method, metallurgical methods, radiation techniques, thermo-chemical reactions and more and as each one is discussed in more details in chapter 8.

In this study tool temperature in turning and the drilling operations has been experimentally studied using thermocouples embedded in the tools. This was chosen as it gives good results in a short interval, and because of its ease in implementation after it has been calibrated, and its low cost. In the turning operation, two thermocouples were used in different positions on the tool as can be seen in figure 8.2, as well as further illustration in figure 8.3 and 8.4 in chapter 8. In the drilling operation the position of the thermocouple can be seen in figure 8.5, and further illustration can also be seen in figure 8.6.

The temperature changes rapidly with time and this has been taken into account in chapter 8 that the measurements for temperature is taken every 0.1 of a second for turning and 0.25 for drilling, therefore giving an accurate and instantaneous recordings which are needed in order to determine the state the tool is undergoing.

The cutting temperature readily reacts to instantaneous changes in the cutting conditions. And as has been demonstrated in the above tests, cutting speed has the largest influence on the temperature, in that as the cutting speed increases so does the temperature. This is shown in figure 8.12 for turning and figure 8.21 for drilling. It is also seen that as the temperature increases the tool wear increases, this can also be seen in the same figures above where it is seen that the temperature with the worn tools is higher.

The fact that the machining temperature has a critical influence on tool wear and tool life has been well recognised since the work of Taylor. Trigger and Chao found that the growth of crater wear at the tool-chip interface was directly governed by the temperature distribution along the interface. Furthermore, Sata showed, experimentally, a close correspondence between crater wear and the cutting temperature. Young (1996) argues that in practice, the amount of flank wear is used more often in determining the tool life and his experiment results show a steady increase in the cutting temperature as the flank wear progresses.

The tool temperature is also seen to increase rapidly, which is due to corresponding to a sudden breakdown of the sharp cutting edge; this is followed by a slight increase in the temperature with increasing uniform wear, and then by acceleration after a critical wear value has been reached. The temperature is seen to reach steady state between 2-5 seconds. This seems an average time to reach steady state in comparison to other studies where it took Levy et al. (1976) 1.5 - 2 minutes and Leshock et al. (1997) 0.33 second to reach steady state as can be seen and was further discussed in chapter 8.

The temperature, as mentioned above, is related to the type of wear mechanism, in that as the cutting speed increases so does the temperature. Therefore the temperature influences the type of wear mechanism that occurs at different stages of the tool's life. This can be seen in the SEM photographs as mentioned above in chapters 6 and 7.

It was shown that for both the turning and the drilling operations, at the low cutting speeds (10 and 20 m/min in turning and 244 rpm in drilling), the adhesion wear

mechanism is dominant as seen in figure 6.42 in chapter 6 and figure 7.20 in chapter 7. The adhesion wear mechanisms is also seen at the cutting speed of 20 m/min in turning, but abrasion wear mechanism seems to be the dominant wear mechanism there, as it is in the cutting speed of 490 rpm in drilling, as seen in figure 6.44 in chapter 6 and figure 7.23 in chapter 7.

At the higher cutting speeds of 40 m/min in turning in figure 6.45 and 735 rpm in drilling in figure 7.24, the dominant wear mechanism is diffusion wear. This can be seen to relate to the figures in chapter 2 of 2.16 and 2.17 where Barth and Hastings respectively show the different stages that the wear mechanisms seen to occur in relation to the cutting speeds and temperature.

In turning, bar diameter was used as a parameter and demonstrated to have an effect on the temperature, this was proven to be the case as can be seen in chapter 8. Using bar diameters, for differentiating temperature, have not been used before as known. It is shown and proven that the smaller the bar diameter then the higher the temperature. This is due to the temperature distribution in the bar diameter. Therefore, if when attempting to develop a tool wear model the effect of the variation of the bar diameter was not taken into account, then a replication of the model with a different bar diameter will not produce a fit.

The chip colour changes according to the temperature was shown in chapter 8 and in figure 8.16 it is shown that the chip colour changes with the bar diameter and therefore reflecting the temperature.

The tests for the 13 mm helix angles that were carried out in drilling were where the cut was 2 mm only and a full cut. Figures 8.20 and 8.21 show the results obtained from testing a new drill, a drill with wear and a drill with 2 mm cut only. The worn drill produced the higher temperatures, then the new drill and the lowest temperature is shown for the drill with the 2 mm cut only. This is due to the area of plastic deformation is much smaller than that of the full cut, therefore less energy converted to heat, and so there is less friction area between the tool and the chip, and the tool and the workpiece.

In chapter 8 a technique that was used in this work is by analysing the oxide in the chip surface was shown. By analysing the amount of oxide iron in the chip surface, therefore, one can work out the temperature of the chip, and the higher the oxide level then the higher the temperature. The process of calculation and more details of the technique is shown in chapter 8 section 8.4.2. It is shown from figure 8.22 that the ratio between oxide iron and free iron increases as the speed increases.

It was concluded that the temperature in the drilling operation is higher than that in the turning operation when similar conditions were used. This was due to the difference in the way the cutting was carried out as well as how the chip had an effect on transmitting some heat while leaving the tool. Thermal conditions in drilling differ significantly from those of turning. The chip is formed at the bottom of the hole and remains in contact with the drill over a comparatively long distance, which increases by the fact that the drill point moves slowly into the portion of the work material being heated by chip formation; in turning, the work material approaching the cutting edge is generally cooler, and the chip is contact with the tool for a shorter time than in drilling. The cutting speed varies across the lip of the drill, so that temperatures are highest near the outer corner or margin of the drill, and temperature-activated margin wear often limits maximum spindle speeds.

It is evident from the above that a knowledge of cutting temperature is essential when studying most metal cutting problems and it is not surprising, therefore, that considerable efforts have been made to assess cutting temperatures by both experimental and theoretical means.

11.7 MODELLING OF PREDICTION APPROACH

The complexity of tool wear was again highlighted in chapters 9 and 10 when examining predictive approaches by using forces. The idea was to take an already existing predictive model in forces and apply the results obtained in this research to it. The chapters showed previous researchers' attempts to develop models, and as

explained in the two chapters the model chosen was that of Taibi, partly because it used a wider range of machining conditions than had previously been attempted and partly because the work had been undertaken by a previous research student at Aston University, so this would be a natural progression for the research to head. Also a third factor was that by using the same equipment, material and laboratory conditions then one can eliminate the difference of all these factors when there is a discretion between the results.

Taibi's model was a predictive model for forces in turning. Taibi also produced an equation where he added wear to the model, this was also used in this work. It was found that when the model was applied to the force results in the turning operation it showed a good fit. Both the experimental and predicted results were close for both the cutting and feed forces. The increase between the gap of the experimental and predicted forces occurred during the higher cutting speeds. This reinforces the point made earlier that the higher the cutting speeds the higher the temperatures. This was discussed in chapter 8 and where it was shown that for example figures 8.7 and 8.8 show the higher the cutting speed then the higher the temperature.

The effect of angles was shown in figures 9.5, 9.6 and 9.7 in chapter 9 for turning. It was seen that angles (rake and flank) effect the forces. A negative angle increases the forces as seen in figure 9.7, this was also discussed earlier where Smith (1989) pointed this out.

When attempting to fit Taibi's model with wear added then the results did not fit. It was shown in figures 9.8 to 9.13 that the experimental and predicted results were not similar. More will be discussed on this with the results of the drilling below.

An attempt was then made to extrapolate this model to the drilling process to see whether it would be possible to use the same model. This extrapolation was made possible due to the work of Webb, a previous research student at Aston University who developed a geometric model to work out the speed and angle values at any point in the drill lip. As can be seen from the results in chapter 10, when the model was developed

for the forces in drilling then it produced a good fit. Figures 10.5 and 10.6 show that the experimental and predicted results were very similar.

Again it was then attempted to use the model that was used for the forces in the drill with the addition of wear. It is again shown that the results do not fit the model. The experimental and predicted results are far apart, as shown in figures 10.7, 10.8 and 10.9 for the thrust and 10.10, 10.11 and 10.12 for the torque for all the three cutting speeds used. As in the turning it was found that the higher the cutting speeds the higher the wear rate.

Therefore for both turning and drilling it was shown that the model gave a good fit when used for predicting the forces in the tool. But when wear was added to the model, it did not fit. This, as suggested in chapters 9 and 10, was due the different wear mechanisms acting at the different stages of the tool life. It was shown in figures 9.14 and 9.15 in chapter 9 and figure 10.10 in chapter 10 that different wear mechanisms are acting in different stages of the tool life. This was explained earlier and shown with the SEM photographs, and the graphs of the forces in chapter 6 and 7, as well as the graphs in chapter 8 of the temperatures, that as the cutting speed increases the temperature increases. This in turn effects the wear mechanisms acting at the different stages in the tool life. It was shown, as discussed earlier, by Barth (1985) and Hastings (1976) in chapter 2 in figures 2.16 and 2.17 respectively how different wear mechanisms act as the temperature increases, that is, due to the temperature, different effects start to take place in the tool.

The reason that the model did not fit when wear was added to it in both turning and drilling was stated in chapters 9 and 10 and that it was due to the fact that Taibi did not think the wear mechanisms would influence his equation only the wear scar, and therefore did not take account of the wear mechanisms in his model.

The two chapters of 9 and 10 highlighted the whole theory and idea of using someone else's model for one's results, as well as the additions to a model and the extrapolation from one operation to another. As it was stated in the beginning of the discussion if it is

shown that an extrapolation process was shown to be successful between two machining operations as it was shown here, especially between single point turning and drilling for reasons explained above, then this is could be the start of a whole new area of research.

11.8 FINAL COMMENTS

From the above, it is seen that it is not always possible to replicate other researchers' work, not because they did not perform what they had claimed they did, but because of the matters that they have not considered, or because they had overlooked some points. These are the factors which can not be replicated.

If one looks at the factors which influence the way heat gets out of the chip, the workpiece and the tool, then ideally one could account for all the factors that one said they have in the way a prediction theory does. Another words, one has to account for every factor which directly and indirectly influences temperature. Temperature is the key to all the parameters which was demonstrated in the above work.

The bar diameter is an excellent example which supports this argument. The bar diameter is a factor which researchers had never taken into account as far as this research found. It was demonstrated in this work that it has an influence on the temperature, and therefore without question influences wear. Therefore, as an example, if one has taken any researcher's work and replicated all the factors but used a different size bar, then one would have obtained a different result which the reason as to why would not have been known, unless the researchers had specifically stated the bar size used and that the same size must be used if the tests were to be replicated to obtain the exact same results.

Looking at the implication of this, it means also that anything which influences the tool or the chip, and that any change that is made or any difference that exists between a set up of two researchers then completely throw out a wear prediction. This difference could be due to the tool holder or the age of the machine tool which could well have a significant influence.

This in the opinion of the author opens up a whole new realm, the results of this work state that anything which influences heat flow is important. Therefore everything which influences heat flow efficiency is important, and any attempts to predict wear really has to in some way or other account for these, and if any attempt will be made to replicate the work to obtain the same results then one has to specify much more tightly the circumstances of the work that was taken. Also the approaches that researchers make between their approaches to wear prediction and the wear mechanisms that actually take place are very unbound. It is clearly that this is important because these mechanisms influence the kind of variations that one is going to obtain, and that if one would like to extrapolate, then the process is an influencing factor too.

Chapter 12

CONCLUSION AND FURTHER WORK

12.1 CONCLUSIONS

The main outcomes of this work are:

- An important finding of this work was indeed that bar diameter does have an influence on the temperature as shown, by the readings taken from the thermocouples in the tool and by the change in the chip colour, in chapter 8. This therefore demonstrates that factors which influence the heat flow efficiency in any of the three sectors; the tool, the workpiece, the chip, have to be taken into account. These factors include dimensions of the three sectors, the materials, the shape of the tool, the way the tool is attached to the machine and so on.

Also related to this is that when wear mechanisms are to be considered in research and predictive equations and models, then accounts must be taken of the machine tool, its age, wear measurement accuracy, and all must be related in the research.

One of the issues in this work was to study what in fact influences wear mechanisms and how. The two major influential areas on the tool that were looked at in details were cutting forces and temperature.

- A number of points which emerged simply confirmed what researchers' expectations would be. The higher the cutting speed the higher the temperature. The temperature influences the wear mechanisms acting on the different stages of the tool's life. Usually at the lower cutting speed, the dominant wear mechanism tended to be adhesion. As the cutting speed increases the abrasion wear mechanism tends to be the dominant wear mechanism. And the dominant wear mechanism as the cutting speed increases then becomes diffusion.

- When plotted on the graph a linear line usually can be related to the abrasion wear mechanism, while a non-linear line tends to be associated with the diffusion wear mechanism, where the temperature is usually higher than the former graph.

- As the cutting speed increases the temperatures increase and therefore the forces tend to decrease. This is due to the metal softening.

- As the cutting speed increases the tool wear increases. Again this is due to the increase in temperature.

Throughout this work it was found that there was a paucity in the literature and research in the drilling operation as compared to the single point turning. The main reason for this was due to the complex geometry of the drill. This was particularly the case when prediction models were involved. This scarcity in the information on drilling was extended to the lack in the existence of standards, which due to this the author developed standards for wear measurements in drilling to be used in this work and which could be used by other researchers in their work.

The two machining operations of single point turning and drilling were investigated over a range of cutting conditions in order to understand the various similarities and differences that exist between them. The predominant aim of this research was to look into the above goal in order to formulate ideas about the prediction models and their extrapolation from one operation to the other as well as additions of extra factors.

In this work, a prediction model which was developed for the forces in turning (by Taibi), was used so that it could be replicated to be compared with the results of the experimental tests in this work. The model was to be extrapolated to the drilling operation, and therefore compared with the results obtained in the tests of this work in drilling. Then the model with wear added to it was to be used also to be compared with results of the tests of this work in both the turning and drilling operation.

The above situation produced four results:

- When the model was used for the prediction of forces in the sharp tool in the turning operation and compared to the test results obtained in this work, then it was found that a good agreement between predictions and experiments were achieved over a wide range of cutting conditions.

- When the model was used for the prediction of forces in the worn tool the turning operation with wear added to it, and compared to the test results obtained in this work, then it was found that results did not give a good fit.

- When the model was used for the prediction of forces in the sharp drill in the drilling operation and compared to the test results obtained in this work, then it was found that a good agreement between predictions and experiments were achieved over a wide range of cutting conditions.

- When the model was used for the prediction of forces in the worn drill in the drilling operation with wear added to it and compared to the test results obtained in this work, then it was found that results did not give a good fit.

It was therefore concluded that the Taibi predictive model for the forces in turning gave a good result over the ranges of tests employed for a sharp tool in the turning operation and the drilling operation despite the complexity of the drill, but not for a worn tool in both operations.

One of the reasons for this is could be that when Taibi developed his model he did not take account of the wear mechanisms acting on the different stages of the tool's life, he only accounted for the wear scar. This accounts for why the model did not give a good fit when wear was added to the model.

The above situations highlights the issue of replication of a model from one research to another. It demonstrates that many issues have to be taken into account when

considering this. Not only issues of the same materials and conditions, but also same machine tool etc. As it was discussed in the thesis that even the age of a machine can alter the results of the tests.

Another issue that was highlighted is about the extrapolation of information and specifically predictive models from one operation to another. Throughout the thesis, it was mentioned that there was paucity in the literature as far as drilling was concerned, but this scarcity of literature is further extended to the subject of extrapolation from one machining process to another.

Problems in extrapolation relate to all those factors which influence temperature, for example, tool geometry, drill shape etc., problems arise in extrapolation due to the differences of the two operations, in this case, the heat in the drilling is much more rapid than in turning, and the tool temperature is considerably higher than for turning. But despite these, the research shows that it is possible to extrapolate information and even predictive models from one operation to another as it was proven possible in this research.

In conclusion, factors such as geometry, cutting speed, angles etc. all effect wear because they are all influenced by the temperature. Therefore the temperature influences the forces, tool wear, wear mechanisms and so on. Extrapolation of predictive models is possible but any prediction must take account of the wear mechanisms at play at the different stages of the tool's life otherwise the possibility of failure is very high.

12.2 RECOMMENDATIONS FOR FURTHER WORK

Recommendations for future consideration can be perhaps directed towards the following areas:

- Bar size had been shown to be a significant influencing factor. Therefore more research should be carried out with regards not just the bar size, but other factors related either to the workpiece, the tool, or the chip which could have similar effects and which have not been considered such as a comparison between a tip held in a tool holder and a solid bar. Considerations of this should be taken when formulating equations and its effect as a variable.

- In this work, the analysis and the calculation of free iron and oxide iron content on the surface of the chip to find out the temperature was used. However, this technique is only possible for steel. Therefore, with further research it may be possible to find similar techniques for other materials.

- The measurement of temperature in the drill was taken from a thermocouple in the oil hole as shown in chapters 4 and 8. It may be possible for more work to be done on the different positioning of the thermocouple in the oil hole and how much the temperature is effected and changed by this. In this work there was the opportunity to be able to work out the variation in the angles and speed across the lip of the drill due to the Webb geometric model. Therefore with further work on the above point about the different positioning of the thermocouple then it may be possible to come out with a similar model for working out the temperature variation across the lip.

It was shown in this work that the bar diameter has an influence on tool temperature and wear. Two major points that involve bar diameter that could be considered for future work are:

- There is a possibility that the angle of contact between the bar and the tool has an influence on the shear plane angle. The change in shear plane angle will cause a

change in the forces. Therefore different bar diameters and their influence can be tested by, for example, by measuring the forces for any change, or by using quick-stop tests in order to gain more information on chip formation, using different bar diameters.

- Another point for future work is to test the effect of different bar diameters by analysing the temperature in the bar. This can be achieved by for example placing a thermocouple in the bar or using infrared techniques in order to measure the temperature changes in the workpiece which might account for the amount of heat going into the bar which is influenced by convection.

- There is a need for predictive equations and models to take account of the wear mechanisms. Wear mechanisms and their consideration in predictive models should be carefully thought about, for instance between the first cut and the second cut a different wear mechanism may begin to take place or become dominant. It must also be considered that more than one wear mechanism may be at play at any one time.

- In principal the turning and the drilling operations are similar, but the drill geometry is much more complex hence the paucity of the literature and research in drilling. More research in this area, that is, drilling, would provide more knowledge on the operation, and therefore this will lead to a better understanding of the complexity of the operation. Therefore, with more research it may be found that more similarities exist between the two operations so for example, data on tool life may be compared.

One major point found in this work is that much more needs to be done on the extrapolation of information, equations and models from the turning operation to the drilling operation. Furthermore, much more work needs to be carried out for the extrapolation from one cutting operation to another no matter what the operations are.

REFERENCES

- AGAPIOU, J.S., and DEVRIES, M.F., (1990a) On the determination of thermal phenomena during drilling - Part 1: Analytical models of twist drill temperature distributions, *International Journal of Machining Tools Manufacture*, V.30, N.2, pp 203-215.

- AGAPIOU, J.S., and DEVRIES, M.F., (1990b) On the determination of thermal phenomena during drilling, Part 2: Comparison of experimental and analytical twist drill temperature distributions, *International Journal of Machining Tools Manufacture*, V.30, N.2, pp 217-226.

- AGAPIOU, J.S., and STEPHENSON, D.A., (1994) Analytical and experimental studies of drill temperatures, *ASME Transactions - Journal of Engineering for Industry*, V.116, Feb, pp 54-60.

- AHMAD, M.M., DERRICOTT, R.T., & DRAPER, W.A., (1989) A photoelastic analysis of the stresses in double rake cutting tools, *International Journal of Machine Tools Manufacture*, V.29, N.2, pp 185-195.

- ALDEN KENDALL, L., (1989) Tool wear and tool life, in *Metals Handbook, V.16: Machining*, 9th ed., Ohio: ASM International, pp 37-48.

ARMAREGO, E.J.A., and BROWN, R.H., (1969) *The Machining of Metals*, New Jersey: Prentice Hall.

- BAHADUR, S., (1978) Wear research and development, *ASME Transactions - Journal of Lubrication Technology*, V.100, pp 449-454.

- BAILEY, J.A., (1975) Friction in metal machining-mechanical aspects, *Wear*, V.31, pp 245-276.

- BANDYOPADHYAY, B.P., (1984) A nonlinear analysis of metal cutting in the built-up edge region, *West Indian Journal of Engineering*, V.9, N.1, pp 45-52.

- BARNES, S., PASHBY, I.R., and MOK, D. K., (1995) The effect of workpiece temperature on the machinability of an aluminium/SiC MMC, *Manufacturing Science and Engineering*, MED-Vol. 2-1/MH-Vol. 3-1, ASME, pp 219-228.

- BARROW, G., (1973) A review of experimental and theoretical techniques for assessing cutting temperatures, *CIRP* V.22, N.2, pp 203-211.

- BARROW, G., (1972) Tool-life equations and machining economics, *Proceedings of the 12th International Machine Tool Design and Research Conference*, 15-17/9/1971, Manchester, in Koenigsberger, F. and Tobias, S.A. (eds), Macmillan, pp 481-493.

- BARTH, C.F., (1985) ,Turning, in King, R.I., *Handbook of High Speed Machining Technology*, Chapman & Hall, pp 173-193.

- BAYER, A.M., & BECHERER, B.A., (1989) High speed tool steels, in *Metals Handbook, V.16: Machining*, 9th ed., Ohio: ASM International, pp 51-59.

- BER, A., (1972) Relationship between thermal properties and flank wear of cemented carbide tools, *CIRP*, V.21, N.1, pp 21-22.

- BHATTACHARYYA, A., & HAM, I., (1969) Analysis of tool wear, Part 1: Theoretical models of flank wear, *ASME Transactions - Journal of Engineering for Industry*, pp 790-798.

- BHATTACHARYYA, A.A., GHOSH, A., & HAM, I., (1970) Analysis of tool wear - Part 2: Applications of flank wear models, *ASME Transactions - Journal of Engineering for Industry*, pp 109-114.

- BILLMAN, E.R., MEHROTRA, P.K., SHUSTER, A.F., & BEEGHLY, C.W., (1988) Machining with Al_2O_3-SiC-Whisker cutting tools, *Ceramic Bulletin*, V.67, N.6, pp 1016-1019.

- BOOTHROYD, G., & KNIGHT, W.A., (1989) *Fundamentals of Machining and Machine Tools*, 2nd ed., New York: Marcel Dekker.

- BOULGER, F.W., (1978) Machining Characteristics of Steels, In *Metals Handbook, V.1*, 9th ed., Ohio: ASM International, pp 565-585.

- British Standards Institution. (1998) Correspondence.

- BRANDT, G., (1986) Flank and crater wear mechanisms of alumina-based cutting tools when machining steel, *Wear* V.112, pp 39-56.

- BRUN, M.K., LEE, M., & GORSLER, F., (1985) Wear characteristics of various hard materials for machining Sic-reinforced aluminium alloy, *Wear*, V.104, pp 21-29.

- BS 1296:1972 - Specifications for Single-point cutting tools. Part 2 - Nomenclature.

- BS 328:1993 - Drills and Reamers. Part 1 - Specification for twist drills.

- BULJAN, S.T., & WAYNE, S.F., (1989) Wear and design of ceramic cutting tool materials, *Wear*, V.133, pp 309-321.

- CAMPBELL, P.Q., CELIS, J.P., ROOS, J.R., & VAN DER BIEST, O., (1994) Fretting wear of selected ceramics, *Wear*, V.174, pp 47-56.

- CARLSSON, T.E., & STRAND, F., (1992) A Statistical model for prediction of tool life as a basis for economical optimisation of the cutting process, *CIRP*, V.41, N.1, pp 79-82.

- CHANDRASHEKHAR, S., OSURI, R.H., and CHATTERJEE, S., (1990) A preliminary investigation into the prediction of drill wear using acoustic emission, in B.E. Klamecki and K.J. Weinmann (eds), *Fundamental Issues in Machining*, New York: ASME, pp 123-137.

- CHAPMAN, W.A.J., (1981) *Workshop Technology*, Part 3, 3rd ed., London: Edward Arnold.

- CHEN, S.J., HINDUJA, S., & BARROW, G., (1989) Automatic tool selection for rough turning operations, *International Journal of Machine Tools and Manufacture*, V.29, N.4, pp 535-553.

- CHERRY, J., (1961) Practical Investigation in metal cutting, *A paper presented to the Wolverhampton Section of The Institution of Production Engineers on 30th March*, pp 90-103.

- CHO, S.S., and KOMVOPOULOS, K., (1988) Cutting force variation sue to wear of multi-layer ceramic coated tools, *ASME Transactions - Journal of Tribology*, V.120, pp 75-81.

- COOK, N.H., (1973) Tool wear and tool life, *ASME Transactions - Journal for Engineering for Industry*, V.95, pp 931-938.

- DAMODARASAMY, S., & RAMAN, S., (1993) An inexpensive system for classifying tool wear states using pattern recognition, *Wear*, V.170, pp 149-160.

- DAN, M.C., & MATHEW, J., (1990) Tool wear and failure monitoring techniques for turning - A review, *International Journal of Machine Tools and Manufacture*, V.30, N.4, pp 579-598.

- DASCHENKO, A.I., and REDIN, V.N., (1988) Control of cutting tool replacement by durability distributions, *International Journal of Advanced Manufacturing Technology*, 3 (5), 39-60.

- DEARNLEY, P.A., (1985) A metallurgical evaluation of tool wear and chip formation when machining pearlitic grey cast irons with dissimilar graphite morphologies, *Wear*, V.101, pp 33-68.

- DEVRIES, M.F., SAXENA, U.K., and WU, S.M., (1968) Temperature distributions in drilling, *ASME Transactions - Journal of Engineering for Industry*, May, pp 231-238.

- DEVRIES, W.R., & MURRAY, S.F., (1994) Tribology at the cutting edge: cutting and grinding fluids, *Tribology Symposium*, Louisiana, USA, 23-26 Jan., pp 23-33.

- EDWARDS, L., & ENDEAN, M., (1990) *Manufacturing with Materials*, The Open University.

- EHRENREICH, E., and LENZ, (1971) Dynamometer for drilling force measurement, *ASME Paper 71-PROD-7*, pp 1-8.

- EL WARDANY, T.I. and ELBESTAWI, M.A., (1997) Prediction of tool failure rate in turning hardened steels, *International Journal of Advanced Technology*, V.3, pp 1-16.

- ELANAYAR, S., and SHIN, Y.C., (1996) Modelling of tool forces for worn tools: flank wear effects, *ASME Transactions - Journal of Manufacturing Science and Engineering*, V.118, Aug, pp 359-366.

- ELBESTAWI, M.A., SRIVASTAVA, A.K., & EL-WARDANY, T.I., (1996) A model for chip formation during machining of hardened steel, *CIRP*, V.45, N.1, pp 71-76.

- EMA, S., FUJII, H., and MARUI, E., (1991) Cutting performance of drills with three cutting edges (effects of chisel edge shapes on the cutting performance), *International Journal of Machine Tools and Manufacture Design, Research and Application*, V.31, N.3, pp 361-369.

- FANG, X.D., (1994) Experimental investigation of overall machining performance with progressive tool wear at different tool faces, *Wear*, V.173, pp 171-178.

- FIELD, M., KAHLES, J.F., & KOSTER, W. P., (1989) Surface finish and surface integrity, in *Metals Handbook, V.16: Machining*, 9th ed., Ohio: ASM International, pp 19-36.

- FISCHER, A., (1996) Well-founded selection of materials for improved wear resistance, *Wear*, V.194, pp 238-245.

- FORTIN, C., BALAZINSKI, K., MONDALSKI, K., SLOMSKI, J., (1990) Study of the influence of feed variation on tool wear, *American Society of Mechanical Engineers, Production Engineering Division, PED, Vol. 43, Winter Annual Meeting of the American Society of Mechanical Engineers*, Dallas, Texas, USA, 25-30 Nov., pp 115-122.

- GARBAR, I.I., (1995) Structure-based selection of wear-resistant materials, *Wear*, 181-183, pp 50-55.

- GOLLER, J.A., & BARROW, G., (1995) The prediction of surface finish in turning operations, *Matador Conference*, Manchester 20-21, April, pp 229-237.

- GORCZYCA, F.E., (1987) *Application of metal cutting theory*, New York: Industrial Press.

- GROOVER, M.P., (1996) *Fundamentals of Modern Manufacturing*, New Jersey: Prentice Hall.

- GRUSS, W.W., (1988) Ceramic tools improve cutting performance, *Ceramic Bulletin*, V.67, N.6, pp 993-996.

- GRUSS, W.W., (1989) Cermets, in *Metals Handbook, V.16: Machining*, 9th ed., Ohio: ASM International, pp 90-97.

- HAM, I., (1968) Fundamentals of tool wear, *Technical paper MR68-617*, ASTM, Michigan, USA.

- HASTINGS, W.F., & OXLEY, P.L.B., (1976) Predicting tool life from fundamental work material properties and cutting conditions, *CIRP*, V.25, N.1, pp 33-38.

- HEATH, D.J., (1989) Ultrahard tool materials, in *Metals Handbook, V.16: Machining*, 9th ed., Ohio: ASM International, pp 105-117.

- HOGLUND, U., (1976) Cutting edge wear in microscale physical conditions - wear processes, *CIRP*, V.25, N.1, pp 99-103.

- HONG, H.A.T., RIGA, A.T., CAHOON, J.M., & SCOTT, C.G., (1993) Machinability of steels and titanium alloys under lubrication, *Wear*, V.162-164, pp 34-39.

- HOWARTH, B., (1998) Application and Design Engineer, Dormer Tools Ltd., Private Communication.

- ISO 3685:1993 - Tool-life testing with single-point turning tools.

- ISO 5419:1982 - Twist drills - Terms, definitions and types.

- JALILII, S.A., and KOLARIK, W.J., (1991) Tool life and machinability models for drilling steels, *International Journal Machine Tools Manufacturing*, V.31, N.3, pp 273-282.

- JAWAHIR, I.S., & FANG, X.D., (1995) A knowledge-based approach for designing effective grooved chip breakers - 2D and 3D chip flow, chip curl and chip breakability, *International Journal of Advanced Manufacturing Technology*, V.10, pp 225-239.

- JUNEJA, B.L., (1987) *Fundamentals of Metal Cutting and Machine Tools*, USA: Halstead Press.

- KALDOR, S., and LENZ, E., (1980) Investigation in tool life of twist drills, *CIRP*, V.29, N.1, pp 23-27.

- KANNATEY-ASIBU, E., (1985) A transport-diffusion equation in metal cutting and its application to analysis of the rate of flank wear, *ASME Transactions - Journal of Engineering for Industry*, V.107, February, pp 81-89.

- KATO, T., and FUJII, H., (1996) PVD Film method for measuring the temperature distribution in cutting tools, *ASME Transactions - Journal of Engineering for Industry*, V.118, Feb, pp 117-122.

- KEMPSTER, M.H., (1984) *Materials for Engineers*, London: Hodder & Stoughton.

- KIBBE, R.R., NEELY, J.E., MEYER, R.O., & WHITE, W.T., (1995) *Machine Tool Practices*, 5th ed., New Jersey: Prentice Hall.

- KING, R.I., (ed), (1985) *Handbook of High-Speed Machining Technology,* New York: Chapman Hall.

- KOBAYASHI, S., and THOMSEN, E.G., (1960) The role of friction in metal cutting, *ASME Transactions - Journal of Engineering for Industry*, V.82, pp 324-332.

- KOELSCH, J.R., (1993) Stop problem chips, *Manufacturing Engineering*, Aug, pp 65-68.

- KOMANDURI, R., & SAMANTA, S.K., (1989) Ceramics, in *Metals Handbook, V.16: Machining*, 9th ed., Ohio: ASM International, pp 98-104.

- KOMARAIAH, M., & NARASIMHA REDDY, P., (1993) Relative performance of tool materials in ultrasonic machining, *Wear*, V.161, pp 1-10.

- KOPALINSKY, E.M., & OXLEY, P.L.B., (1984) An investigation of the influence of feed and rake on the ratio of feed force to cutting force when machining with negative rake angle tools, *CIRP*, V.33, N.1, pp 43-46.

- KOREN, Y., (1978) Flank wear model of cutting tools using control theory, *ASME Transactions - Journal of Engineering for Industry,* V.100, February, pp 103-109.

- KOREN, Y., and ULSOY, A.G., (1984) State model for flank wear in metal cutting, *Manufacturing Engineering Transactions,* 12th NAMRC, North American Manufacturing Research Conference Proceedings, Houston, MI, USA, 30 May-1 June, pp 260-264.

- KOREN, Y., ULSOY, A.G., and DANAI, K., (1986) Tool wear and breakage detection using a process model, *CIRP,* V.35, N.1, pp 283-288.

- KOREN, Y., KO, T-R., ULSOY, A.G., and DANAI, K., (1991) Flank wear estimation under varying cutting conditions, *ASME Transactions - Journal of Dynamic Systems, Measurement and Control,* V.113, July, pp 300-307.

- KOZAK, J., RAJURKAR, K.P., & WANG, S.Z., (1994) Material removal in WEDM of PCD blanks, *ASME Transactions - Journal of Engineering for Industry*, V.116, pp 363-369.

- KRAMER, B.M., (1986) A comprehensive tool wear model, *CIRP*, V.35, N.1, pp 67-70.

- KRAMER, B.M., (1987) On tool material for high speed machining, *ASME Transactions - Journal of Engineering for Industry*, V.109, pp 87-91.

- KRAMER, B.M., (1993) Tribological aspects of metal cutting, *ASME Transactions - Journal of Engineering for Industry*, V.115, pp 372-376.

- KRONENBERG, M., (1970) Replacing the Taylor formula by a new tool life equation, *International Journal of Machine Tool Design Research*, V.10, pp 193-202.

- LAU, W.S., and RUBENSTEIN, C., (1978) The influence of tool geometry on the Taylor constant, *International Journal of Machine Tool Design and Research*, V.18, pp 59-66.

- LAU, W.S., and RUBENSTEIN, C., (1982) The influence of the plan approach angle in orthogonal cutting, *International Journal of Machine Tool Design and Research*, V.22, N.1, pp 65-74.

- LEE, L.C., (1986) A study of noise emission for tool failure prediction, *International Journal of Machine Tool Design and Research*, V.26, N.2, pp 205-215.

- LEE, L.C., LAM, K.Y., and LIU, X.D., (1994) Characterisation of tool wear and failure, *Journal of Materials Processing Technology*, V.40, pp 143-153.

- LEE, L.C., LEE, K.S., & GAN, C.S., (1989) On the correlation between dynamic cutting force and tool wear, *International Journal of Machine Tools and Manufacture*, V.29, N.3, pp 295-303.

- LESHOCK, C.E., & SHIN, Y.C., (1995) Investigation on tool rake face temperature in turning by a tool-work thermocouple technique, *Manufacturing Science and Engineering MED-vol.2-1/MH-vol.3-1, V.1*, ASME, pp 189-202.

- LESHOCK, C.E., and SHIN, Y.C., (1997) Investigation on cutting temperature in turning by a Tool-Work Thermocouple Technique, *Journal of Manufacturing Science and Technology,* V.119, Nov, pp 502-508.

- LEVY, B., and DEVRIES, M.F., (1976a) Use of drill forces as a measure of machinability, *SME Technical Paper MR76 - 340*, pp 1-12.

- LEVY, E.K., TSAI, C.L., and GROOVER, M.P., (1976b) Analytical Investigation of the Effect of Tool Wear on the Temperature Variations in a Metal Cutting Tool, *ASME Transactions - Journal of Engineering for Industry,* February, V.98, No. 1, pp 251-257.

- LI, X., KOPALINSKY, E.M., & OXLEY, P.L.B., (1995) A numerical method for determining temperature distribution in machining with coolant, Part 1: Modelling the process, *Journal of Engineering for Industry*, Part B, V.209, pp 33-43.

- LIM, S.C., LEE, S.H., LIU, Y.B., & SEAH, K.H.W., (1993a) Wear maps for uncoated high-speed steel cutting tools, *Wear*, V.170, pp 137-144.

- LIM, S.C., LIU, Y.B., LEE, S.H. & SEAH, K.H.W., (1993b) Mapping the wear of some cutting-tool materials, *Wear*, V.162-164, pp 971-974.

- LIU, T.I., and ANATHARAMAN, K.S., (1994) Intelligent Classification and Measurement of Drill Wear, *ASME Transactions - Journal of Engineering for Industry,* V.116, Aug, pp 392 - 397.

- LIU, H., and XUE, Q., (1996) Wear mechanisms of zirconia/steel reciprocating sliding couple under water lubrication, *Wear*, V.201, pp 51-57.

- LO CASTRO, S., LO VALVO, E., RUISI, V.F., LUCCHINI, E., & MASCHIO, S., (1993) Wear mechanism of ceramic tools, *Wear*, V.160, pp 227-235.

- LOLADZE, T.N., (1976) Tribology of metal cutting and creation of new materials, *CIRP*, V.25, N.1, pp 83-88.

- LOLADZE, T.N., (1981) On the theory of diffusion wear, *CIRP*, V.30, N.1, pp 71-76.

- LUDEMA, K.C., (1974) A Perspective on Wear Models, *ASTM Standardization News*, V.2, No. 9, pp 3-17.

- MANSOUR, W.M., OSMAN, M.O.M., SANKAR, T.S., and MAZZAWI, A., (1973) Temperature Field and Crater Wear in Metal Cutting using a Quasi-finite Element Approach, *International Journal of Production Research,* V.11, No. 1, pp 59-68.

- MATSUMURA, T., OBIKAWA, T., SHIRAKASHI, T., & USUI, E., (1993) Autonomous turning operations planning with adaptive prediction of tool wear and surface roughness, *Journal of Manufacturing Systems*, V.12, N.3, pp 253-262.

- McADAMS, H.T., and ROSENTHAL, P., (1961) Forces on a Worn Cutting Tool, *ASME Transactions - Journal of Engineering For Industry,* V.83, Series B, Nov, pp 505-512.

- MENG, H-C., (1994) *Wear Modelling: Evaluation and Categorization of Wear Models*, PhD Thesis, University of Michigan.

- MERCHANT, M.E., (1945a) Mechanics of the Metal Cutting Process. I - Orthogonal Cutting and a Type 2 Chip, *Journal of Applied Physics,* V.16, N.5, May, pp 267-275.

- MERCHANT, M.E., (1945b) Mechanics of the Metal Cutting Process. II - Plasticity Conditions in Orthogonal Cutting, *Journal of Applied Physics,* V.16, N.5, June, pp 318-324.

- MILLS, B., and REDFORD, A.H., (1983) *Machinability of Engineering Materials*, New York: Applied Science Publishers.

- MORIN, E., MASOUNAVE, J., and LAUFER, E.E., (1995) Effect of drill wear on cutting forces in the drilling of metal-matrix composites, *Wear*, V.184, pp 11-16.

- MURAKA, P.D., BARROW, G., and HINDUJA, S., (1979) Influence of the process variables on the temperature distribution on orthogonal machining using the finite element method, *International Journal of Mechanical Science,* V.21, N.8 , pp 445-456.

- NACHTMAN, E.S., (1989) Metal cutting and grinding fluids, in *Metals Handbook, V.16: Machining*, ASM International, 9th ed., pp 121-132.

- NAGASAKA, K., and HASHIMOTO, F., (1982) The establishment of a tool life equation considering the amount of tool wear, *Wear*, V.81, pp 21 - 31.

- NAIR, R., DANAI, K., & MALKIN, S., (1990) Turning process identification through force transients, *The winter annual meeting of the ASME*, Texas, USA, Nov. 25-30, pp 59-66.

- NARASIMHA, K., OSMAN, M.O.M., CHANDRASHEKHAR, S., FRAZAO, J., (1987) An investigation into the influence of helix angle on the torque-thrust coupling effect in twist drills, *International Journal of Advanced Manufacturing Technology*, V.2, N.4, pp 91 - 105.

- NARUTAKI, N., YAMANE, Y., HAYASHI, K., & KITAGAWA, T., (1993) High speed machining of Inconel 718 with ceramic tools, *CIRP*, V.42, N.1, pp 103-106.

- NEALE, M.J., (ed.), (1995) *The Tribology Handbook*, 2nd Edition, Oxford:Butterworth-Heinmann.

- OHGO, K., (1978) The adhesion mechanism of the built-up edge and the layer on the rake face of a cutting tool, *Wear*, V.51, pp 117-126.

- OLBERTS, D.R., (1959) A Study of the Effects of Tool Flank Wear on Tool Chip Interface Temperature, *ASME Transactions - Journal of Engineering for Industry*, May, pp 152-158.

- ORABY, S.E., & HAYHURST, D.R., (1991) Development of models for tool wear force relationships in metal cutting, *International Journal of Mechanical Science*, V.33, N.2, pp 125-138.

- OXFORD, C.J., (1955) On the Drilling of Metals: Part 1 - Basic Mechanics of the process, *ASME Transactions*, February, pp 103 - 114.

- PASHBY, I.R., (1992) *The effect of heat treatment on the machinability of austempered ductile iron*, PhD Thesis, Warwick University.

- PASHBY, I.R., WALLBANK, J., & BOUD, F., (1993) Ceramic tool wear when machining austempered ductile iron, *Wear*, V.162-164, pp 22-33.

- PETERSON, M.B., (1974) Understanding Wear, *ASTM Standardisation News*, V.2, N.9, pp 9-12.

- POLLACK, H.W., (1988) *Materials Science and Metallurgy*, 4th ed., New Jersey: Prentice Hall.

- PRINS, O.D., (1971 The Influence of Wear on the Temperature Distribution at the Rake Face, *CIRP* V.19, pp 579-584.

- RADFORD, J.D., and RICHARDSON, D.B., (1980) *Production engineering Technology*, London: Macmillan.

- RAHMAN, M., (1988) In process detection of chatter threshold, *ASME Transactions - Journal of Engineering for Industry*, V.110, pp 44 - 50.

- RAMASWAMI, R., (1971) The effect of the BUE on the wear of cutting tools, *Wear*, V.18, pp 1-10.

- RAVINDRA, H.V., SRINIVASA, Y.G., and KRISHNAMURTHY, R., (1993) Modelling of tool wear based on cutting forces in turning, *Wear*, V.169, pp 25 - 32.

- REDFORD, A.H., and AKHTAR, S., (1976) Temperature - Tool Life Relationships for Resulphurised Low Carbon Free Machining Steels, *CIRP*, V.25, N.1, pp 89-91.

- ROWE, G.W., & SPICK, P.T., (1967) A new approach to determination of the shear-plane angle in machining, *Journal of Engineering for Industry*, V.89B, pp 530-538.

- RUBENSTEIN, C., (1976) An analysis of tool life based on flank-face wear, Part 1: Theory, *Journal of Engineering for Industry - ASME Transactions*, February, pp 227 - 232.

- RUBENSTEIN, C., (1991a) The Torque and Thrust Force in Twist Drilling - I - Theory, *International Journal Machine Tools Manufacturing*, V.31, N.4, pp 481-489.

- RUBENSTEIN, C., (1991b) The Torque and Thrust Force in Twist Drilling - II - Comparison of Experimental Observations with Deductions from Theory, *International Journal Machine Tools Manufacturing*, V.31, N.4, pp 491-504.

- RUFF, A.W., and LUDEMA, K.C., (1986) Wear, in BEVER, Michael B., (ed.), *Encyclopaedia of Materials Science and Engineering*, V.7, Oxford:Pergamon Press Ltd., pp 5273-5278.

- SADAT, A.B., (1994) Tool wear measurement and monitoring techniques for automated machining cells, *The Energy-Sources Technology Conference*, Louisiana, USA, Jan 23-26, pp 103-115.

- SANTHANAM, A.T., & TIERNEY, P., (1989) Cemented Carbides, in *Metals Handbook, V.16: Machining*, ASM International, 9th ed., pp 71-89.

- SCHAIBLE, J., (1991) Inserts turn to the future, *Cutting Tool Engineering*, pp 92-97.

- SCHMIDT, A.O., and ROUBIK, J.R., (1949) Distribution of Heat Generated in Drilling, *ASME Transactions* - April, pp 245-252.

- SELVAM, M.S., & RADHAKRISHNAN, V., (1974) Groove wear, built-up edge and surface roughness in turning, *Wear*, V.30, pp 179-188.

- SHAW, M.C., and OXFORD, C.J., (1957) On the Drilling of Metals - 2- The Torque and Thrust in Drilling, *ASME Transactions*, V.79, pp 139-148.

- SHAW, M.C., (1991) *Metal Cutting Principles*, Oxford: Clarendon Press.

- SINGPURWALLA, N.D., and KUEBLER, A.A., (1966) A quantitative evaluation of drill life, *ASME Paper 66-WA/PROD-11*, pp 1 - 11.

- SMITH, G.T., (1989) *Advanced Machining - The handbook of cutting technology*, Bedford: IFS Publications.

- SODERBERG, S., (1978) Wear of twist drills, *Fagersta High-Speed Steel Symposium*, pp 34 - 45.

- STEPHENSON, D.A., and AGAPIOU, J.S., (1997) *Metal Cutting Theory and Practice*, New York: Marcel Dekker.

- STERN, E.L., and PELLINI, R.P., (1993) A Study on the Effect of Tool Wear on Machining Forces, in Ehmann, K.F., (Ed.), *Manufacturing Science and Engineering*, PED-Vol. 64, New York: ASM, pp 445-451.

- STEVENSON, M.G., WRIGHT, P.K., and CHOW, J.G., (1983) Further Developments in Applying the Finite Element Method to the Calculation of Temperature distributions in Machining and Comparisons with Experiment, *ASME Transactions - Journal of Engineering for Industry*, V.105, Aug, pp 149-154.

- SUBRAMANIAN, K., and COOK, N.H., (1977) Sensing of Drill Wear and Prediction of Drill Life, *ASME Transactions - Journal of Engineering for Industry*, May, pp 295 - 300.

- SUKVITTAYAWONG, S., & INASAKI, I., (1991) Identification of chip forming turning process, *JSME (Japan Society of Mechanical Engineers), International Journal, Vibration, Control Engineering, Engineering for Industry*, V.34, N.4, pp 553-560.

- TAIBI, S., (1994) *Modelling the Dynamics of Cutting During Turning*, PhD Thesis, University of Aston in Birmingham.

- TAKEYAMA, H., and MURATA, R., (1963) Basic investigation of tool wear, *Journal of Engineering for Industry - ASME Transactions*, February, pp 33 - 38.

- TAYLOR, F.W., (1907) On the Art of Cutting Metals, *Journal of engineering for Industry, ASME Transactions*, V.28, pp 315-350.

- TAYLOR, J., (1962) The tool wear-time relationship in metal cutting, *International Journal Machine Tool Design Research*, V.2, pp 119-152.

- THANGARAJ, A., and WRIGHT, P.K., (1988) Computer-assisted prediction of drill-failure using in-process measurements of thrust force, *ASME Transactions - Journal of Engineering for Industry*, V.110, May, pp 192 - 200.

- TONSHOFF, H.K., & BARTSCH, S., (1988) Wear mechanisms of ceramic cutting tools, *Ceramic Bulletin*, V.67, N.6, pp 1020-1027.

- TRENT, E.M., (1988) Metal cutting and tribology of seizure, Part 3: Temperatures in metal cutting, *Wear*, V.128, pp 65-81.

- TRENT, E.M., (1991) *Metal Cutting*, Oxford: Butterworth-Heinemann.

- TUCKER, R.C., (1986) Wear Failures, in *Metals Handbook Vol. 11: Failure Analysis and Prevention*, 9th Edition, Ohio: American Society For Metals, pp 145-162.

- USUI, E., SHIRAKASHI, T., & KITTAGAWA, T., (1978) Analytical prediction of three dimensional cutting process - Part 3: Cutting temperature and crater wear of carbide tool, *Journal of Engineering for Industry*, V.100, pp 236-243.

- VENKATESH, V.C., (1978) On a diffusion wear model for High Speed Steel tools, *Journal of Lubrication Technology - ASME Transactions*, V.100, July, pp 436 - 441.

- VENUVINOD, P.K., & DJORDJEVICH, A., (1996) Towards active chip control, *CIRP*, V.45, N.1, pp 83-86.

- WADA, R., KODAMA, H., & NAKAMURA, K., (1980) Wear characteristics of single crystal diamond tool, *CIRP*, V.29, N.1, pp 47-52.

- WALLACE, P.W., and BOOTHROYD, G., (1964) Tool Forces and Tool-Chip Friction in Orthogonal Machining, *Journal Mechanical Engineering Science*, V.6, N.1, pp 74-87.

- WATSON, A.R., (1985a) Drilling model for cutting lip and chisel edge and comparison of experimental and predicted results: part 1 - Initial cutting lip model, *International Journal of Machine Tool Design Research*, V.25, N.4, pp 347 - 365.

- WATSON, A.R., (1985b) Drilling model for cutting lip and chisel edge and comparison of experimental and predicted results: part 2 - Revised cutting lip model, *International Journal of Machine Tool Design Research*, V.25, N.4, pp 367 - 376.

- WATSON, A.R., (1985c) Drilling model for cutting lip and chisel edge and comparison of experimental and predicted results: part 3 - Drilling model for chisel edge, *International Journal of Machine Tool Design Research*, V.25, N.4, pp 377 - 392.

- WATSON, A.R., (1985d) Drilling model for cutting lip and chisel edge and comparison of experimental and predicted results: part 4 - Drilling tests to determine chisel edge contribution to torque and thrust, *International Journal of Machine Tool Design Research*, V.25, N.4, pp 393 - 404.

- WEBB, P.M., (1990) *The Influence of Cutting Tool geometry upon Aspects of Chip Flow and Tool Wear - A theoretical, three dimensional examination of the cutting geometry and the shape of the twist drill*, PhD Thesis, University of Aston in Birmingham.

- WICK, C., (1988) Ceramic cutting tools update, *Manufacturing Engineering*, April, pp 81-87.

- WILKINSON, P., REUBEN, R.L., JONES, J.D.C., BARTON, J.S., HAND, D.P., CAROLAN, T.A., & KIDD, S.R., (1997) Surface finish parameters as diagnostics of tool wear in face milling, *Wear*, V.205, pp 47-54.

- WILLIAMS, R.A., (1973) A Study of the Drilling Process, *ASME Paper N73-WA/PROD 6*, Nov 11-15, pp 1-9.

- YAGUCHI, H., (1988) Built-up edge in low-carbon resulfurized free-machining steels, *1st International Conference on Behaviour of Materials in Machining*, Stratford-upon-Avon, Nov 8-10, pp 24.1-24.9.

- YANG, K., & JEANG, A., (1994) Statistical surface roughness checking procedure based on a cutting tool wear model, *Journal of Manufacturing Systems*, V.13, N.1, pp 1-8.

- YEE, K.W., BLOMQUIST, D.S., DORNFELD, D.A., & PAN, C.S., (1986) An acoustic emission chip-form monitor for single-point turning, *Proceedings of the 26th International Machine Tool Design and Research Conference*, UMIST, Manchester, Sep 17-18, pp 305-312.

- YOUNG, H-T., (1996) Cutting temperature responses to flank wear, *Wear*, V.201, N.1-2, pp 117-120.

- ZAKARIA, A.A., & EL GOMAYEL, J.I., (1975) On the reliability of the cutting temperature for monitoring tool wear, *International Journal of Machine Tool Design Research*, V.15, pp 195-208.

APPENDIX 1

TEST CONDITIONS

A1 MACHINING

A1.1 Turning

A1.1.1 Moly M2 HSS

Due to CNC machine breakdown the experiments had to begin by using the Elliot Superomnispeed 4000 lathe. On this lathe each test was carried out using the conditions listed in table A1.1.

A - Ordinary lathe

Speed (m/min)	Feed rate (mm/rev)	DOC (mm)	Flank angle (deg)	Rake angle (deg)
15.2	0.18	2	12^{o} 15`	14^{o} 38`
20.2	0.18	2	11^{o} 40`	13^{o} 25`
25.7	0.18	2	8^{o} 12`	15^{o} 15`
27.8	0.18	2	9^{o} 23`	13^{o} 7`

Table A1.1 Cutting conditions: Moly M2 HSS, cooling 4% Shell Dromus B @ 2 litres / min. no nose radius

B - Torshalla CNC

Using the Torshalla CNC lathe, the cutting conditions are shown in tables A1.2 to A1.9. Tables A1.2 and A1.3 show the condition for cutting tests using 2 mm for DOC, and 1 mm for DOC respectively:

Speed (m/min)	Feed rate (mm/rev)	DOC (mm)	Flank angle (deg)	Rake angle (deg)
10	0.18	2	7° 20'	14° 45'
20	0.18	2	7° 21'	15° 20'
30	0.18	2	7° 18'	14° 45'
40	0.18	2	8° 9'	15° 21'

Table A1.2 Cutting conditions: Moly M2 HSS, cooling 4% Shell Dromus B @ 4 litres / min. no nose radius

Speed (m/min)	Feed rate (mm/rev)	DOC (mm)	Flank angle (deg)	Rake angle (deg)
10	0.18	1	7° 30'	15° 33'
20	0.18	1	7° 28'	15° 50'
30	0.18	1	7° 27'	15° 50'
40	0.18	1	7° 24'	15° 52'

Table A1.3 Cutting conditions: Moly M2 HSS, cooling 4% Shell Dromus B @ 4 litres / min. no nose radius

The tool material Moly M2 HSS was cut by using various speeds of 10, 20, 30 and 40 m/min., four different rake angles of 30, 10, 6 and -6 degrees, and three different flank angles of 5, 10 and 15 degrees. The cutting conditions can be seen in table A1.4 below.

Speed (m/min)	Flank angle (deg)	Rake angle (deg)	Speed (m/min)	Flank angle (deg)	Rake angle (deg)
10	4° 37'	6° 23'	20	4° 19'	6° 18'
30	4° 52'	6° 9'	40	5° 26'	5° 55'
10	8° 58'	6° 30'	20	9° 26'	6° 15'
30	9° 20'	5° 22'	40	11° 18'	6° 10'
10	14° 28'	5° 44'	20	14° 18'	6°
30	14° 34'	6° 28'	40	14° 41'	6° 28'
10	4° 45'	10° 7'	20	4° 11'	10° 24'
30	4° 5'	10° 51'	40	4° 19'	10° 25'
10	9° 48'	10° 40'	20	9° 21'	9° 44'
30	9° 11'	10° 16'	40	9° 15'	9° 39'
10	15° 38'	8° 51'	20	16° 10'	8° 40'
30	15° 42'	8° 37'	40	16° 48'	8° 41'
10	4° 54'	29° 38'	20	4° 40'	30° 20'
30	4° 56'	30° 49'	40	4° 56'	30° 8'
10	8° 50'	30° 2'	20	9° 28'	30° 12'
30	10° 32'	28° 55'	40	9° 28'	29° 50'
10	17°	28° 25'	20	17° 02'	27° 45'
30	16° 04'	28° 42'	40	16° 40'	28° 10'
10	4° 56'	-6° 26'	20	4° 58'	-6° 34'
30	5° 17'	-6° 32'	40	5° 38'	-6° 37'
10	9° 57'	-6° 15'	20	10°	-6° 27'
30	10° 17'	-6° 04'	40	10° 09'	-5° 34'
10	14° 46'	-6° 22'	20	14° 40'	-6° 22'
30	15° 28'	-6° 17'	40	15° 21'	-6° 37'

Table A1.4 Cutting conditions: Moly M2 HSS with 0.15 mm/rev. feed rate, 2 mm DOC, no nose radius at various rake and flank angles and dry cut

A1.1.2 BT42 HSS

Tables A1.5 to A1.8 show the cutting conditions that were used for the BT42 HSS tests:

Speed (m/min)	Feed rate (mm/rev)	wet / dry 4% @ 4 l/min	Flank angle (deg)	Rake angle (deg)
10	0.18	wet	5°	6°
20	0.18	wet	5°	6°
30	0.18	wet	5°	6°
40	0.18	wet	5°	6°
10	0.15	dry	5°	6°
20	0.15	dry	5°	6°
30	0.15	dry	5°	6°
40	0.15	dry	5°	6°

Table A1.5 Cutting conditions: uncoated BT42 HSS, with 0.4 mm nose radius

The purpose of this uninterrupted test is to see the effect of the interruptions on tool life and forces.

Cutting time (sec)	Speed (m/min)	Feed rate (mm/rev)	DOC (mm)	Flank angle (deg)	Rake angle (deg)
3600	10	0.15	2	5°	6°
1800	20	0.15	2	5°	6°
1080	30	0.15	2	5°	6°
60	40	0.15	2	5°	6°

Table A1.6 Cutting conditions: uncoated BT42 HSS, with 0.4 mm nose radius dry cut

The purpose of this test was to cut six tools, each time using a new one, varying the times by five minutes increments in order to see the effect on the wear scar size.

Cutting time (sec)	Speed (m/min)	Feed rate (mm/rev)	DOC (mm)	Flank angle (deg)	Rake angle (deg)
300	20	0.15	2	5°	6°
600	20	0.15	2	5°	6°
900	20	0.15	2	5°	6°
1200	20	0.15	2	5°	6°
1500	20	0.15	2	5°	6°
1800	20	0.15	2	5°	6°

Table A1.7 Cutting conditions: uncoated BT42 HSS, with 0.4 mm nose radius dry cut

Speed (m/min)	Feed rate (mm/rev)	wet / dry 4% @ 4 l/min	Flank angle (deg)	Rake angle (deg)
30	0.18	wet	5°	6°
45	0.18	wet	5°	6°
50	0.18	wet	5°	6°
60	0.18	wet	5°	6°
70	0.18	wet	5°	6°
10	0.15	wet	5°	6°
30	0.15	wet	5°	6°
50	0.15	wet	5°	6°
10	0.15	dry	5°	6°
30	0.15	dry	5°	6°
50	0.15	dry	5°	6°

Table A1.8 Cutting conditions: TiN coated BT42 HSS, with 0.8 mm nose radius

A1.1.3 Carbide.

KC850 compostition - A TiC/TiCN/TiN coating on an extra-strong cobalt enriched substrate.

K68 compostion - A tough WC/Co unalloyed grade.

K313 composition - An unalloyed WC/Co fine-grained grade.

The cutting conditions used for the Carbide tests are shown in table A1.9 below:

Tool Material	Speed (m/min)	Feed rate (mm/rev)	Nose radius (mm)	wet / dry 4% @ 4 l/min
K68	40	0.15	0.4	dry
K68	50	0.15	0.4	dry
K68	60	0.15	0.4	dry
K68	40	0.15	0.8	dry
K68	50	0.15	0.8	dry
K68	60	0.15	0.8	dry
K68	30	0.18	0.8	wet
K68	40	0.18	0.8	wet
K68	50	0.18	0.8	wet
K68	55	0.18	0.8	wet
K68	60	0.18	0.8	wet
KC850	30	0.18	0.8	wet
KC850	40	0.18	0.8	wet
KC850	50	0.18	0.8	wet
KC850	60	0.18	0.8	wet
KC850	70	0.18	0.8	wet
KC850	40	0.18	0.4	dry
K313	40	0.18	0.4	wet
K313	50	0.18	0.4	wet
K313	60	0.18	0.4	wet
K313	40	0.15	0.4	dry
K313	50	0.15	0.4	dry
K313	60	0.15	0.4	dry
K313	40	0.15	0.8	dry
K313	50	0.15	0.8	dry
K313	60	0.15	0.8	dry

Table A1.9 Cutting conditions: Carbide tool, depth of cut 2 mm, flank angle = 5^0 and Rake angle = 6^0

A1.2 Drilling

The cutting conditions for the tests carried out for the drilling operations are shown below in tables A1.10 to A1.12:

Speed (rpm)	Feed rate (mm/rev)	Drill Size (mm)	Helix angle	Hole Nº. tested for wear and forces
354	112	9	Standard	1
244	78	13	Slow	1, 10, 20, 30, 40 & 50
354	112	9	Standard	1, 10, 20, 30, 40 & 50
244	78	13	Standard	1, 10, 20, 30, 40 & 50
354	112	9	Standard	1, 10, 20
354	112	13	Fast	1, 10
707	226	9	Standard	1, 4, 8, 12
490	156	13	Slow	1, 4, 8, 12
707	226	9	Standard	1, 4, 8, 12
490	156	13	Standard	1, 4, 8, 12
707	226	9	Standard	1, 4, 8, 12
490	156	13	Fast	1, 4, 8, 12
1061	349	9	Standard	1, 3, 4, 6
735	234	13	Slow	1, 3, 4, 6
1061	349	9	Standard	1, 3, 4, 6
735	234	13	Standard	1, 3, 4, 6
1061	349	9	Standard	1, 3
735	234	13	Fast	1,

Table A1.10 Cutting conditions: tool material M2 HSS, dry cut

Tables A1.11 and A1.12 show the drill specifications for 13 mm diameter and 9 mm diameter respectively where measurements had been taken before the tests were carried out using the Swiss toolmakers microscope as shown in figure 5.5 in chapter 5.

Drill label	SLH8	STH6	FH9	SLH4	STH10	FH6	SLH9	STH5	FH4
Drill type	slow	stand	fast	slow	stand	fast	slow	stand	fast
Speed (rpm)	244	244	244	490	490	490	735	735	735
Feed (mm/rev)	78	78	78	156	156	156	234	234	234
Helix angle (deg)	12° 33'	31° 11'	40° 12'	11° 49'	32° 06'	41° 28'	12° 42'	8° 41'	39° 37'
Web thickness (mm)	1.846	2.235	2.519	1.911	1.983	2.423	1.933	2.173	2.150
Chisel angle (deg)	126° 55'	125° 36'	128° 21'	126° 30'	129° 36'	125° 50'	126° 42'	122° 21'	127° 37'
Point angle (deg)	121° 40'	121° 36'	113° 50'	120° 08'	118° 31'	114° 24'	121° 31'	121° 44'	114° 31'
Total body clearance (mm)	0.673	0.632	0.823	0.537	0.810	0.561	0.625	0.447	0.835
Lip clear (mm)	9.333	11.23	9.658	9.775	12.56	9.450	10.8	10.25	10.0
Total point clear (mm)	0.631	0.427	0.642	0.537	0.810	0.768	0.551	0.447	0.612
Fluted land width (mm)	9.771	8.806	6.006	10.387	8.011	6.088	10.348	8.691	5.527
Cylindrical land width (mm)	0.887	0.673	0.684	0.835	0.892	0.861	0.809	1.031	0.716

Table A1.11 Drill specifications for 13 mm diameter

Drill label	P10	P13	P15	P12	P17	P18	P14	P16	P11
Drill type	stand	stand	stand	stand	stand	stand	stand	stand	stand
Speed (rpm)	354	354	354	707	707	707	1061	1061	1061
Feed (mm/rev)	112	112	112	226	226	226	340	340	340
helix angle (deg)	27° 46'	29° 45'	28° 10'	30° 08'	28° 28'	28° 40'	29° 30'	29° 45'	31° 23'
Web thickness (mm)	1.515	.515	1.548	1.550	1.555	1.507	1.639	1.569	1.553
Chisel angle (deg)	131° 01'	131° 05'	131° 20'	130° 22'	132°	131° 22'	130° 14'	132°	130° 35'
Point angle (deg)	119° 50'	120° 36'	120° 52'	119° 25'	119° 36'	119° 38'	120° 06'	119° 48'	119° 57'
Total body clearance	0.440	0.419	0.369	0.467	0.411	0.562	0.377	0.394	0.405
Lip clear (mm)	14.5	14.62	14.47	15.25	14.57	14.62	13.7	14	15
Total point clear (mm)	0.461	0.441	0.532	0.467	0.579	0.562	0.528	0.553	0.456
Fluted land width (mm)	6.010	6.327	6.284	6.335	6.384	6.250	6.473	6.417	6.278
Cylindrical land width	0.733	0.736	0.665	0.644	0.767	0.588	0.909	0.778	0.656

Table A1.12 Drill specifications for 9 mm diameter

A2 TEMPERATURE

A2.1 Turning

The tool material that was used for these tests was uncoated BT42 HSS triangle insert. According to the Kennametal technical data its specification is TPUN160304. The test conditions can be seen in tables A1.13 to A1.17.

A2.1.1 New tool

Speed (m/min)	Cutting time (sec)	No. of therm-ocouple	Feed rate (mm/rev)	DOC (mm)
10	110.6	2	0.15	2
20	113.3	2	0.15	2
30	122.2	2	0.15	2
40	64.5	2	0.15	2

Table A1.13 Test conditions: tool material is uncoated BT42 HSS, with nose radius 0.4 mm, dry cut

Speed (m/min)	Cutting time (sec)	No. of therm-ocouple	Feed rate (mm/rev)	DOC (mm)
10	14.4	2	0.15	2
20	12.4	2	0.15	2
30	13.8	1	0.15	2
40	14.4	1	0.15	2

Table A1.14 Test conditions: tool material is uncoated BT42 HSS, with nose radius 0.4 mm, dry cut

Speed (m/min)	Cutting time (sec)	No. of therm-ocouple	Feed rate (mm/rev)	DOC (mm)
30	9.8	1	0.15	2
40	8.8	1	0.15	2

Table A1.15 Test conditions: tool material is uncoated BT42 HSS, with nose radius 0.4 mm, dry cut

Speed (m/min)	Cutting time (sec)	No. of therm-ocouple	Feed rate (mm/rev)	Depth of cut (mm)
30	7.2	2	0.15	2
40	9.4	2	0.15	2
10	16.8	2	0.15	2
20	11.7	2	0.15	2

Table A1.16 Test conditions: tool material is uncoated BT42 HSS, with nose radius 0.4 mm, dry cut

A2.1.2 Worn tool

For table A1.17 the tool material is uncoated BT42 HSS, with nose radius 0.4 mm, dry cut, with flank wear: 0.177 mm max., 0.118 mm ave., 0.299 mm notch wear and 0.243 mm nose wear, and depth of rake face wear 0.1 mm, bar diameter was 50 mm.

Speed (m/min)	Cutting time (sec)	No. of therm-ocouple	Feed rate (mm/rev)	Depth of cut (mm)
10	8	2	0.15	2
20	14	2	0.15	2
30	13	2	0.15	2
40	13	2	0.15	2

Table A1.17 Test conditions: tool material is uncoated BT42 HSS.

A2.1.3 Bar diameter

The test conditions for turning are shown in tables A1.18 and A1.19 below:

Speed (rpm)	Cutting time (sec)	Number of thermocouple	Bar Diameter (mm)	Feed rate (mm/rev)	Depth of cut (mm)
20	19	2	31	0.15	2
20	23	1	53	0.15	2
20	16	1	75	0.15	2

Table A1.18 Test conditions: tool material is uncoated BT42 HSS, with nose radius 0.4 mm, dry cut

Speed (m/min)	Cutting time (sec)	Bar Diameter (mm)	No. of therm-ocouple	Wear (mm)					
				Before			After		
				ave	max.	nose	ave	max.	nose
10	18	31	2	.122	.170	.354	.153	.229	.383
10	14	51	2	.122	.170	.354	.153	.229	.383
10	16	75	2	.122	.170	.354	.153	.229	.383
20	16	31	2	.153	.229	.383	.174	.252	.494
20	17	51	2	.153	.229	.383	.174	.252	.494
20	16	75	1	.153	.229	.383	.174	.252	.494
30	18	31	1	.174	.252	.494	.215	.284	.560
30	18	51	1	.174	.252	.494	.215	.284	.560
30	20	75	1	.174	.252	.494	.215	.284	.560
40	10	31	1	.215	.284	.560	.250	.341	.662
40	13	51	1	.215	.284	.560	.250	.341	.662
40	12	75	1	.215	.284	.560	.250	.341	.662

Table A1.19 Test conditions: tool material is uncoated BT42 HSS, with nose radius 0.4 mm, feed rate 0.15 mm/rev. dry cut

A2.2 Drilling

An ordinary lathe machine was used to test the drill temperature. During the test the drill was stationary while the workpiece rotated. The test conditions for M2 HSS 8 mm with oil hole drill worn and unworn at 3 different speeds in drilling are shown in tables A1.20 to A1.25 below:

A2.2.1 New tool.

Speed (rpm)	Cutting time (sec)	No. of thermocouple	Feed rate (mm/rev)
310	10.25	1	0.15
700	13.75	1	0.15
900	10.0	1	0.15
900	10.0	1	0.15

Table A1.20 Test conditions: tool material is M2 HSS, standard helix angle drill 8 mm diameter with wear, dry cut

Speed (rpm)	Cutting time (sec)	No. of thermocouple	Feed rate (mm/rev)
310	10.5	1	0.15
700	12.5	1	0.15
900	14.75	1	0.15

Table A1.21 Test conditions: tool material is M2 HSS, standard helix angle drill 8 mm diameter new, dry cut

Speed (rpm)	Cutting time (sec)	No. of thermocouple	Feed rate (mm/rev)
310	10	2	0.15
700	8	2	0.15
900	8	2	0.15

Table A1.22 Test conditions: tool material is M2 HSS, standard helix angle drill 8 mm diameter resharpened, dry cut

A2.2.2 Worn tool.

Speed (rpm)	Cutting time (sec)	No. of thermocouple	Feed rate (mm/rev)
900	10.5	2	0.15
700	11.25	2	0.15
310	13.5	2	0.15

Table A1.23 Test conditions: tool material is M2 HSS, standard helix angle drill 8 mm diameter, dry cut

For table A1.24 the tool material is M2 HSS, standard helix angle drill 8 mm diameter, dry cut. Conditions of the lip height before the test were 0.079 mm for the first three tests and 0.013 mm for the last three tests

Speed (rpm)	Cutting time (sec)	Feed rate (mm/rev)	No. of therm-ocouple	Wear (mm)					
				Before			After		
				corn	max.	ave	corn	max.	ave
310	13.5	0.15	2	.139	.138	.051	.280	.209	.124
				.158	.132	.072	.239	.202	.109
700	16.75	0.15	2	.139	.138	.051	.280	.209	.124
				.158	.132	.072	.239	.202	.109
900	14.75	0.15	2	.139	.138	.051	.280	.209	.124
				.158	.132	.072	.239	.202	.109
310	10	0.15	2	.280	.209	.124	.409	.332	.169
				.239	.202	.109	.328	.320	.145
700	13	0.15	2	.280	.209	.124	.409	.332	.169
				.239	.202	.109	.328	.320	.145
900	10.5	0.15	2	.280	.209	.124	.409	.332	.169
				.239	.202	.109	.328	.320	.145

Table A1.24 Test conditions: tool material is M2 HSS

A2.2.3 Lip cutting 2 mm only.

Speed (rpm)	Cutting time (sec)	No. of thermocouple	Feed rate (mm/rev)
310	9	2	0.15
700	10	2	0.15
900	10	2	0.15

Table A1.25 Test conditions: tool material is M2 HSS, standard helix angle drill 8 mm diameter, dry cut

APPENDIX 2

TERMS AND DEFINITIONS

Twist drills - Terms and definitions (ISO 5419: 1996)

3.1 Axis: the longitudinal centre-line of the drill (figure A2.1).

3.2 Shank: the portion of the drill by which it is held and driven (figure A2.1 A and B).

3.2.1 Taper shank: (figure A2.1 A).

3.2.2 Parallel Shank: (figure A2.1 B).

3.2.3 Parallel shank with tenon drive (figure A2.1 B).

3.3 Tang: the flattened end of a taper shank intended to fit into the slot in the socket and to be used for ejection pruposes (figure A2.1 A).

3.4 Tenon: the flattened end of a parallel shank intended for driving purposes (figure A2.1 B).

3.5 Body: the proportion of the drill extending from the shank to the chisel edge (3.26) (figures A2.1 A and A2.1 B).

3.7 Overall length: the distance between two planes normal to the drill axis through the chisel edge (3.26) and the end of the shank (including any tenon or tang) respectively (figure A2.1 A and B).

3.8 Flute length: the distance between two planes normal to the drill axis through the chisel edge (3.26) and the shank end of the flutes respectively (figures A2.1 A and B).

3.9 Flute: a groove in the body of the drill which, at the intersection with the flank (3.21) provides a major cutting edge (3.23), thus permitting removal of chips and allowing cutting fluid to reach the major cutting edge (figure A2.1 A).

3.10 Fluted land: the helical portion of the body (3.5), including both the land (3.14) and the body clearance (3.17) (figure A2.1 A).

3.11 Width of flute land: the distance between the leading edge of the land (3.16) and the heel (3.19), measured at right angles to the leading edge of the land (figure A2.1 A).

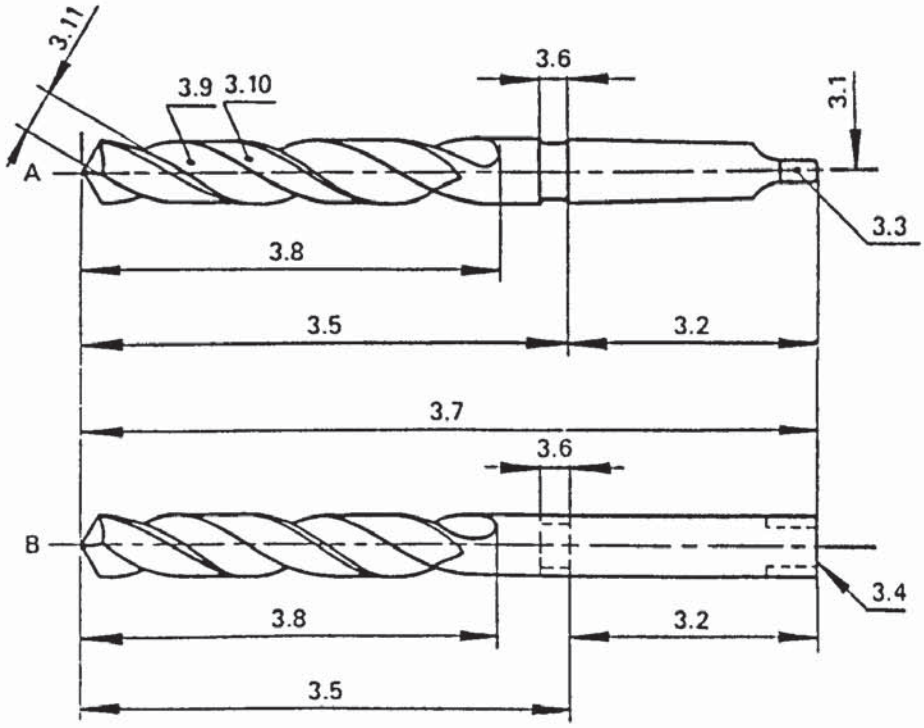

Figure A2.1 Drill body (ISO)

3.12 Web: the central portion of the drill situated between the roots of the flutes over the flute length (figure A2.2).

3.13 Web thickness: the minimum dimension of the web measured in a plane normal to the axis. The web thickness is usually measured at the point end (figure A2.2).

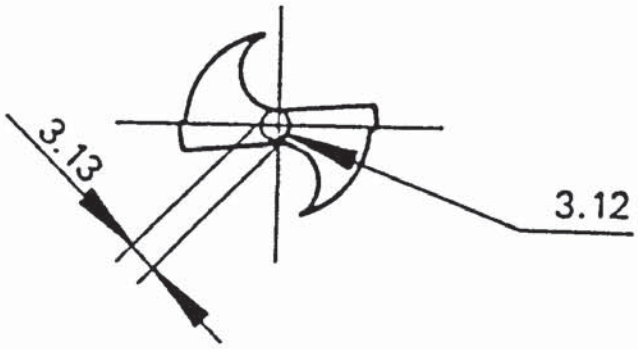

Figure A2.2 Drill web (ISO)

3.14 Land: the cylindrical or conical leading surface of the drill (figure A2.4).

3.15 Width of land: the dimension measured at right angles to the leading edge of the land (3.16) across a land (3.14) (figure A2.4).

3.16 Leading edge of a land (minor cutting edge): the edge formed by the intersection of a land (3.14) and a flute (3.9) (figure A2.4).

3.17 Body clearance: the portion of a fluted land reduced in diameter to provide diametrical clearance (figure A2.4).

3.18 Depth of body clearance: the radial distance between the land (3.14) and the corresponding body clearance (3.17). It is generally measured at the outer corners (figure A2.3).

3.19 Heel: the edge formed by the intersection of a flute (3.9) and the body clearance (3.17) (figure A2.4).

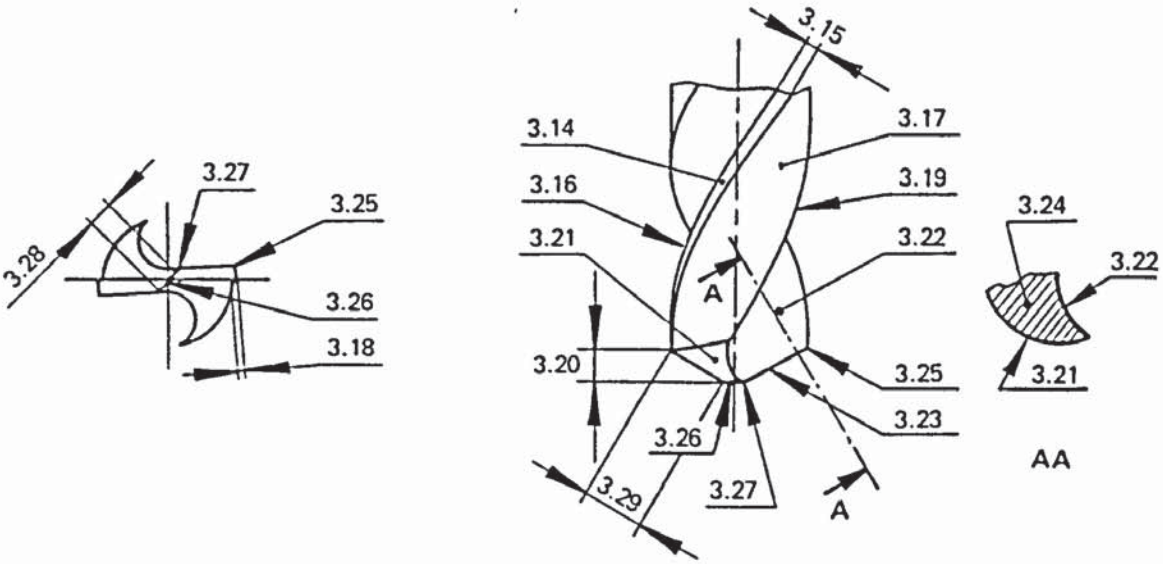

Figure A2.3 Drill chisel edge and Figure A2.4 Drill cutting edge (ISO)

3.20 Point (cutting part): the functional part of the drill comprised of chip-producing elements. The major cutting edges (lips 3.23), chisel edge (3.26), faces (3.22) and flanks (3.21) are therefore elements of the point (cutting part) (figure A2.4).

3.21 Flank (major flank): the surface on the drill point bounded by the major cutting edge (3.23), the fluted land (3.18), the following flute and the chisel edge (3.26) (figure A2.4).

3.22 Face: the portion of the surface of a flute adjacent to the major cutting edge (3.23) and on which the chip impinges as it is cut from the workpiece (figure A2.4).

3.23 Major cutting edge (lip): the edge formed by the intersection of a flank (3.21) associated with the major cutting edge (3.23).

3.24 Wedge: the portion of the point enclosed between a face (3.22) and a flank (3.22) (figure A2.4).

3.25 Outer corner: the corner formed by the intersection of a major cutting edge (3.23) and the leading edge of the land (3.16) (figure A2.3 and A2.4).

3.26 Chisel edge: the edge formed by the intersection of the flanks (3.21) (figures A2.3 and A2.4).

3.27 Chisel edge corner: the corner formed by the intersection of a major cutting edge (3.23) and the chisel edge (3.26) (figure A2.3 and A2.4).

3.28 Chisel edge length: the distance between the chisel edge corners (3.27) (figure A2.3).

3.29 Major cutting edge (lip) length: the minimum distance between the outer corner (3.25) and the corresponding chisel edge corner (3.27) of the major cutting edge (3.23) (figure A2.4).

3.30 Drill diameter: the measurement across the lands (3.14) at the outer corners (3.25) of the drill. Measured immediately adjacent to the point (3.20) (figures A2.5 and A2.6).

Figure A2.5 Drill body clearance diameter and Figure A2.6 Drill diameter (ISO)

3.31 Body clearance diameter: the diameter of the body clearance (3.17) behind the lands (3.14) (figure A2.5).

3.32 Back taper: the reduction in diameter (3.30) from the outer corner (3.25) towards the shank. It is expressed by the ratio of the reduction in diameter and the length of measurement.

3.33 Web taper: the increase in web thickness (3.13) from the point (3.20) of the drill to the shank end of the flutes. It is expressed by the ratio of the increase in diameter and the length of measurement.

3.34 Rotation of cutting: the primary motion of the cutting edge relative to the workpiece.

3.35 Right-handed cutting drill: a drill that rotates in a clockwise direction relative to the workpiece when viewed on the shank end of the drill (counter-clockwise) when viewed on the point end).

3.36 Left-handed cutting drill: a drill that rotates in a clockwise direction relative to the workpiece when viewed on the shank end of the drill (counter-clockwise) when viewed on the point end).

3.37 Lead of helix: the distance measured parallel to the drill axis (3.1) between corresponding points on the leading edge of a land (3.16) in one complete revolution of the land (3.14) (figure A2.7).

3.38 Helix angle (may be classified as normal, slow and quick): the acute angle between the tangent to the helical leading edge and a plane containing the axis and the point in question. This angle lies in a plane normal to the radius at the point on the edge (figure A2.7).

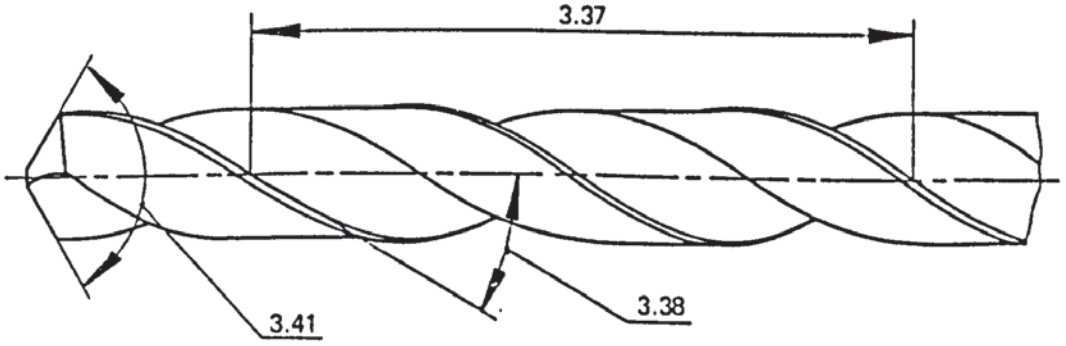

Figure A2.7 Drill helix angle (ISO)